Analysis of RNA-protein interactions involved in calicivirus translation and replication

by

Ioannis Karakasiliotis

Thesis submitted for the degree of

Doctor of Philosophy

Imperial College London

2008

Department of Virology, Imperial College London, Faculty of Medicine, St. Mary's Campus, Norfolk Place

London

Abstract

The interaction of host-cell nucleic acid-binding proteins with the genomes of positive-stranded RNA viruses is known to play a role in the translation and replication of many viruses. To date, however, the characterisation of similar interactions with the genomes of members of the *Caliciviridae* family has been limited to *in vitro* binding analysis. In this study, feline calicivirus (FCV) and murine norovirus (MNV) have been used as model systems to identify and characterise the role of host-cell factors that interact with the viral RNA and RNA structures that regulate virus replication. It was demonstrated that RNA-binding proteins such as polypyrimidine tract-binding protein (PTB), poly(C)-binding proteins (PCBPs) and La protein interact with the extremities of MNV and FCV genomic and subgenomic RNAs. PTB acted as a negative-regulator in FCV translation and is possibly involved in the switch between translation and replication during the late stages of the infection, as PTB is exported from the nucleus to the cytoplasm, where calicivirus replication takes place. Furthermore, using the MNV reverse-genetics system, disruption of 5' end stem-loops reduced infectivity ~15-20 fold, while disruption of an RNA structure that is suspected to be part of the subgenomic RNA synthesis promoter and an RNA structure at the 3' end completely inhibited virus replication. Restoration of infectivity by repair mutations in the subgenomic promoter region and the recovery of viruses that contained repressor mutations within the disrupted structures, in both the subgenomic promoter region and the 3’ end, confirmed a functional role for these RNA secondary structures. Overall this study has yielded new insights into the role of RNA structures and RNA-protein interactions in the calicivirus life cycle.

Table of Contents

Abstract 2

Table of Contents 3

Table of Figures 7

Table of Tables 11

Abbreviations 12

Acknowledgements 16

Declaration 17

1. General Introduction 19

1.1. *Caliciviridae* 21

1.2. Disease and Epidemiology 21

1.2.1. Human caliciviruses 21

1.2.2. Murine norovirus 22

1.2.3. Feline calicivirus 23

1.3. Morphology and genome organisation 25

1.4. Viral proteins 28

1.4.1. NS1 and NS2 28

1.4.2. NS3 (NTPase) 29

1.4.3. NS4 29

1.4.4. NS5 (VPg) 30

1.4.5. NS6 and NS7 (Protease and Polymerase) 31

1.4.6. VP1 (major capsid protein) 32

1.4.7. VP2 (minor capsid protein) 33

1.5. Virus life cycle 33

1.6. RNA as a functional molecule 37

1.6.1 AU-rich elements (AREs) 39

1.6.2. Iron response elements (IREs) 40

1.7. RNA structures in (+) sense RNA viruses 42

1.7.1. IRESs 42

1.7.2. Other structures involved in viral translation 48

1.7.3. RNA structures involved in viral replication 50

1.8. Host RNA-binding proteins 51

1.8.1 Polypyrimidine tract binding protein (PTB) 52

1.8.2 Lupus autoantigen (La) 54

1.8.3 Poly(C) binding protein (PCBP) 57

1.8.4 Other host cell RNA binding proteins 59

1.9. Aim of the study..... 59

2. Materials and Methods 61

2.1. Antisera 62

2.2. Viruses and Cell lines 62

2.3. Western blot 62

2.4. Northern blot 63

2.5. Reverse transcription (RT) and Polymerase chain reaction (PCR) 64

2.6. Viral RNA immunoprecipitation 67

2.7. T7 transcription 68

2.8. RNA affinity columns 69

2.9. Protein purification 70

2.9.1 GST-PTB 70

2.9.2 His-PTB, His-PCBP1 and His-PCBP2 71

2.10. Electrophoretic mobility shift assays (EMSAs) 72

2.11. VPg-linked viral RNA purification 72

2.12. *In vitro* translation 73

2.13. RNase H treatment of FCV RNA 74

2.14. Bioinformatics tools 74

2.14. MNV and FCV reverse genetics 76

2.15. Determination of viral titre (TCID50/ml) 78

2.16. MNV plaque assays 79

2.17. DNA and RNA and siRNA transfection 79

2.18. Plasmid preparation 80

2.19. Luciferase assay 80

2.20. Confocal microscopy 80

3. Analysis of the role of PTB in the calicivirus life cycle 82

3.1. Introduction 83

3.2. PTB interacts with the 5' extremities of the calicivirus genomic and subgenomic RNAs *in vitro* 84

3.3. PTB interacts with the FCV RNA in infected cells 90

3.4. FCV replication is not affected by overexpression of PTB 91

3.5. RNAi-mediated knockdown of PTB 92

3.6. FCV replication is affected by RNAi-mediated knockdown of PTB in a temperature dependent manner 94

3.7. PTB binds at least on two sites of FCV genomic RNA 5’ end in a synergistic manner 100

3.8. Viruses with reduced affinity for PTB have the same growth kinetics as the wild-type virus in tissue culture 105

3.9. PTB inhibits FCV *in vitro* translation 108

3.10. Inhibition of FCV *in vitro* translation is temperature dependent 112

3.11. FCV translation is enhanced by RNAi-mediated knockdown of PTB 112

3.12. PTB translocates from the nucleus to the cytoplasm during FCV infection 115

3.13. Discussion 121

4. Functional analysis of RNA structures in the MNV genome 130

4.1. Introduction 131

4.2. Prediction of higher order RNA structures in the MNV genome 132

4.3. Specific RNA structures are required for the MNV replication 138

4.4. Deletion of the MNV 3' UTR polypyrimidine hairpin loop does not affect viral replication in tissue culture 140

4.5. Characterisation of naturally revertant viruses 144

4.6. Compensation of the disrupting mutations 149

4.7. Discussion 150

5. Characterisation of the Interaction of PCBPs and La with calicivirus RNA 156

5.1. Introduction 157

5.2. The MNV 5' genomic and 5' subgenomic RNA extremities interact with poly(C)-binding proteins 158

5.3. The MNV 3' UTR interacts with PTB and PCBP2 162

5.4. The La protein interacts with the 5' extremity of FCV genomic RNA 165

5.5 La protein assists PTB binding to the 5' extremity of the FCV genomic RNA .. 166

5.6 Discussion 169

6. Conclusion and future work 173

References 179

Table of Figures

Figure 1.1. Phylogenetic relationship among caliciviruses 20

Figure 1.2. Calicivirus capsid morphology 25

Figure 1.3. Graphic illustration of the coding region of representatives from the four calicivirus genera 26

Figure 1.4. FCV and MNV Genomic and subgenomic RNAs 27

Figure 1.5. Virus induced vesicles 35

Figure 1.6. Termination reinitiation for translation of ORF3 36

Figure 1.7. Iron responsive elements 41

Figure 1.8. Structures of picornaviral IRESs 43

Figure 1.9. Structures of hepatitis C virus genomic RNA 48

Figure 1.10. End to end interaction of poliovirus RNA 51

Figure 1.11. Polypyrimidine tract binding protein alternative splicing variants 53

Figure 1.12. The functional domains of La protein 55

Figure 1.13. Poly(C) binding proteins 57

Figure 2.1. Mutagenesis by extension PCR 65

Figure 2.2. Overlapping mutagenesis PCR 77

Figure 3.1. Riboproteomic and bioinformatic analysis of PTB binding on FCV and MNV RNA 86

Figure 3.2. Bioinformatics analysis of the 5' end of the MNV genomic RNA 87

Figure 3.3. PTB binds specifically to the FCV 5' genomic and 5' subgenomic RNA extremities 88

Figure 3.4. PTB binds specifically to the MNV 5' genomic and 5' subgenomic RNA extremities 89

Figure 3.5. PTB interacts with the viral RNA *in vivo* 90

Figure 3.6. FCV replication is not affected by overexpression of PTB1 92

Figure 3.7. RNAi-mediated PTB knockdown has a dramatic effect on poliovirus translation 93

Figure 3.8. Limited effect of RNAi-mediated knockdown of PTB on calicivirus replication at 37 ^{o}C 95

Figure 3.9. FCV replication is affected by RNAi-mediated knockdown of PTB in a temperature dependent manner 96

Figure 3.10. FCV yield is reduced by RNAi-mediated knockdown of PTB at 32 ^{o}C .. 97

Figure 3.11. FCV protein expression is inhibited by PTB knockdown at 32 ^{o}C 98

Figure 3.12. FCV RNA production is inhibited by PTB knockdown at 32 ^{o}C 99

Figure 3.13. Mapping of the PTB binding site(s) on the FCV 5'G_{1-245} 100

Figure 3.14. Mapping of the PTB binding site(s) on the FCV 5'G_{1-245} 102

Figure 3.15. Mutational analysis of PTB binding sites on the FCV 5'G_{1-202} by electrophoretic mobility shift assays 104

Figure 3.16. Recovery of genetically defined FCV which contain mutations in the PTB binding sites 107

Figure 3.17. Inhibition of FCV *in vitro* translation by PTB 109

Figure 3.18. Effect of PTB on cap-dependent and FMDV-IRES dependent *in vitro* translation 110

Figure 3.19. The inhibition of FCV *in vitro* translation by PTB is temperature dependent 111

Figure 3.20. Isolation of FCV sgRNA and the effect on its translation during RNAi 114

mediated knockdown of PTB .....

Figure 3.21.1 Distribution of PTB in FCV infected cells at 37 ^{o}C 116

Figure 3.21.2 FCV infected cells have reduced levels of PTB in the nucleus 117

Figure 3.22. FCV infected cells have increased levels of PTB in the cytoplasm 118

Figure 3.23. FCV infected cells have increased levels of PTB in the cytoplasm and decreased levels in the nucleus 119

Figure 3.24. Correlation between p76 levels and the levels of PTB in the nucleus in FCV infected cells 119

Figure 3.25. Localisation of PTB in the cytoplasm of FCV infected CRFK cells 120

Figure 4.1. Predicted RNA structures in the MNV genome 133

Figure 4.2. A stem loop structure upstream of the subgenomic RNA start is predicted for a variety of representative caliciviruses 136

Figure 4.3. Alignment of the 3' end stem loop of MNV RNA 137

Figure 4.4. Phenotypes of the mutated viruses recovered by reverse genetics 139

Figure 4.5. Phenotype of the 3' polypyrimidine loop-deletion virus after reverse genetics recovery 141

Figure 4.6. Growth kinetics and temperature sensitivity analysis of the 3' end polypyrimidine loop deletion virus 143

Figure 4.7. Reversion determinants of naturally revertant viruses 145

Figure 4.8. Phenotype of the m53RevA revertant of the m53 lethal phenotype 146

Figure 4.9. Thermodynamically predicted secondary structures involved in the reversion of the m54 lethal phenotype 148

Figure 4.10. Compensation of the stem loop upstream of the subgenomic RNA start . 149

Figure 5.1. Bioinfomatically predicted secondary structure of the MNV 5'G_{1-250} 159

Figure 5.2. Interaction of PCBP1 and PCBP2 with the MNV 5'G_{1-250} and 5'SG_{1-200} RNAs 160

Figure 5.3. Comparison of the interaction of PCBP1 and PCBP2 with the MNV 5'G_{1-250} and 5'SG_{1-200} RNAs 161

Figure 5.4. PCBP2 and PTB interact with the 3' extremity of the MNV genome 164

Figure 5.5. PTB interacts specifically with the 3' extremity of the MNV genome 165

Figure 5.6. La protein interacts specifically with the 5' end of the FCV genomic RNA 165

Figure 5.7. La assists PTB binding on the 5' end of the FCV genomic RNA 168

Figure 6.1. The hypothesis for the regulation of FCV replication by PTB 177

Figure 6.2. The RNP complex that regulates FCV translation 177

Table of Tables

Table 2.1. FCV oligonucleotides 65

Table 2.2. MNV sequencing oligonucleotides 66

Table 2.3. MNV oligonucleotides 67

Table 2.4. GenBank accession numbers of FCV and MNV strains 75

Table 6.1. RNA-protein interactions in FCV and MNV 172

Abbreviations

α-CPs	α-complex proteins
ARE	AU-rich elements
BHK-21	baby-hamster kidney cells
BSRT7	BHK-derived cell line exopressing T7 polymerase
CAT	chloramphenicol acetyltransferase
cDNA	copy DNA
Ci	Curie
CMV	cucumber mosaic virus
CMV	cytomegalovirus
CnBr	cyanogen bromide
Cre	cis-acting replication element
CRFK	Crandel Reese feline kidney
CrPV	cricket paralysis virus
DAPI	4',6-diamidino-2-phenylindole
ddH2O	double distilled H2O
DMEM	Dulbecco MEM
dsRNA	double stranded RNA
DTT	Dithiothreitol
EBERs	Epstein-Barr encoded RNAs
EBV	Epstein Barr virus
EDTA	ethylenediaminetetraacetic acid
eIF	eukaryotic initiation factor
EMCV	encephalomyocarditis virus
EMSA	electrophoretic mobility shift assay
FCS	foetal calf serum
FCV	feline calicivirus
FMDV	foot and mouth disease virus
FUT2	α(1,2)-fucosyltranferase
GAPDH	glyceraldehyde-3-phosphate dehydrogenase
GE	gastroenteritis
GFP	green fluorescence protein

GM-CSF	granulocyte-macrophage-colony-stimulating factor
GNRA	guanine, any nucleotide, purine, adenine
gRNA	genomic RNA
GST	glutathione-S-transferase
HAV	hepatitis A virus
HCV	hepatitis C virus
HEPES	4-(2-hydroxyethyl)-1piperazineethane sulfonic acid
hnRNP	heterogeneous nuclear ribonucleoprotein
HRPO	horseradish peroxidase
HuCV	human calicivirus
IFN-γR	interferon-γ receptor
IPTG	isopropyl-b-D-thiogalactopyranoside
IRE	iron responsive element
IRES	internal ribosomal entry site
IRP	iron regulatory protein
ITAF	IRES trans-acting factor
JAM-1	feline junctional adhesion molecule 1
kb	kilobases
kDa	kilo Daltons
KH	hnRNP K-homology
La	lupus autoantigen
LB	Luria broth
LC	leader capsid
LDH	lactate dehydrogenase
LOX	15-lipoxygenase
LUC	firefly luciferase
MES	2-(*N*-morpholino) ethenesulfonic acid
MgOAc	magnesium acetate
MHV	mouse hepatitis virus
miRNAs	micro RNAs
MNV	murine norovirus
m.o.i	Multiplicity of infection
mRNA	messenger RNA

MRP	mitochondrial RNA processing
MVAT7.	modified vaccinia virus Ankara T7
mwt	molecular weight
NMR	nuclear magnetic resonance
nPTB	neuronal PTB
NS	non-structural
nt(s)	nucleotide(s)
NTPs	nucleocide (A,U,G,C) triphosphates
NV	Norwalk virus
ORF	open reading frame
PABP	polyA-binding protein
PAGE	sodium dodecyl sulfate polyacrylamide gel electrophoresis
PAM	peptidylglycine alpha-amidating monooxygenase
PBS	phosphate buffered saline
PCBPs	polyC-binding proteins
PCR	polymerase chain reaction
p.i.	post infection
PKA	Protein kinase A
PMSF	phenylmethylsulphonyl fluoride
P-Num	p-number
polyU/C	poly uridine/cytosine
pT7SG+R	plasmid expressing the FCV subgenomic RNA + 3' ribozyme
PTB	polypyrimidine tract-binding protein
PVDF	polyvinylidene fluoride
RAG1	recombination-activating gene 1
RAG2	recombination-activating gene 2
RAW	mouse leukaemic monocyte macrophage cell line
RdRp	RNA-dependent RNA polymerase
RHDV	rabbit hemorrhagic disease virus
RIPA	radioimmunoprecipitation
RNase	ribonuclease
RNP	ribonucleoprotein complex
RRL	rabbit reticulocyte lysate

RRM	RNA recognition motif
rRNA	ribosomal RNA
RT	reverse transcription
Rz	ribozyme
S	stem
SDS	sodium dodecyl sulphate
sgRNA	subgenomic RNA
siRNAs	small interfering RNAs
SL	stem-loop
SLa	stem-loop antigenomic
SMSV	San Miguel sea lion virus
snoRNAs	small nucleolar RNAs
snRNAs	small nuclear RNAs
ssRNA	single stranded RNA
STAT-1	signal transducer activator of transcription 1
SVEV	swine vesicular exanthema virus
TCID50	50% tissue culture infective dose
TfR1	transferrin receptor 1
TIA-1	T cell intracellular antigen-1
TIAR	TIA-1 related protein
TNF	tumour necrosis factor
tRNA	transfer RNA
TURBSs	termination upstream ribosomal binding sites
unr	upstream of N-ras protein
UTR	untranslated region
VP1	virus capsid protein 1
VP2	virus capsid protein 2
VPg	virus protein linked to genome
vRNA	viral RNA
XIAP	X-linked inhibitor of apoptosis
α-CPs	α-complex proteins

Acknowledgements

First of all I would like to thank my supervisor Ian Goodfellow for his endless help and encouragement during this project. I would also like to thank the rest of the members of the calicivirus lab: Yasmin Chaudhry, Dalan Bailey, Nora McFadden, and Lillian Chung, for their great help and for making the three years of this project enjoyable. Last but not least I would like to thank my parents, Nikos and Aggeliki, as well as my girlfriend Niki for their support and patience during my stay in the UK.

Declaration

All the work presented in this thesis is the result of my own work (except where indicated) and in no way forms part of any other thesis. This work was carried out at the Department of Virology, Faculty of Medicine, Imperial College London under the supervision of Dr. Ian Goodfellow.

"*Εις τον πατέραν μου οφείλω το ζείν καί εις τον διδασκαλόν μου το ευ ζειν*"

Ο Αλέξανδρος ο Γ' ο Μακεδών 356 π.Χ. – 323 π.Χ.

"*To my father I owe my being and to my teacher I owe my well-being*"

Alexander III the Macedon 356 B.C. – 323 B.C.

Chapter 1.

General Introduction

Gastroenteritis (GE) is one of the most common diseases in humans. More than 700 million cases per year are reported worldwide, resulting in approximately 3.5 to 5 million deaths (mainly in developing countries) (reviewed by Atmar & Estes, 2001). The causal agent for acute gastroenteritis can be bacterial, parasitic or viral. Bacterial GE is caused mostly by *Salmonella* and *Campylobacter*, parasitic GE mainly by *Giardia* and viral GE by caliciviruses, rotaviruses and astroviruses.

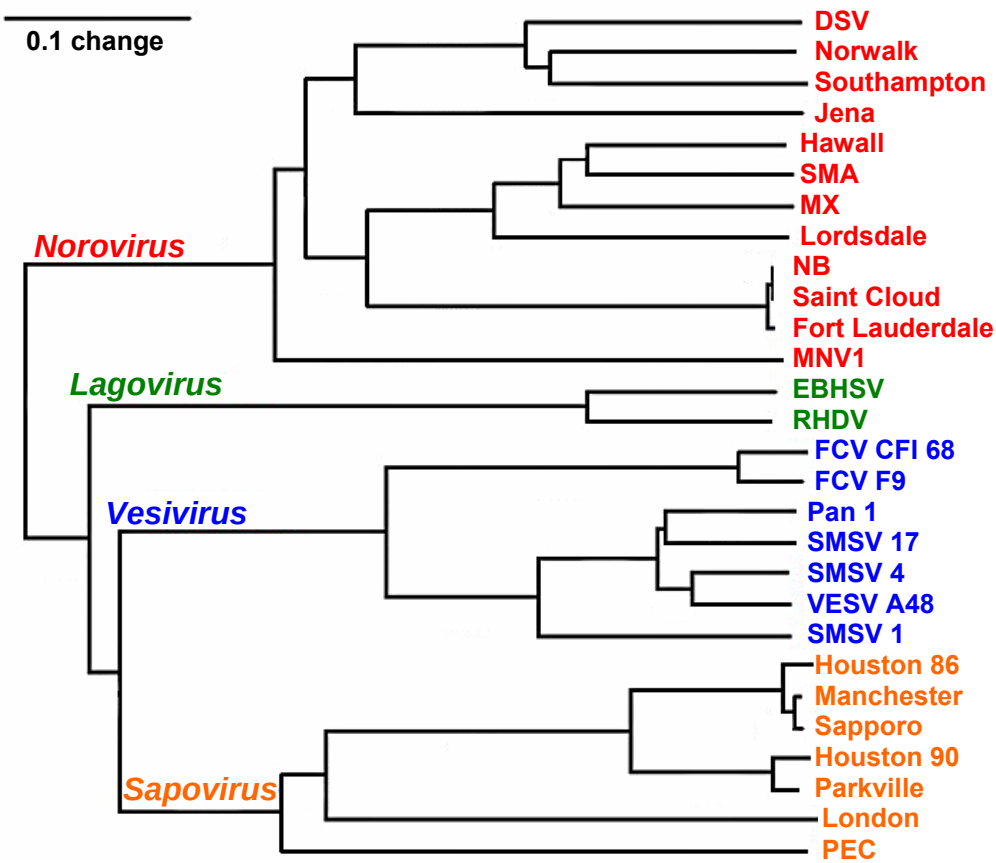


Figure 1.1. Phylogenetic relationship among caliciviruses Phylogenetic tree of caliciviruses based on the sequences of the capsid protein. Adapted from (Karst et al., 2003)

1.1. *Caliciviridae*

Gastroenteritis caused by Norwalk virus (NV), a human calicivirus (HuCV) was first described in Norwalk, Ohio in 1968 (Adler & Zickl, 1969). The name calicivirus is derived from the Latin word *calyx* (=cup) because of the cup-like structures on their capsid. Since 1998 the *Caliciviridae* family has been divided into four genera (updated later for more formal nomenclature Büchen-Osmond, 2003) the *Norovirus* genus, comprising among others Norwalk virus and murine norovirus (MNV), the *Sapovirus* genus, with the Sapporo virus to be designated as the type species, *Lagovirus* genus, comprising mainly of rabbit hemorrhagic disease virus (RHDV) and the *Vesivirus* genus, containing swine vesicular exanthema virus (SVEV) and feline calicivirus (FCV). A phylogenetic tree showing the evolutionary interrelationships among the various genogroups of caliciviruses is presented in **Fig. 1.1**.

1.2. Disease and Epidemiology

1.2.1. Human caliciviruses

Caliciviruses which cause disease in humans (Human caliciviruses) can be found in both the *Norovirus* and *Sapovirus* genera. HuCV have been reported to be responsible for 75% of all gastroenteritis cases of viral aetiology and 60% of all gastroenteritis cases as estimated by CDC for the United States (Mead et al., 1999). HuCVs are commonly isolated during outbreaks of gastroenteritis in hospitals, restaurants, cruise ships, schools and other settings that combine food with large numbers of people. The transmission of HuCVs mainly follows the faeco-oral route,

but aerosolised vomit can become an alternative method of transmission (Graham et al., 1994). The symptoms of a HuCV infection last for 12 to 60 hours, and they include nausea, vomiting, abdominal cramps and diarrhoea. Children experience mainly vomiting, while in adults, diarrhoea is the most common symptom. Due to the vomiting caused by HuCVs and the seasonality, the disease is often referred as "winter vomiting disease". The illness can be fatal when it leads to dehydration in susceptible persons. However, in the majority of cases in the developed world, the symptoms are mild and the infection is resolved within several days.

The large number of people affected by HuCVs along with the required decontamination of the setting where an outbreak has occurred makes the HuCVs of high economic importance. The 35,000 hospitalisations in England and Wales and the 283 episodes of infectious intestinal disease per 1000 person each year, support estimates of the profound economic effect of HuCV (reviewed by Lopman et al., 2002). It was estimated that during 2003 and 2004, HuCV outbreaks in hospitals resulted in the loss of 3400 bed-days. The overall impact of outbreaks occurring in hospital environments alone, including the cost of replacing staff due to illness, has been estimated at ~70 million pounds Sterling per year (Lopman et al., 2004).

1.2.2. Murine norovirus

Another important member of the *norovirus* genus is murine norovirus (MNV). MNV (MNV-1) was first identified in transgenic mice lacking the recombination-activating gene 2 and the signal transducer activator of transcription 1 (RAG2/STAT-$1^{-/-}$). In these severely immunocompromised mice MNV-1 caused a

lethal infection that was associated with encephalitis, vasculitis of the cerebral vessels, meningitis, hepatitis, and pneumonia (Karst et al., 2003). STAT-1 is part of the signalling pathway responsible for innate immunity and is required for the clearance of the virus. The defect in STAT1 was the main determinant of the lethal phenotype as in $STAT1^{-/-}$ mice the mortality was high, while in $RAG2^{-/-}$ mice MNV-1 showed only limited replication and lead to an asymptomatic infection, similar to that observed in immunocompetent mice (Karst et al., 2003). MNV-1 showed a clear tropism for murine dendritic cells and macrophages, while a macrophage cell line, (RAW 264.7), could support viral growth (Wobus et al., 2004). Recent studies have identified additional MNV strains (Hsu et al., 2006, Muller et al., 2007, Thackray et al., 2007), among them MNV-2, 3 and 4. In these cases the viruses were isolated from the mesenteric lymph nodes of persistently infected immunocompetent mice (Hsu et al., 2006). In a recent survey carried out in an animal facility, 67.5% of the laboratory kept mice were found positive for MNV (Muller et al., 2007). Thus, MNV is not only a good system for the study of the basic biology of noroviruses, but is also an important pathogen of research mice.

1.2.3. Feline calicivirus

Feline calicivirus (FCV), of the *Vesivirus* genus, causes an acute oral and upper respiratory system disease in domestic and wild cats. The disease is often called ‘cat flu’ because of the similarities of the clinical signs to those caused by influenza virus in humans (TerWee et al., 1997). Recently, more virulent strains have become prevalent in the USA which cause a systemic infection. These highly virulent strains cause outbreaks of a systemic illness similar to the hemorrhagic disease caused by

RHDV in rabbits, which leads to the death or euthanasia of 50% of the infected cats (Pedersen et al., 2000). To date, only one outbreak of highly virulent FCV has been reported in the UK (Coyne et al., 2006). In most cases the virus is shed in oropharyngeal secretions for about 30 days. However, a small part of the cat population remain as carriers (persistence) shedding virus for more than a month or even for the rest of their life (Radford et al., 2007). The prevalence of FCV ranges from 10% for domestic cats, to 25%-40% in feral cats or those living in large colonies. FCV is one of the very few caliciviruses which replicate efficiently in tissue culture, leading to the availability of a wide range of live-attenuated vaccines (reviewed by Radford et al., 2007). A report in 2006 presented a potential link between vesiviruses and undiagnosed human diseases. Using antigens from the San Miguel sea lion virus (SMSV) and the FCV vaccine strain F9 a high prevalence of anti-vesivirus antibodies was detected in individuals with undiagnosed hepatitis (Smith et al., 2006). Interestingly, ongoing viremia was detected in the 10% of these cases (Smith et al., 2006).

Despite the advanced epidemiological knowledge on human caliciviruses, the molecular mechanisms that these viruses use for replication are still unknown. This is largely due to the fact that until very recently, cell lines or animal models that can be infected with HuCVs have not been available. Recent work by Asanaka et al. demonstrated limited evidence of Norwalk virus replication and packaging after transfection of cells with a full length clone (Asanaka et al., 2005). In 2006 an animal model for human caliciviruses was developed as HuCV demonstrated efficient infection in gnotobiotic pigs (Cheetham et al., 2006). In 2007 there was a report of a 3-dimentional cell culture system that could support HuCV growth on an organoid

model of the human small intestinal epithelium (Straub et al., 2007). Despite these recent advances, FCV and MNV (Wobus et al., 2004) that can be propagated in cell culture are still the best readily available systems with which to study the basic mechanisms of viral genome translation and replication. MNV is the only norovirus that can replicate in a small animal model (mice) thereby boosting pathogenicity studies in noroviruses. Recently, a replicon system for Norwalk virus was developed, in which a self-replicating RNA representing the viral RNA was stably expressed in cells providing the first tool for the study of HuCV replication (Chang et al., 2006).

1.3. Morphology and genome organisation

The particles (virions) of caliciviruses exhibit T=3 icosahedral symmetry and are 35-39nm in diameter (Prasad et al., 1999). Images taken by electron microscopy revealed small pits on the virus surface leading to the name calicivirus, from the Latin calyx (= cup) (**Fig. 1.2a**). However, the surface of Norwalk virus, in contrast to the other caliciviruses, seems to be less well defined by EM (**Fig. 1.2b**). X-ray crystallography has also revealed the fine structure of the capsid from several

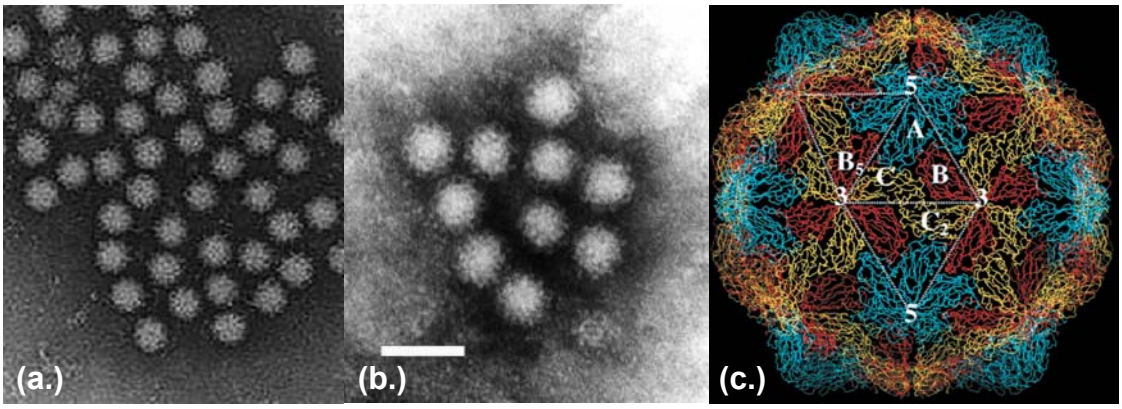


Figure 1.2. Calicivirus capsid morphology. **(a.)** Electron microscopy image of RHDV (microbes.otago.ac.nz) **(b.)** Electron microscopy image of Norwalk virus; bar = 50nm (www.epa.gov) **(c.)** X-ray crystallography structure of Norwalk virus (Prasad et al., 1999).

members of the family as 180 copies of a single capsid protein, organised into 90 dimers (**Fig. 1.2c**). In addition to the major capsid protein (VP1), two copies of the minor capsid protein (VP2) are present in each virion (Konig et al., 1998, Sosnovtsev & Green, 2000). More details about the capsid and receptor binding are discussed later in this chapter.

The capsid encloses the genome of the virus which is a positive sense RNA molecule of approximately 7.5 kb in length with a protein covalently linked to the 5' end (VPg) and a poly(A) tail at the 3' end. The genome is divided into three open reading frames (ORFs) flanked by two short untranslated regions (UTRs). The overall

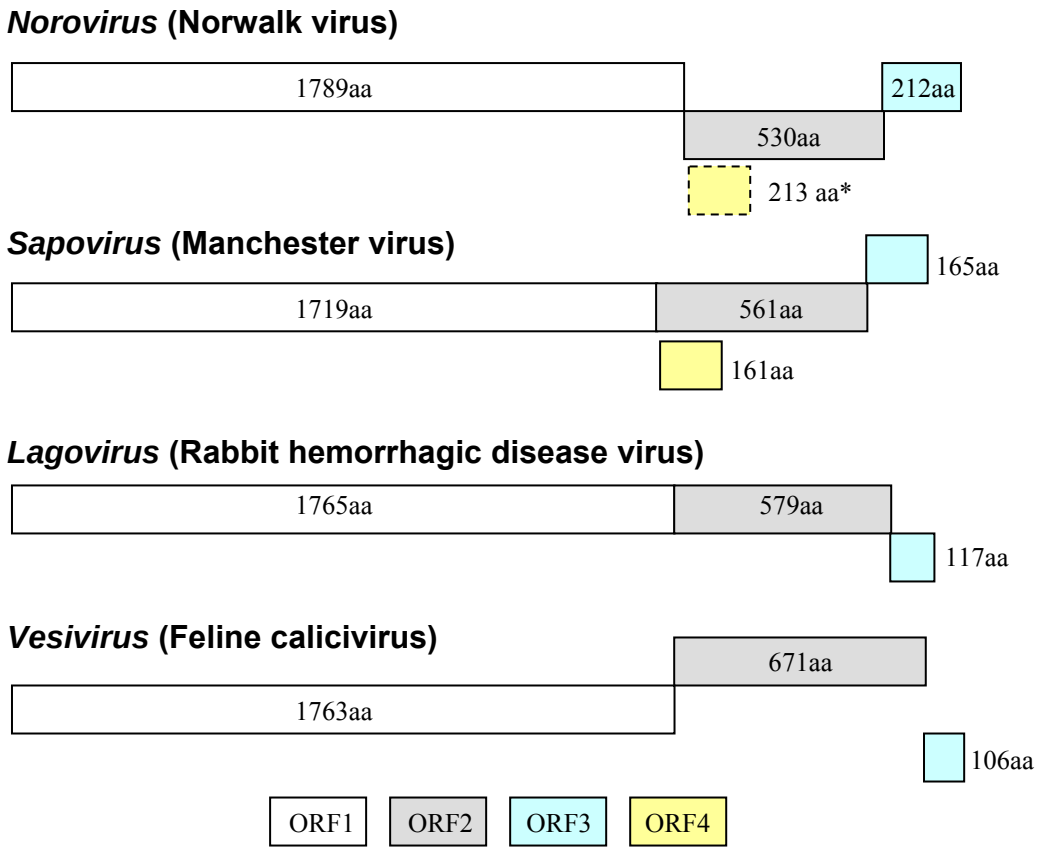


Figure 1.3. Graphic illustration of the coding region of representatives from the four calicivirus genera. The different open reading frames of all the viruses are presented; white for ORF1, grey for ORF2, blue for ORF3 and yellow for the additional ORF present in Manchester virus (reviewed by Atmar & Estes, 2001). In sapoviruses and lagoviruses ORF1 and ORF2 are fused but ORF2 is independent in the context of the subgenomic RNA. (* = potential ORF4 present in MNV)

structure of the genome is conserved in all the caliciviruses, with the only differentiation being the length of each ORF and the reading frame in which each ORF is encoded (**Fig. 1.3**). An additional ORF is predicted to exist in the *Sapovirus* genus (Manchester virus) and in the *Norovirus* genus (MNV), with the start codon very close to the N terminus of ORF2.

During the virus replication cycle, a subgenomic RNA is produced which encodes the major (VP1) and minor (VP2) capsid proteins (**Fig. 1.4**). This subgenomic RNA is 2.4 kb in length and shares the same 3' UTR as the genomic RNA, from which it is produced. The sequences of the 5' UTRs of the genomic and

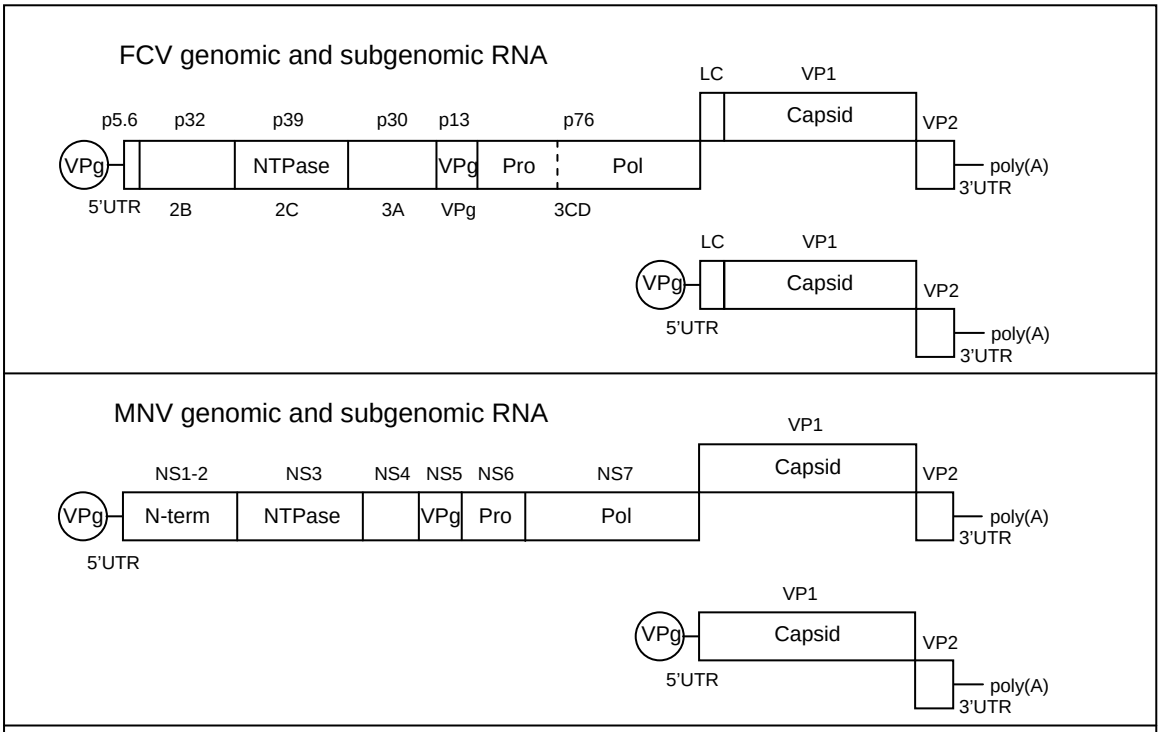


Figure 1.4. FCV and MNV Genomic and subgenomic RNAs. Graphic illustration of the genomic and subgenomic RNAs of FCV and MNV highlighting the proteins generated from the expression and processing of the three ORFs. Both RNAs in MNV and FCV have a VPg protein linked to the 5' end of a short 5'UTR, while a poly(A) follows the 3'UTR. As the nomenclature in the bibliography is still obscure there are multiple designations for the different peptides. p5.6 – p76 is the nomenclature of FCV proteins (Sosnovtsev et al., 2002), 2B -3CD is the nomenclature according to the homology of the proteins in terms of function or genome position in picornaviruses and NS1-NS7 is the current nomenclature for the MNV proteins (Sosnovtsev et al., 2006). N-term = N-terminal peptide, Pro = protease, Pol= polymerase, VP1 = major capsid protein, VP2 =minor capsid protein, LC = premature leader-capsid

subgenomic RNAs are similar, signifying an involvement in a common mechanism. Similarly to the genomic RNA, the subgenomic RNA is covalently linked to VPg and has a poly(A) tail at the 3' end. Encapsidation of the subgenomic RNA has been reported for RHDV (Meyers et al., 1991) and in a similar study on FCV, particles produced during a high multiplicity of infection, resulted in a subpopulation of lower density virions that were found to carry the 2.4 kb subgenomic RNA alone (Neill, 2002). These findings suggest that encapsidation of the subgenomic RNA is a common phenomenon among caliciviruses.

1.4. Viral proteins

Caliciviruses produce a large polyprotein from ORF1 that is processed by the viral protease to generate the mature non-structural proteins and a number of precursor proteins. For FCV the co-translational processing of the polyprotein yields 6 proteins p5.6, p32, p39,p13, p30, p76 and a variety of precursor proteins (Sosnovtsev et al., 2002) (**Fig. 1.4**). For MNV, the processing of the polyprotein also yields 6 proteins but with 2 main differences; p5.6 and p32 are merged to NS1-2, while p76 is split into NS6 and NS7 (Sosnovtsev et al., 2006).

1.4.1. NS1 and NS2

The first non-structural peptides encoded in ORF1 of FCV are p5.6 and p32 (NS1-2 for MNV). The RHDV 23-kDa protein is believed to be the analog of the FCV p32 protein and is predicted to have functional similarities with the 2B protein of picornaviruses. The picornavirus 2B protein contains hydrophobic membrane

association domains and is involved in the membrane rearrangements observed during infection. These rearrangements include vesicle formation and changes in the permeability of host cell membranes (Agirre et al., 2002). The FCV p32 protein has been found in the membranous replication complexes (Green et al., 2002), while the NV analog p48 interacts with VAP-A, a protein known to be involved in vesicle transport (Ettayebi & Hardy, 2003). Expression of p48 in cells disrupted vesicle transport and the Golgi apparatus (Ettayebi & Hardy, 2003, Fernandez-Vega et al., 2004)

1.4.2. NS3 (NTPase)

The FCV p39 protein (or MNV NS3) is predicted to possess an NTP-binding domain similar to the conserved picornavirus 2C-NTPase. The 2C-like protein in RHDV and Southampton virus (*Norovirus*) has been shown to hydrolyse nucleoside triphosphates *in vitro* (Marin et al., 2000, Pfister & Wimmer, 2001). Co-localisation of p39 with viral replication complexes is also indicative of a possible role in replication (reviewed by Sosnovtsev et al., 2002).

1.4.3. NS4

The FCV p30 (MNV NS4) is predicted to have an amphipathic helix which may give membrane association properties (reviewed by Sosnovtsev et al., 2002). It is likely that p30 is functionally analogous to the 3A protein of picornaviruses, recruiting VPg to the membrane vesicles in the replication complexes (Green et al.,

2002). In addition to its mature form, p30 is present as p30-VPg and p30-VPg-p76 precursors during infection (Sosnovtsev et al., 2002).

1.4.4. NS5 (VPg)

The FCV p13 or VPg protein is linked to the 5' end of the genomic and subgenomic RNAs (Herbert et al., 1997). The linkage of VPg to the viral RNA is crucial for infectivity as treatment of the viral RNA with proteinase K leads renders the RNA non-infectious (Burroughs & Brown, 1978). In addition, mutations in VPg can result in a decrease or even complete loss of infectivity in the case of Tyr 24 (Mitra et al., 2004). *In vitro* transcribed 5' capped RNAs produced from a full length cDNA clone of FCV are infectious when transfected into cells (Sosnovtsev & Green, 1995). These observations led to the speculation that VPg might be involved in the initiation of the translation in caliciviruses. The translation initiation factor eIF3 has been demonstrated to interact with the Norwalk virus VPg protein using the yeast two-hybrid system and *in vitro* binding assays (Daughenbaugh et al., 2003). Furthermore, the translation initiation factor eIF4E interacts with the Lordsdale virus (HuCV) and FCV VPg proteins. Inhibition of eIF4E activity was found to impede FCV translation *in vitro* confirming a functional role for the VPg:eIF4E interaction (Goodfellow et al., 2005). MNV-1 VPg also interacts with eIF4E, although sequestration of eIF4E did not inhibit *in vitro* translation of MNV VPg-linked RNA (Chaudhry et al., 2006). It has been speculated that eIF3 bridges the interaction of eIF4G with MNV VPg, as the domain of eIF4G which interacts with eIF4E is not required in MNV translation (Chaudhry et al., 2006).

1.4.5. NS6 and NS7 (Protease and Polymerase)

The p76 protein is the homolog of the picornaviral 3CD protein and has two distinct regions relative to their function. The first half has been characterised as a trypsin-like serine protease and is related to the picornaviral 3C protease (and as such is named 3C-like protease). The second half is the viral RNA-dependent RNA polymerase (RdRp) related to the picornaviral 3D polymerase. In contrast to the FCV protein, in RHDV (Martin Alonso et al., 1996), NV (Blakeney et al., 2003) and MNV (Sosnovtsev et al., 2006) the protease-polymerase protein is further processed and the two functions are separated into two distinct proteins (NS6 and NS7).

The 3C-like protease has been characterised in NV, RHDV and FCV. In NV the protein has been characterised *in vitro* as both a *cis* and *trans* acting protease (Blakeney et al., 2003) with high substrate specificity (Someya et al., 2000). In RHDV and FCV, mutagenesis of the cleavage sites demonstrated a high substrate specificity and that the 3C-like protease is the only protease required for complete processing of the polyprotein (reviewed by Clarke & Lambden, 1997, Sosnovtsev et al., 2002). The 3C-like protein, in addition to the processing of the polyprotein, is thought to inhibit cap-dependant protein synthesis by cleavage of the eukaryotic initiation factor eIF4G (Willcocks et al., 2004) and poly(A)-binding protein (Kuyumcu-Martinez et al., 2004).

The p76 protein (3CD) also possesses RNA-dependent RNA polymerase (RdRp) activity in the 3D-like domain of the protein. The RdRp activity, as mentioned above, is separated from the protease activity in RHDV and NV during

polyprotein processing. However, in FCV, despite the existence of minor cleavage sites between protease and polymerase, the active form of the RdRp and the only form found during the infection, is full-length p76 (Wei et al., 2001). In noroviruses the separated polymerase moiety retains the RdRp activity (Belliot et al., 2005). Norovirus and Sapovirus RdRp have been shown to act in a primer independent manner and are capable of *de novo* initiation (Fukushi et al., 2004, Fullerton et al., 2007). Crystal structures are now available for a number of the calicivirus RdRp's and that they look similar to other RdRps (Ng et al., 2002).

1.4.6. VP1 (major capsid protein)

The second ORF (ORF2) codes for the major capsid protein (VP1) and is thought to be produced from the subgenomic RNA alone. However, in lagoviruses and sapoviruses a portion of capsid is produced from the genomic RNA as ORF2 is fused to ORF1 giving a polyprotein that contains non-structural proteins and the major capsid protein (Clarke & Lambden, 1997). The capsid protein, as mentioned above, forms dimers that can be assembled to form the viral particle (90 dimers) in the absence of either RNA or other viral proteins (Bertolotti-Ciarlet et al., 2002). In FCV only, the capsid protein contains a leader peptide (leader of the capsid or LC) at its N terminus that is cleaved by p76 to give the mature capsid protein. The structure of the capsid protein, as determined using VLP's, demonstrates that VP1 can be divided into two domains, S and P (Prasad et al., 1999). The S domains interact with each other to form the major contacts between the subunits, while the P domains protrude from the surface forming cup like structures on the surface of the virion. The two domains are separated by a flexible hinge (Prasad et al., 1999). The P domain is further divided

into P1 and P2, while P2 is the most variable region of the capsid and the determinant of the species-specific binding to the respective receptor (Tan et al., 2004).

1.4.7. VP2 (minor capsid protein)

The third ORF (ORF3) of FCV codes for a small protein (VP2) of unknown function. The protein is basic leading to the speculation that it may interact with nucleic acids. This hypothesis, along with the observation that the inner surface of the virion is rather acidic, has led to the idea that VP2 may contribute to the encapsidation of the viral RNA (reviewed by Glass et al., 2000), however no direct evidence for such a role has been reported as yet. The VP2 protein of Norwalk virus, expressed from baculovirus in insect cells, exists in two forms, both phosphorylated (35 kDa) and non-phosphorylated (23 kDa). Only 1 or 2 copies of the protein are present in each particle (Glass et al., 2000, Glass et al., 2003). VP2 protein has been shown to stabilise VLPs when VP1 and VP2 are co-expressed in the baculovirus system, while VP2 also protects VLPs from proteolytic degradation (Bertolotti-Ciarlet et al., 2003). A two hybrid screen also confirmed an interaction between VP2 and VP1 (Kaiser et al., 2006). Finally, VP2 protein is required for the production of infectious FCV particles and for virus replication (Sosnovtsev et al., 2005).

1.5. Virus life cycle

Very little is currently known about the life cycle of caliciviruses and most of our knowledge is inferred from our current understanding of other related positive strand RNA viruses, such as picornaviruses. The virus life cycle begins with the

attachment of the particle to specific receptors, which in some cases is a carbohydrate moiety, on the membrane of the host cells. NV infection has been associated with ABO histo-blood group type (Hennessy et al., 2003) as Norwalk virus can bind the human ABO, Lewis and secretor histo-blood group antigens (Huang et al., 2003). During experimental human infections a proportion of individuals were found to be resistant to NV infection (Lindesmith et al., 2003). This resistance was later attributed to a mutation in α(1,2)-fucosyltranferase (*FUT2*) gene (Thorven et al., 2005), which regulates the expression of ABH antigens in saliva, mucosal tissues and secretions. Feline junctional adhesion molecule 1 (JAM-1) was recently identified as a receptor for FCV (Makino et al., 2006). Expression of JAM-1 in non permissive hamster lung cells led to infection by a variety of FCV strains (Makino et al., 2006). Studies also suggest that α2,6-linked sialic acid may play a role in virus binding (Stuart & Brown, 2007).

After the attachment to the cell surface, the viral RNA is released in the cytoplasm where it is recognised by the translation system of the cell. VPg acts as a *cis*-acting translation element that by interaction with translation initiation factors leads to the recruitment of the ribosome. This leads to the translation of the first ORF (ORF1) of the genomic RNA. ORF1 codes for the viral polyprotein which, in the case of Sapporo virus and RHDV includes, at its C terminus, the capsid protein. However, in the case of FCV, the ORF1 polyprotein stops at the end of the RdRp. The polyprotein is subsequently cleaved by the 3C-like protease of the virus first in *cis*, as it is part of the polyprotein, and then in *trans* producing the mature viral proteins (Sosnovtsev et al., 2002).

The non-structural proteins cause rearrangements in the cellular membranes that lead to the formation of vesicles, similar to those observed during poliovirus infection (**Fig. 1.5**). The replication complexes are formed on these vesicles and produce, via a negative strand RNA intermediate, new positive strand RNAs. All the viral proteins, structural and non-structural, and their precursors have been detected in these replication complexes. In addition to the newly synthesised genomic RNA, subgenomic RNA is also formed during genome replication. Both have negative sense RNA intermediates as two species of negative sense RNA can be detected by Northern blot in purified FCV replication complexes (one at ~8 kb and the other at ~2.5 kb) (Green et al., 2002).

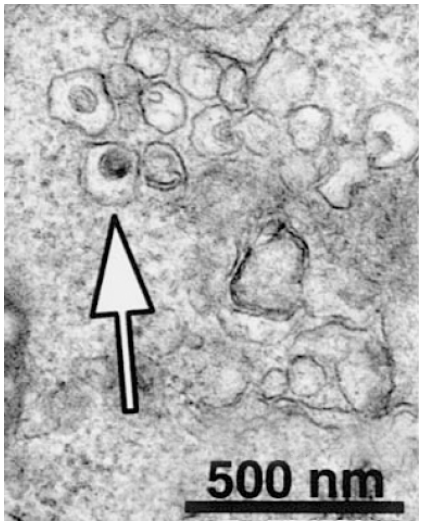


Figure 1.5. Virus induced vesicles. Vesicles (arrow) produced during replication of FCV in CRFK cells (Green et al., 2002)

The mechanism which caliciviruses use for subgenomic RNA synthesis is not known, however two mechanisms have been proposed. The first one implicates premature termination of the negative sense RNA synthesis that then serves as a template for the subgenomic RNA synthesis. The second is based on an internal initiation mechanism that utilizes a full length antisense genomic RNA and a *cis*-acting RNA element that is recognised by RdRp. The initiation of positive sense subgenomic RNA synthesis would occur in the region upstream of the ORF2 initiation codon. Deletion analysis has shown that the RHDV RdRp requires 50 bases upstream of the start of subgenomic RNA sequence in order to produce RNA with the same size as the subgenomic RNA *in vitro*. The above result infers the existence of a

cis-acting RNA element that initiates the subgenomic RNA synthesis on the negative sense genomic RNA (Morales et al., 2004).

The replication of the subgenomic RNA is followed by its translation, again through VPg-dependent translation initiation. ORF2 is translated to produce the capsid protein with the leader peptide attached to the N terminus in the case of FCV. This leader peptide is subsequently removed by the viral protease to produce the mature capsid protein. A termination reinitiation mechanism has been proposed for the translation of ORF3 (VP2) in RHDV, as the stop codon of ORF2 is required for the efficient initiation of ORF3 translation (Meyers, 2003). Also, some sequence elements upstream of ORF3 (in ORF2) are required for ORF3 translation as any RNA with less than 100 nt preceding ORF3 can not express ORF3 (Meyers, 2003). Subsequent analysis of the synthesis of VP2 in FCV revealed an identical termination reinitiation mechanism (Luttermann & Meyers, 2007). Furthermore, two sequence motifs, referred to as TURBSs (termination upstream ribosomal binding sites) essential for reinitiation were identified upstream of ORF3 one of which is conserved among caliciviruses and is complementary to part of the 18S rRNA (Luttermann & Meyers, 2007) **Fig. 1.6**.

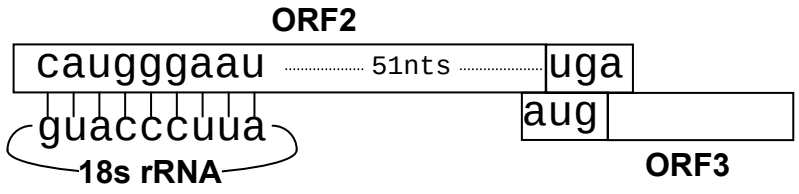


Figure 1.6. Termination reinitiation for translation of ORF3. The junction region between ORF2 and ORF3 of FCV, where the termination reinitiating takes place. ORF2 stop codon and the ORF3 start codon as well as the sequence complementary to the 18s rRNA are highlighted (Luttermann & Meyers, 2007).

The last step of the virus life cycle is the production of new virus particles. The genomic RNA, and in some cases the subgenomic, is encapsidated possibly with the help of VP2 (Glass et al., 2000). Progeny FCV viruses have been reported to arise as early as 30 minutes post infection (reviewed by Green et al., 2002). It is thought that the newly assembled particles are then released during the virus induced cell lysis.

1.6. RNA as a functional molecule

Until twenty years ago the view of an RNA was that of a passive information carrying molecule (mRNA) or part of the protein-synthesis machinery, either transferring the amino-acids (tRNA), or providing a scaffold for the ribosomal proteins (rRNA). During the 1980s, revolutionary discoveries in the biology of RNA pointed towards a new era where RNA was found to play a central role in the regulation of all cellular mechanisms due to its ability to form functional complex structures. Findings such as the autocatalytic excision of an intervening sequence in Tetrahymena's 26S rRNA (Kruger et al., 1982) , and the ribozyme activity of RNase P (Guerrier-Takada et al., 1983) were some of the first discoveries in this new era for the RNA. The propensity of RNA to form complex higher order structures can be only compared with the folding ability of proteins (Storz et al., 2005). Since the discovery of the first functional RNA structures a cascade of identifications of new functional RNA molecules took place. siRNAs (small interfering RNAs) (Fire et al., 1998), miRNAs (micro RNAs) (Lai, 2002), snRNAs (small nuclear RNAs) and snoRNAs (small nucleolar RNAs) (Storz et al., 2005) were found to regulate gene expression and alternative splicing. The peptidyltransferase activity of ribosomes was

found to be situated in the RNA moiety (Nissen et al., 2000) placing the ribosome in the growing list of enzymaticaly active RNAs, the ribozymes.

Most of the RNAs described above have evolved their structures in order to interact with proteins and in most cases the function of these RNAs is only apparent as part of a specific ribonucleoprotein complex (RNP). An obvious transition towards more complicated RNPs is the evolution of RNase P. The RNase P RNP complex consists of an RNA molecule and an increasing, on the evolutionary ladder, number of proteins: 1 in bacteria, 4 in archaea, 9 in yeast, and 10 in mammalian RNase P. The most important finding though is the relative dependence of the enzymatic activity on the protein moiety. The RNA moiety in bacteria is active in the absence of protein, while its activity in archea is reduced and drops dramatically in eukaryotic RNase P (Kikovska et al., 2007).

Higher life forms have developed more complex networks for regulating gene expression. A big part of this transition resides in the increase of functional RNA molecules (Mattick, 2001). Genes in eukaryotic organisms contain more of, what were thought to be, “junk” sequences (Mattick, 2004). Recently it was made obvious that these sequences are part of a regulatory interaction network that acts, in part, at the RNA-protein interaction level. These sequences code for small functional RNAs (Lai, 2002) or alternative splicing regulators (Singh, 2002) and untranslated regions (UTRs) in the mRNAs that regulate the export from the nucleus, localization in the cytoplasm and translational control (Jansen, 2001, Kozak, 2005).

The sequences flanking the coding region of a eukaryotic mRNA (and to a lesser extent of the prokaryotic) contain regulatory structures recognized by a variety of proteins or even by other RNAs (Staton et al., 2000, Jansen, 2001, Kozak, 2005, Ciesla, 2006). The presence of these regulatory structures on every mRNA signifies their important role in the regulation of gene expression. Some of the best studied functional RNA elements are the AU-rich elements (ARE) and the iron responsive element (IRE) that are present in a variety of mRNAs.

1.6.1 AU-rich elements (AREs)

AU-rich elements were first identified in the 3' UTR of tumour necrosis factor (TNF) mRNA (Caput et al., 1986). The AU rich sequence (UUAUUUAU) was conserved between human and murine TNF mRNAs while it was present in variety of others including the mRNA for human and mouse interleukin 1, human and rat fibronectin, and most of the sequenced human and mouse interferons (Caput et al., 1986). Since then, the list of mRNAs containing AREs has grown enormously and it is now estimated that 5–8% of human mRNAs contain AREs (reviewed by Barreau et al., 2005). AREs are usually 50–150 nts in length and regulate the stability of an mRNA. When the ARE motif of the 3' UTR of human granulocyte-macrophage-colony-stimulating factor (GM-CSF) mRNA was inserted into the 3' UTR of β-globin mRNA the later was destabilized, despite the fact that it is naturally a very stable mRNA (Shaw & Kamen, 1986). The regulation of mRNA stability by AREs is mediated by the control of length of the 3' poly(A) tail. Shortening of the poly(A) tail of c-fos mRNA, rapidly increased its degradation, leading to reduced protein production (Chen & Shyu, 1994). AREs are binding targets for a variety of RNA-

binding proteins with one of the best studied examples being the mRNA stability regulation by the proteins Hu and AUF1 (or hnRNPD). HuR (member of Hu family) increased the stability of p21 mRNA by binding to its ARE (Wang et al., 2000), while binding of AUF1 to mRNAs triggered their degradation (DeMaria & Brewer, 1996). Amongst the proteins that have been identified to interact with AREs are polypyrimidine tract binding protein (PTB or hnRNPI) and hnRNPC (Hamilton et al., 1993), T cell intracellular antigen-1 (TIA-1) with its related protein TIAR (Piecyk et al., 2000), and a number of RNA-binding metabolic enzymes such as glyceraldehyde-3-phosphate dehydrogenase (GAPDH), lactate dehydrogenase (LDH) and enoyl-CoA hydratase (reviewed by Ciesla, 2006). The wide distribution of AREs in the transcriptome and the regulation of high importance aspects of the cell biology by ARE-binding proteins signify the importance of these elements.

1.6.2. Iron response elements (IREs)

Some of the most conserved RNA structures in eukaryotic cells are the iron response elements (IREs). IREs are hairpin structures located at the 5' or 3' end of mRNAs involved in the iron homeostasis of the cell, regulating their expression (Thomson et al., 1999). The loop of the hairpin, usually consisting of 5-6 nucleotides (CAGYGX)[1], and a single nucleotide cytosine bulge at the 5' part of the stem are the most conserved parts of the structure. Regulation via IREs is mediated by the interaction of the RNA element with the iron regulatory proteins 1 and 2, (IRP1 and IRP2) in responce to the levels of iron in the cell. Binding of IRPs to the IRE is induced under low intracellular iron concentration while high levels of iron inhibit the

[1] Y = C or U and X any nucleotide expect for G

interaction (Thomson et al., 1999) **(Figure 1.7)**. When the IRE is situated at the 5' UTR of an mRNA, like the mRNAs for H (heavy) and L (light) ferritin subunits, the interaction of the IRE with IRP1 or 2 with the IRE prevents the formation of the 43s translation initiation complex (Goessling et al., 1998) **(Figure 1.7)**. The inhibition is thought to involve sterical blocking of access to the 5' cap by the translation initiation cap-binding complex eIF4F (Muckenthaler et al., 1998). A different effect is observed when the IREs are situated at the 3'UTR of the mRNA. The 3'UTR of transferrin receptor (TfR1) mRNA encompasses 5 IREs able of binding IRP1/2 (Erlitzki et al., 2002). In this instance binding of IRPs prevents degradation of the mRNA by an endonuclease, increasing the half-life of the mRNA and thus its translation efficiency (Erlitzki et al., 2002, Rouault, 2006) **(Figure 1.7)**.

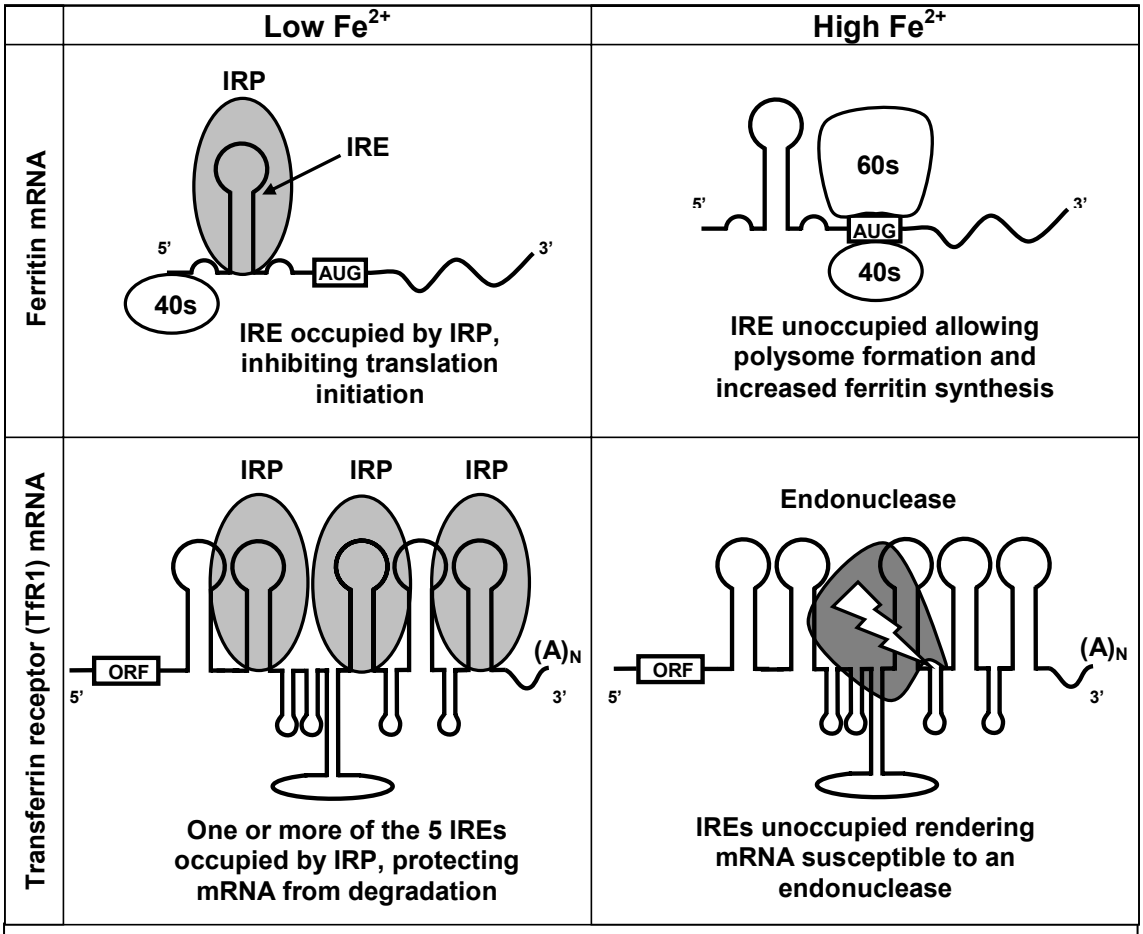


Figure 1.7. Iron responsive elements. The role of IREs in the regulation of ferritin and transferrin receptor mRNA translation depending on the intracellular levels of iron (Fe^{2+}) (Rouault, 2006)

The regulation of important processes, such as those described above, by RNA structures and RNA-binding proteins, as well as the variety of genetic diseases associated with specific RNA protein interactions (Bakheet et al., 2001, Hollams et al., 2002, Rouault, 2006) signify their central role in the regulation of post transcriptional gene expression.

1.7. RNA structures in (+) sense RNA viruses

1.7.1. IRESs

It is well established that at the initial stages of infection the genomes of positive sense RNA viruses must be recognised by the host cell translational machinery in order to generate the proteins essential for virus replication. Different positive strand RNA viruses have evolved a variety of mechanisms to exploit the translation machinery of the cell. Some viruses have become adapted to the use of normal cap-dependent translation of the host cell e.g. rotaviruses (Vende et al., 2000) and some flaviviruses (West Nile virus; Ray et al., 2006), while others have developed alternative methods such as the VPg-dependent translation of caliciviruses (Chaudhry et al., 2006) and the internal ribosomal entry site (IRES) dependent translation of picornaviruses and hepatitis C virus (HCV) (Jang, 2006).

IRESs are RNA structures present in the 5' UTRs of a number of viral and cellular mRNAs which lead to the placement of the 40s ribosomal subunit at the correct site to allow protein synthesis initiation (Baird et al., 2006). The recruitment of the 40s ribosomal subunit to the IRES is accomplished through the direct interaction

of the IRES with several canonical translation initiation factors including eIF2, eIF3, eIF4A, eIF4B, eIF4E and eIF4G, often with the assistance of non-canonical translation factors or IRES trans-acting factors (ITAFs) (reviewed by Jackson, 2005). The only known IRES to differ from this norm is the Cricket paralysis virus (CrPV) IRES which is able to bind the ribosome directly via a t-RNA like domain and promote an initiation factors independent translation initiation (Jan & Sarnow, 2002).

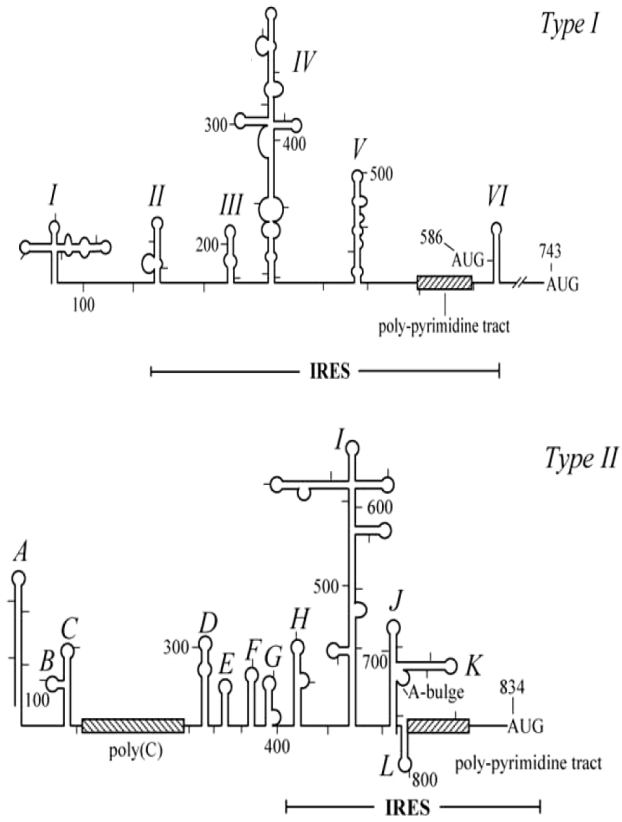


Figure 1.8. Structures of picornaviral IRESs. Graphical illustration of the two main types of internal ribosomal entry sites (IRESs) found in picornaviruses. The nomenclature of structural domain is presented above each stem-loop. I – VI for type I and A – L for type II. AUG is the initiation codon and poly(C) is the poly-cytosine stretch present in type II IRESs. (Adapted from Jang, 2006)

The encephalomyocarditis virus (EMCV) IRES was the first to be discovered and characterised using the dicistronic translation assay where two reporter genes are expressed from the same mRNA, the first under cap-dependent translation and the second under IRES-dependent translation (Pelletier & Sonenberg, 1988). Soon after it became obvious that all picornaviruses contain an IRES element in their 5' UTRs (Jackson, 2005). Using phylogenetic and biochemical analysis picornavirus IRESs can be divided into two groups: type I IRESs, which includes the enterovirus and rhinovirus IRESs (**Fig. 1.8**) and type II, which includes the cardiovirus (e.g. EMCV), aphthovirus (e.g. foot and mouth disease virus or FMDV), and hepatovirus IRESs (e.g. HAV) (**Fig. 1.8**) (Jang, 2006).

Several stem loop elements of the picornaviral IRESs have been shown to interact with the canonical and non canonical translation factors. For example, eIF4G and eIF4B interact with stem loop V of the poliovirus IRES (**Fig. 1.8**) (Ochs et al., 2002). Disruption of the interaction between stem loop V and eIF4G by a mutation in the IRES of Sabin type 1 poliovirus vaccine strain resulted in impaired translation efficiency, that conferred the attenuated phenotype of the strain (Ochs et al., 2003). Similar requirements have been demonstrated for the type II IRESs. The J/K elements of EMCV IRES recruit eIF4A (Kolupaeva et al., 1998), while the interaction of eIF4A with eIF4G increases the affinity of eIF4G for the EMCV IRES (Lomakin et al., 2000) A structural rearrangement of the downstream RNA structures induced by eIF4G/eIF4A binding is thought to be required for the efficient recruitment of the ribosome (Kolupaeva et al., 2003).

The picornavirus IRESs which have been extensively studied, all interact with a variety of non-canonical translation factors (or IRES *trans*-acting factors, ITAFs). ITAFs are usually members of the heterogeneous nuclear ribonucleoprotein (hnRNP) family of RNA binding proteins involved in post transcriptional control of mRNAs (discussed in more detailed later). Initial studies using RRLs to study IRES function indicated that additional supplementary factors were required for efficient translation initiation in enteroviruses and rhinoviruses (Dorner et al., 1984, Borman et al., 1993). The stimulatory ITAFs, include the polypyrimidine tract binding protein (PTB), poly(rC) binding protein (PCBP), the Lupus autoantigen (La) and the upstream of N-ras protein (unr). PTB has been shown to bind the EMCV, poliovirus, FMDV and rhinovirus IRESs (Kaminski et al., 1995, Hunt & Jackson, 1999, Back et al., 2002a). Poliovirus IRES activity is greatly dependent on PTB and proteolytic cleavage of the protein, as occurs late in the infection, reduces significantly the translation efficiency (Back et al., 2002a). Interestingly the attenuation of the poliovirus type 3 Sabin vaccine strain has been attributed to the reduced affinity of its IRES for the neuronal variant of PTB (nPTB) (Guest et al., 2004). PTB was shown to be required for the translation initiation from the FMDV IRES as it was found to bind simultaneously to the H and the J/K/L stem loop elements using different RNA binding domains (Song et al., 2005). A rather complicated situation has been described with regards to the role of PTB binding to the EMCV IRES. Initially, it was thought that PTB was required for the translation initiation from the EMCV IRES as its activity in the established dicistonic reporter system was dependent on PTB (Kaminski et al., 1995). However, further studies revealed that the sequences downstream of the IRES were determining the requirement for PTB and that in its natural context, the IRES was rather PTB independent (Kaminski & Jackson, 1998). The importance of the size of

an oligo-adenine RNA bulge was raised by the authors and that the maintenance of a higher order RNA structure was found to determine the requirement for PTB. Both findings pointed towards an RNA chaperone activity of PTB on the IRES function.

Further work on ITAFs demonstrated that the La protein was required for efficient translation from the poliovirus IRES as addition of La to *in vitro* translation systems resulted in stimulation of IRES activity and reduced production of aberrant translation initiation products (Meerovitch et al., 1993). The poliovirus IRES demonstrated a requirement for PCBP (Walter et al., 2002), while the unr protein was found to be required for the translation initiation from type I IRESs but not type II IRESs (Boussadia et al., 2003). Another factor called $ITAF_{45}$ or ebp1 is required for the efficient translation initiation from the FMDV IRES (Pilipenko et al., 2000). Despite the fact that $ITAF_{45}$ displayed similar affinities for both the EMCV and FMDV IRESs, siRNA mediated knockdown had no effect on the EMCV IRES (Monie et al., 2007).

An important common structural element of the picornavirus IRESs is the 20-nucleotide long polypyrimidine (Yn) tract downstream of the structural elements which bind the canonical translation initiation factors (stem loop V for type I IRESs and stem loops J, K and L for type II IRESs) (**Fig. 1.8**). The length of this Yn track and the nucleotides between Yn and the start codon have been shown to be important for the function of the IRES (Jang & Wimmer, 1990, Pilipenko et al., 1992).

Another IRES element is present in the hepatitis C virus (HCV) 5'UTR which is substantially different from that found in picornavirus IRESs. Only porcine

teschovirus IRES, a newly identified picornavirus, has a remarkably similar structure to HCV and is speculated that it was the result of an interspecies recombination event (Pisarev et al., 2004). HCV IRES is closely related structurally and functionally to the pestivirus IRES (Pestova et al., 1998, Fletcher & Jackson, 2002). In contrast to picornavirus IRESs, the HCV IRES is independent of the eIF4 factors. Cryo electron microscopy reconstruction of HCV IRES with the 40s ribosomal subunit confirmed a direct interaction (Spahn et al., 2004). However, it is believed that interaction of the HCV IRES with eIF3 enhances the formation of the initiation complex (Spahn et al., 2001). Interestingly most of the ITAFs found to interact with picornaviral IRESs also interact with the HCV IRES (Lu et al., 2004). The La protein enhances HCV translation by binding to the initiation codon and neighbouring sequences (Ali & Siddiqui, 1997, Costa-Mattioli et al., 2004). The role of PTB in HCV translation is rather unclear. Early experiments on HCV IRES activity showed that immunodepletion of PTB from rabbit reticulocyte lysates resulted in a reduction in translation efficiency from the HCV IRES (Ali & Siddiqui, 1995). However, addition of recombinant PTB failed to reverse the effect of depletion, signifying that factors associated with PTB may be responsible for the reduction of translation efficiency (Ali & Siddiqui, 1995). Further experiments using RNA aptamers designed against PTB showed a reduction in HCV IRES driven translation, recovered by addition of recombinant PTB (Anwar et al., 2000). Importantly, in the same publication the authors supported the *in vitro* results by *in vivo* data. Recently, however, the situation has become more complicated as results using different approaches contradicted the initial view of the PTB requirement in HCV translation. Overexpression of PTB in cells inhibited the translation from the HCV IRES, while expression of the antisense RNA for PTB gene reduced the levels of PTB and stimulated HCV translation

(Tischendorf et al., 2004). The different results produced using different constructs demonstrated the need of a natural context in which HCV IRES activity can be assessed. Also, the above studies revealed the potential involvement of more RNA elements in the regulatory mechanism of HCV translation such as the X region of the 3' UTR that is discussed in more details later.

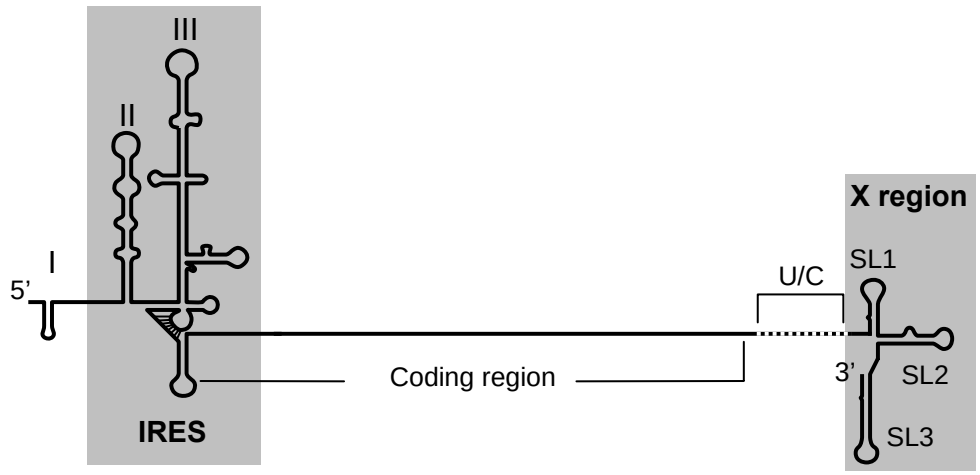


Figure 1.9. Structures of hepatitis C virus genomic RNA. Graphic representation of the HCV genomic RNA highlighting the IRES and the 3' end X region. Structural domains of the 5' end I, II and III as well as the three 3' stem loops SL1, SL2 and SL3 are represented. U/C = polypyrimidine tract

1.7.2. Other structures involved in viral translation

A feature common among mRNAs and viral RNAs is the existence of specific RNA elements, usually at the 3' end of the RNA, which function as *cis*-acting regulators of translation. A well known example is the so called "X" region situated at the 3'end of the HCV genome which stimulates IRES driven translation (Ito et al., 1998). This region is comprised of 98 nucleotides, is highly conserved among HCV strains and forms 3 stem loop structures which interact with a variety of proteins (Tsuchihara et al., 1997). Addition of this element to the 3'end of constructs

expressing a reporter under the control of the HCV or EMCV IRES, stimulated translation (Ito et al., 1998). In the same report, deletion of the PTB binding site in the X region hampered its stimulatory role (Ito et al., 1998). Recent studies have added a further level of complexity to the role of PTB in HCV translation; a pyrimidine rich stretch in the core-coding region of HCV, with high affinity for PTB, was shown to inhibit HCV translation while addition of the X region to the 3' end of the transcripts restored the translation efficiency (Ito & Lai, 1999). Subsequent reports using different systems also produced contradicting results. Whilst some groups agreed that the X region stimulated the HCV IRES mediated translation (Michel et al., 2001, McCaffrey et al., 2002) others argued that the X region had no effect (Fang & Moyer, 2000, Friebe & Bartenschlager, 2002). There was even a report claiming that the X region (or rather the SL3 part of it) had an inhibitory effect on HCV translation (Murakami et al., 2001). However, recently, an extensive analysis using a variety of methods and constructs concluded that the result varied with different approaches. A precise 3' terminus was a key factor for the effect observed, while the U/C rich stretch before just before X region and the 1st stem loop were mostly responsible for stimulation (Song et al., 2006). A remarkable result came from the *in vivo* experiments included in the same report as they observed that stimulation of HCV IRES-dependent translation by the 3' UTR was only obvious in hepatoma cell lines such as Huh-7 and HepG2 cells, indicating a role for a cell specific factor (Song et al., 2006). This observation adds to the accumulated evidence towards the importance of RNA-protein interactions in viral tropism. However, the role of PTB is still obscure while the protein required to bridge the interaction between 5' and 3' UTRs is unknown.

1.7.3. RNA structures involved in viral replication

A crucial step in the life cycle of positive stranded RNA viruses is the switch from translation to replication. This transition is very important as translation proceeds in a 5' to 3' direction while the synthesis of the negative strand RNA proceeds in 3' to 5' direction. This conflict, which favours the more robust ribosome, inhibits replication (Gamarnik & Andino, 1998, Barton et al., 1999). Poliovirus, which is arguably the best studied positive stranded RNA virus, has provided the best example of such regulation. The poliovirus 3CD protein, a homologue of the FCV p76 protein, was found to participate in the formation of a ribonuleoprotein (RNP) complex on the cloverleaf structure of the poliovirus 5'UTR. In addition to 3CD, this RNP complex was found to contain a 36 kDa cellular protein (**Fig. 1.6**) (Andino et al., 1993) which was subsequently identified as the PCBP2 protein (Parsley et al., 1997). The interaction of 3CD with the 5'cloverleaf (5'CL) was found to increase the affinity of PCBP2 for the 5' CL (Walter et al., 2002). The proposed hypothesis is that increasing amounts of 3CD produced by viral RNA translation trigger the displacement of PCBP2 from the IRES (Perera et al., 2007). 3CD assists binding of PCBP2 to the 5'CL where it promotes the interaction between the 5'CL and the 3'UTR through a 3CD/PCBP-3CD/PABP protein bridge (Barton et al., 2001, Herold & Andino, 2001). This interaction induces the negative strand RNA synthesis after the 3'UTR bound 3CD is cleaved to $3D_{pol}$ which is the active polymerase (Gohara et al., 2000). This interaction was also shown to be required for VPg uridylation thereby providing the protein primer for the negative strand RNA synthesis (Lyons et al., 2001), while evidence suggest that the same complex decreases the sensitivity of the RNA to RNases (Barton et al., 2001).

There is currently limited data on the transition from translation to replication in other animal positive-strand RNA viruses. A similar end to end interaction through a protein bridge has been suggested to be a possible trigger of the switch in HCV (Song et al., 2006). Down-regulation of HCV translation by the core and/or NS5A protein may also be part of the mechanism (Zhang et al., 2002, Kalliampakou et al., 2005).

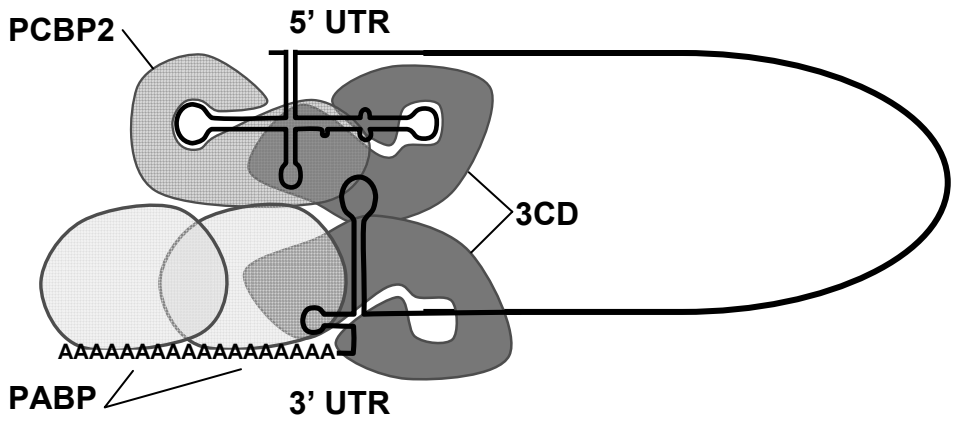


Figure 1.10. End to end interaction of poliovirus RNA. Graphic representation of the 3CD/PCBP-3CD/PABP protein bridge between 5' and 3' UTRs that triggers the initiation of the negatives strand RNA synthesis in polioviruses (Barton et al., 2001, Herold & Andino, 2001)

1.8. Host RNA-binding proteins

The recruitment of host cell proteins is a general observation in all studied RNA viruses and is believed to occur mainly due to the evolutionary need of these viruses to keep the size of their genome small. PTB, PCBP and La, as mentioned in the previous section, have been extensively studied as they have been found to interact with a number of viral RNAs (Hellen et al., 1993b, Ali & Siddiqui, 1995, Gamarnik & Andino, 1998).

1.8.1 Polypyrimidine tract binding protein (PTB)

Polypyrimidine Tract Binding protein (PTB), also known as hnRNP-I, has four RNA recognition motifs (RRMs) and four variants; PTB-1,-2,-4 (**Fig. 1.11**) and neuronal PTB (nPTB). The major physiological role of PTB is to regulate the alternative mRNA splicing of a variety of mRNAs. PTB acts as a splicing repressor by excluding selected 3' splice sites during mRNA maturation (Valcarcel & Gebauer, 1997). PTB negatively regulates the splicing of a plethora of mRNAs, such as γ2 subunit of the $GABA_A$ receptor (Ashiya & Grabowski, 1997), α-actinin (Southby et al., 1999), Fas (Izquierdo et al., 2005) and FosB (Marinescu et al., 2007). This exon exclusion is mediated by the competition of PTB with other splicing regulating proteins. For example, during the regulation of Fas mRNA splicing, TIA-1 protein recruits the U1 snRNP that induces the exon exclusion, while competition of TIA-1 binding on the RNA by PTB inhibits the splicing (Izquierdo et al., 2005). However, in the case of calcitonin and calcitonin gene-related peptide mRNAs, PTB has been shown to act as a positive regulator of the exclusion of a 3'-terminal exon (Lou et al., 1999). Involvement of PTB in the regulation of RNA polyadenylation (Lou et al., 1999), localisation (Cote et al., 1999) and stability (Pautz et al., 2006) have also been reported. The localisation of PTB is mainly nuclear, concentrated in the perinucleolar compartment, but under certain circumstances it may appear in the cytoplasm shuttling between cytosol and the nucleus (Kamath et al., 2001). Alteration of the nuclear pore permeability and composition during poliovirus (Gustin & Sarnow, 2001) and rhinovirus (Gustin & Sarnow, 2002) infection has been shown to induce the flow of nuclear proteins to the cytoplasm, while protein kinase A (PKA) phosphorylation of PTB at Ser-16 results in the redistribution of PTB to both nucleus

and cytoplasm (Xie et al., 2003). The phosphorylation state of PTB is very likely to play a role in the cytoplasmic function of PTB as phosphorylated PTB has been found to be associated with HCV replication complexes (Chang & Luo, 2006). PTB binds short, single strand polypyrimidine motifs such as UCUU, UCUUC, UUCUCU or CUCUCU and it is believed to have a chaperone activity, stabilising a functional RNA conformation (reviewed by Simpson et al, 2004). Binding of PTB and PCBP1 to the IRES present in *Bag-1* mRNA results in a conformational change in the IRES which induces ribosome recruitment (Pickering et al., 2004).

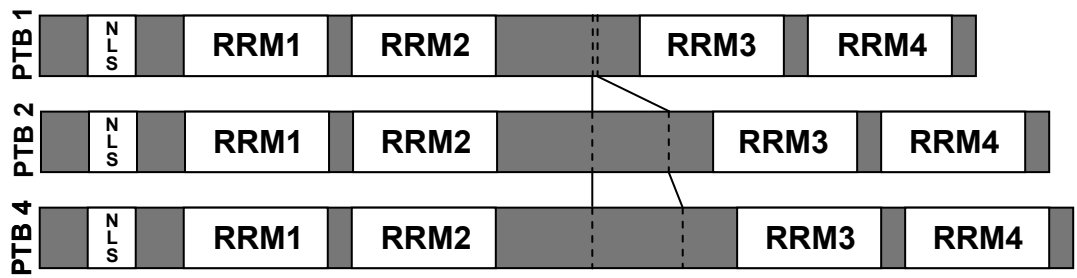


Figure 1.11. Polypyrimidine tract binding protein alternative splicing variants. The main PTB variants PTB1, 2 and 4. The 4 RNA recognition motifs (RRMs) and the nuclear localisation signal (NLS) are depicted (Wagner & Garcia-Blanco, 2001)

PTB protein has been found to interact with the RNA of a variety of positive strand-RNA viruses. The interaction of PTB with the 5' UTR of poliovirus and encephalomyocarditis virus (EMCV) is required for the efficient translation of the RNA (Hellen et al., 1993a). As mentioned before, the attenuation of the poliovirus vaccine strain Sabin type 3 has been attributed to the reduced affinity of the viral IRES to the neuronal variant of PTB (nPTB) (Guest et al., 2004). In foot-and-mouth disease virus (FMDV) PTB protein was found in the translation complexes bound on the IRES, while mutations in the major binding site had a direct effect on translation

efficiency of FMDV RNA. Rabbit reticulocyte lysates depleted of the PTB demonstrated a reduced translation from the FMDV IRES, while addition of recombinant PTB restored the original translation levels (Niepmann et al., 1997). *In vivo* experiments with transient overexpression of the PTB demonstrated increased translation under several picornaviral and flaviviral IRESs (Gosert et al., 2000). In mouse hepatitis virus (MHV), a coronavirus, PTB has been shown to bind to the leader sequence of its RNAs on specific UCUAA repeats. Deletion of these repeats led to impairment of transcription (Li et al., 1999). In the same virus PTB was also found to interact with the 3' UTR altering the secondary structure of the RNA, opening up a double-stranded region that may expose important sequences for the regulation of subgenomic RNA synthesis (Huang & Lai, 1999). In vitro binding assays have shown that PTB is binding the 5' and 3' extremities of Norwalk virus genome (Gutierrez-Escolano et al., 2000, Gutierrez-Escolano et al., 2003). The PTB binding site has been roughly located into the first 110 nucleotides of the Norwalk virus genomic RNA (Gutierrez-Escolano et al., 2000), a region that has been predicted to form a stem-loop structure (Jiang et al., 1993).

1.8.2 Lupus autoantigen (La)

La (Lupus autoantigen) protein has also been shown to interact with the RNA of many positive sense RNA viruses. La, a 52-kDa protein, has been characterised as an autoantigen in patients with systemic lupus erythematosus and Sjogren's syndrome (Buyon, 1989). La is comprised of an RNA binding La motif (present as well in other non-related proteins) an RRM and an NLS at the C-terminus (**Fig. 1.12**). A potential second RRM (maybe residual) has been proposed for the La

protein of vertebrates (Birney et al., 1993) and *Drosophila melanogaster* (Wolin & Cedervall, 2002) (**Fig. 1.12**). La is an abundant protein with mainly nucleoplasmic and nucleolar localisation (Graus et al., 1985). However, as in the case of PTB, La seems to shuttle between the nucleus and cytoplasm under certain circumstances, such as poliovirus (Meerovitch et al., 1993) and dengue virus (Yocupicio-Monroy et al., 2007) infection, apoptosis (Ayukawa et al., 2000), and treatment with metabolic inhibitors (Bachmann et al., 1989) either due to alteration in phosphorylation state, cleavage or modification of the permeability of nucleopores.

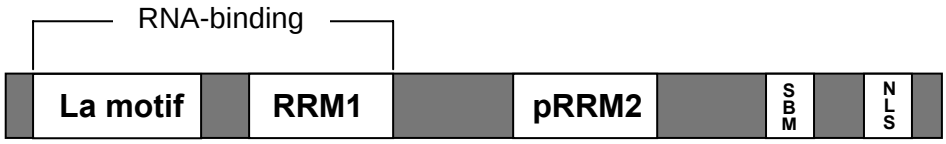


Figure 1.11. The functional domains of La protein. The RNA-binding region encompasses the La motif and the well characterised RNA recognition motif (RRM1). pRRM2 is the predicted second RRM in the La protein of some organisms. The small basic motif (SBM) as well as the nuclear localisation signal (NLS) is depicted (Wolin & Cedervall, 2002).

Extensive study of La has revealed that the physiological role of the protein is to stabilise and protect the 3'ends of small nascent RNA transcripts (Wolin & Cedervall, 2002). This protective role has been shown to be required for t-RNA maturation as binding of La to the 3' end of the pre-t-RNAs inhibits the exonucleolytic 3'→ 5' degradation of the RNA while facilitating an endonucleolytic removal of the 3' extension (Yoo & Wolin, 1997). Furthermore, La protein seems to stabilise a functional t-RNA structure, as certain mutations that inhibit either the maturation or the aminoacylation by disrupting the t-RNA conformation are compensated by La (Wolin & Cedervall, 2002). The spliceosomal U1, U2, U4, U5 RNAs and the small nucleolar RNA U3 RNA are another group of La targets. Binding

of La aids the maturation as it blocks the exonucleolytic degradation when it reaches a poly(U) stretch (Chanfreau et al., 1997, Xue et al., 2000). Other RNA targets that La has been demonstrated to bind are the 5S pre-rRNA, RNase P RNA, rodent $4.5S_I$ and $4.5S_{II}$ RNAs, Y RNAs, the mitochondrial RNA processing (MRP) complex RNA and the Epstein Barr virus (EBV) EBERs (Wolin & Cedervall, 2002).

During poliovirus infection the La protein relocates to the replication sites in the cytoplasm where it aids viral translation by minimising the production of aberrant peptides (Meerovitch et al, 1993; Svitkin et al, 1994). The role of La in IRES-dependent translation has also been demonstrated in the case of Hepatitis C virus (Ali & Siddiqui, 1997, Costa-Mattioli et al., 2004). In caliciviruses La protein has been shown to bind on the 5' and 3' extremities of the NV genomic RNA in the same 110 nts where PTB appears to bind (Gutierrez-Escolano et al., 2000, Gutierrez-Escolano et al., 2003).

In addition to its regulatory role in the organisation and biogenesis of the translation machinery, the La protein regulates directly the translation of several proteins by interacting with their mRNAs. A dominant negative form of La selectively inhibited the translation under the X-linked inhibitor of apoptosis (XIAP) IRES element (Holcik & Korneluk, 2000), while translation of the protein chaperone BiP mRNA was enhanced in the presence of La (Kim et al., 2001). A different mechanism of translation regulation has been observed for the peptidylglycine alpha-amidating monooxygenase (PAM) mRNA. Binding of La to the 3' UTR of the mRNA induced the nuclear retention of the mRNA, while addition of La protein lacking its

own nuclear retention element resulted to the export of the mRNA from the nucleus (Brenet et al., 2005).

1.8.3 Poly(C) binding protein (PCBP)

Another protein that has been extensively studied for its RNA-binding activity is poly(rC) binding protein (PCBP). The best studied PCBPs are those belonging in the group of the α-complex proteins (α-CPs) and are known as α-CP1, α-CP2, α-CP3 and α-CP4 or most commonly known as PCBP1, PCBP2, PCBP3 and PCBP4. In contrast to the three different PTBs, PCBPs are not the result of alternative spliced mRNAs, but they exist in the genome as four different genes. Moreover, a variety of alternative splicing products have been identified for PCBP1 and PCBP4 (Makeyev & Liebhaber, 2002). All four PCBPs are comprised of three hnRNP K-homology (KH) domains (**Fig. 1.13**) that have the ability to bind single stranded RNA individually (Dejgaard & Leffers, 1996). However, a more complicated collaboration of all three KH domains results in the high affinity of hnRNP K for poly(C) (Siomi et al., 1994).

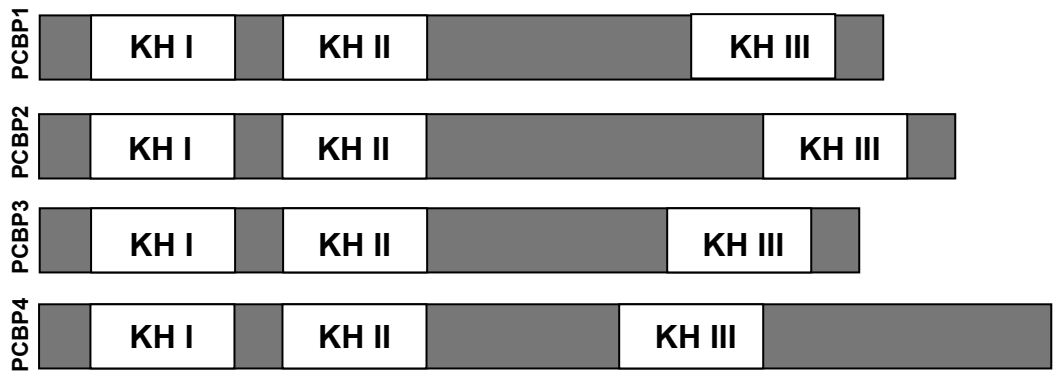


Figure 1.13. Poly(C) binding proteins. The domain layout of the four major PCBPs. The three hnRNP K-homology (KH) domains are depicted (Makeyev & Liebhaber, 2002)

PCBPs are involved in the translation of several mRNAs by regulating their stability. Formation of an RNP complex between PCBP1 or PCBP2 and a pyrimidine rich element at the 3' UTR of α-globin mRNA leads to increased mRNA stability (Chkheidze et al., 1999, Kong et al., 2003), while interruption of the pyrimidine rich element results in reduced mRNA stability (Weiss & Liebhaber, 1995). Similar regulatory roles of PCBPs have been observed for the mRNAs of β-globin (Yu & Russell, 2001) and collagen α1 (I) (Stefanovic et al., 1997) suggesting the involvement of PCBPs in a general mechanism of mRNA stabilisation by interaction with the 3' UTR. Inhibition of mRNA translation is another aspect of PCBPs' function. PCBP1, PCBP2 and hnRNP K interact with a CU-rich element at the 3' UTR of 1,5-lipoxygenase (LOX) mRNA leading to translational silencing (Ostareck et al., 1997). This inhibition is achieved by blockage of the 40S ribosomal subunit accessibility to the 60S subunit at the initiation complex of the 5' end (Ostareck et al., 2001). The involvement of PCBPs in the regulation of picornavirus translation and replication has already been discussed in the section dedicated to IRESs. Another level of regulation that PCBPs are involved in is transcriptional as several PCBPs have been shown to interact with pyrimidine rich single stranded DNA elements. PCBPs have been shown to activate the transcription of human c-myc (Tomonaga & Levens, 1996), the neuronal nicotinic acetylcholine receptor (Du et al., 1998) and μ-opioid receptor gene (Kim et al., 2005)

In caliciviruses, PCBP2 has been found to interact with the 5'extremity of the NV genomic RNA in supershift mobility assays, while the binding seems to take place in the first 110 nt of the 5'extrermity, the same region in which PTB and La have been found to bind (Gutierrez-Escolano et al., 2000). A strong binding of PCBP2

to the 3'UTR of the NV genomic RNA has also been observed, in the region where a predicted stem-loop structure is located (Gutierrez-Escolano et al., 2003).

1.8.4 Other host cell RNA binding proteins

In addition to PTB, La and PCBP there are several other host cell proteins that have been reported to bind on the RNA of positive stand RNA viruses. The upstream of n-Ras protein (Unr) has been shown to bind to the poliovirus and rhinovirus IRES (Boussadia et al., 2003). Glyceraldehyde-3-phosphate dehydrogenase (GAPDH) was been found to interact with the 5' UTR of Hepatitis A virus, hnRNP A1 interacts with the 5' leader of both positive and negative sense RNA in mouse hepatitis virus, Sam68 and EF-1α bind to poliovirus RNA, while the latter has been demonstrated also to interact with the 3' UTR of Dengue 4 virus (reviewed by Lai, 1998). In addition, in NV, the hnRNP L protein has been found to participate in the formation of an RNP complex at the 5' extremity of the genomic RNA (Gutierrez-Escolano et al., 2000). Finally, poly(A) binding protein (PABP) has been shown to interact with the poly(A) tail of positive strand RNA viruses genomes, often participating in the formation of a protein bridge between the 5' and 3' UTRs (Herold & Andino, 2001).

1.9. Aim of the study

The aim of this project was to identify host cell RNA-binding proteins that interact with the extremities of the genomic and subgenomic RNA of caliciviruses, forming the viral ribonucleoprotein complexes (RNPs). As no functional data exists

up to date for any RNA-protein interaction involved in calicivirus life cycle the role of PTB in FCV translation and replication was examined. For this purpose *in vitro* and *in vivo* translation studies were used in conjunction with replication studies in the FCV tissue culture infection system. Furthermore, using the MNV reverse genetics system that became available in the 3rd year of this project, an attempt was made to identify functional cis-acting RNA elements in the MNV genome. Such elements could be possibly involved in the regulation of the translation and replication of MNV. The long term goal for this second part of my study was to identify potential binding sites of host cell and viral RNA-binding proteins on the viral RNA. The characterisation of the RNA-protein interactions that regulate calicivirus replication can shed light on the mechanism of calicivirus replication and may reveal potential targets for the synthesis of drugs or the production of attenuated calicivirus strains that can be used as vaccines against caliciviruses.

Chapter 2.

Materials and Methods

2.1. Antisera

Antiserum to the FCV RdRp (p76) was generated by immunization of New Zealand white rabbits with recombinant p76 previously purified in the lab. Goat antiserum to hnRNP I (PTB) (Cat# sc-16547), used for the western blots, was purchased from Santa Cruse Biotechnology, while mouse monoclonal DH3, DH7 and DH17 antisera to PTB were kindly provided by Eckard Wimmer (Stony Brook University, New York, USA). Antiserum to GAPDH (Cat# AM4300) was purchased from Ambion. Antiserum to FCV Urbana capsid was kindly provided by Stanislav Sosnovtsev (National Institutes of Health, Bethesda, Maryland, USA).

2.2. Viruses and Cell lines

FCV was propagated in Crandel Reese feline kidney (CRFK) cells at 37 ^{o}C 10 % CO_2. CRFK cells were maintained in Dulbecco MEM (DMEM) with 10 % foetal calf serum (FCS) at 37 ^{o}C with 10% CO_2. MNV was propagated in the murine leukaemia macrophage cell line RAW 264.7 cells using DMEM at 37 ^{o}C 10 % CO_2. Baby-hamster kidney cells (BHK-21) expressing T7 DNA polymerase (BSRT7 cells) used during reverse genetics recovery of MNV from the cDNA clones were cultured in DMEM containing 1mg/ml G418 at 37 ^{o}C 10 % CO_2.

2.3. Western blot

For western blot analysis, cells were lysed in radioimmunoprecipitation (RIPA) buffer (50 mM Tris–HCl pH 8.0, 150 mM NaCl, 1 mM EDTA, 1% Triton X-100 and 0.1% SDS). The protein concentration was determined using the BCA protein

assay (Pierce) and equal quantities of protein from each lysate in reducing SDS-PAGE sample buffer were separated by SDS-PAGE. The proteins were transferred to a polyvinylidene fluoride (PVDF) Immobilon-P transfer membrane (Millipore) by semi-dry blotting according to the manufacturer's instructions (Biorad). The membrane was blocked with 5% milk powder in PBST (0.1% Tween 20 / PBS), subjected to the primary antibody for 2 h and subsequently washed 3 times. The secondary, horseradish peroxidase (HRPO) conjugated, antibody was applied for 1 h and the membrane was washed twice in PBST and twice in PBS. For the final visualisation, ECL detection substrate (Amersham-Biosciences) was used according to manufacturer's instructions.

2.4. Northern blot

Total RNA was extracted from cells using the GenElute Total RNA isolation kit (Sigma) following the protocol described by the manufacturer. The concentration of RNA was determined by measuring the absorbance at 260 nm (A260) in a spectrophotometer. RNA was mixed with an equal volume of 2x glyoxal RNA loading buffer (Ambion) and incubated at 55 ^{o}C for 30 minutes. Equal amounts of RNA (10 μg) were separated on a 0.7% agarose gel. Electrophoresis was performed in 0.5xTBE buffer. The RNAs were transferred to a positively charged nylon membrane Hybond N+ (Amersham Biosciences), using capillary transfer under mildly alkaline conditions to partially hydrolyse the RNA as described (Sambrook, 2001). The membrane was pre-hybridised for 1 h with Rapid-Hyb solution (Amersham Biosciences) at 70 ^{o}C and the RNA probe was added in tube. Hybridisation was performed at 70 ^{o}C for 2 h, after which the membrane was washed in 2x SSC (300mM NaCl, 30 mM Na-Citrate pH 7.0), 0.1% SDS at room temperature for 10

minutes, then in 1x SSC (150 mM NaCl, 15 mM Na-Citrate pH 7.0), 0.1 % SDS at 65 ^{o}C for 20 minutes. Exposure of membrane to a phosphor imager screen allowed its visualisation.

2.5. Reverse transcription (RT) and Polymerase chain reaction (PCR)

RT reactions were performed on 5μg of total RNA from infected cells using SuperScript II Reverse transcriptase (Invitrogen) according to the manufacturer. For PCR amplifications, Triple Master Taq polymerase (Eppendorf) or KOD Hot start (Novagen) was used according to the manufacturer's protocol in an Eppendorf thermal cycler. For mutagenic extension PCRs 500 ng of the first PCR product, after purification with GFX PCR DNA and Gel Band Purification Kit (GE Healthcare), was used as the forward primer in a subsequent PCR reaction containing a reverse primer downstream on the template (**Fig. 2.1**). The primers used for amplification of FCV sequences from the FCV full-length cDNA clone, pQ14, are listed in **Table 2.1**. The primers used for the sequencing of MNV and amplifications from the MNV full-length cDNA clone, pT7:MNV 3'Rz and mutant derivatives are listed in **Tables 2.2** and **2.3**.

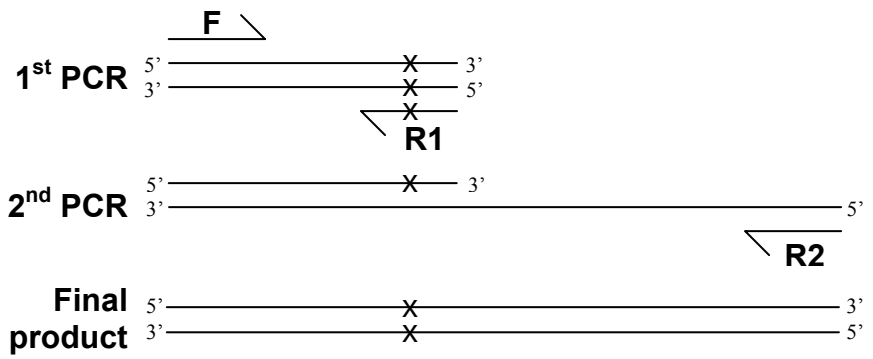


Figure 2.1. Mutagenesis by extension PCR. The extension PCR used a mutagenic 1st PCR amplification by a forward (F) and a mutagenic reverse primer (R1) as forward primer in conjunction with a second reverse primer (R2) further downstream. X is the mutation introduced.

Table 2.1. FCV oligonucleotides

oligo†	oligo sequence 5' → 3'‡	Pol§	Description¶
IGRDG13	TAATACGACTCACTATAGGGGTAAAAGAAATTTGAG	F	5'G_{1-x} PCR
IGRDG157	TAATACGACTCACTATAGGGCTGAGCTTCGTGCTTAAAAC	F	5'G_{32-245} PCR
IGRDG158	TAATACGACTCACTATAGGGTATCTTTATAACAAGCTTTCTCGC	F	5'$G_{118-245}$ PCR
IGRDG159	TAATACGACTCACTATAGGGACAAGCTTTCTCGCCCTATAAG	F	5'$G_{128-245}$ PCR
IGRDG18	GGATCTGTCCTTTGGAAG	R	5'G_{x-245} PCR
IGRDG14	TAATACGACTCACTATAGGGAGTCCTTACGGACACTGTG	R	5'G_{72-245} PCR
IGRDG15	TAATACGACTCACTATAGGGTCGCGCCTCCGTTGAAGCG		5'$G_{111-245}$ PCR
IGRDG16	TAATACGACTCACTATAGGGACAAGCTTCTGCCCTTATAG	R	5'$G_{164-245}$ PCR
IGRDG17	TAATACGACTCACTATAGGGTGTGCAGTTAGGACAAAC	R	5'$G_{202-245}$ PCR
IGIC3	GCTTGTTATAAAGATACTGCAAGTCGCGCCTCCGTTCAAGCG	R	mBS1 Syn PCR
IGIC4	GCTTGTTATAAAGATACTTTTTTTCGCGCCTCCGTTCAAGCG	R	mBS1 F(A) PCR
IGIC48	GGGCGAGAAAGCTTGTTATACAAGTACTGAAGATCGCGCCTCCG	R	mBS2 Syn PCR
IGIC49	GGGCGAGAAAGCTTGTTATTTTTTTACTGAAGATCGCGCCTCCG	R	mBS2 F(A) PCR
IGRDG135	TGTGCAGTTAGGACAAACGTCATAACTGGCACTTTTTTTTCAAG CTTCTGCCCTTATAG	R	mBS3 F(A) PCR
IGRDG137	TGTGCAGTTAGGACAAACGTCATAACTGGCACAACTTGGACAAG CTTCTGCCCTTATAG	R	mBS3 Syn PCR
IGIC67	GGGCGAGAAAGCTTGTTATACAAGTACTGCAAGTCGCGCCTCCG TTGAAGCG	R	mBS1+mBS2 Syn PCR
IGRDG19	TAATACGACTCACTATAGGGGTGTTCGAAGTTTGAGCATG	F	5'SG_{1-285} PCR
IGRDG28	TTGGCCAGAGCTCCATTCCAGTGCATTGGAGGG	R	
IGRDG26	TAATACGACTCACTATAGGGAAGGGTACAAGGCCCCCTCC	F	3' extremity 7493-7683 PCR
IGRDG22	CCCTGGGGTTAGGCGCAAATG	R	
IGRDG54	GCGGGATCCTTATTCTTCAGCAAAGCTAAC	R	p76-coding region specific for RNase H digestion of the genomic RNA
M13/Puc R	ACACAGGAAACAGCTATGACCA	R	M13/Puc pGemT reverse primer

† The primers used on the FCV full length cDNA clone, pQ14, or cDNA from cells infected with FCV
‡ The underlined nucleotides highlight the T7 RNA polymerase promoter sequence
§ Polarity: F and R represent forward and reverse primer respectively.
¶ x = nucleotide between 1 and 245 Syn = synonymous mutations, F(A) = full adenosine substitution

Table 2.2. MNV sequencing oligonucleotides

oligo †	oligo sequence 5' → 3'	Pol§	Position in MNV genome
1F	GTGAAATGAGGATGGCAACGCCATCTTCTGCGCCC	F	1
404F	GGAGCCTGTGATCGGCTCTATCTTGGAGCAGG	F	404
491R	GCCTGGCAGACCGCAGCACTGGGGTTGTTGACC	R	491
922F	GCATTGTCAATGCCCTGATCTTGCTTGCTGAGC	F	922
1139R	GGCGAACTTGCCCATCTCTTGGGCGGCCTTGAGAGCC	R	1139
1540F	GCTTTTGCCAAAACCTAGCCAAGAGGATTGCTG	F	1540
1540R	CAGCAATCCTCTTGGCTAGGTTTTGGCAAAAGC	R	1540
1954F	GGCCCGATTACAGCCACATCAATTTCATCTTGG	F	1954
1954R	CCAAGATGAAATTGATGTGGCTGTAATCGGGCC	R	1954
2392F	GTGTCAGAAGGATAAAGGAGGCCCGCCTCCGCTGC	F	2392
2392R	GCAGCGGAGGCGGGCCTCCTTTATCCTTCTGACAC	R	2392
2616R	GCCCCCGGCCCTTCTTGTTCTTGCCCTTCTTTCC	R	2616
2902F	GCAAGCCGATCGACTGGAATGTGGTTGGCC	F	2902
2902R	GGCCAACCACATTCCAGTCGATCGGCTTGC	R	2902
3394F	CGGGCGACTGTGGCTGTCCCTATGTTTATAAGAAGGGTAAC	F	3394
3394R	GTTACCCTTCTTATAAACATAGGGACAGCCACAGTCGCCCG	R	3394
3734F	GCGAGATCAGCTTAAGCCCTATTCAGAACCACGCG	F	3734
3734R	CGCGTGGTTCTGAATAGGGCTTAAGCTGATCTCGC	R	3734
4450F	GCCCTTGCACCACACAGCTGAATAGTTTGG	F	4450
4450R	CCAAACTATTCAGCTGTGTGGTGCAAGGGC	R	4450
4839R	GCAGGGCCATTAGTTGGGAGGGTCTCTGAGCATGTCC	R	4839
5052F	GTGAATGAGGATGAGTGATGGCGCAGCGCCAAAAGCCAATGGC	F	5052
5332R	GTTCCCAACCCAGCCGGTGTACATGGCTGAGAGGTGGGC	R	5332
5722R	CACGGGCAAGTCGACCATCCGGTAGATGGTTCTCTC	R	5722
6034F	GGTTACCCCGATTTCTCTGGGCAACTGGAGATCGAGGTCC	F	6034
6034R	GGACCTCGATCTCCAGTTGCCCAGAGAAATCGGGGTAACC	R	6034
6427F	GTCTCCTGGTTCGCGTCTAACGCGTTCACCGTGCAGTCC	F	6427
6427R	GGACTGCACGGTGAACGCGTTAGACGCGAACCAGGAGAC	R	6427
6733F	GCAATTCCATCTCAAATGTTCAAAACCTTCAGGCAAAC	F	6733
6733R	GTTTGCCTGAAGGTTTTGAACATTTGAGATGGAATTGC	R	6733
7155F	GTGGACACATCCCCTCTACCGATCTCGGGTGGACGCTTGCC	F	7155
7400R	TTTTTTTTTTTTTTTTTTTTTTTTTTTTTTTAAAATGCATCTAACTACCACA AAG	R	7400

† The primers used on the MNV full length cDNA clone, pT7:MNV 3'Rz and mutant derivatives or cDNA from cells infected with MNV

§ Polarity: F and R represent forward and reverse primer respectively.

Table 2.3. MNV oligonucleotides

oligo†	oligo sequence 5' → 3'‡	Pol§	Description¶
IGIC50	GAGCTCACTAGTTAATACGACTCACTATAGTGAAATGAGGATGGCAACACC CAGTAGTGCGCCCTCTGTGCGCAACA	F	m50 mutagenic primer
IGIC51	GAGCTCACTAGTTAATACGACTCACTATAGTGAAATGAGGATGGCAACGCC ATCTTCTGCGCCTTCGGTACGCAACACAGAGAAACGCA	F	m51 mutagenic primer
IGIC52	GCCGGCGCTAGCTTTTTTTTTTTTTTTTTTTTTTTTTTTTAAAATGCATCTAA CTACCACTTACGCAGTAAGCAGAAATCATTTTCAC	R	m52 mutagenic primer
IGIC53	CAAAGACTGCTGAGCGTTCCTGCGGGGTTTCGGCGTCCATTGTTCCAAAGC GCACCC	R	m53 mutagenic primer
IGIC54	GCCGGCGCTAGCTTTTTTTTTTTTTTTTTTTTTTTTTTTTAAAATGCACGAAA CTGTCATAAAGAAAAGAAAGCAGTAAGC	R	m54 mutagenic primer
IGIC16	TAATACGACTCACTATAGGGGTGAAATGAGGATGGCAACGC	F	5'G_{1-x} PCR
IGIC17	AGCACGCGTGCATCACTACGCG	R	5'G_{x-250} PCR
IGIC143	GCCTTCTTGTTTTTGCGTTTC	R	5'G_{1-73} PCR
IGIC144	TTTCGTCTTCGCTCTCCG	R	5'G_{1-138} PCR
IGIC145	TGAGCTTCCTGCTCAGGAGGG	R	5'G_{1-172} and 5'G_{73-172} PCRs
IGIC146	TAATACGACTCACTATAGGGTTCGTCTAAAGCTAGTGTCTCC	F	5'G_{73-250} and 5'G_{73-172} PCRs
IGIC147	TAATACGACTCACTATAGGGACATGACCCCTCCTGAGCAGG	F	5'$G_{138-250}$ PCR
IGIC148	TAATACGACTCACTATAGGGAGCCCGGCGCCCTTGCGGCCC	F	5'$G_{172-250}$ PCR
IGIC18	TAATACGACTCACTATAGGGGTGAATGAGGATGAGTGATGGC	F	5'SG_{1-200} PCR
IGIC19	CACCAAGGGGGCACTGGAC	R	
IGIC127	TAATACGACTCACTATAGGGACATCCCCTCTACCGATCTCGG	F	3'extremity nts
IGIC128	TTTTTTTTTTTTTTTAAAATGC	R	7161-7382 + $(A)_{15}$
IGIC161	GGAACAATGGACGCCGAAACCCCGCAGGAACGTTCGGCGGTCTTTGTGAAT G	F	m53R mutagenic primer
IGIC162	CATTCACAAAGACCGCCGAACGTTCCTGCGGGGTTTCGGCGTCCATTGTTC C	R	

† The primers used on the MNV full length cDNA clone, pT7:MNV 3'Rz and mutant derivatives
‡ The underlined nucleotides highlight the T7 RNA polymerase promoter sequence
§ Polarity: F and R represent forward and reverse primer respectively.
¶ x = nucleotide between 1 and 250, (A)15 = poly(A) tail of 15 adenines.

2.6. Viral RNA immunoprecipitation

For the immunoprecipitation of viral RNP complexes, 2 x 10^7 CRFK cells were infected for 16 h with FCV (m.o.i of 0.1). The cells were harvested in 2 ml of polysome lysis buffer (100 mM KCl, 5 mM Mg_2Cl, 10 mM HEPES pH 7.0, 0.5 % Nonidet P-40, 1mM DTT, 100 U/ml RNasin RNase inhibitor (Promega), 1x complete EDTA free protease inhibitor (Roche Applied Sience)). Cell lysis was assisted by passing the lysates through a blunt end 23G needle (20x). The lysates were centrifuged at 16,000 g for 15 min in a 4 ^oC centrifuge. The supernatant was

supplemented with polysome lysis buffer up to a final volume of 5 ml was precleared using 200 µl of protein-A agarose beads (50 % slurry) for 2 h at 4 ^{o}C with rotation in a 15 ml tube. In parallel, 10 µl of antibody (400 ng for α-GAPDH) was incubated with 40 µl of protein-A agarose (50 % slurry) equilibrated in polysome lysis buffer for 2 h at 4 ^{o}C. The excess antibody was removed by 4x wash in 1 ml of polysome lysis buffer and 1 ml of precleared lysates was added to the beads. The antibody carrying beads and the precleared lysates were incubated at 4 ^{o}C overnight (~16 h) with rotation. The beads were washed with 1 ml of polysome lysis buffer (4x) and with 1 ml of polysome lysis buffer containing 1 M urea at 4 °C for 5 min for each wash. The beads were resuspended in 100 µl of polysome lysis buffer with 0.1 % SDS and 30 µg proteinase K (Promega). The reaction was incubated at 50 °C for 30 min, the RNA was extracted with phenol–chloroform and precipitated using ethanol with 1 µg of glycogen as a carrier. After precipitation, the pellet was resuspended in 20 µl of ddH_2O and cDNA was synthesised using $d(N)_6$ random primers (Promega). The detection of viral cDNA was performed by PCR amplification of the 5'$G_{1\text{-}245}$ region (**Table 2.1**) of the viral genome and the PCR products were analysed on a 2 % agarose gel.

2.7. T7 transcription

For the preparation of RNA probes for northern blot analysis, T7 transcription reactions contained 40 mM Tris (pH 8.0), 40 mM DTT, 6 mM $MgCl_2$, 2 mM spermidine, 0.5 mM ATP, CTP, GTP, 10 µM UTP, 4 µl αP^{32}UTP (10 µCi/µl, 3000 mCi/mmol) (at a 1:15 proportion hot:cold), 300 ng of PCR product and 0.5 µg/µl T7 polymerase. The reaction was incubated at 37 ^{o}C for 2 h and DNase I treated (2 U) for

15 min at 30 ^{o}C. The riboprobes were purified using a G50 column and the purified probe was mixed with 1 ml of Rapid-Hyb buffer (Amersham Biosciences).

RNA probes for the electrophoretic mobility shift assay (EMSA), competitor RNAs and RNAs for the RNA affinity columns were synthesised by *in vitro* T7 transcription after PCR amplification of the respective regions from pQ14. Radioactive probes were synthesised using Megashortscript T7 (Ambion) with α-^{32}P UTP according to manufacturer's protocol. Transcription reactions contained 40 mM Tris, 32 mM MgOAc, 40 mM DTT, 2 mM spermidine, 7.5 mM NTPs, 0.7 μg/μl T7 RNA polymerase and high concentration of template DNA. The radioactive probes were purified by electrophoresis in a 6% acrylamide, 7M urea gel and overnight diffusion in 0.1% SDS, 10 mM Tris, 1 mM EDTA solution. The RNAs were phenol-chloroform extracted, ethanol precipitated and resuspended in 50 μl of ddH_2O. The concentration of each probe was determined by spectrometry quantification at 260 nm.

The 5'cap-CAT-FMDV IRES-LUC bicistronic RNA was produced using the Megashortscript kit (Ambion) using 210 ng of *Xho*I linearised pGEMCATLUC:FMDV IRES plasmid according to the manufacturer with the addition of 6 mM of Ribo m^{7}G cap analog (Promega).

2.8. RNA affinity columns

0.75 g of activated CNBr-sepharose 4B beads was washed once with 50 mls of 1mM HCl and twice with 10 mls of double distilled water. 250 μl of CnBr-Sepharose (Pharmacia) (bead volume) was added to 750 μl of 0.2 M MES pH 6.0 containing 200

µg of RNA. The reactions were incubated for 2 h at 4 ^{o}C with rotation. The absorption at 260 nm was measured for each column after coupling to ensure that equal amounts of RNA were coupled to the column. The beads were washed with 100 mM Tris pH 8.0 and incubated in 100 mM Tris pH 8.0 for 1 h at 4 ^{o}C to block the non-reacted groups. The beads were washed three times in S10 dilution buffer (50 mM HEPES pH 8.0, 120 mM potassium acetate, 5.5 mM magnesium acetate, 10 mM KCl, 6 mM DTT) prior to use. 100 µl of RNA beads (bed volume) were incubated with 100 µl of HeLa S10 extracts, prepared previously in the lab, for 1 h at 4 ^{o}C. Finally the beads were washed 4 times with S10 dilution buffer and the bound proteins were eluted with 100 µl of reducing SDS PAGE loading buffer. The final elutions were separated by 12.5% acrylamide SDS PAGE and stained using silver stain (Biorad).

2.9. Protein purification

2.9.1 GST-PTB

DH5α *E. coli* cells were transformed with the pGEX6P-1 PTB plasmid, provided by Richard Jackson (University of Cambridge, UK). Cells from a single colony were grown in LB at 37 ^{o}C up to an OD600 of 0.6. Isopropyl-β-D-thiogalactopyranoside (IPTG) was added at a final concentration of 0.1 mM and the protein expression was induced for 2 hours. The cells were lysed using a French press under high pressure (1000 bar) in PBS containing 0.5 mM DTT, 10 mM EDTA, 3 µg/ml leupeptine and pepstatin, 1% Triton X-100, 1 mM PMSF. The clarified lysate was passed through a glutathione-sepharose column and washed with PBS containing

0.5 mM DTT, 10 mM EDTA and 1% Triton X-100. A second wash with 50 mM Tris pH 8.0, 150 mM NaCl and 0.5 mM DTT followed. The protein was then eluted in 10 mM reduced glutathione, 50 mM Tris pH 8.0, 150 mM NaCl and 0.5 mM DTT and dialysed against 50 mM HEPES pH 7.6, 1 mM DTT, 1 mM MgCl2 and 20 % glycerol.

2.9.2 His-PTB, His-PCBP1 and His-PCBP2

SG13009 *E. coli* cells were transformed with the pQE9 PTBI1 plasmid for His-PTB and JM109 *E. coli* cells were transformed with the pQE30:PCBP1 and pQE:PCBP2 plasmid for His-PCBP1 and His-PCBP2 respectively. Cells from a single colony were grown in LB at 37 ^{o}C up to an OD600 of 0.6. Isopropyl-β-D-thiogalactopyranoside (IPTG) was added at a final concentration of 0.1 mM and the protein expression was induced for 2 hours. For His-PTB, the cells were lysed using a French press under high pressure (1000 bar) in PBS containing 0.5 mM DTT, 10 mM EDTA, 3 μg/ml leupeptine and pepstatin, 1% Triton X-100, 1 mM PMSF. For His-PCBP1 and His-PCBP2, the cells were pelleted and resuspended in lysis buffer (50 mM Tris pH 8.0, 20% glycerol, 500 mM NaCl) containing lysozyme (1 mg/ml). The cells were incubated on ice for 30 min and sonicated for complete lysis. The protein purification was performed using Ni-NTA (Qiagen) according to the manufacturer. His-PTB was dialysed against 50 mM HEPES pH 7.6, 1 mM DTT, 1 mM MgCl2 and 20 % glycerol. His-PCBP1 and His-PCBP2 preparations were dialysed against 5 mM Tris pH 7.5, 100 mM KCl, 1 mM DTT, 0.05 mM EDTA and 5 % glycerol.

2.10. Electrophoretic mobility shift assays (EMSAs)

The 7.5 µl EMSA reactions contained 85 nM radioactive probe, GST-PTB at varying concentrations, 0.67 µg/µl yeast t-RNA, 5 mM HEPES pH 7.6, 25 mM KCl, 2.5 mM $MgCl_2$, 1 mM DTT and 4% glycerol. For the competition assays containing 5'G_{1-245} RNA probes, 0.5 µg of GST-PTB or 0.75 µg of La protein was used per reaction. For the competition assays which contained the FCV 5'SG_{1-285} RNA probes, 0.5 µg of GST-PTB was used per reaction. For the competition assays that contained the MNV 5'G_{1-250} RNA probe 1 µg of GST-PTB was used per reaction. For the competition assays that contained the MNV 3'extremity RNA probe (nts 7133-7382) 0.125 µg of GST-PTB was used per reaction. Competitor RNAs were used at 850nM and 8.5 µM, while the non-specific competitor RNAs only at 8.5 µM. All reactions were incubated for 10 min at 30 ^{o}C and for all but three probes the reactions were analysed using a 4 % acrylamide gel (acrylamide:bis-acrylamide 19:1) containing 5 % glycerol. EMSAs containing FCV nts 1-111, 118-245 and 128-245 were analysed on a 5 % acrylamide gel (acrylamide:bis-acrylamide 19:1) containing 5 % glycerol. The EMSA gels were dried and visualised on a phosphor imager screen. Band quantification was performed using the ImageQuant 5.0 software package (Molecular Dynamics).

2.11. VPg-linked viral RNA purification

FCV VPg-linked RNA was extracted from viral replication complexes in infected CRFK cells (Green et al., 2002). Four T175 flasks of CRFK cells were infected for 6 hours with FCV (m.o.i. of 10) at 37 ^{o}C. The cells were harvested and pelleted at 500 g for 5min. The pellets were washed in 10 ml of PBS and the aliquots

combined into a 50 ml Falcon tube. The cells were pelleted at 500g for 5 min and resuspended in ice cold TN buffer (10mM Tris pH 7.8, 10mM NaCl), in which they were incubated for 15 min to swell. Lysis was performed in a dounce homogeniser (60x), the lysate was aliquoted in 1.5 ml tubes and centrifuged at 800g for 5 min 4 ^{o}C to pellet the nuclei and the unlysed cells. The supernatant was subsequently centrifuged at 13,000 rpm on a desk-top centrifuge for 20 min at 4 ^{o}C to pellet the replication complexes. The pellets were resuspended in 120 µl TN buffer containing 15 % glycerol and combined. The RNA from the replication complexes was purified using the GenElute Total RNA isolation kit (Sigma) following the protocol described by the manufacturer.

2.12. *In vitro* translation

For *in vitro* translation assays, FCV RNA purified from replication complexes and *in vitro* synthesised bicistronic 5'cap-CAT-FMDV IRES-Luc RNA were translated using the Flexi rabbit reticulocyte lysates (RRLs) (Promega). Each 12.5 µl translation reaction included 6.25 µl of RRL, 20 µM amino acid mixture minus methionine, 100 mM KCl, 2 mM DTT, 0.5 mM MgOAc, 5µCi ^{35}S methionine (1000 Ci/mmol) (GE Healthcare) and 312.5 ng of preparation containing FCV VPg-linked RNA or bicistronic RNA. Translation reactions occasionally contained 1 µl of His-PTB or buffer at various concentrations, and 5'$G_{1\text{-}245}$ RNA transcripts at various concentrations. The reactions were incubated at 30 ^{o}C for 1.5 h. However, for the assessment of the role of temperature in the inhibition of FCV translation by His-PTB, the reactions were incubated at a range of temperatures. For the translation of the RNase H treated FCV RNA 3.5 µl of the RNase H reaction was added in the translation reactions.

The translation reactions were mixed with equal volume of 2x reducing SDS-PAGE sample buffer and 5 µl of each reaction were separated in a 12.5% acrylamide gel. The gel was fixed using fixation solution (10 % ethanol and 10 % glacial acetic acid in ddH_2O) and dried. The dried gels were visualised on a phosphor imager screen. Band quantification was performed using the ImageQuant 5.0 software package (Molecular Dynamics).

2.13. RNase H treatment of FCV RNA

The specific digestion of the FCV genomic RNA in the viral RNA preparation from infected cells was carried out by using RNase H and the IGRDG54 oligonucleotide that is complementary to p76 coding region or the non-specific M13/Puc R primer. RNase H reactions contained 1.26 µg of VPg-linked RNA preparation, 25 pmol of IGRDG54, 10 U RNAsin (Promega), 37.5 mM KCl, 25 mM Tris-HCl pH 8.3, 1.5 mM $MgCl_2$, 5 mM DTT and 50 U of RNase H (Ambion). The reaction was incubated at 37 ^oC for 20 min.

2.14. Bioinformatics tools

Alignments of MNV and FCV sequences were performed with the ClustalW online software (www.ebi.ac.uk/Tools/clustalw/index.html) using sequences submitted in GenBank (www.ncbi.nlm.nih.gov/Genbank/index.html) or obtained by sequencing of PCR products by the MRC Sequencing Service (Imperial College, UK). The FCV and MNV GenBank strains used in the present study are listed in **Table 2.4**.

Table 2.4. GenBank accession numbers of FCV and MNV strains

Strain	Accession Number	Strain	Accession Number
Urbana	L40021	CR6	EU004676
DD/2006/GE	DQ424892	CR7	EU004677
USDA	AY560118	CR10	EU004678
UTCVM-H1	AY560116	CR11	EU004679
UTCVM-H2	AY560117	CR13	EU004680
UTCVM-NH1	AY560113	CR15	EU004681
UTCVM-NH2	AY560114	CR17	EU004682
UTCVM-NH3	AY560115	CR18	EU004683
FCV2024	AF479590	WU11	EU004663
F4	D31836	WU12	EU004664
F9	M86379	WU20	EU004665
F65	AF109465	WU21	EU004666
CFI/68	U13992	WU22	EU004667
MNV1	DQ285629	WU23	EU004668
MNV2	DQ223041	WU24	EU004669
MNV3	DQ223042	WU25	EU004670
MNV4	DQ223043	WU26	EU004671
CR1	EU004672	MNV1/2002/USA	AY228235
CR3	EU004673	Berlin/04/06	DQ911368
CR4	EU004674	Berlin/05/06	EF531290
CR5	EU004675	Berlin/06/06	EF531291

For the thermodynamic prediction of RNA structures three online software packages were used. Single sequence based thermodynamic predictions were performed using mfold (frontend.bioinfo.rpi.edu/applications/mfold/cgi-bin/RNA-form1.cgi) (Zuker, 2003). Alignment based thermodynamic predictions were performed using pfold (www.daimi.au.dk/~compbio/RNAfold/) (Knudsen & Hein, 2003). Single sequence based thermodynamic predictions for RNA structures that included pseudoknots were performed using Kinefold (http://kinefold.curie.fr/) (Xayaphoummine et al., 2005).

2.14. MNV and FCV reverse genetics

Synonymous mutations in the RNA structures present at the 5' end of the MNV genomic RNA were introduced by PCR amplification using the 5' mutagenic primer IGIC50 to generate m50 and IGIC51 to generate m51, in combination with the 3' primer 1139R. The resultant PCR products were digested with *Spe*I and *Fse*I and cloned into the MNV infectious clone pT7:MNV G3'Rz. Synonymous changes were introduced into the stem loop immediately upstream of the initiation site for subgenomic RNA synthesis at the NS/S junction by PCR amplification of the region using primers IGIC53 and 4450F. The resultant PCR product was digested with *Bip*I and *Nsi*I and cloned into the MNV transfer vector pSL301:MNV *Afe*I-*Sac*II. The mutated region was then transferred to the MNV infectious clone pT7:MNV G 3'Rz by digestion with *Afe*I and *Sac*II to generate the mutated derivative m53. Mutations for the RNA structures present in the 3' UTR of MNV (m52, m54) were generated by PCR amplification of the 3' end of the MNV genome using the 5' mutagenic primer IGIC52 or IGIC54 (for m52 and m54 respectively) in combination with 6427F. The resultant product was digested with *Nhe*I and *Bst*API before insertion into a transfer vector containing the MNV subgenomic RNA (pSL301:MNV SG 3'Rz). The mutated fragment was subsequently transferred to the MNV infectious clone pT7:MNV G 3'Rz using the *Sac*II and *Nhe*I restriction sites. The region that included the mutations in m53RevA was PCR amplified using primers 4450F and 5332R. The resultant PCR product was digested with *Bip*I and *Nsi*I and cloned into the MNV transfer vector pSL301:MNV *Afe*I-*Sac*II. The mutated region was then transferred to the MNV infectious clone pT7:MNV G 3'Rz by digestion with *Afe*I and *Sac*II to generate the mutated derivative m53RevA. Compensatory mutations for the m53 MNV mutant

were introduced by overlap PCR[2]. For m53R mutagenic PCR, the IGIC161 and IGIC162 complementary mutagenic primers were used in combination with primers 3394F and 6034R as distal vector primers (**Fig. 2.2**). The restriction sites used to clone this mutagenised region back into the m53 clone were *Hind*III and *Sac*II. In all cases, the insertion of the correct mutations was subsequently confirmed by sequencing.

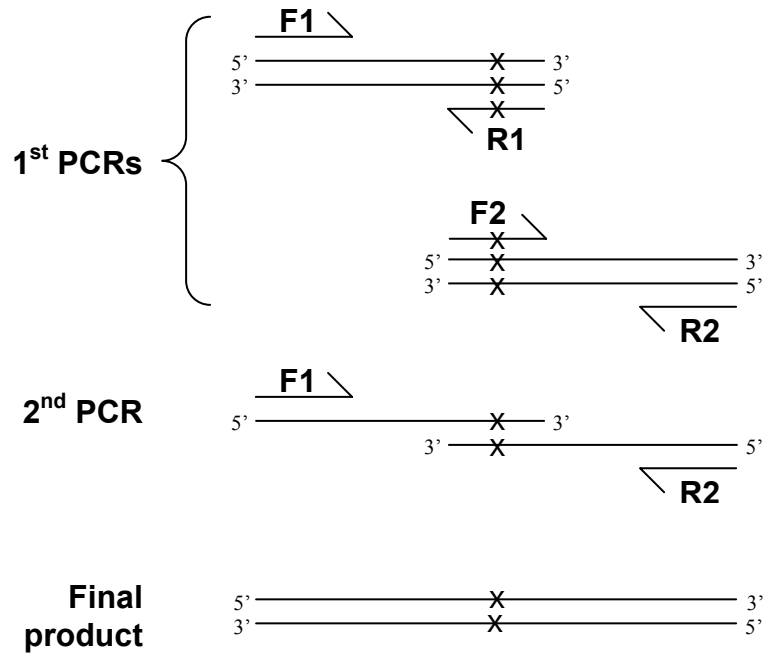


Figure 2.2. Overlapping mutagenesis PCR. A set of initial PCR reactions was carried out using primer pairs F1-R1 and F2-R2. R1 and F2 are the mutagenic primers and are complementry to each other. The resulted PCR products were annealed at the region of the mutagenic primers and were extended. A second PCR was performed using primers F1 and R2 to amplify the mutated product.

BSRT7 cells were plated in 6-well plates at a density of 7.5 x 10^5 cells/well in antibiotic free DMEM with 10 % FCS and incubated overnight at 37 ^oC 5 % CO_2. The cells were incubated for 1 h with a fowlpox virus expressing T7 RNA polymerase at an m.o.i. (based on the virus titre in chick embryo fibroblasts) of 0.5 p.f.u. per cell in 700 μl of antibiotics free DMEM (10 % FCS). Antibiotics free DMEM (10 % FCS)

[2] m53R cloning was performed by Dalan Bailey.

media were subsequently supplemented up to a final volume of 2 ml. 1 μg of each MNV cDNA construct was transfected using Lipofectamine 2000. To analyse protein expression, cells were harvested 24 h post-transfection for Western blot analysis. To examine the presence of infectious norovirus, cells were harvested 24 h post-transfection, virus was released by two freeze–thaw cycles and the titres of virus were determined as TCID50/ml in RAW 264.7 cells, using microscopic visualization for the appearance of cytopathic effect.

FCV, strain Urbana, and FCV mutants were recovered using the FCV full length infectious cDNA clone pQ14 and mutant derivatives (Sosnovtsev & Green, 1995) after transfection of 1 μg of plasmid into CRFK cells infected with a Vaccinia poxvirus expressing T7 RNA polymerase (MVAT7).

2.15. Determination of viral titre (TCID50/ml)

The titre of FCV and MNV was determined by serial dilutions of the virus containing media in a 96 well plate with dilutions spanning from 10^{-1} to 10^{-8}. The fraction (%) of the infected wells in a number of repeats for each dilution was determined by the cytopathic effect of the virus on the cells. The viral titre was calculated using the following formulas:

$$y = 1 - \left(\sum_{i=1}^{8} xi \times 100^{-1} + 0.5 \right) \times 20$$

xi = % infected wells per dilution, i = dilution as 10^{-i}

$$TCID50/ml = 10^{y}$$

2.16. MNV plaque assays

Plaque morphology of the recovered MNVs was examined by plaque assay (Wobus et al., 2004). RAW 264.7 cells, maintained in media (MEM with 10% low-endo FCS, 10mM HEPES pH7.6, 1% Penicillin/Streptomycin, 1% Glutamate), were seeded into 6 well plates (3.5 cm diameter) at a density of 3 x 10^6 cells per well and left overnight to reach a 80-90 % confluency. 1.5 ml 10-fold dilutions in complete DMEM media of virus inoculum were applied to the cell monolayer for 1 h at room temperature. The inoculum was aspirated and 1.5 ml 3 % low melting point SeaPlaque agarose (42 ^oC) (Lonza, Switzerland) mixed with 1.5ml 2x overlay MEM (37 ^oC) (Invitrogen) was added over the monolayer. After the agarose was solidified at room temperature the plates were incubated upside-down at 37 ^oC. Three days later methylene blue solution (1:1:1 of 1 % ethylene blue in ethanol: 1x PBS: Formalin [35-40 % formaldehyde in solution]) was applied to the agarose and the cells were stained for 3-4 h. The agarose plug was removed, the stained monolayer was washed in water and the plate was dried.

2.17. DNA and RNA and siRNA transfection

Cells were transfected with 1 μg of plasmid or RNA using 4 μl of Lipofectamine 2000 (Invitrogen) according to the manufacturer. For siRNA transfection, CRFK cells were plated at 4 x 10^5 cells per well in a 6-well dish. After 2 h, the cells were transfected with 220 pmol/well of PTB P1 siRNAs (Domitrovich et al., 2005) using 4 μl of Lipofectamine 2000 following manufacturers protocol. After overnight incubation at 37 ^oC 5% CO_2, the cells were split using trypsin into two

wells of a 6-well dish. A second transfection with 55 pmol/well of siRNAs followed and the cells were incubated overnight at 37 ^{o}C 5% CO_2. The media was replaced and the cells were grown for a further 3 days. To control for non-specific effect of siRNAs cells were treated following the same procedure with siRNAs against GFP.

2.18. Plasmid preparation

DH5α cells were incubated on ice with 1μg of plasmid or 2 of ligation for 30 minutes. The cells were heat shocked at 42 ^{o}C for 30 seconds and incubated for 1 h in SOC media (Invitrogen). The plasmid DNA was extracted from 1 ml of bacterial culture using alkaline lysis, phenol chloroform extraction and ethanol precipitation (Sambrook, 2001) Plasmid DNA from 100 ml cultures was extracted using Wizard Plus Midipreps DNA Purification System (Promega) according to the manufacturer.

2.19. Luciferase assay

The luciferase assay in cell lysates was performed using 100 μl of luciferase reagent (Promega) onto 5 μg of total protein from each cell lysate and the luciferase activity was measured in a luminometer.

2.20. Confocal microscopy

CRFK cells were plated on round glass cover slips and infected with FCV (m.o.i of 0.5) for 9 h at 37 ^{o}C or for 16 h at 32 ^{o}C. The glass cover slips were washed with chilled PBS and fixed in 4 % paraformaldehyde solution containing 250 mM

HEPES pH 7.4 for 10 min on ice. An 8 % paraformaldehyde solution containing 250 mM HEPES pH 7.4 was applied for 20 min at room temperature and the cells were subsequently washed 3x with PBS. 50 mM ammonium chloride was applied for 10 min at room temperature and the cells were washed 3x with PBS. Permeabilisation of the cells was performed using 0.2 % Triton-X 100 in PBS for 10 min at room temperature and block buffer (1 % bovine serum albumin in PBS) was applied for 5 min (3x).

Staining of cells for p76 and PTB was performed using a rabbit polyclonal antibody for p76 and a mouse monoclonal antibody for PTB (DH17). Image-iT FX signal enhancer was used according to the manufacturer (Invitrogen). The antibodies were diluted 1:200 in block buffer and applied on cells for 1 h. The excess antibody wash removed by 3x wash with block buffer for 5 min and the secondary antibodies were applied at an 1:500 dilution for 1h. Alexa Fluor 488 α-rabbit (Cat# A11030) (Invitrogen) was used as a secondary antibody for p76 and Alexa Fluor 546 α-mouse (Cat# A31628) was used as a secondary antibody for PTB. The cells were washed 3x with PBS for 5 min and instantly in ddH_2O. The glass cover slips were mounted on a glass slide with 40 µl of Mowiol 4-88 (Calbiochem) containing 1 µg/ml of 4',6-diamidino-2-phenylindole (DAPI). The cells were viewed with a Zeiss LSM 510 Meta confocal microscope, and the images were processed with Zeiss Meta 510 software (Carl Zeiss). For the quantification of staining intensity in specific areas of the confocal images Image Quant 5.0 software (Molecular Dynamics) was used as described previously (Henics & Zimmer, 2006).

Chapter 3.

Analysis of the role of PTB in the calicivirus life cycle

3.1. Introduction

A large number of cellular proteins have been identified which interact with the 5' and 3' ends of cellular mRNAs (Erlitzki et al., 2002, Thomson et al., 2005) as well as the 5' and 3' ends of many viral RNAs (Gamarnik & Andino, 2000, Guest et al., 2004, Lu et al., 2004). As detailed in **Chapter 1**, these interactions often play a central role in genome translation and replication for many positive strand RNA viruses. A variety of techniques have been developed for the identification of host cell factors that interact with specific RNA structures, for example electrophoretic mobility shift assays (EMSAs) and functional analysis using fractions of cell extracts prepared by traditional chromatographic fractionation procedures, have previously been used to demonstrate the importance of PTB and unr for rhinovirus IRES activity (Borman et al., 1993, Hunt et al., 1999). In contrast, components of human telomerase were identified using a yeast three hybrid system in which the RNA component of the enzyme was used to screen a library of cellular proteins (Le et al., 2000). Northwestern analysis of EMSA complexes formed between iron response elements (IREs) and cellular extracts has been used to identify a wider variety of IRE regulatory proteins (IRPs) (Popovic & Templeton, 2005). More sophisticated methods which combine RNA affinity chromatography and mass spectrometry, have also been used for the identification of proteins which interact with the poliovirus (Blyn et al., 1996) and HCV IRESs (Lu et al., 2004). The aim of the work presented in this chapter was to characterise the interaction between PTB and the calicivirus RNA and assess the role of the protein in the calicivirus life cycle. Although FCV and MNV data is presented side by side, MNV was only available during the latter part the project, hence, the studies on MNV were less developed.

3.2. PTB interacts with the 5' extremities of the calicivirus genomic and subgenomic RNAs *in vitro*.

RNA affinity columns were generated in order to identify proteins which interact with the 5' extremities of calicivirus genomic and subgenomic RNAs. These regions of the viral genomes were chosen as bioinformatics analysis indicated that they are predicted to contain a high degree of RNA structure (data not shown). In addition, RNA structures required for the translation and replication of positive strand RNA viruses are generally located at the extremities of the viral genome. RNA affinity columns were generated by coupling *in vitro* transcribed RNAs corresponding to the 5' extremities of the FCV or MNV[3] genomic and subgenomic RNAs to cyanogen bromide activated sepharose. The RNAs used in this study represented the first 245 nts of the FCV genomic RNA (5'$G_{1\text{-}245}$), the first 285 nts of the FCV subgenomic RNA (5'$SG_{1\text{-}285}$), the first 250 nts of the MNV genomic RNA (5'$G_{1\text{-}250}$) and the first 200 nts of the MNV subgenomic RNA (5'$SG_{1\text{-}200}$). Cytoplasmic extracts from HeLa cells, which are permissive to calicivirus replication, were applied to the RNA affinity columns. After extensive washing, proteins retained on the columns were analysed by SDS-PAGE. Silver staining revealed the proteins that were selectively retained by the RNA on the column (**Fig. 3.1a**). Western blot analysis using specific antisera was used as an initial approach to identify proteins which bound the calicivirus RNAs. A small number of proteins are regularly found in RNPs formed on the 5' extremity of positive stranded RNA viral genomes, often playing crucial roles in translation or replication. As highlighted in chapter 1, one such protein is PTB, which has been found to interact not only with genomes of HCV,

[3] MNV columns were made by Yasmin Chaudhry

coronaviruses and picornaviruses, but has also been reported to interact with the Norwalk virus genome, the prototype human calicivirus. PTB consensus binding sequences (Y_x-UCUU-Y_z)[4] were identified in the FCV genomic and subgenomic RNA 5' extremities. The thermodynamic predictions of the FCV 5'G_{1-245} and the MNV 5'G_{1-250} RNA secondary structures are presented in **Figures 3.1c** and **3.2** respectively, with the potential PTB binding sequences highlighted. To determine if PTB was specifically retained by the calicivirus RNA sequences coupled to the affinity columns, elutions were analysed by Western blot for the presence of PTB (**Fig. 3.1b**). PTB was selectively retained by both the 5' genomic and 5' subgenomic extremities of FCV and MNV. The levels of PTB retained on the column containing non-specific control RNA (*E. coli* 5S ribosomal RNA) were similar to the background levels of protein retained by the beads alone, indicating that the retention of PTB was specific for the calicivirus RNA sequences.

A drawback of using RNA affinity columns is that they do not always demonstrate a direct binding of the identified proteins to the RNA target as proteins may be retained indirectly via interactions with other proteins which interact directly with the target. In order to address the direct nature of the interaction, recombinant GST-tagged PTB was used in EMSAs in which the selected viral RNA transcripts were used as radiolabeled probes (**Fig. 3.3** and **3.4**). In order to limit non-specific RNA-protein interactions, the reactions contained a 280 fold excess of non-specific yeast t-RNA. Increasing concentrations of PTB were incubated in EMSA reactions

[4] Y=pyrimidine x,z=random numbers

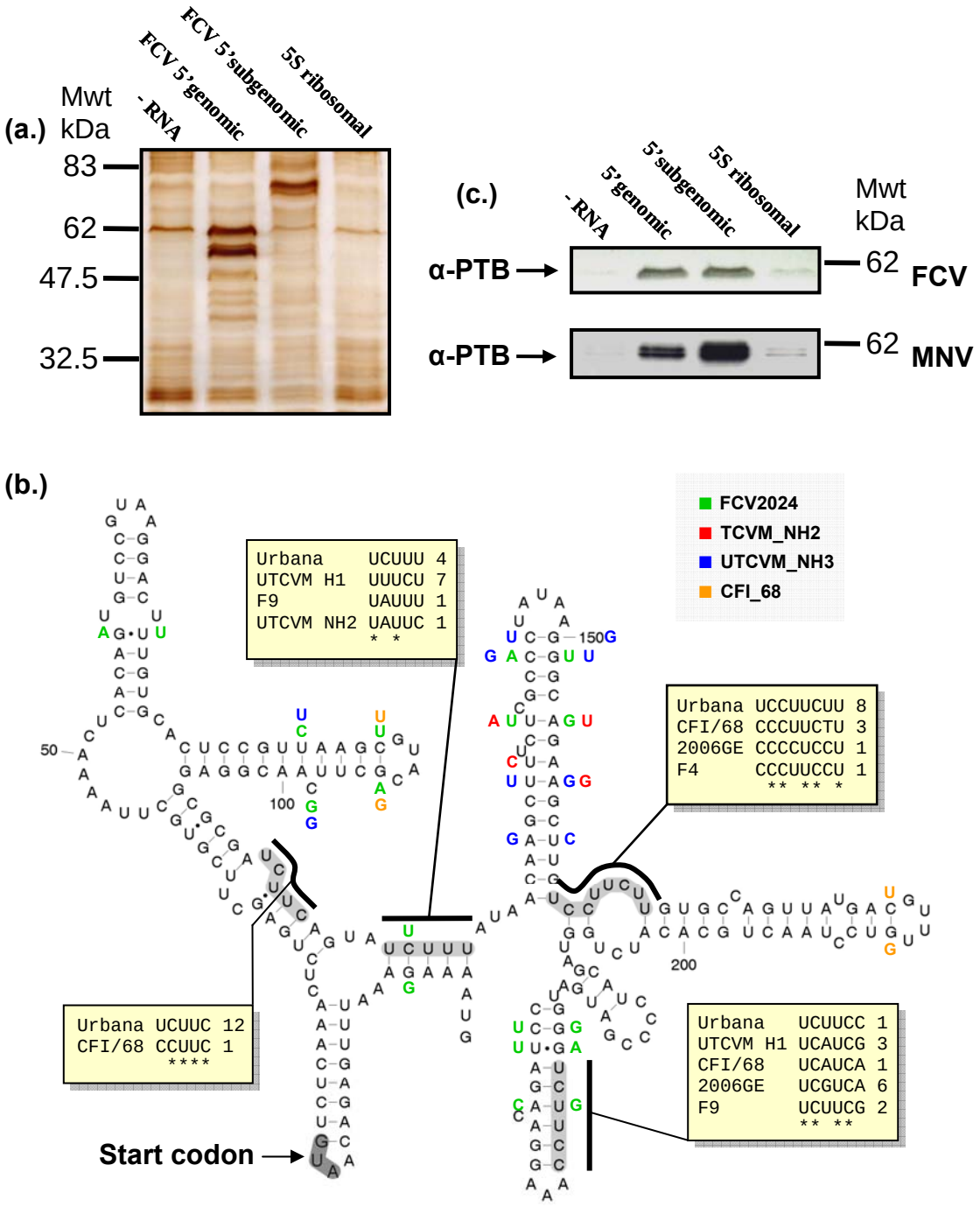


Figure 3.1. Riboproteomic and bioinformatic analysis of PTB binding on FCV and MNV RNA. (**a.**) Proteins retained by the RNA affinity columns containing the 5' genomic and 5' subgenomic RNAs analysed on a 12.5% polyacrylamide gel. The 5S ribosomal RNA and sepharose beads without RNA (-) were used as controls (**b.**) The thermodynamically predicted secondary structure of FCV 5'$G_{1\text{-}245}$. The coloured bases show the sites of co-variation in some of the FCV strains that verify evolutionally the conservation of the secondary structure. The polypyrimidine stretches conserved among the different FCV strains are highlighted with a black line. Alignments of all the different strains of FCV for the polypyrimidine stretches are presented in the boxes and the numbers next to sequences show the number of strains in which a specific altered sequence is found (**c.**) Western blot for PTB of the proteins isolated on RNA affinity columns containing the FCV and MNV 5'G and 5'SG RNAs. Columns containing the 5S ribosomal RNA or without RNA (-) were used as controls.

containing the FCV 5'G_{1-245} and 5'SG_{1-285} RNA probes and the amount of protein required to retard the mobility of approximately 40 – 50 % of the probe was determined (**Fig. 3.3a**). The optimum amount of PTB (0.5 μg) was subsequently used in competition EMSAs in order to address the specificity of the interaction. The formation of the PTB:5'G_{1-245}-RNA complex was inhibited by the addition of unlabelled 5'G_{1-245} and 5'SG_{1-285} RNA transcripts (**Fig. 3.3b**). The same procedure was repeated using the FCV 5'SG_{1-285} RNA as radiolabeled probe (**Fig. 3.2c**) demonstrating the specific interaction of PTB with these important regions of the FCV genome. In both cases an RNA transcript representing the poliovirus 2C *cis*-acting replication element (2C *Cre*) was used as a non-specific competitor RNA and did not inhibit complex formation. The band that was observed to have the same mobility as the complex, but which formed in the absence of recombinant protein

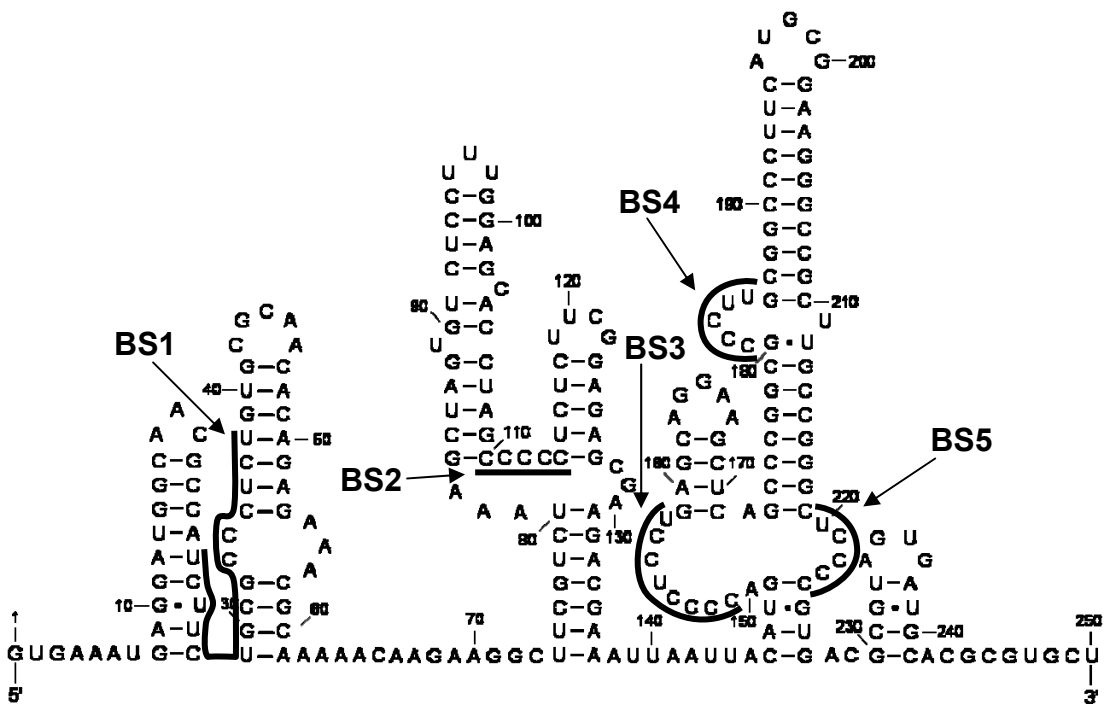


Figure 3.2. Bioinformatics analysis of the 5' end of the MNV genomic RNA. The thermodynamically predicted secondary structure of MNV 5'G_{1-250}. The polypyrimidine stretches conserved among the different MNV strains are highlighted with a black line (BS1-5).

(highlighted by an asterisk in the PA lane in **Figure 3.3b)**, was likely to represent either an alternative fold of the RNA probe or a probe duplex. This complex was removed in most of the subsequent EMSAs by denaturing and reannealing the RNA probe prior to use.

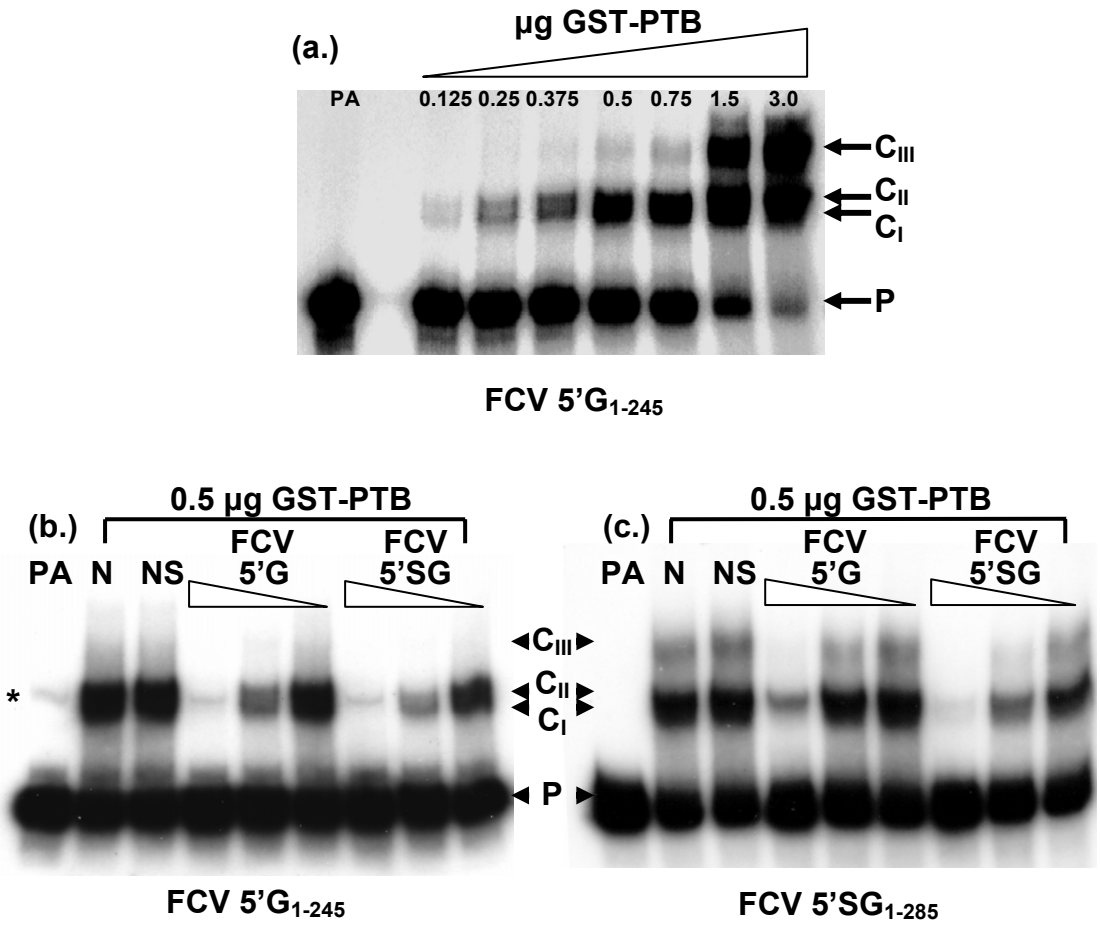


Figure 3.3. PTB binds specifically to the FCV 5' genomic and 5' subgenomic RNA extremities (**a.**) EMSA analysis examining the ability of PTB to interact with the 5' extremity of the FCV genome (5'$G_{1\text{-}245}$). RNA probes encompassing nts 1-245 of the FCV genome were incubated with increasing concentrations of protein and the reactions separated on an 4 % native acrylamide gel. (**b.**, **c.**) EMSAs demonstrating successful inhibition of complex formation, between recombinant PTB and labelled FCV 5' genomic (5'$G_{1\text{-}245}$, b.) and 5' subgenomic (5'$SG_{1\text{-}250}$, c.) RNA probe upon addition of non-labelled 5' genomic (5'G) and 5' subgenomic RNA (5'SG). (PA = probe alone, N = no competitor RNA, NS = non specific RNA, C_I = complex I, C_{II} = complex II C_{III} = complex III and P= probe *=alternative structure of the RNA probe or probe dimer)

Similar EMSAs were performed for the MNV 5'genomic and 5' subgenomic extremities (**Fig. 3.4a,b**). In agreement with my previous data using RNA affinity columns, PTB bound less well to the MNV 5'genomic extremity than on the MNV 5' subgenomic end in the EMSA experiments. The specificity of the interaction was also demonstrated using competition assays (**Fig. 3.4c**).

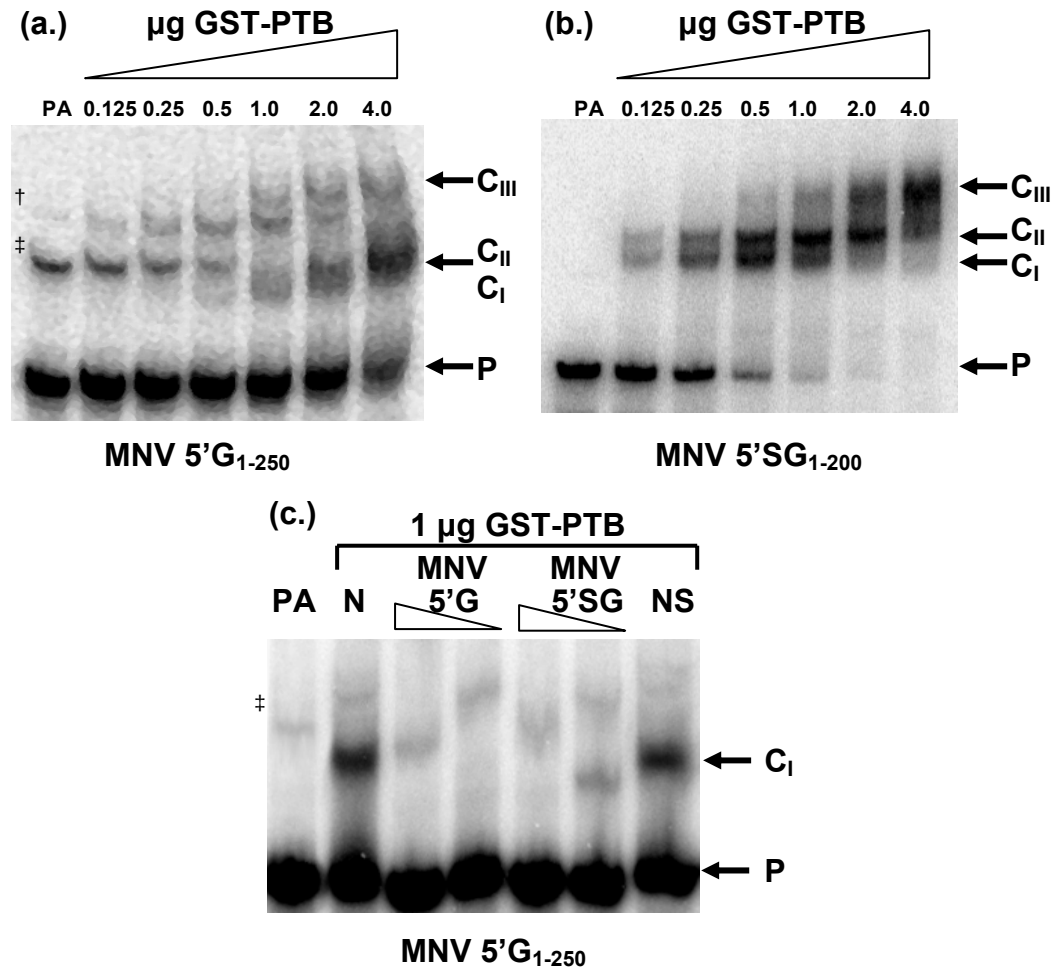


Figure 3.4. PTB binds specifically to the MNV 5' genomic and 5' subgenomic RNA extremities (**a., b.**) EMSA analysis examining the ability of PTB to interact with the 5' extremity of the MNV genome (5'G_{1-250}). RNA probes encompassing nts 1-250 of the MNV genomic RNA and nts 1-200 of MNV subgenomic RNA were incubated with increasing concentrations of protein and the reactions separated on an 4 % native acrylamide gel. (**c.**) EMSAs demonstrating successful inhibition of complex formation, between recombinant PTB and labelled 5' G_{1-250} RNA probe, by non-labelled MNV 5'G_{1-250} (5'G) and 5'SG_{1-200} RNA (5'SG). (PA = probe alone, N = no competitor RNA, NS = non specific RNA, C_I = complex I, C_{II} = complex II C_{III} = complex III and P= probe, † and ‡ are alternative RNA conformations or probe multimers)

3.3. PTB interacts with the FCV RNA in infected cells.

Although the *in vitro* data demonstrated PTB binding to the FCV and MNV genomes, it was important to demonstrate that this interaction also occurred during infection. To address this question, immunoprecipitation combined with RT-PCR (IP-RT-PCR) was used to determine if PTB was associated with the viral genome during replication. Antibodies to PTB were first assayed for their ability to efficiently immunoprecipitate PTB from cell extracts (**Fig. 3.5a**). Two monoclonal antibodies (DH7 and DH17) to PTB were able to immunoprecipitate PTB efficiently from cell extracts (**Fig. 3.5a**) and were also able co-precipitate the FCV RNA from infected cells (**Fig. 3.5b**). One monoclonal (α-PTB DH3) and two polyclonal antibodies (mouse α-PTB St Cruz and guinea pig α-PTB) to PTB were either unable or not

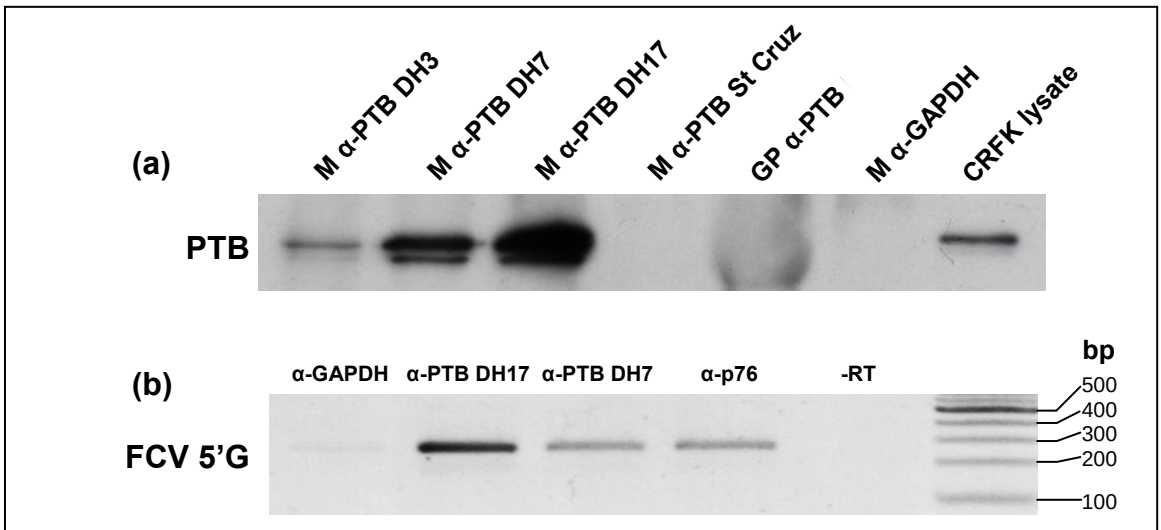


Figure 3.5. PTB interacts with the viral RNA *in vivo*. (**a.**) Western blot for PTB showing the ability of a variety of antibodies to immunoprecipitate PTB. (**b.**) RT-PCR for the 5'$G_{1\text{-}245}$ of the vRNA pulled down during the immunoprecipitation of PTB and p76 (protease-polymerase) from infected feline kidney cell cytoplasmic lysates. RT-PCR of the RNA extracted from the immunoprecipitation of GAPDH from infected cytoplasmic lysates and the α-PTB DH17 RNA (-RT) were used as controls. (bp = base pairs)

efficient enough in PTB immunoprecipitation and thus they were not used for RNA immunoprecipitation (**Fig. 3.5a**). The viral RNA was detected by RT-PCR using primers which amplified the 5'G_{1-245} region of the FCV genomic RNA (**Fig. 3.5b**). Antisera to the viral RdRp, p76, was used as a positive control in the assay as it is in direct contact with the viral RNA during genome replication, while an α-GAPDH antibody was used as negative control in both PTB and FCV RNA immunoprecipitation (**Fig. 3.5a,b**).

3.4. FCV replication is not affected by overexpression of PTB

To begin to elucidate a role for the interaction of PTB with the viral RNA, PTB1 was overexpressed in CRFK cells and the effect on virus replication monitored (**Fig. 3.6a**). The hypothesis was that if PTB regulated calicivirus life cycle its overexpression could stimulate or repress viral replication. Transient expression of PTB1 in CRFK cells resulted in a 90% increase of PTB1 levels. To assess the effect of PTB overexpression on calicivirus replication, CRFK cells overexpressing PTB1 and control cells were infected with FCV at a multiplicity of infection (m.o.i.) of 4. The one step growth curve of FCV showed that the viral titre was unaffected by the increased PTB levels (**Fig. 3.6b**). The lack of effect of PTB overexpression on viral replication was further confirmed by northern blot detection of the genomic and subgenomic RNA levels, as well as the detection of the viral polymerase, p76 by western blot (**Fig. 3.6c**).

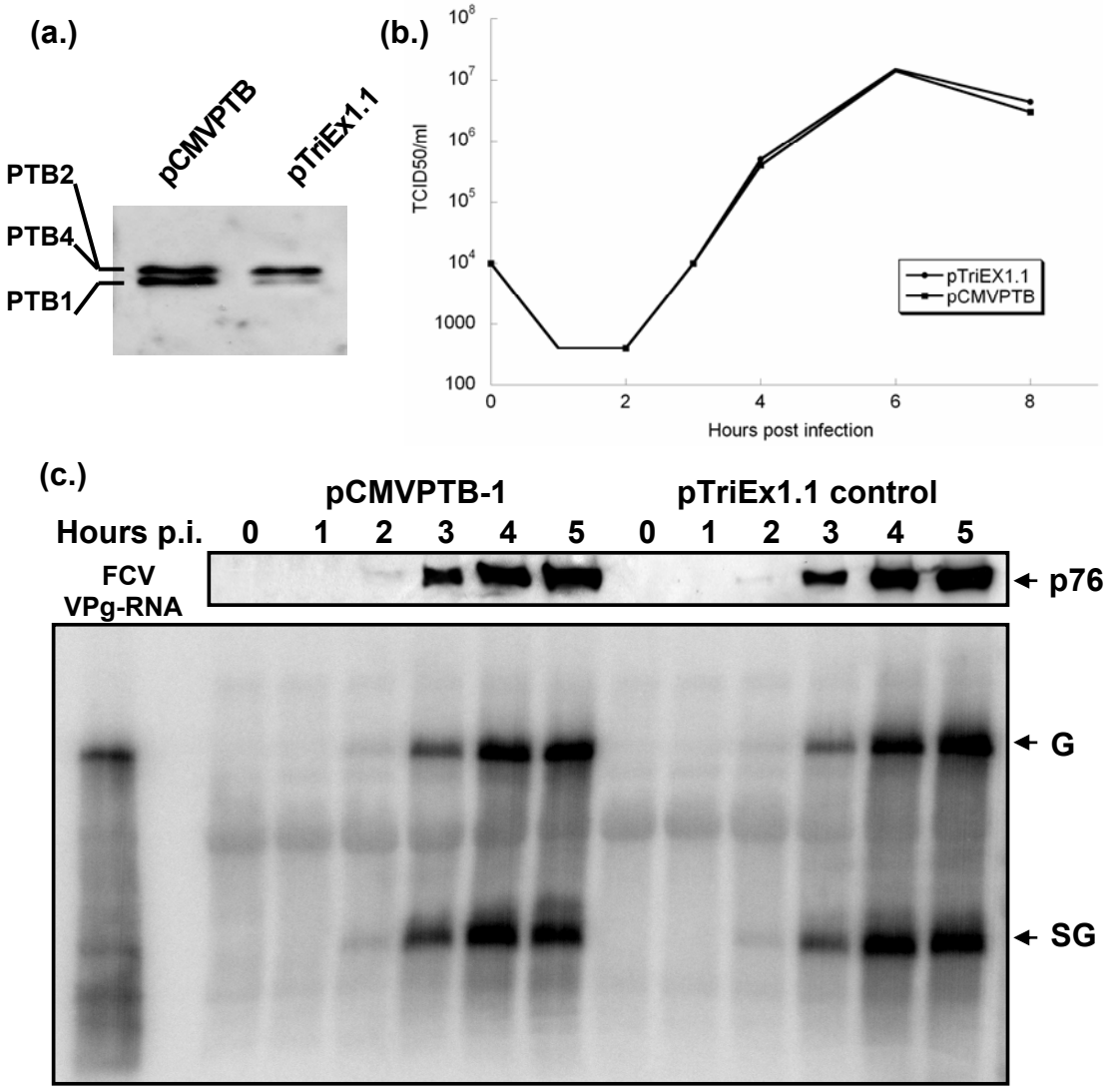


Figure 3.6. Calicivirus replication is not affected by overexpression of PTB1
(**a.**) Western blot for PTB demonstrating increased levels of PTB1 after transient expression in CRFK cells. (**b.**) One step growth curve of FCV (m.o.i. of 4) in cells overexpressing PTB and control cells. (**c.**) Western blot analysis of the expression of the viral polymerase, p76, in cells overexpressing PTB and control cells at various time points post infection (p.i.) and northern blot detection of genomic (G) and subgenomic (SG) RNAs at the same time points.

3.5. RNAi-mediated knockdown of PTB

An approach that has been increasingly used for the study of the role of proteins in cells is RNAi mediated knockdown of protein expression. When siRNAs, small RNA sequences specific for the target mRNA, are transfected into cells, they

activate the RNA induced silencing system of the cell, leading to specific degradation of the target mRNA (Elbashir et al., 2001). siRNA mediated knockdown of PTB has been shown to effectively impede HCV replication (Domitrovich et al., 2005) and poliovirus translation (Florez et al., 2005). PTB siRNAs (Domitrovich et al., 2005) were used to reduce PTB expression in CRFK cells. Western blot analysis demonstrated that the levels of PTB were decreased by 80% (**Fig. 3.7a**). Since the knockdown was not complete, very common in RNAi experiments, the effect of the PTB reduction on translation of the PTB dependent IRES of poliovirus (Toyoda et al., 1994) was examined (**Fig. 3.7b**). An RNA construct expressing luciferase under the control of the poliovirus IRES was transfected into CRFK cells which had been previously transfected with the PTB specific siRNAs. The luciferase signal from the cells underexpressing PTB was reduced by 99.5 % compared to the cells transfected with the control green fluorescence protein (GFP) specific siRNAs (**Fig. 3.7b**). The almost complete inhibition of the poliovirus IRES function demonstrated that the levels of PTB knockdown were sufficient to demonstrate a role of PTB in cells.

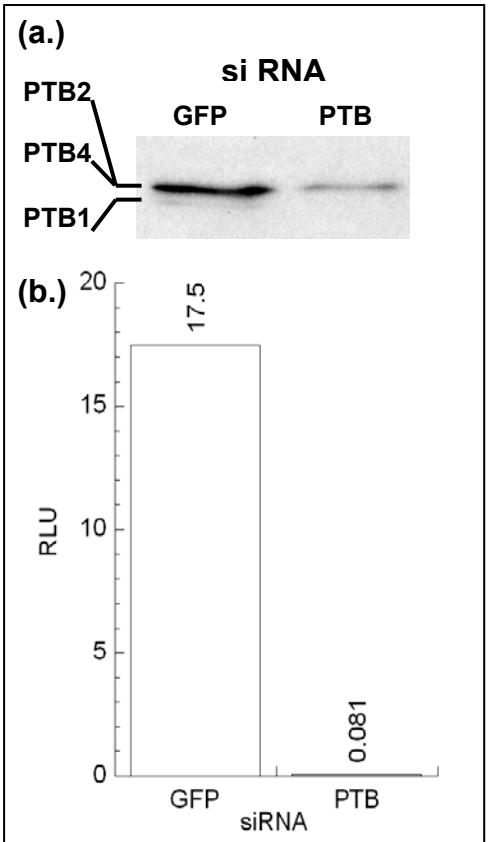


Figure 3.7. RNAi-mediated PTB knockdown has a dramatic effect on poliovirus translation (**a.**) Western blot analysis of PTB demonstrating decreased levels of all PTB isoforms after transfection of CRFK cells with PTB and GFP (control) specific siRNAs. (**b.**) Luciferase production driven by the poliovirus IRES in CRFK cells treated with PTB and GFP specific siRNAs.

3.6. FCV replication is affected by RNAi-mediated knockdown of PTB in a temperature dependent manner

As the levels of PTB knockdown were sufficient to inhibit poliovirus translation, the ability of FCV to grow under reduced PTB levels was investigated. CRFK cells transfected with either PTB or control GFP siRNAs, were infected with FCV at an m.o.i of 4 and the growth kinetics of the virus was examined (**Fig. 3.8a**). The growth curve demonstrated only a small decrease in virus production of not more than 40 % at 6 hours post infection (p.i.), while the titre at 3 and 9 hours post infection was essentially unaffected (**Fig. 3.8a**). Western blot analysis demonstrated that PTB knockdown had a limited effect on the production of the viral polymerase, p76. Band quantification using a densitometry scanner demonstrated a reduction of p76 expression of approximately 30 % at 3 h p.i., 35 % at 6 h p.i., and 25 % at 9 h p.i. (**Fig. 3.8b**). Such a limited effect on the viral protein expression may explain the insignificant effect of PTB knockdown on the overall virus yield.

A major parameter affecting RNA conformation and consequently its interactions with RNA binding proteins is temperature (Moulton et al., 2000). At lower temperatures unfavourable base pairing can be stabilised, while at higher temperatures base paring essential for the functionality may be disrupted. CRFK cells transfected with PTB and control (GFP) siRNAs were infected in suspension and subsequently incubated on a PCR block in order to achieve an accurate (±0.1 ^{o}C) and constant temperature. Infection of cells at a range of temperatures (32-39 ^{o}C) with FCV (m.o.i. of 4), showed a differential effect of PTB knockdown on viral polymerase (p76) production 6 hours p.i. (**Fig. 3.9**). The effect was more apparent at

extreme temperatures (32 and 39 ^{o}C) where the viral polymerase levels (p76) were approximately 20 % of the levels observed in the control cells at the same temperature. In contrast, at 37 ^{o}C the levels of p76 were 65 % of the control (**Fig. 3.9**), verifying the limited effect discussed in the previous paragraph.

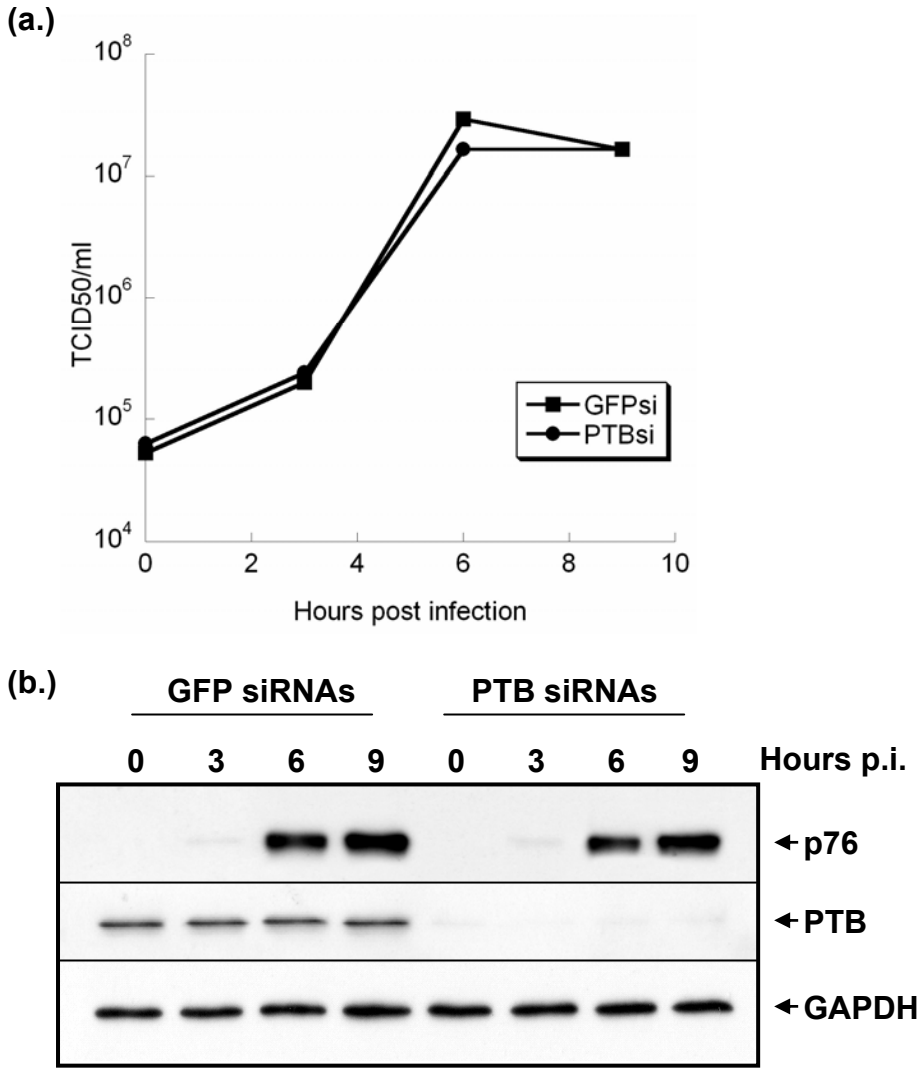


Figure 3.8. Limited effect of RNAi-mediated knockdown of PTB on FCV replication at 37 ºC (**a.**) One step growth curve of FCV (m.o.i of 4) in cells treated with PTB and control GFP specific siRNAs. (**b.**) Western blot for viral polymerase (p76), PTB and GAPDH (control) during the FCV infection in the PTB and GFP siRNA treated cells. (p.i. = post infection)

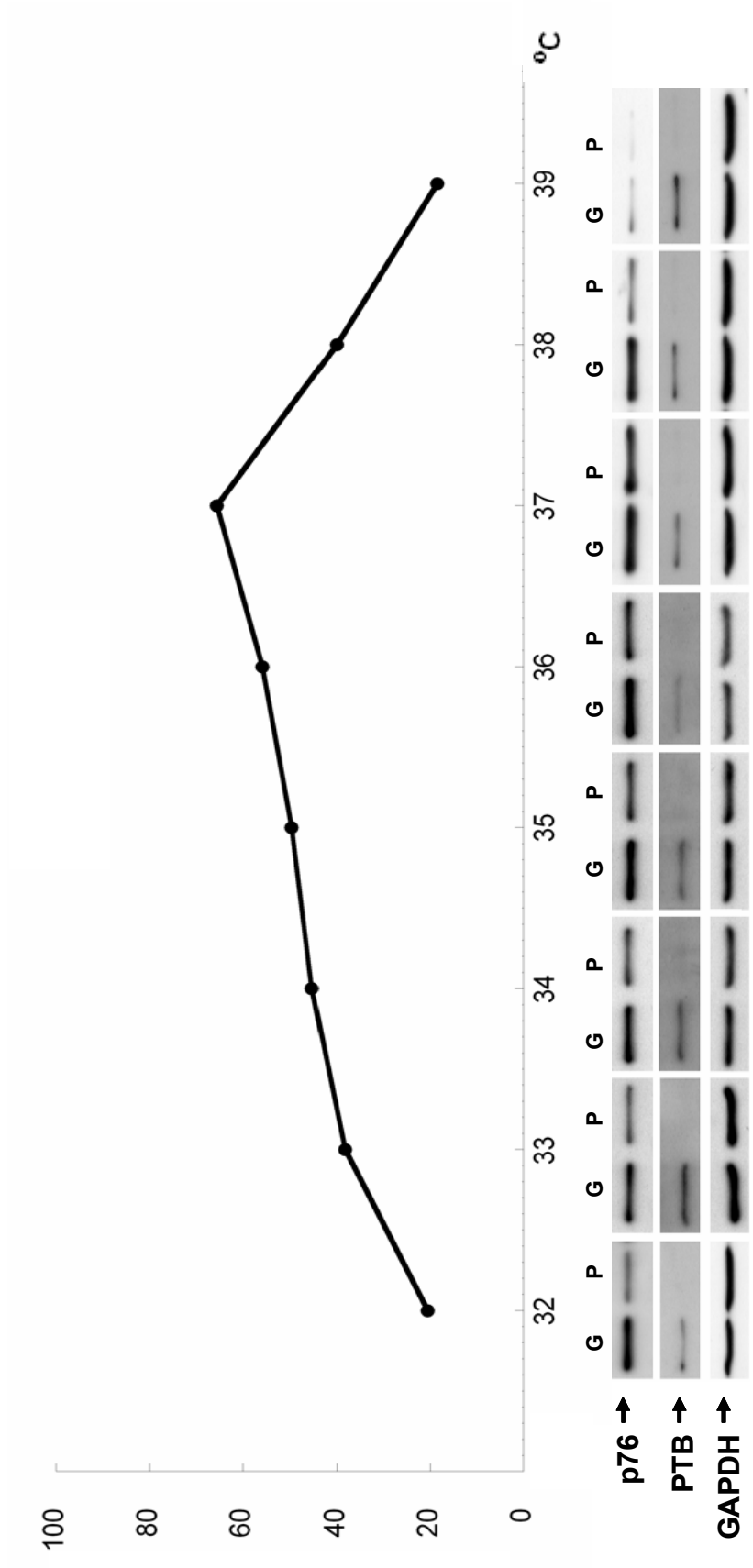


Figure 3.9. FCV replication is affected by RNAi-mediated knockdown of PTB in a temperature dependent manner FCV polymerase (p76) production 6 hour p.i. and graphical representation of p76 levels in PTB siRNAs transfected cells (P) as percent of the control (GFP siRNAs (G)) levels at various incubation temperatures. GAPDH was used as control for equal loading.

In order to determine the effect of PTB knockdown on calicivirus replication at a temperature in which this effect was apparent, FCV (m.o.i of 4) was used for the infection of PTB and control siRNA treated cells at 32 ^{o}C. 32 ^{o}C was chosen for further analysis as the virus replication, even in the control cells, was severely inhibited at 39 ^{o}C. During the course of the infection, virus yield was measured at 3, 6, 9, and 18 hours p.i. (**Fig. 3.10**). At 6 hours p.i. a 99 % reduction of virus production was observed and at the consecutive time points, 9 and 18 hours p.i., virus yield was reduced by 95 % and 93 % respectively in PTB siRNA transfected cells compared to control transfected cells (**Fig. 3.10**).

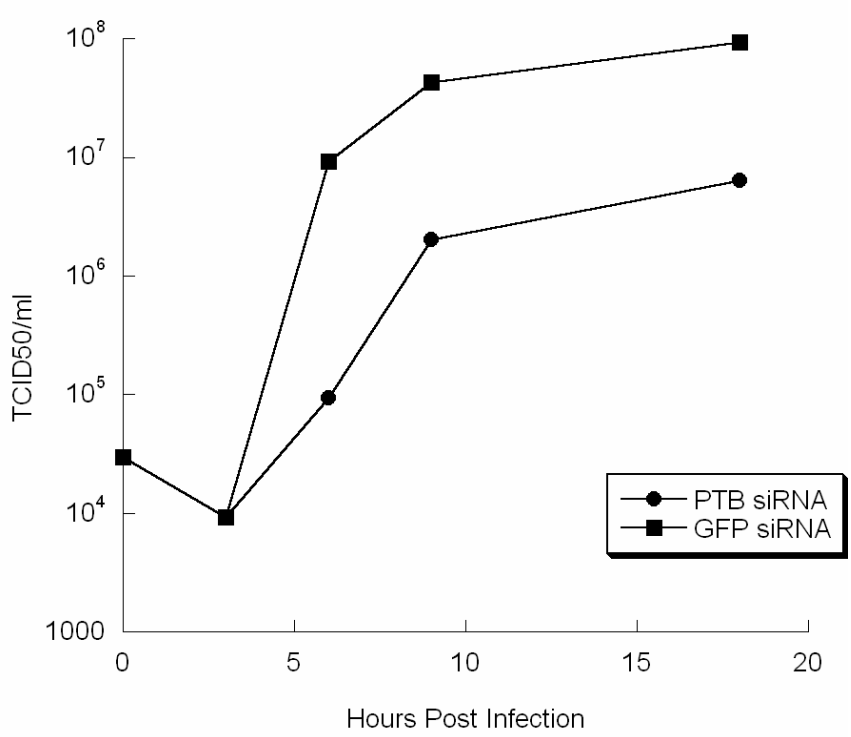


Figure 3.10. FCV yield is reduced by RNAi-mediated knockdown of PTB at 32 ^{o}C. FCV growth kinetics after infection of CRFK cells treated with PTB and GFP (control) siRNA cells at a multiplicity of infection of 4.

Calicivirus non-structural proteins, such as the polymerase p76, are produced by translation of the genomic RNA, while the major (VP1) and minor (VP2) capsid proteins are produced by the translation of the subgenomic RNA. The levels of the viral polymerase (p76) and major capsid protein were determined by western blot for all the time points p.i. (**Fig. 3.11a**). The production of both proteins was severely affected demonstrating a similar response to the PTB knockdown. At 6 hours post

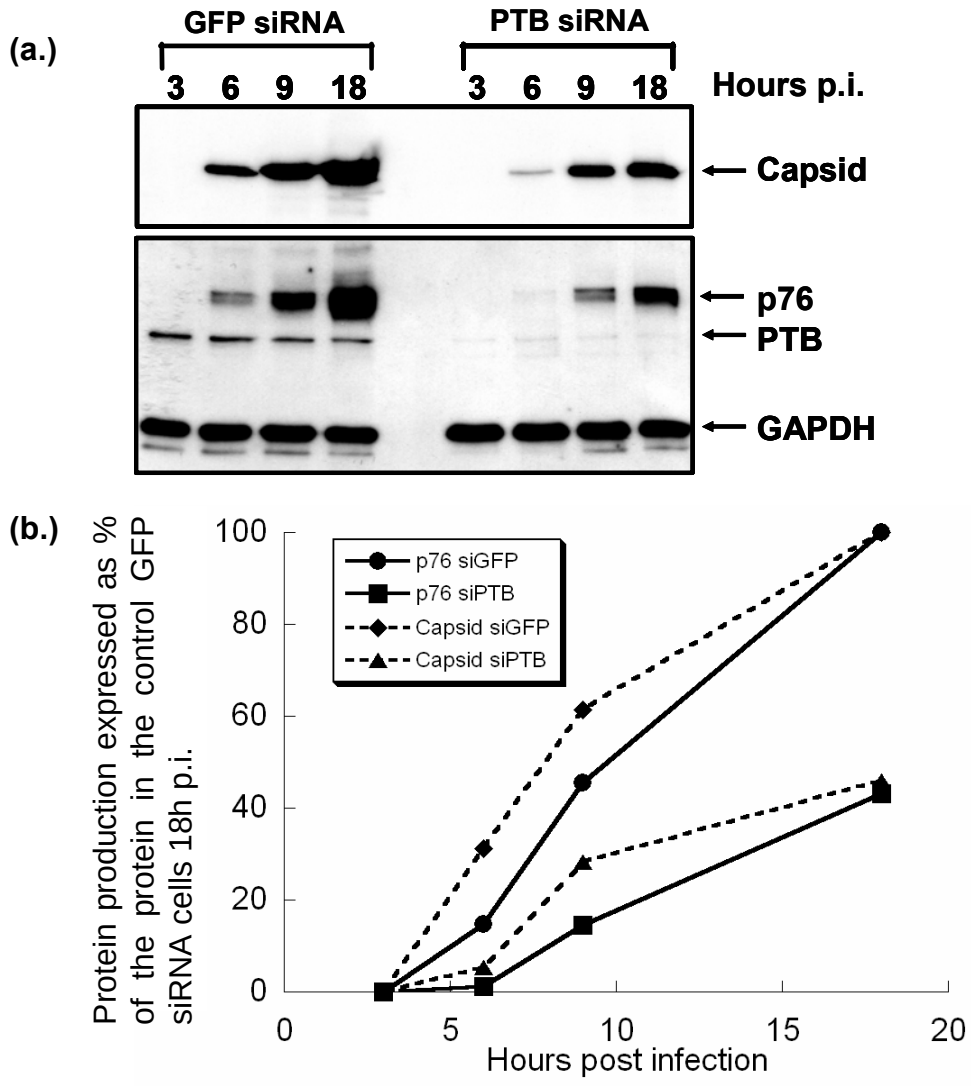


Figure 3.11. FCV protein expression is inhibited by PTB knockdown at 32 ºC. (**a.**) FCV polymerase (p76) and major capsid protein were detected by western blot during infection of PTB siRNA transfected and control (GFP siRNAs) cells. (**b.**) The levels of both proteins are plotted as percentage of the respective protein production in control cells at 18 hours p. i..

infection protein production was reduced by 90 %, by 79 % at 9 h and by 60 % at 18 h p.i. (**Fig. 3.11b**). RNA production was also affected by PTB knockdown, as shown by northern blot analysis for genomic and subgenomic RNAs (**Fig. 3.12a**). The production of both RNAs was equally inhibited with the inhibition ranging from 60% at 6 h p.i. to 30 % at 18 h p.i. (**Fig. 3.12b,c**). Such a profound effect on the viral replication signified a role of PTB in the viral life cycle. The fact that translation and replication are highly interdependent during a normal virus infection meant that no specific role for PTB in one or the other stage could be attributed as part of this study; but an attempt to address this is described later in this chapter.

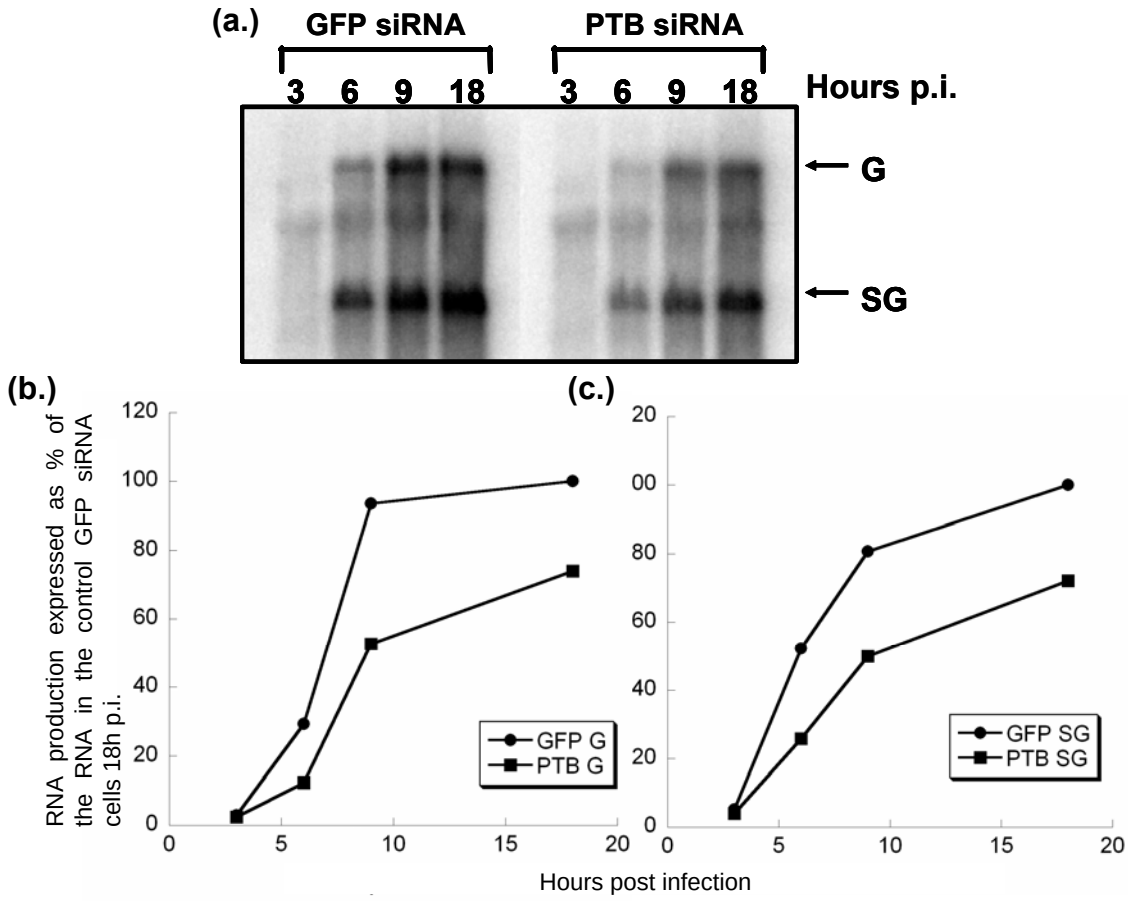
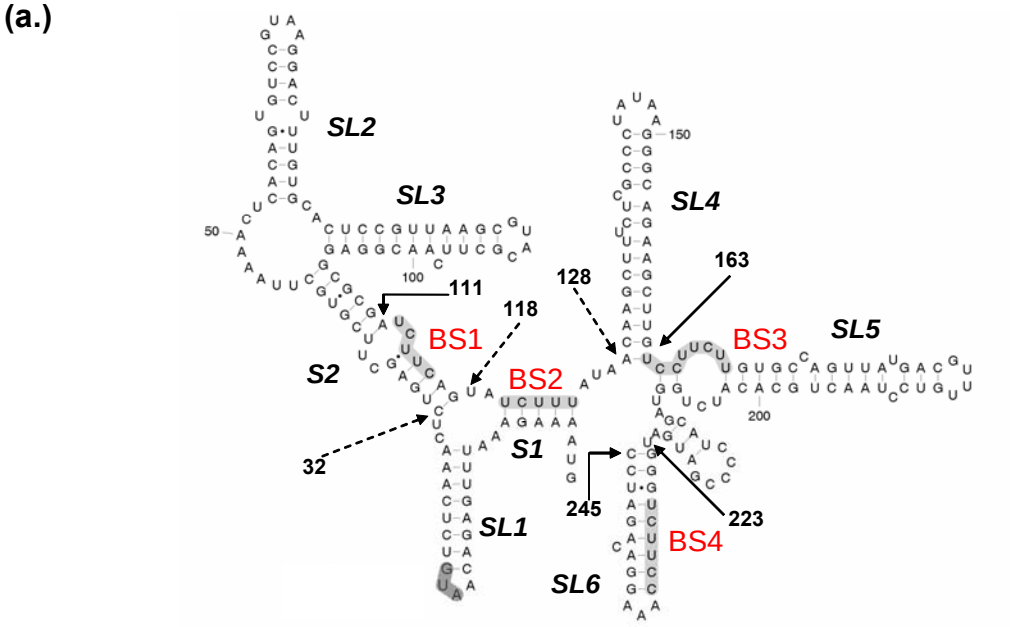


Figure 3.12. Calicivirus RNA production is inhibited by PTB knockdown at 32 ^{o}C. (**a.**) Genomic (G) and subgenomic (SG) RNA from calicivirus infected cells underexpressing PTB (PTB siRNA) or control (GFP siRNA) cells was detected by Northern blot analysis of RNA from cells infected at 32^{o}C. The levels of (**b.**) genomic and (**c.**) subgenomic RNA were plotted as percentage to the levels of genomic RNA production at 18 hours p.i. in the control GFP siRNA transfected cells.

3.7. PTB binds at least on two sites of FCV genomic RNA 5' end in a synergistic manner.

To further characterise the interaction between PTB and the FCV genomic RNA 5'$G_{1\text{-}245}$, truncations of the region were used as radiolabeled probes for EMSA analysis. The predicted PTB consensus binding sequences (**Fig. 3.13a**) were taken into consideration during the design of the truncations in order to analyse different combinations of the potential binding sites. The secondary structure of the region was



(b.)

	BS1	BS2	BS3
	R R D L Q Y	L Q Y L Y N	A C P S C A
mt	AGGCGCGACTTGCAGTAT	CTTCAGTACTTGTATAAC	GCTTGTCCAAGTTGTGCC
wt	AGGCGCGATCTTCAGTAT	CTTCAGTATCTTTATAAC	GCTTGTCCTTCTTGTGCC
FA	AGGCGCGAAAAAAAGTAT	CTTCAGTAAAAAAATAAC	GCTTGTAAAAAAAGTGCC

Figure 3.13. Mapping of the PTB binding site(s) on the FCV 5'$G_{1\text{-}245}$. (**a.**) The secondary structure of nucleotides 1-245 of the FCV genomic RNA (5'$G_{1\text{-}245}$) as predicted thermodynamically. The four potential binding sites of PTB are highlighted with red letters and the structural elements (stems,*S* and stem-loops,*SL*) are annotated in *italics*. The continuous arrows indicate the nucleotide positions which represent the 3' end of RNA transcripts that start from 1st nucleotide of the 5'$G_{1\text{-}245}$ (3'end truncations), while the dashed arrows indicate the nucleotide positions that represent the 5' end of RNA transcripts that terminate at nucleotide 245 of the 5'$G_{1\text{-}245}$ (5'end truncations) (**b.**) Alignment of the synonymous mutations (mt) with the wild-type (wt) sequence of FCV in three of the potential binding sites that were used in the mutational analysis of PTB binding on the FCV 5'$G_{1\text{-}245}$. Underneath each alignment the full-adenine substitutions for each potential biding site are presented

also taken also into account in order to reduce, where possible, the effect of truncations on the native RNA conformation (**Fig. 3.13a**). As no biochemical data existed on the structure of the FCV 5' end, free energy minimisation algorithms and evolutional co-variation were used to predict the RNA secondary structure presented in **Figures 3.1 and 3.13a**.

Two sets of truncations were tested for their ability to form a complex with PTB. The FCV 5'$G_{1\text{-}245}$ was truncated at the 3' end producing RNA transcripts encompassing nucleotides (nts) 1-111, 1-163, 1-202 and 1-223. Nts 1-111 did not contain any of the PTB consensus sequences, 1-163 encompassed the BS1 and BS2 potential binding sites and 1-223 sequence contained the BS1, BS2 and BS3 consensus sequences (**Fig. 3.13a**). The FCV 5'$G_{1\text{-}245}$ was also truncated at its 5' end producing transcripts that encompassed nts 32-245, 118-245 and 128-245 RNAs. Nts 32-245 contained all predicted PTB consensus sequences, but lacked the first stem loop of the original 5'$G_{1\text{-}245}$, 118-245 encompassed BS2, BS3 and BS4 potential binding sites and nts 128-245 contained BS3 and BS4 consensus sequences (**Fig. 3.13a**). As the only purpose of this series of EMSAs was to crudely identify the PTB binding site(s), the affinities are expressed using a rather arbitrary scale in which the affinity of PTB for the RNA probe representing the 5'$G_{1\text{-}245}$ RNA sequence is represented as: "++++" (**Fig. 3.14**). Also, the fact that the preparation of PTB used in these experiments had a small quantity of truncated products made difficult the accurate calculation of affinities. Titration of PTB on the 1-111 sequence demonstrated that it has no ability to interact with PTB, not unexpected since there is no pyrimidine rich stretch in this region. Addition of the first two potential binding

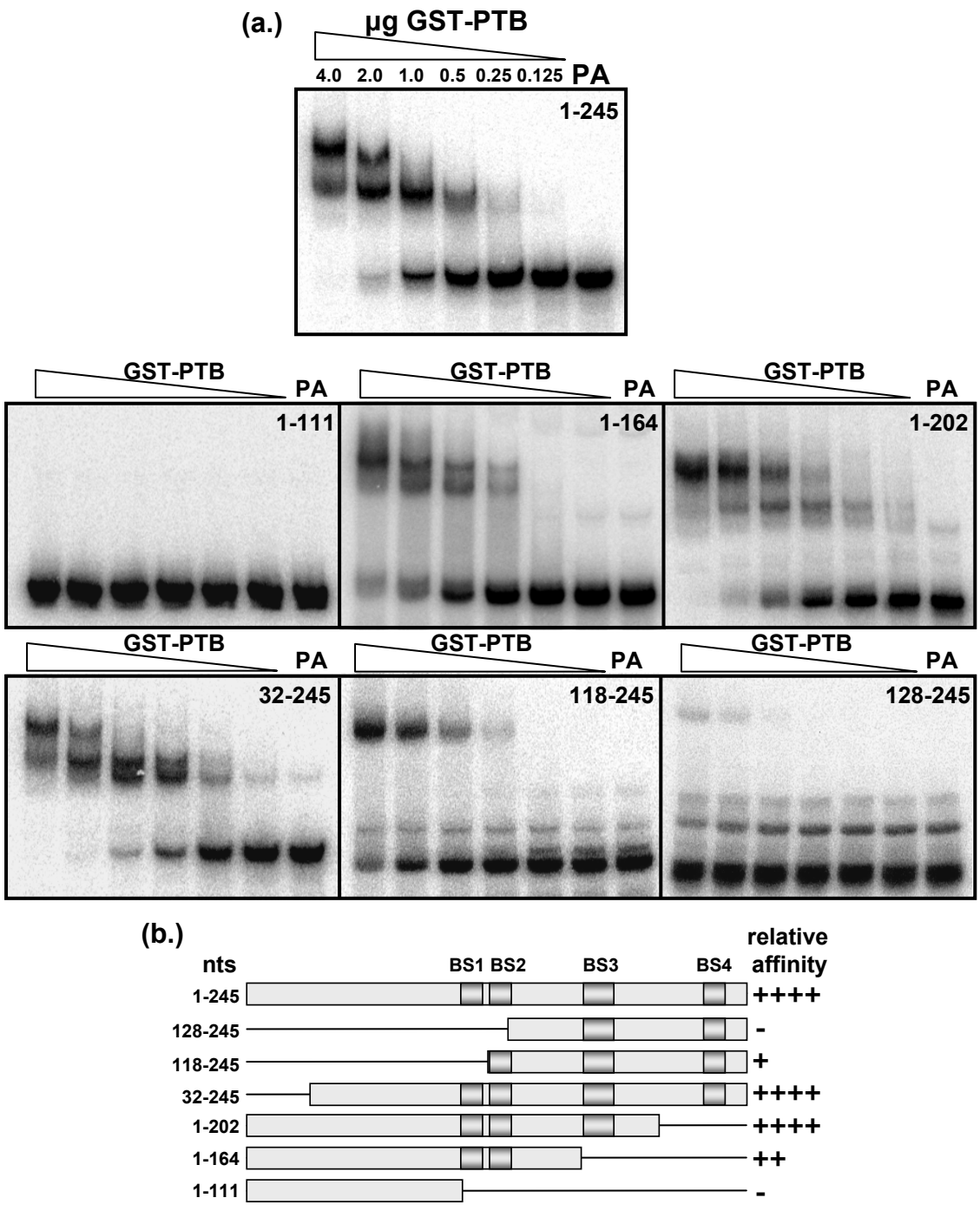


Figure 3.14. Mapping of the PTB binding site(s) on the FCV 5'G$_{1\text{-}245}$. (**a.**) Titration of PTB on RNA probes that represent the 3' and 5' end truncation of the 5'G$_{1\text{-}245}$ RNA. (**b.**) Graphic illustration of the different RNA transcripts used to evaluate the contribution of the different potential binding sites (▭) in PTB binding (PA = probe alone, ++++ = 5'G$_{1\text{-}245}$ affinity for PTB, - = absence of or residual affinity to PTB, nts = nucleotides)

sites and stem loop 4 (*SL4*) (1-164) dramatically increased the affinity of the RNA for PTB. The further addition of BS3 and *SL5* (1-202) restored the affinity of the RNA for PTB to the 5'G_{1-245} level. The deletion analysis demonstrated that BS4 and sequences downstream of nucleotide 202 did not contribute to PTB binding. Indeed, BS4 was not conserved in FCV sequences that became available later (**Fig. 3.1c**). Deletion analysis from the 5' end of the 5'G_{1-245} RNA demonstrated that deletion of the nucleotides 1-127, containing BS1 and BS2 (128-245), led to the abolishment of PTB binding, while addition (to this probe) of BS2 (118-245) partially restored PTB binding. Interestingly, deletion of nucleotides 1-31 increased the binding of PTB on the RNA, possibly because disruption of stem 1 (*S1*) made the BS2 region single stranded (**Fig. 13a**). Finally, deletion of nts 1-31 and 118-245, producing an RNA that encompassed BS1 only, was not able to form a complex with PTB. The above deletion analysis showed that the most critical potential binding site was BS2 as all RNA probes containing BS2 were able to bind PTB, while probes lacking this region demonstrated minimal or no PTB binding activity.

The deletion analysis was followed by mutational analysis of the potential PTB binding sites (**Fig. 3.15**). However, as all the potential binding sites were located in the protein-coding region, the mutations had to preserve the original amino-acid sequence (synonymous nucleotide changes) while changing the pyrimidine rich sequence. This was not as important for the *in vitro* binding assays as it was for the assessment of the effect of these mutations in virus replication. A synonymous mutant RNA produced for BS2 was tested in EMSAs and demonstrated wild-type levels of PTB binding (**Fig. 3.13b**). Synonymous mutations were introduced in the other

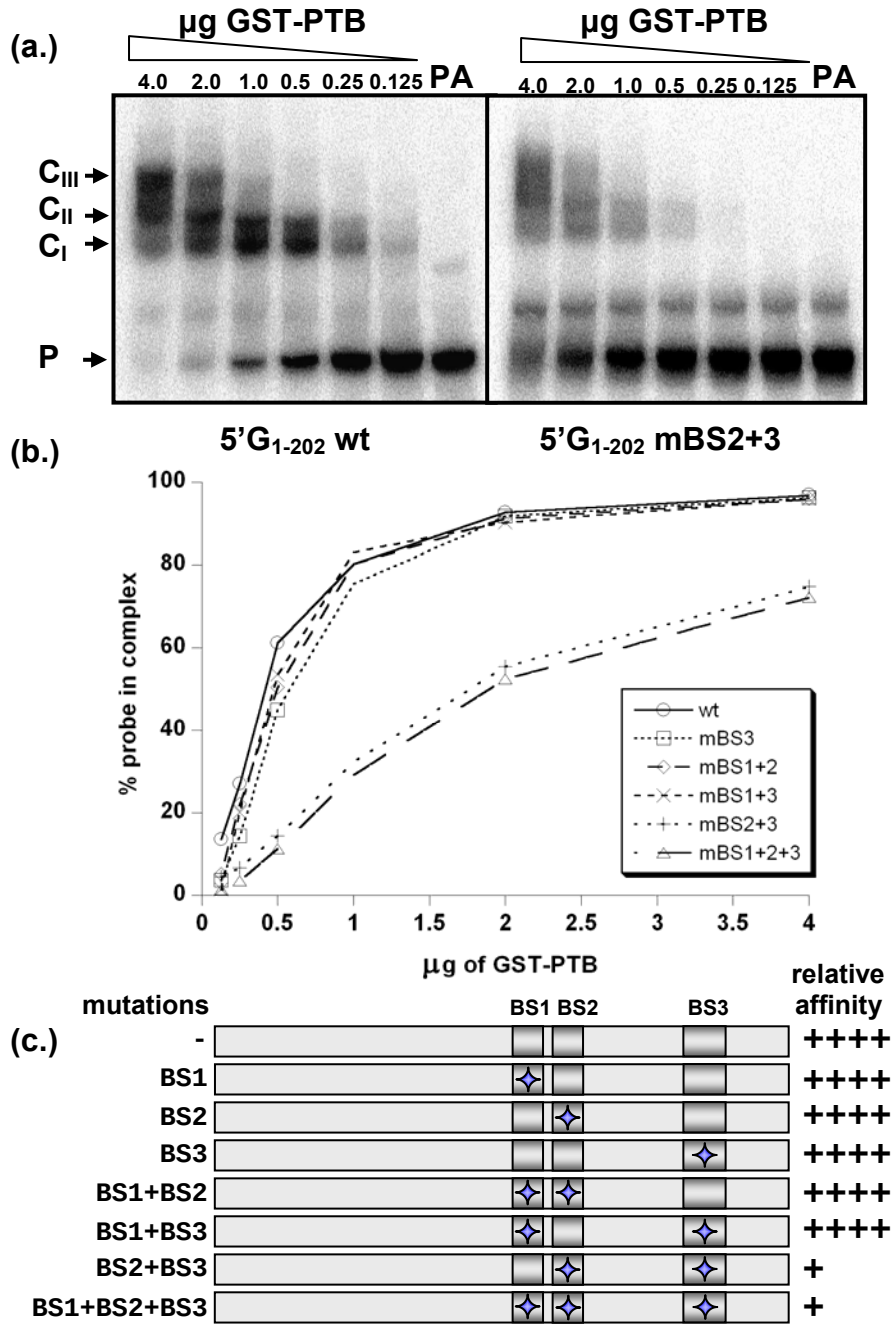


Figure 3.15. Mutational analysis of PTB binding sites on the FCV 5'G$_{1-202}$ by electrophoretic mobility shift assays. (**a.**) EMSAs in which increasing amounts of PTB are incubated with wild-type (wt) and mutated (mBS2+3) FCV 5'G$_{1-202}$ RNA probes. (**b.**) The fraction (%) of the probe in complex under increasing amounts of GST-PTB for EMSAs that contain 5'G$_{1-202}$ probes with different combinations of the mutations in the PTB potential binding sites BS1, BS2 and BS3. (**c.**) Graphic illustration of the different RNA transcripts used to evaluate the contribution of the different potential binding sites (▭) in PTB binding after the mutational analysis. The blue stars highlight the potential binding sites that were mutated in each RNA probe. (PA= probe alone, ++++ = wt affinity of 5'G$_{1-202}$ for PTB)

potential binding sites (**Fig. 3.13b**) and as for BS2, demonstrated wild-type affinity for PTB (**Fig. 3.15**). A second set of mutant RNAs was constructed in which synonymous mutations in the potential binding sites of PTB were introduced in all possible combination (BS1+BS2, BS1+BS3, BS2+BS3 and BS1+BS2+BS3). The triple RNA mutant showed a dramatic reduction in PTB binding while the only double mutant that demonstrated a defect in PTB binding was BS2+BS3 (**Fig. 3.15**). As the PTB binding curve for the BS2+BS3 mutant RNA was the same as the triple mutant it was considered as the minimum combination of mutations required for the reduction in PTB binding.

Even if *in* vitro PTB binding was significantly reduced in the mutated RNAs, some residual binding activity remained. This signified that at least one additional region, which did not correspond to any of the evolutionally conserved pyrimidine rich tracts, contributed the observed lower binding affinity of the RNA to PTB. All the above mutational analysis was repeated using RNAs in which the polypyrimidine tract had been fully substituted by adenines ($full_{(A)}$ substitutions). PTB binding of the $full_{(A)}$ mutant RNAs was exactly the same as with the synonymous mutations, showing that the binding that was observed for the synonymous mutant RNAs was not due to the remaining pyrimidines in the potential binding sites (data not shown).

3.8. Viruses with reduced affinity for PTB have the same growth kinetics as the wild-type virus in tissue culture

The main reason for the identification of the PTB binding site was to investigate a potential defect of a virus with a reduced ability to bind PTB. The

synonymous mutations that reduced PTB binding at the 5' genomic extremity were cloned into the FCV full length clone, pQ14, either individually (m14:BS2, m26:BS3) or in combination (m2:BS2+BS3)[5]. The viruses were produced through transfection of the mutated FCV infectious clones into BSRT7 cells infected with a modified strain of Vaccinia virus expressing T7 polymerase (**Fig. 3.16a**). This Vaccinia virus strain although unable to go through a full replication cycle in BSRT7 cells shows limited expression, which produces recombinant T7 polymerase. The T7 polymerase, using the promoter upstream of the viral cDNA, creates a large number of transcripts that express the viral proteins, while a minority of them are able to replicate and produce infectious virus. The recovered viruses were amplified, their sequence confirmed and their growth kinetics compared to the wild-type virus (**Fig. 3.16b**). All three mutant viruses were able to replicate at rates similar to the wild-type indicating that the introduced mutations did not confer any significant attenuation to the virus in CRFK cells. No increase in temperature sensitivity of virus replication was observed at 32 or 39 ^{o}C for all three mutant viruses while they also demonstrated the same response to PTB knockdown as wild-type virus (data not shown).

[5] FCV mutant clones were made by Stanislav Sosnovtsev (NIH, Maryland, USA)

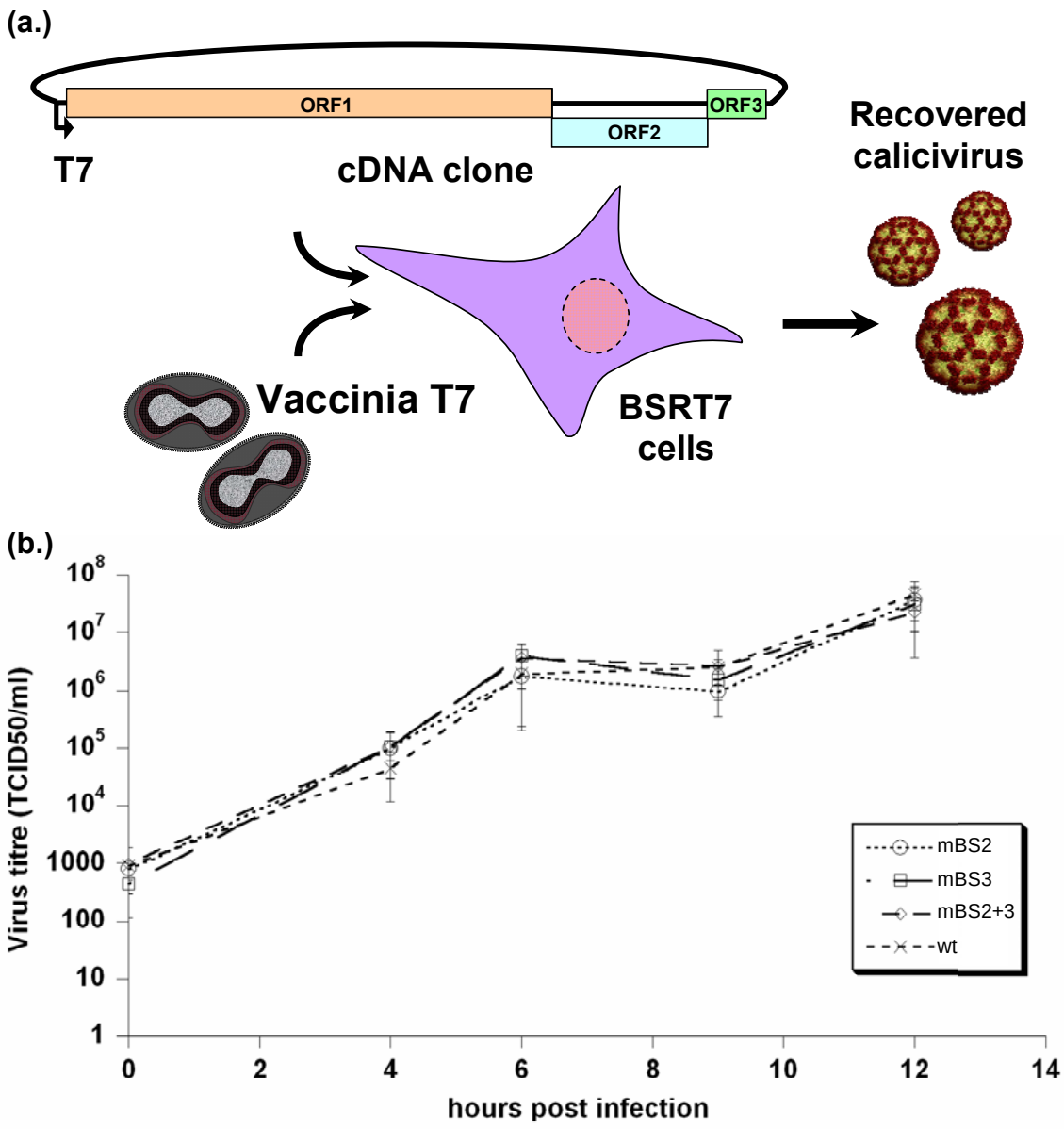


Figure 3.16. Recovery of genetically defined FCV which contain mutations in the PTB binding sites. (**a.**) Schematic representation of the procedure followed during the reverse genetics recovery of the mutant viruses. Briefly, the viral cDNA infectious clone was transfected into BSRT7 cells infected with Vaccinia virus T7 and the recovered viruses were harvested amplified and retitred. The sequence was confirmed prior to use in growth curves (**b.**) Growth kinetics of the infection in CRFK cells for the mutant FCVs (m14 = mBS2, m26 = mBS3 and m2 = mBS2+3) at 37 ^{o}C and at a multiplicity of infection of 0.4.

3.9. PTB inhibits FCV *in vitro* translation

In order to define the stage of the virus life cycle at which PTB might be involved, isolation of the two main processes, translation and replication, was required. The lack of a replicon system for FCV made the study of a translation independent FCV replication almost impossible. Additionally, the unique mechanism of calicivirus translation made the investigation of FCV translation in cells rather difficult. As explained thoroughly in the general introduction, FCV and the vast majority of caliciviruses require the interaction of the translation machinery with the VPg protein linked to the 5' end of the viral RNA. Transfection of an *in vitro* synthesised RNA would require the prior attachment of VPg to its 5' end in order to be translated, but such a method is not yet available. However, an *in vitro* translation system was recently developed (Goodfellow et al., 2005), thereby allowing the investigation of the requirements of the calicivirus translation machinery. As PTB is a well known regulator of picornavirus translation (Niepmann et al., 1997) its effect on FCV translation was assessed by titration of recombinant his-PTB in a rabbit reticulocyte lysate (RRL) FCV *in vitro* translation assay (**Fig. 3.17**). Addition of increasing amounts of PTB was followed by declining production of *in vitro* synthesised FCV proteins (**Fig. 3.17**). In order to verify that the inhibition of FCV translation by PTB was specific, *in vitro* synthesised 5'$G_{1\text{-}245}$ RNA was titrated into the reactions containing exogenous PTB (**Fig. 3.17**). Results indicated that addition of the FCV 5'$G_{1\text{-}245}$ RNA restored FCV translation back to normal levels (**Fig. 3.17**).

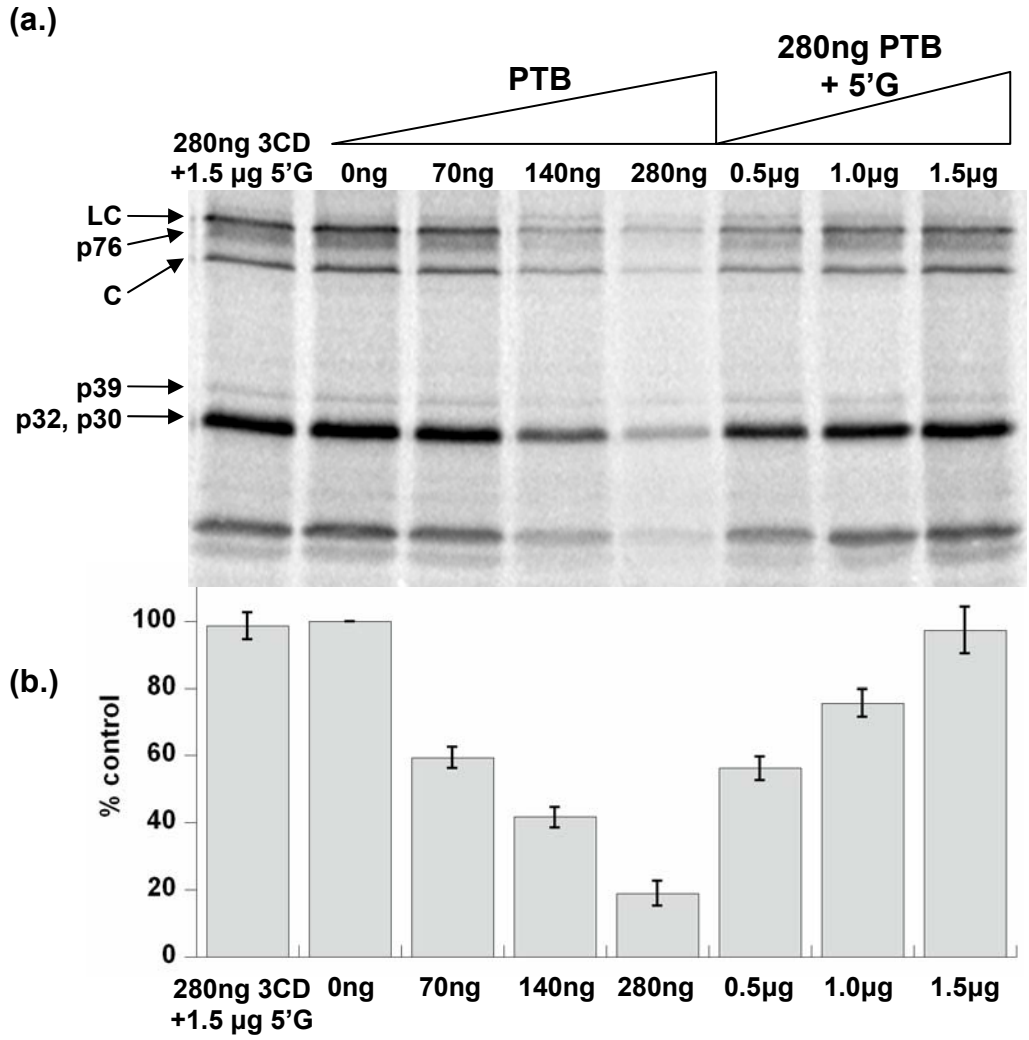


Figure 3.17. Inhibition of FCV *in vitro* translation by PTB. (**a.**) Effect of addition of his-PTB on FCV *in vitro* translation that demonstrates the reduced expression of FCV proteins that are produced by the translation of ORF1 (from the genomic RNA) and ORF2 (from the subgenomic RNA). The ^{35}S methionine labelled FCV proteins were analysed by SDS-PAGE. Addition of increasing amounts of 5'$G_{1\text{-}245}$ RNA on top of PTB led to the recovery of the FCV translation. (**b.**) Bar chart illustrating the efficiency of FCV translation as % of the control (0ng PTB) as measured by phosphor-imager densitometry quantification. LC = leader peptide + capsid, C = capsid p76, p39, p32 and p30 are various other proteins of FCV. 3CD is the poliovirus protease-polymerase and 5'G is the FCV 5'$G_{1\text{-}245}$. Error bars represent the standard deviation from three different experiments

A capped and polyadenylated bicistronic RNA expressing the CAT enzyme from the 5' cap structure and firefly luciferase from the FMDV IRES (5'cap-CAT FMDV-IRES-Luciferase 3' poly(A)tail) was used to assess the effects of PTB (or the impurities regularly found with purified proteins) on the general cap-dependent and IRES-dependent translation (**Fig. 3.18**). Upon addition of low amounts of PTB into

the translation reactions cap dependent translation was not affected, while FMDV translation demonstrated a rather insignificant increase (**Fig. 3.18**). Under the same conditions FCV translation was reduced by 40 and 60 % at 70ng and 140ng of PTB respectively (**Fig. 3.17**). This fact along with the rescue of FCV translation by 5'G_{1-245} signified that the inhibitory effect of PTB is caused specifically by its interaction with the FCV RNA. Only at the highest concentration of PTB were both FMDV and cap dependent translation affected (**Fig. 3.18**). In contrast to FCV translation, titration of

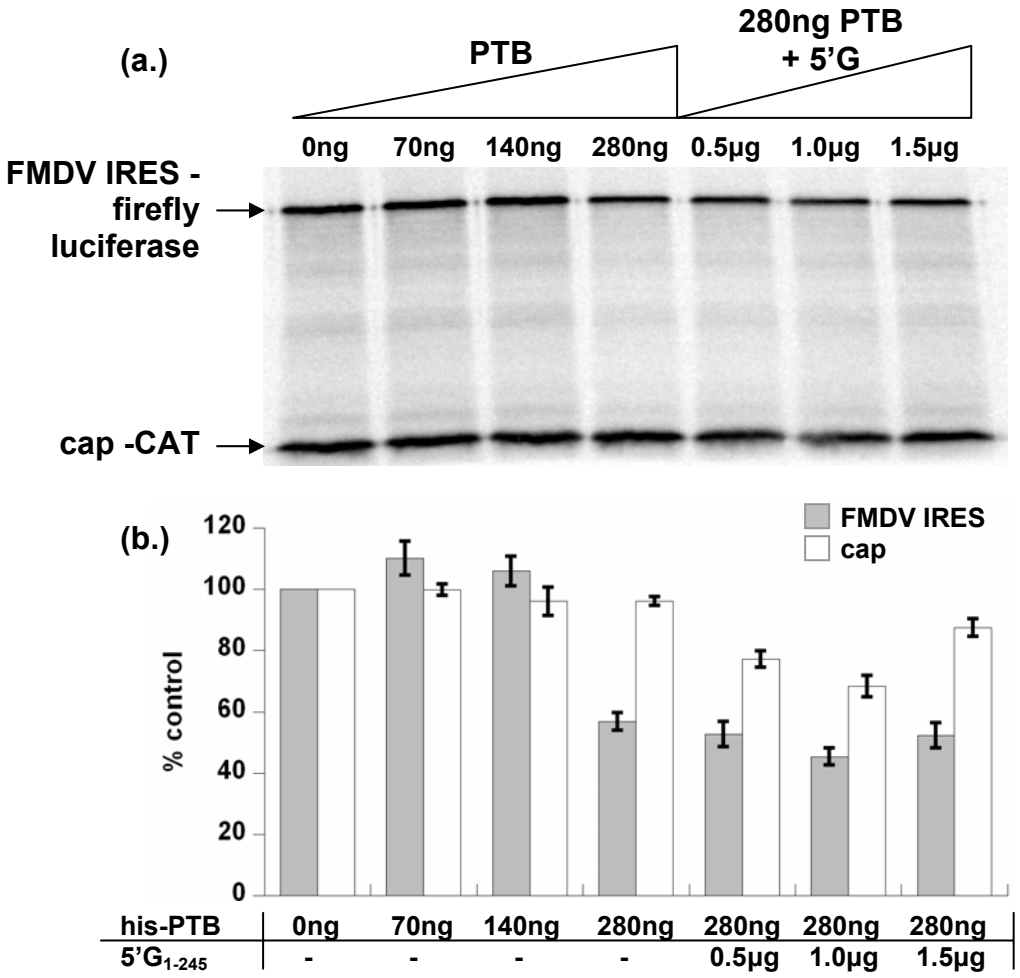


Figure 3.18. Effect of PTB on cap-dependent and FMDV-IRES dependent *in vitro* translation. (**a.**) Increasing amounts of his-PTB and 5'G_{1-245} in the *in vitro* translation of a bicistronic RNA construct that expressed the CAT enzyme under the cap structure and firefly luciferase under the FMDV IRES. Increasing amounts of FCV 5'G_{1-245} RNA on top of PTB were used to asses the specificity of the effect of PTB on translation. The ^{35}S methionine labelled CAT and firefly luciferase were analysed by SDS-PAGE. (**b.**) Bar chart that illustrates the efficiency of cap- and FMDV IRES-dependent translation as % of the control (0ng PTB) as measured by phosphor-imager densitometry quantification. Error bars represent the standard deviation from three different experiments

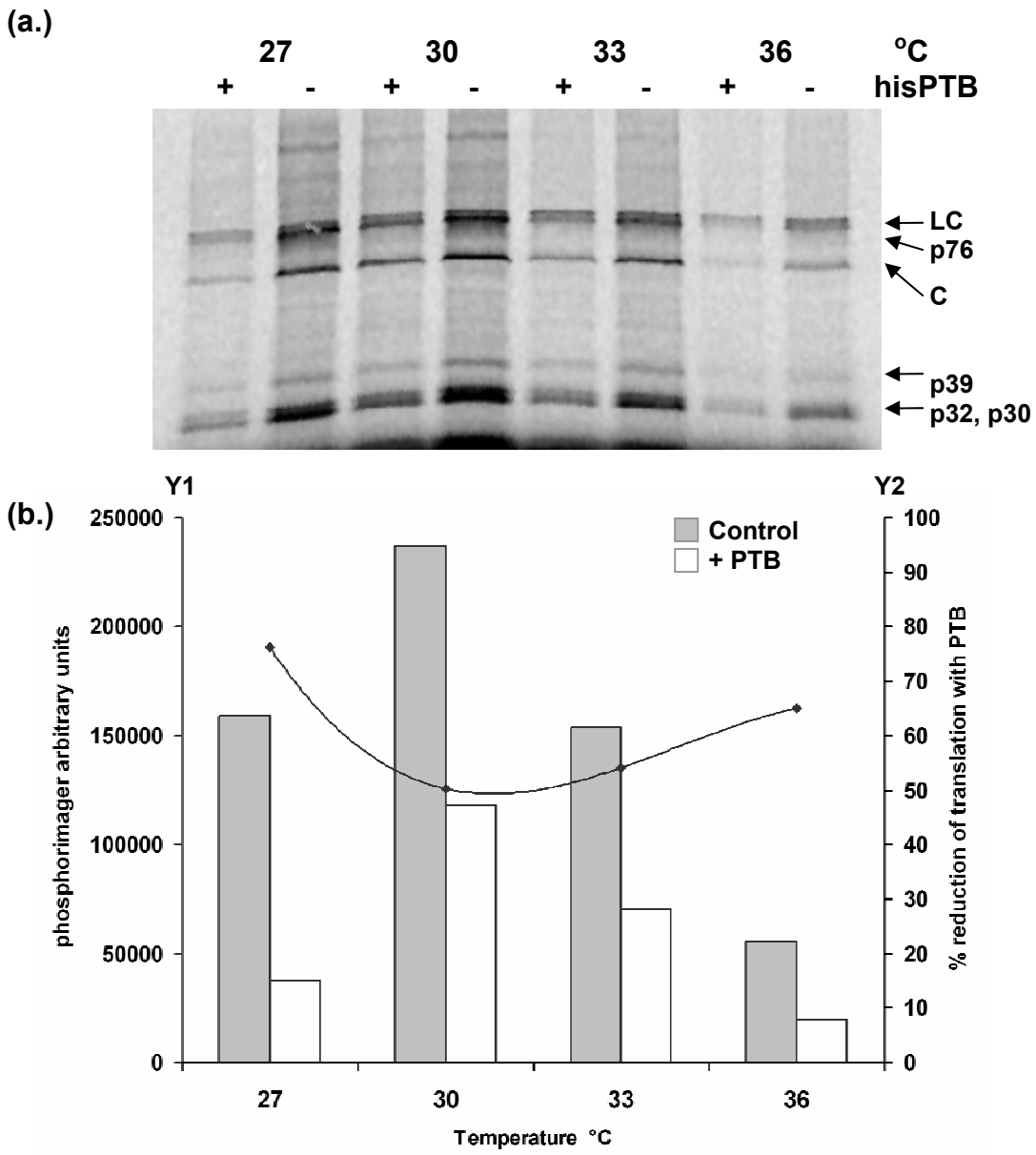


Figure 3.19. The inhibition of FCV *in vitro* translation by PTB is temperature dependent. (**a.**) Addition of 140ng of his-PTB in the FCV *in vitro* translation under different incubation temperatures. The proteins expressed from the FCV genomic and subgenomic RNA labelled with ^{35}S methionine were analysed by SDS-PAGE in 12.5 % polyacrylamide gel. (**b.**) Illustration of the efficiency of FCV translation before and after addition of his-PTB. The raw data in phosphor imager arbitrary units is presented as a bar chart by the Y1 axis for every incubation temperature, while the line (Y2 axis) represents the relative inhibition (as % of the –PTB control) of FCV translation upon addition of his-PTB at every incubation temperature. LC = leader peptide + capsid, C = capsid

the FCV RNA. Only at the highest concentration of PTB were both FMDV and cap dependent translation affected (**Fig. 3.18**). In contrast to FCV translation, titration of 5'G_{1-245} RNA transcript did not restore the levels of either cap-dependent or IRES-dependent translation, leading to the assumption that some other factor(s) co-purified with PTB, rather than PTB itself, may have been responsible for the inhibitory effect.

3.10. Inhibition of FCV *in vitro* translation is temperature dependent

The analysis of the effect of PTB knockdown using siRNAs showed a temperature dependent effect on the virus growth that led to the hypothesis of a potential involvement of the well documented RNA chaperone activity of PTB. Therefore, *in vitro* translation assays were incubated at various temperatures to assess the temperature dependence of the PTB inhibitory effect on FCV translation. Indeed, at 30 ^{o}C, which is the optimum *in vitro* translation temperature, the inhibitory effect of PTB was less apparent than it was at temperatures lower or higher (**Fig. 3.19**).

3.11. FCV translation is enhanced by RNAi-mediated knockdown of PTB

As stated above the requirement of VPg protein at the 5'end of the FCV RNA for its translation excluded the possibility of experiments on calicivirus translation in tissue culture using *in vitro* transcribed RNA. During virus replication a subgenomic RNA (sgRNA) is produced from the 3' half of the viral genomic RNA, which

similarly to the genomic RNA is translated using the VPg protein. However, the sgRNA does not produce the viral polymerase as it codes only for the major (VP1) and minor (VP2) proteins. Thus, if the sgRNA was present in cells without the genomic RNA it would be able to produce the capsid proteins, but lacking the polymerase it wouldn't be able replicate. An attempt to separate the two major processes of calicivirus life cycle, translation and replication, in tissue culture was made by specifically digesting the genomic RNA with RNase H. A DNA oligonucleotide complementary to the coding region of the RdRp (p76) was annealed to the viral RNA preparation and the complex was digested by the DNA:RNA hybrid specific RNase H. The efficiency of RNase H in removing the genomic RNA was assessed by *in vitro* translation of the digestion reaction in RRLs (**Fig. 3.20a**). The viral RNA treated with a non-specific oligonucleotide produced a normal FCV protein profile, while the RdRp specific oligonucleotide resulted in the elimination of all the genomic RNA produced proteins. The FCV major capsid protein is produced as a premature protein (LC) attached to a leader peptide that is subsequently removed by the viral protease that is fused to the RdRp in p76 protein. The absence of p76 in the protein profile is not only apparent directly but also indirectly by the fact that the LC remained uncleaved. The identity of the bands corresponding to the LC and the capsid in the FCV *in vitro* translation were verified by immunoprecipitation using an α-capsid antibody (**Fig. 3.20a**). The RdRp specific RNase H digested viral RNA that contained only the sgRNA was transfected into CRFK cells treated with PTB and GFP specific siRNAs to assess the effect of PTB knockdown in the viral translation. As shown by western blot for the major capsid protein, the production of protein from the subgenomic RNA was highly induced in the absence of PTB. This fact signified that siRNA-mediated knockdown of PTB reduced the inhibition in FCV translation

caused by the presence of PTB (**Fig. 3.20b**). However, the protein that was detected had a similar molecular weight to the mature major capsid protein that is present in infected cells and virions (**Fig. 3.20b**), while the premature LC precursor protein, produced by the subgenomic RNA in the absence of p76, could not be detected. The LC protein produced during transfection of subgenomic RNA construct was used as a control in the assay. The pT7SG+R plasmid that expressed subgenomic RNA under T7 promoter was transfected into CRFK cells infected with MVAT7. The absence of

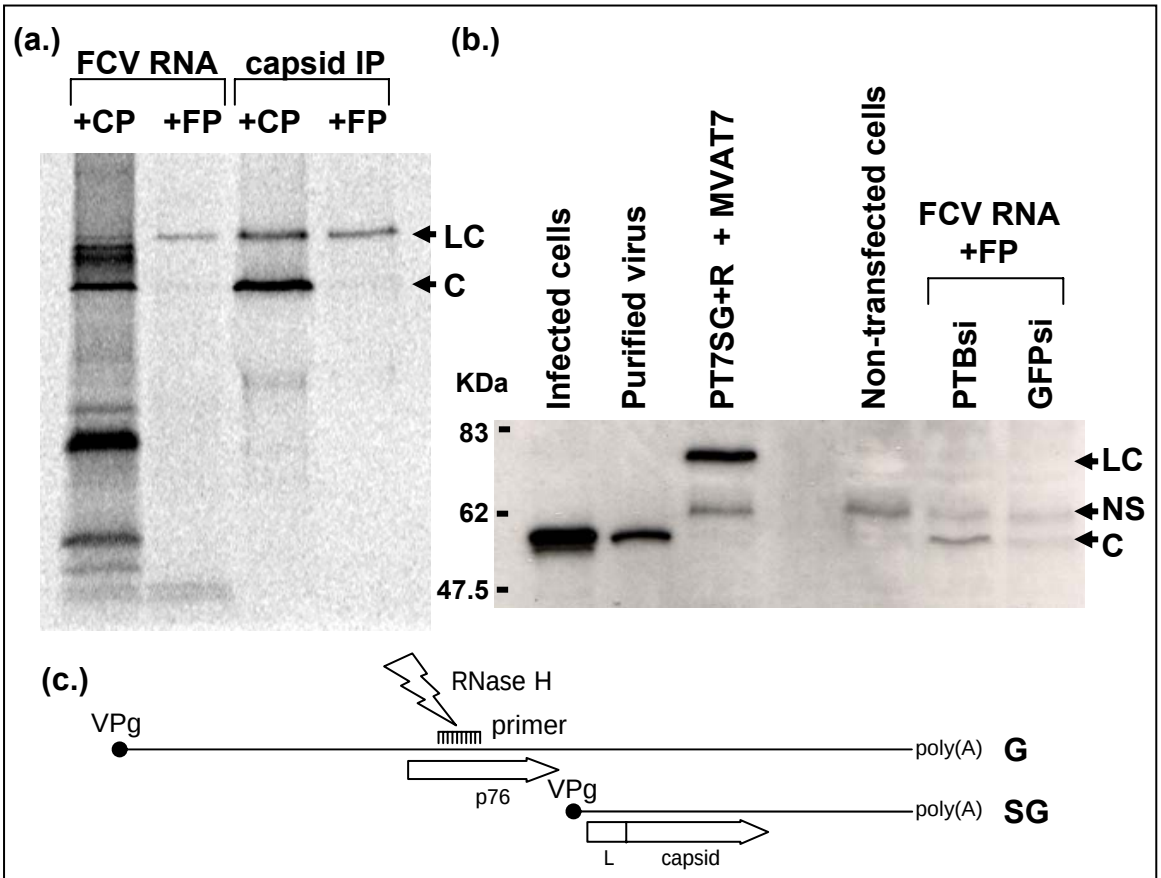


Figure 3.20. Isolation of FCV sgRNA and the effect on its translation during RNAi mediated knockdown of PTB. (**a.**) *In vitro* translation of FCV RNA after RNase H digestion using an FCV genomic RNA specific DNA oligonucleotide (FP) and a control DNA oligonucleotide (CP). Immunoprecipitation with α-major capsid (VP1) from the *in vitro* translation of FCV RNA after RNase H digestion using an FCV genomic RNA specific DNA oligonucleotide (FP) and a control DNA oligonucleotide (CP). The proteins were labelled with ^{35}S methionine and the SDS-PAGE analysis was exposed to a phosphor imager screen (**b.**) Western blot for the major capsid protein (VP1) in infected CRFK cells, purified virus, produced by transfection of the sgRNA-coding pT7SG+R plasmid in CRFK cells after infection with MVAT7, non-transfected CRFK cells, and CRFK cells treated with PTB or GFP siRNAs that have been transfected with FCV RNA digested with RNase H using an FCV specific DNA oligonucleotide (**c.**) Illustration of the specific digestion of the FCV genomic RNA using the IGRDG54 oligonucleotide complementary to p76-coding region (primer) and RNase H. (LC=leader capsid, C=capsid, NS=non specific)

LC could indicate a possible residual presence of p76 in the cells as a consequence of a small proportion of genomic RNA that possibly remained uncleaved after RNase H treatment. However, p76 could not be detected by western blot in the same cell lysates (data not shown).

3.12. PTB translocates from the nucleus to the cytoplasm during FCV infection

To examine the localisation of PTB during FCV infection confocal microscopy was used. Infected CRFK cells were probed for PTB and the viral polymerase, p76, as a marker for the viral replication complexes. The localisation of PTB is normally nuclear, unless the cell undergoes cell division (**Fig. 3.21.1**). During FCV infection of CRFK cells at 37 ^{o}C PTB remained predominantly nuclear, while in a small number of cells a cytoplasmic fraction of PTB was also present (**Fig. 3.21.1**). However, there was no major redistribution of PTB in the vast majority of infected cells (data not shown). The situation was different when the infection was carried out at 32 ^{o}C. At 32 ^{o}C the levels of PTB in the nucleus of the infected cells showed an approximately 70% decrease compared to the non-infected cells (**Fig. 3.21.2** and **3.23**). The cytoplasmic portion of PTB, present at low levels in normal cells, showed an approximately 10x increase in the infected cells (**Fig. 3.22** and **3.23**). An interesting observation was that increasing levels of the viral polymerase, p76, resulted in decreasing levels of nuclear PTB in infected cells (**Fig. 3.7**), while cells at the very late stages of the infection had nearly undetectable levels of PTB (data not

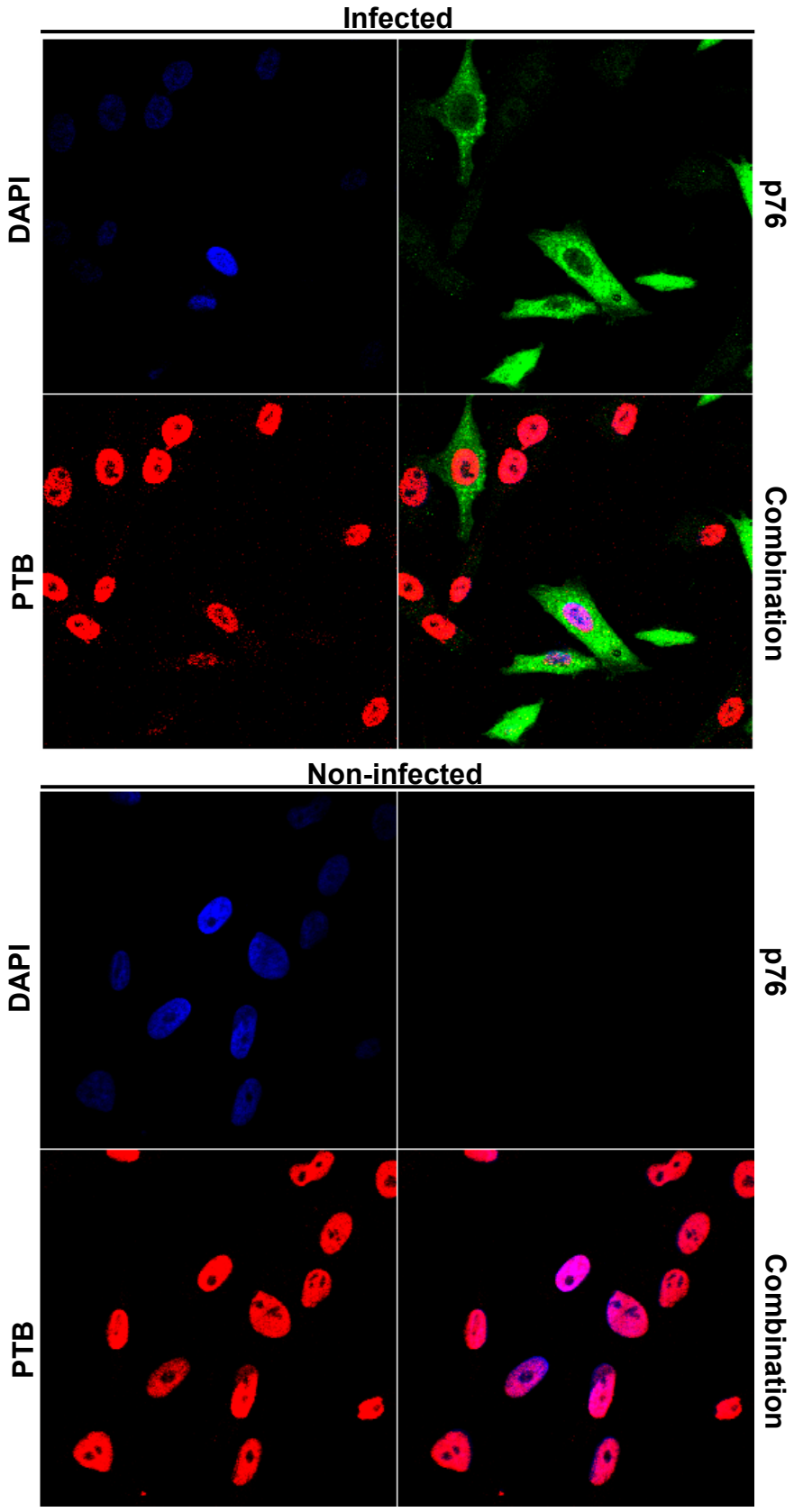


Figure 3.21.1 Distribution of PTB in FCV infected cells at 37 °C. CRFK cells were infected with FCV for 9 h at 37 °C and at an m.o.i. of 0.5. Infected and control cells were fixed and stained for p76 (**green**) and PTB (DH17 monoclonal) (**red**). DAPI was used for nuclei (**blue**) staining. The cells were observed using confocal microscopy.

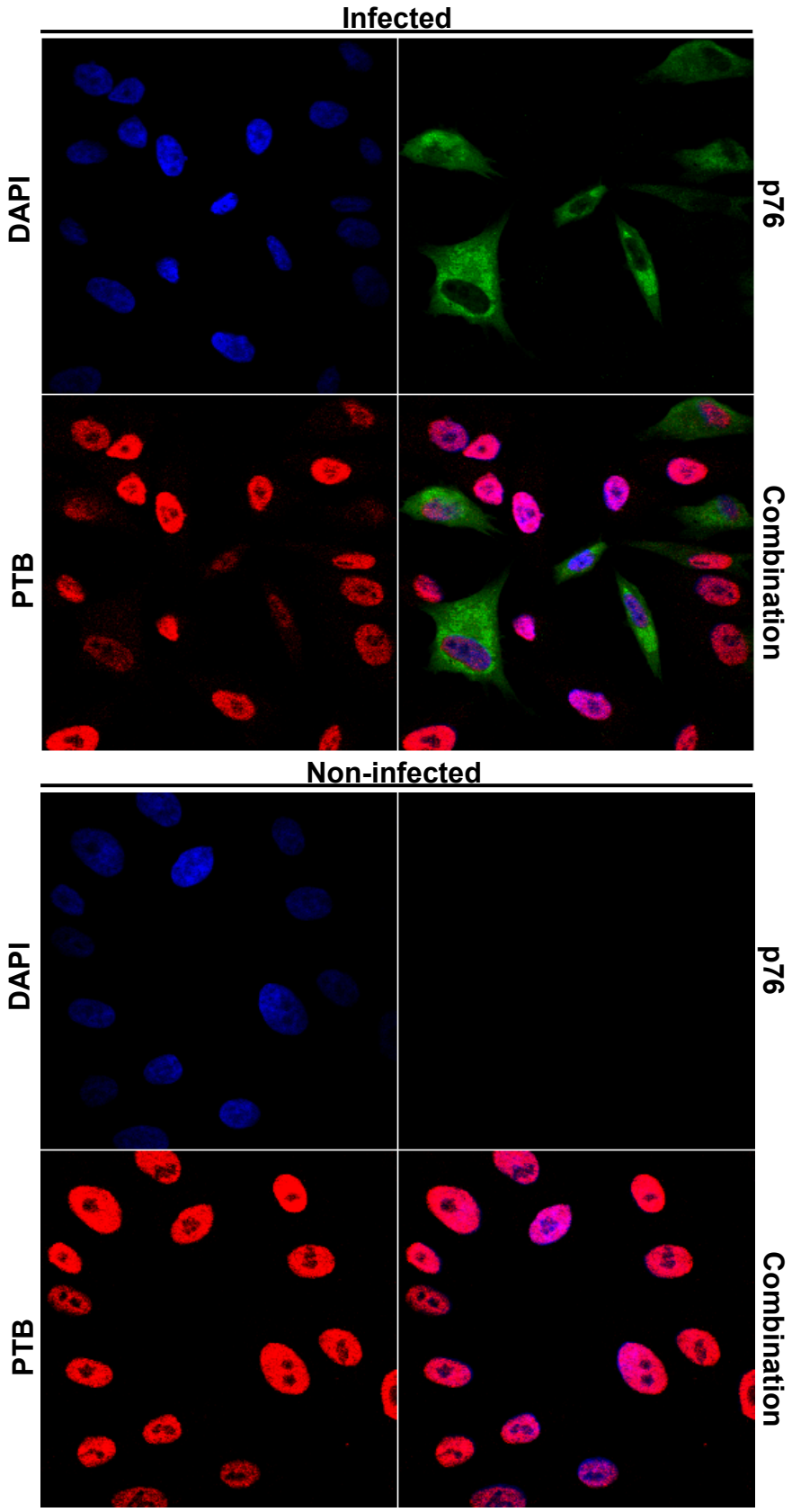


Figure 3.21.2 FCV infected cells have reduced levels of PTB in the nucleus at 32 °C. CRFK cells were infected with FCV for 16 h at 32 °C and at an m.o.i. of 0.5. Infected and control cells were fixed and stained for p76 (**green**) and PTB (DH17 monoclonal) (**red**). DAPI was used for nuclei (**blue**) staining. The cells were observed using confocal microscopy.

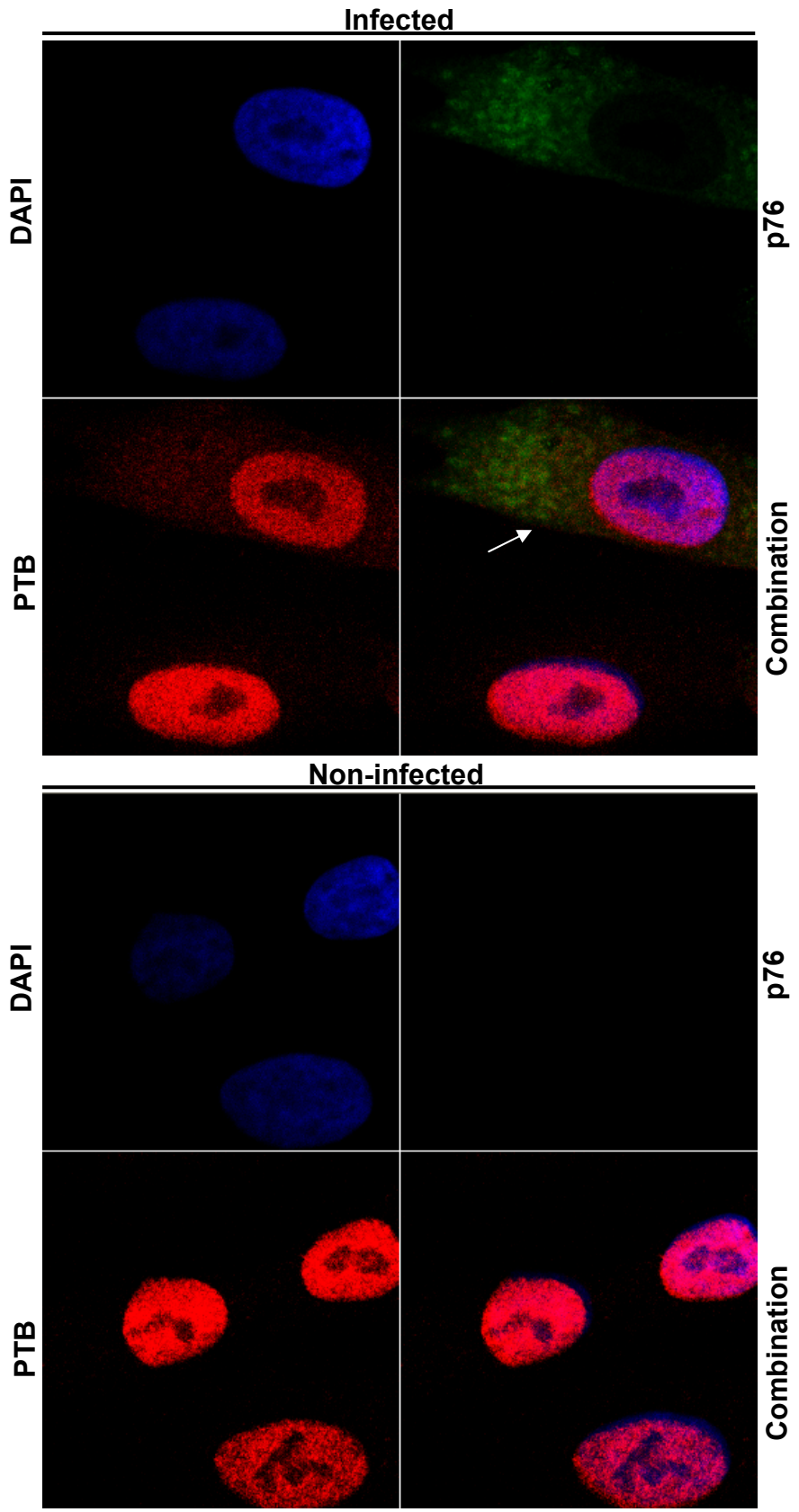


Figure 3.22. FCV infected cells have increased levels of PTB in the cytoplasm. CRFK cells were infected with FCV for 16 h at 32 °C and at an m.o.i. of 0.5. Infected and control cells were fixed and stained for p76 (**green**) and PTB (DH17 monoclonal) (**red**). DAPI was used for nuclei (**blue**) staining. The cells were observed using confocal microscopy. The white arrow indicates the cell with high levels of p76

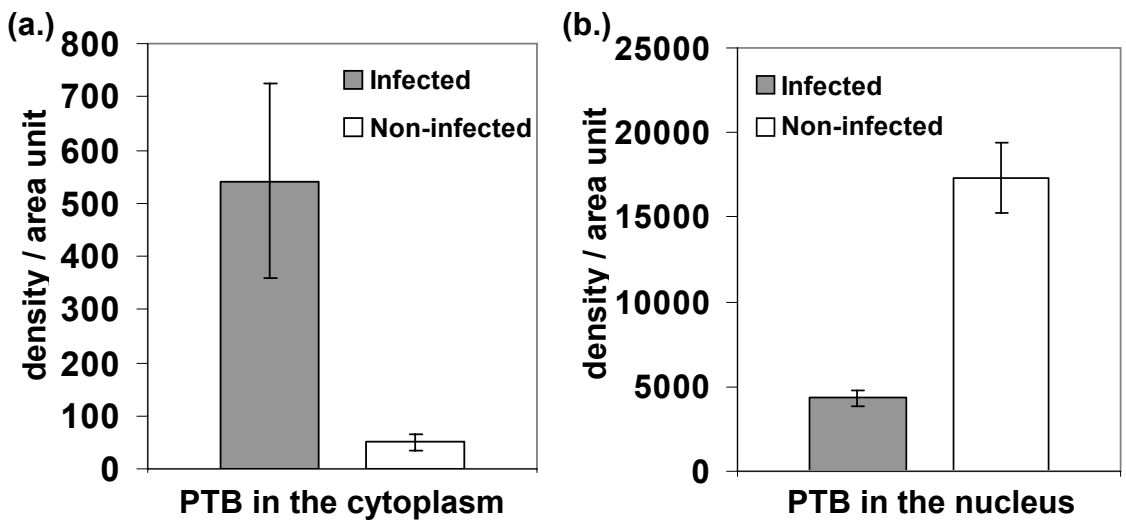


Figure 3.23. FCV infected cells have increased levels of PTB in the cytoplasm and decreased levels in the nucleus. CRFK cells were infected with FCV for 16 h at 32 °C and at an m.o.i. of 0.5. Infected and control cells were fixed and stained for p76 and PTB (DH17 monoclonal). The cells were observed using confocal microscopy and the intensity of cytoplasmic and nuclear PTB staining was determined using the ImageQuant 5.0 software. **(a.)** The density of PTB in the cytoplasm of infected and non-infected cells. **(b.)** The density of PTB in the nucleus of infected and non-infected cells. The density is measured in ImageQuant density arbitrary units per area unit.

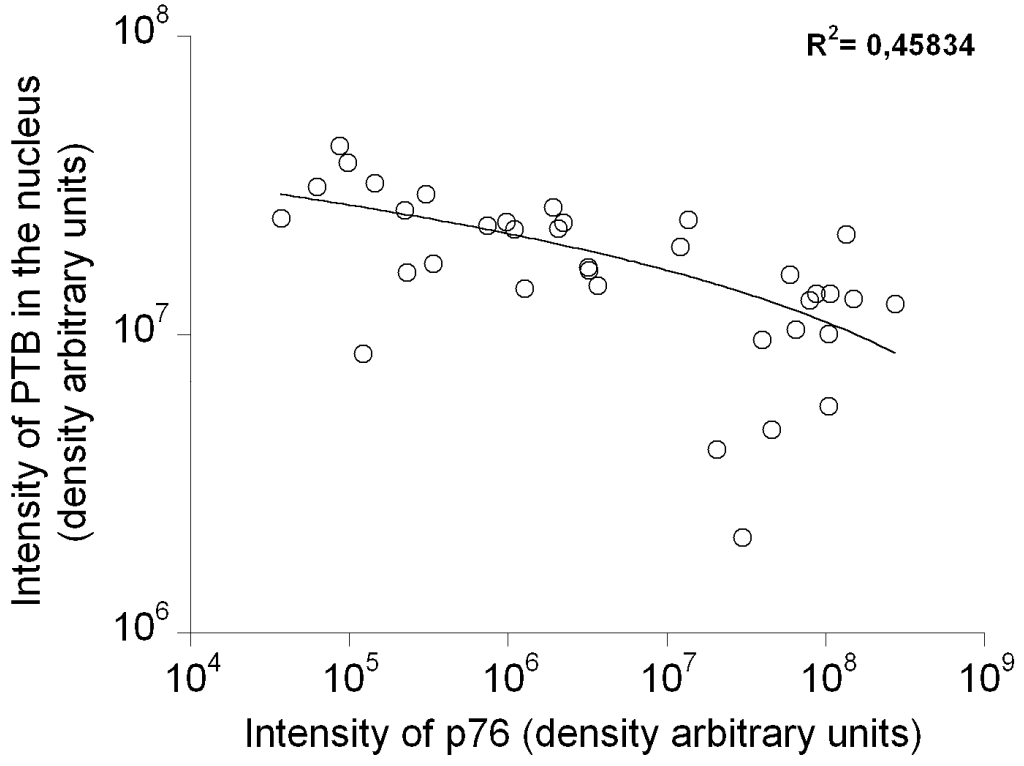


Figure 3.24. Correlation between p76 levels and the levels of PTB in the nucleus in FCV infected cells. CRFK cells were infected with FCV for 16 h at 32 °C and at an m.o.i. of 0.5. Infected and control cells were fixed and stained for p76 and PTB (DH17 monoclonal). The cells were observed using confocal microscopy and the intensity of p76 and nuclear PTB staining was determined using the ImageQuant 5.0 software. The intensity of p76 staining in the cell was plotted against the intensity of PTB staining in the nucleus. The intensity is measured in ImageQuant density arbitrary units.

shown). Thus, during the infection of CRFK cells with FCV, PTB demonstrated redistribution from the nucleus to the cytoplasm but also a reduction in total levels of the protein as the reduction of the nuclear fraction did not match the increase of the cytoplasmic fraction (**Fig. 3.23** and **3.24**). This overall decrease of PTB levels in FCV infected cells can be easily observed in **Figure 3.21.2**. More detailed pictures of FCV infected cells demonstated some overlap of the p76 and PTB signals and in some cases PTB staining was peripherally associated with p76 containing replication complexes (**Fig. 3.25**).

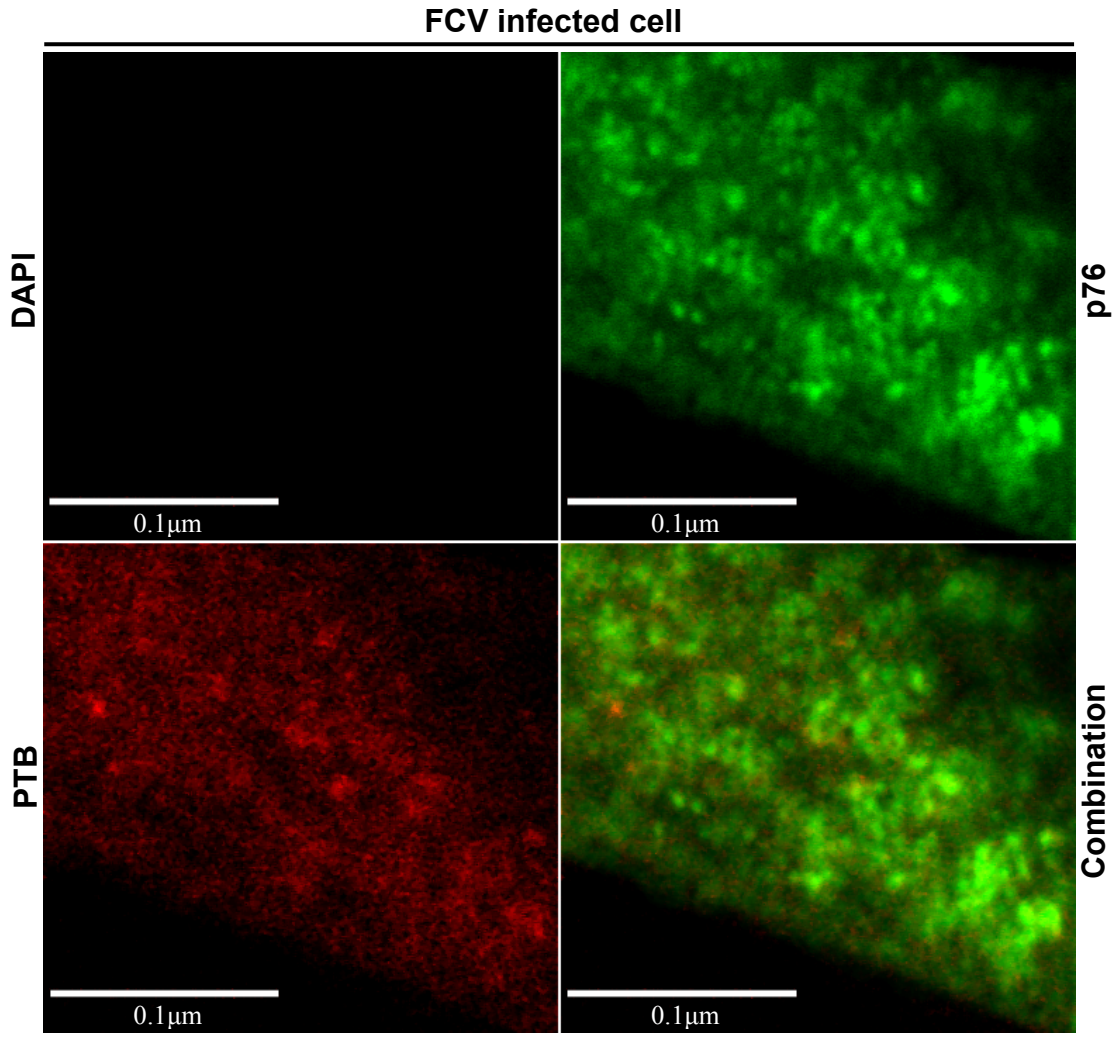


Figure 3.25. Localisation of PTB in the cytoplasm of FCV infected CRFK cells. CRFK cells were infected with FCV for 16 h at 32 °C and at an m.o.i. of 0.5. Infected and control cells were fixed and stained for p76 (**green**) and PTB (DH17 monoclonal) (**red**). DAPI was used for nuclei (**blue**) staining. The cells were observed using confocal microscopy.

3.13. Discussion

In general, the 5' and 3' extremities of viral RNA genomes must fold into defined three-dimensional structures in order to adopt a functional state. As a result of structural promiscuity and an abundance of intramolecular interactions, alternative non-functional conformations are also adopted, significantly slowing the appearance of a functional conformation (Treiber & Williamson, 2001). As a consequence, it has been suggested that RNA folding requires the aid of proteins with chaperone activity that possibly trap or resolve misfolded structures (Herschlag, 1995).

The interaction of host-cell nucleic acid-binding proteins with the genomes of positive-stranded RNA viruses is known to play a role in many aspects of the virus life cycle. The majority of these proteins are predicted to function as RNA chaperones, allowing the viral RNA to adopt a functional conformation. In the case of cellular or viral IRES elements, the binding of host-cell proteins to RNA is thought to lead to structural rearrangements, usually in close proximity to the protein-binding site, resulting in the formation of a conformation suitable for translation initiation (Martinez-Salas et al., 2001, Pickering et al., 2004). These proteins, known as IRES trans-acting factors (ITAFs), include PTB isoforms, poly(rC)-binding protein, La, hnRNP K, unr (upstream of N-ras), nucleolin and many others (reviewed by Stoneley & Willis, 2004).

In the present study PTB was identified as a host-cell protein required for efficient calicivirus replication in a temperature-dependent manner. A more important role for PTB at temperatures above and below 37 °C would agree with the hypothesis

that PTB functions as an RNA chaperone, aiding in the correct folding of viral RNA. The lack of a significant effect of PTB siRNAs on FCV replication at 37 °C, the temperature at which the virus has been repeatedly passaged, is intriguing. Although viral RNA polymerase levels were reduced to 65 % of the levels observed in control siRNA-treated cells (**Fig. 3.11**), no effect on virus titre was observed. It is possible that the RNA chaperone activity of PTB is only required in conditions where non-functional RNA structures are stabilized (e.g. temperatures <37 °C) or functional structures are destabilized (e.g. temperatures >37 °C). It is important to note that although RNA interference-mediated knockdown of PTB significantly reduced PTB levels, detectable PTB remained (**Fig. 3.7**). Hence, the PTB remaining after siRNA-mediated knockdown may be sufficient for correct RNA folding at 37 °C, but increased levels are required to maintain a functional conformation at non-favourable temperatures or in circumstances where other RNA chaperone factors are absent. Previous studies on EMCV IRES-mediated translation have demonstrated that although a wild-type IRES directing EMCV polyprotein synthesis does not require PTB for efficient translation, an IRES with an enlarged A-rich bulge is highly dependent on PTB (Kaminski & Jackson, 1998). As a result, it was presumed that PTB plays a significant role in maintaining an appropriate higher order structure for translation initiation only when non-functional conformations are apparent (Kaminski & Jackson, 1998). This observation would fit with our hypothesis that the function of PTB in the calicivirus life cycle is only required under 'unfavourable' conditions.

An additional factor that may affect the relative requirement of RNA for a particular RNA chaperone is the expression levels of other interacting host-cell factors. The relative expression levels of such factors may be significantly different in

primary tissues compared to the levels observed in immortalized cell lines. The temperature of the environment in which the virus replicates is also likely to be a determining factor in the relative contribution of PTB to the virus life cycle. Given that feline body core temperature ranges from 38 to 39 °C and can rise to 41.5 °C during FCV infection (Poulet et al., 2005), we would predict PTB plays a functional role in FCV replication *in vivo*.

Similar temperature sensitivity of the RNA chaperone activity of PTB has also been highlighted during trans-splicing of the thymidylate synthase group 1 intron (Belisova et al., 2005). Whereas trans-splicing occurs in a protein-independent manner at 55 °C, the reaction is significantly reduced at 37 °C due to an inability of the RNA to fold into a splicing-competent conformation. PTB was found to stimulate the rate of trans-splicing at 37 °C by threefold (Belisova et al., 2005). This increased requirement for PTB at reduced temperature was due to stabilization of RNA structures that were non-functional for splicing.

Previous studies have highlighted that the primary role for PTB in the life cycle of many positive-stranded RNA viruses is at the level of viral translation (Belsham & Sonenberg, 2000, Pilipenko et al., 2001). The only available means for the study of FCV translation is the *in vitro* RRL translation system (Goodfellow et al., 2005). In this system PTB acted as negative regulator of FCV translation in a specific manner as the effect on FMDV IRES and cap-dependent translation was insignificant and at high concentrations non-specific to PTB. (**Fig. 3.17** and **3.18**). An observation that is important to be clarified is the limited increase of the FMDV translation upon addition of PTB as it is well known that FMDV IRES function is dependent on PTB.

During the original investigation of the involvement of PTB in FMDV translation, the dependence on PTB was observed only in RRLs depleted of PTB (Niepmann et al., 1997). Indeed, previous work on PTB depleted RRLs showed that absence of PTB did not affect FCV translation, while FMDV translation was significantly inhibited (data not shown). The temperature dependent effect of PTB on FCV *in vitro* translation was in agreement with a similar temperature dependent requirement for the virus replication in tissue culture and provided additional evidence towards the RNA chaperone activity of PTB (**Fig. 3.19**).

A major difference between the *in vitro* translation and the replication of the virus in tissue culture was that during the viral infection the knockdown of PTB was responsible for the reduction of the viral yield, while in the *in vitro* translation system a reduction of viral translation was observed upon addition of recombinant PTB. How can a virus benefit by the reduction of its translation? Positive strand RNA viruses use their RNA as template for both translation and replication. At the initial stages of infection it is crucial for the virus to transform the intracellular environment in order to achieve its replication (Green et al., 2002, Schwartz et al., 2004). This can only happen by intensive translation from the viral RNA to produce the proteins required for the rearrangement of the cell membranous structures which lead to the formation of the replication complexes (van Kuppeveld et al., 1997). As the microenvironment of each replication complex becomes saturated with viral proteins, translation is decelerated to favour the production of new viral RNAs. This switch between translation and replication must occur as the RdRp proceeds in a direction opposite to the ribosome during negative-strand RNA synthesis. The involvement of PCBP2 in the switch between translation and replication in polioviruses signified the importance

of host-cell RNA binding proteins in this process. It is possible that PTB, through interaction with the calicivirus RNA (possibly as part of a larger RNP complex) decreases the translation rate by sequestration of the 5'extremity from the translational machinery, thereby promoting higher rates of replication at later stages of the virus life cycle.

An attempt to verify the role of PTB as a negative regulator of FCV translation in tissue culture was made by selective digestion of the genomic RNA in the mixture of viral RNAs using RNase H. The inactivation of the genomic RNA allowed translation from only the subgenomic RNA that, in the absence of polymerase, cannot be replicated. The translation of the subgenomic RNA in CRFK cells was significantly increased under low levels PTB that indicated again a repression role for PTB on viral translation. However, the observed processing of the LC into mature major capsid protein indicated the presence of either a cellular or viral protease, capable of capsid cleavage. It has been reported previously that caspase mediated cleavage of capsid protein occurs during FCV infection (Al-Molawi et al., 2003). The caspase cleavage of the 62 kDa mature capsid protein resulted in a product of apparent size of 40 kDa, but the cleavage site on the protein was not mapped (Al-Molawi et al., 2003). If the cleavage occurred closer to the C terminus the deletion from the 67 kDa LC of about 22 kDa would result in a 55 kDa protein[6], similar in size with the mature capsid. The cationic lipid transfection reagents such as Lipofectamine used in this study for the transfection of the viral RNA into cells induce apoptosis activating the caspase cascade that could result in the cleavage of the LC during the overnight exposure to caspases (Iwaoka et al., 2006). Another possibility could be that

[6] The apparent weight as determined by SDS-PAGE. The actual molecular weight could be different.

other cellular proteases induce the capsid maturation as it has been reported previously (Geissler et al., 1999). However, in that study such maturation of FCV capsid did not occur in CRFK cells (Geissler et al., 1999), a result verified in the present study by the expression of LC from the subgenomic RNA construct (**Fig. 3.20**). It is not known if specific proteases are upregulated during transfection of dsRNA that could explain the occurrence of maturation only in the cell transfected with RNA. A final possibility could be, even if p76 could not be detected by western blot, that undetectable amounts of the viral protease could induce the cleavage of the leader peptide from LC.

To further investigate the role of PTB during FCV infection the binding of PTB was mapped on the 5' extremity of the virus. PTB was not restricted on a specific binding site rather it interacted with a variety of pyrimidine stretches on the RNA (**Fig. 3.15**). The presence of four RRMs on PTB is responsible for its complicated binding properties that have been thoroughly dissected for FMDV IRES (Song et al., 2005). A strong PTB-binding site is present in the second domain of the IRES, where a number of pyrimidines in the domain contribute to the interaction with PTB (Luz & Beck, 1991). Additional binding sites for PTB have been identified in several parts of the fourth and fifth RNA domain further downstream on FMDV IRES (Luz & Beck, 1991, Kolupaeva et al., 1996).

Production of viruses that encompassed mutations in the binding sites of PTB was achieved using the FCV reverse genetics system (Sosnovtsev & Green, 1995). However, the mutant viruses (even the double mutant virus) demonstrated no defect during their replication in CRFK cells compared to the wild-type FCV. It has been

well documented that such RNA-protein interactions affect virus replication often in a cell-type specific manner (Chang et al., 1993, Guest et al., 2004, Merrill et al., 2006). For example, the attenuated vaccine strain of poliovirus type 3 (Sabin 3) is able to grow to high titres in the traditional tissue culture cell lines, but is attenuated during the infection of neuronal cells (Guest et al., 2004). This attenuation was attributed to the reduced binding of PTB caused by the alteration of the secondary structure by a single mutation close to one of the PTB binding sites on the poliovirus IRES. The effect of the mutation on the binding of PTB on the Sabin type 3 IRES in combination with the significantly reduced levels of PTB in the neuronal cells conferred a 2.5 to 4 fold decrease in the viral translation compared to the wild-type poliovirus type 3 virus (Leon) (Guest et al., 2004). It is possible that the kidney-origin of the CRFK cell line that has been traditionally used for the study of FCV replication is not representative of the conditions during a normal FCV infection of the upper respiratory tract target cells. Another possibility could be that PTB is affecting FCV replication via interaction with a different region of the viral RNA. A well documented equivalent is the involvement of PTB in HCV life cycle. As discussed previously in **Chapter 1**, PTB was shown to interact with a variety of regions (IRES, core and 3'UTR) of HCV RNA, while the functional data concerning the involvement of the different RNA domains in the regulation network till recently remained rather contradictory (Song et al., 2006). Such a region could be the sgRNA in which translation and/or replication could be affected through PTB binding to its 5' extremity (**Fig. 3.3**). Furthermore this interaction has been evolutionally conserved in the MNV genome as the 5'extremity of the MNV sgRNA demonstrated a good affinity for PTB, while the MNV 5' genomic extremity demonstrated only residual binding (**Fig. 3.3**).

An important aspect of PTB behaviour during FCV infection is its localisation. If PTB remained nuclear during the infection, as it does in non-infected cells, the ensuing discussion of an interaction between PTB and the viral genome in the virus life cycle would be of less significance. The observation by confocal microscopy of CRFK cells infected with FCV, demonstrated that PTB translocated during the infection from the nucleus to the cytoplasm, while the total staining of PTB showed a dramatic decrease. This effect had been observed when the infection was carried out at 37 ^{o}C, but was more obvious when the infections were incubated at 32 ^{o}C. The more apparent translocation of PTB at 32 ^{o}C could provide an additional explanation for the temperature dependent effect of PTB knockdown in FCV replication. Nuclear factors important for viral replication, such as PTB, have been demonstrated to translocate from the nucleus to the cytoplasm during poliovirus (Gustin & Sarnow, 2001) and rhinovirus (Gustin & Sarnow, 2002) infection. Disruption of the nucleopores and the proteolytic cleavage or phosphorylation of PTB are factors that induce the movement of PTB to the cytoplasm (Kamath et al., 2001, Xie et al., 2003). The limited co-localisation between PTB and the viral polymerase, p76, could possibly indicate that PTB may be associated only with a particular form of RNA (e.g. dsRNA intermediate) or that the epitope of the monoclonal antibody used for the confocal microscopy was masked when PTB was in the replication complexes. The translocation of PTB to the cytoplasm was followed by an apparent decrease in the levels of the protein in the cell that was more obvious at 32 ^{o}C than at 37 ^{o}C. During the study of the effect of PTB knockdown in the viral replication the levels of PTB in the control cells (GFP siRNA, **Fig. 3.8**) did not alter during the course of the infection, while in the same cells when the infection was carried out at 32 ^{o}C PTB levels demonstrated a decrease (**Fig. 3.11**). This observation signified a possible

downregulation of PTB during FCV infection or proteolytic cleavage of the protein that could not be detected by western blot (**Fig. 3.11**). The role of such a downregulation of PTB is not known, however, it is known that PTB is cleaved by caspases during apoptosis (Back et al., 2002b) and apoptosis is induced during FCV infection (Sosnovtsev et al., 2003). PTB is also cleaved by poliovirus protease 3CD during poliovirus infection, but such an activity has not been observed for the FCV analog, p76 (Back et al., 2002a).

In light of these data, PTB seems to play a key role in the calicivirus life cycle possibly as component of the switch between translation and replication giving further insight in this important for the virus process. However, further evidence is required to support this role, particularly with use of a wide range of cell lines or the *in vivo* animal model.

Chapter 4.

Functional analysis of RNA structures in the MNV genome

4.1. Introduction

The identification of functional RNA elements in an mRNA or a vRNA provides an alternative to the protein based approach already described for the study of RNA-protein interactions. These functional elements often interact with proteins that constitute or regulate the translation or replication machinery of a virus. Thus the identification of functional RNA structures involved in the major aspects of viral replication is crucial for the understanding of the life cycle of positive stranded RNA viruses such as caliciviruses. During the course of my studies on the role of RNA-protein interactions in FCV life cycle, an alternative model system for the study of calicivirus biology became available, namely murine norovirus (MNV), a newly identified member of the *norovirus* genus, which can be propagated in tissue culture (Wobus et al., 2004). As such, this is also a more representative model for the study of human caliciviruses. However, the lack of a reverse genetics system for MNV to allow the study of the effect of mutations on viral phenotype, as was readily available for FCV, had kept the focus of my studies on FCV. Such a system was successfully developed by my colleagues in October 2006 (Chaudhry et al., 2007) and provided a powerful tool for the study of MNV. The need for a reverse genetics system was so great that soon after the first report another group published an additional method for the production of genetically defined MNV (Ward et al., 2007).

The aim of the work presented in this chapter was to take advantage of this newly developed MNV reverse genetics system and use it to identify functional RNA elements in murine norovirus genome. Characterisation of the mutant viruses would

demonstrate the requirement for a certain RNA structure or sequences while it could also indicate the process of the viral life cycle in which this structure is involved.

4.2. Prediction of higher order RNA structures in the MNV genome

Large scale computational thermodynamic analysis and suppression of synonymous site variation analysis[7] of the MNV genome showed regions of highly structured RNA at the 5' and 3' extremities of the viral genome (**Fig. 4.1b**). In addition, a region overlapping the start of the subgenomic RNA region was also predicted to have higher order RNA structures (**Fig. 4.1b**). Using a variety of free energy minimisation algorithms, such as mfold (Zuker, 2003) and pfold (Knudsen & Hein, 2003), thermodynamically stable RNA structures were predicted for these regions (**Fig. 4.1a**). The regions predicted to form these RNA structures are highly conserved among different MNV strains and in most cases the identity reaches 100 % (data not shown). Such low variability regions in an mRNA have a high possibility of accommodating functional RNA structures. This finding, combined with low p-number (P-Num) values, which represent the number of different base pairs a specific base can form in a set of potential structures predicted for a given RNA sequence, can give a good indication towards the prediction of a stable RNA secondary structure (Zuker, 2003).

[7] A computational method that determines the evolutional variation of a codon in a coding region. When a region of an RNA contains an essential RNA structure, its conservation limits the variation of the nucleotides in the triplet. This codon variation suppression is forced by the combined need for a conserved RNA structure and amino-acid sequence. This analysis was conducted in collaboration with Prof. Peter Simmonds (University of Edinburgh)

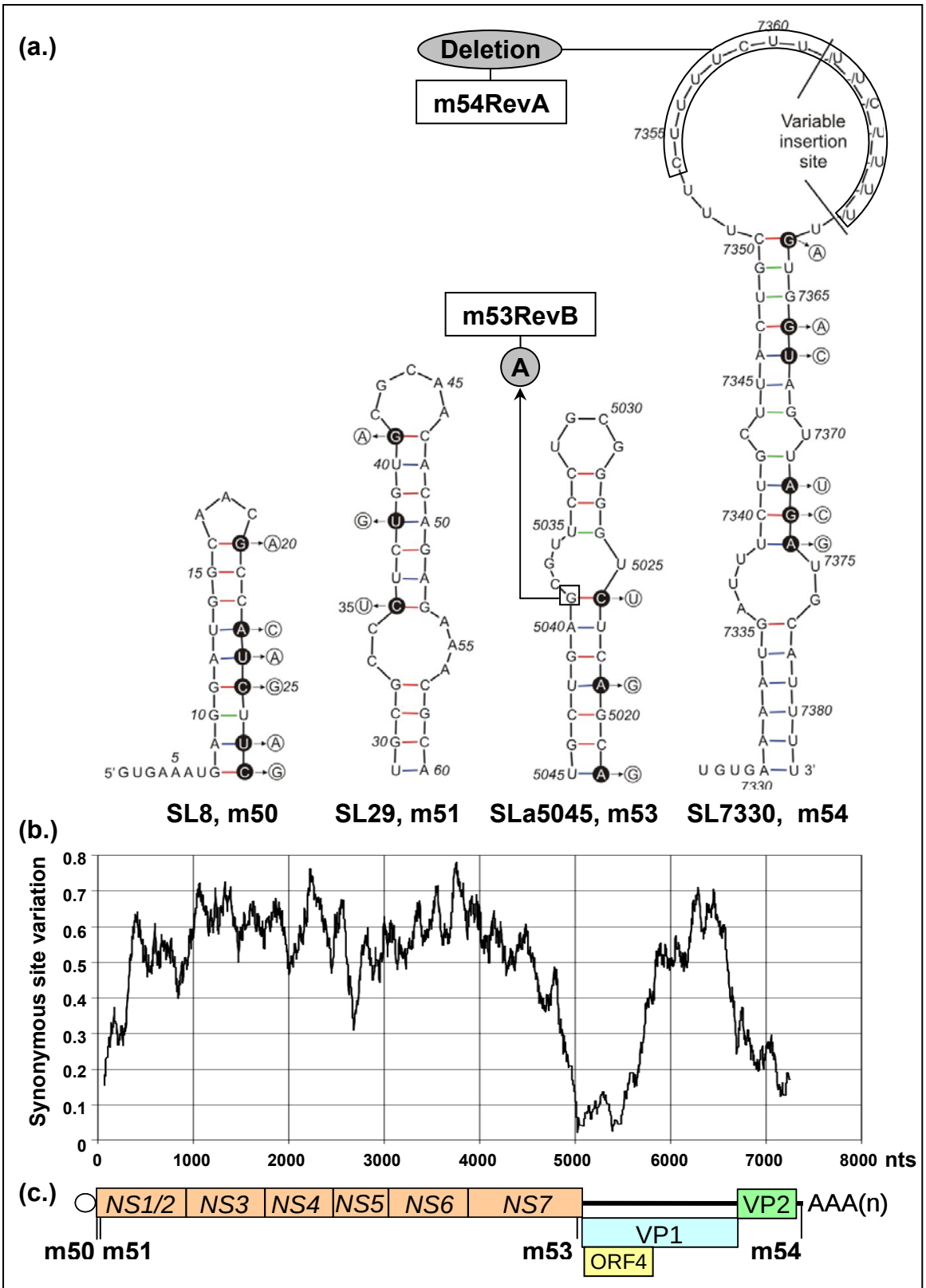


Figure 4.1. Predicted RNA structures in the MNV genome. (**a.**) RNA structures predicted using energy minimisation algorithms. Highlighted in the black circles are the nucleotides mutated to the nucleotides presented into the white circles. (**b.**) Suppression of synonymous site variation (SSSV) analysis for the MNV genome (courtesy Prof. Peter Simmonds, University of Edinburgh). Low values of variation represent a high possibility of conserved RNA structure and vice-versa. The MNV genome is presented under the SSSV graph and shows the position of the predicted stem-loops and the respective mutations. The suppression mutations (grey circle) that reverted the lethal phenotype of m53 and m54 are highlighted in a box, (nts = nucleotides)

Two of the predicted stem loops were situated at the 5'extremity of the MNV genomic RNA just after the short 5'UTR. The first predicted stem loop is situated 8 nucleotides from the 5' end and consists of a 9 base pair stem, terminated by a three nucleotide loop (SL8, **Fig. 4.1a**). Such a stem loop can be predicted for all known caliciviruses, however without any similarity in either primary sequence or stem size (data not shown). In order to assess the importance of this structure in MNV replication, a set of mutations were introduced that destabilised the stem by braking 3 A-U and 3 G-C base pairs (m50, **Fig. 4.1a**). The introduction of mutations was limited by the fact that the stem accommodates nucleotides which form part of the first open reading frame of the virus (ORF1). Such a limitation usually allows the change of the most degenerate in the genetic code third base of a triplet, hence only nucleotide changes that did not alter the amino-acid sequence were introduced. However, in the case of m50 the protein sequence contained two serines that are represented in the genetic code by 6 different codons, giving more flexibility in the choice of nucleotides.

The second stem loop of the 5' extremity was situated just after the first stem loop at position 29 of the MNV genome (SL29). An internal bulge separated a 4-nucleotide bottom and a 7-nucleotide top stem (**Fig. 4.1a)**. The mutations for the disruption of this stem loop were focused on the longer 7-nuclotide top stem (m51, **Fig. 4.1a**). In contrast to the m50 mutant, the amino-acid sequence restrictions in m51 allowed the alteration of only 3 nucleotides which, according to mfold predictions were enough to destabilise the structure. As the altered bases were located at the third base position of the respective ORF1 codon, the introduced nucleotides were selected according to their ability to reform a stable stem by subsequent changes of the

downstream nucleotides, which constituted the 3' partners of the stem base pairs. Such a second 5' extremity stem loop structure can also be predicted for other noroviruses and several other caliciviruses (data not shown).

Another region that showed a computationally high possibility of accommodating functional RNA structures was the junction between ORF1 and ORF2. This junction is also the start of the region which represents the sequence of the MNV subgenomic RNA (sgRNA). The hypothesis was that structures downstream of the junction would represent the 5' extremity of the subgenomic RNA and such structures may regulate sgRNA translation and replication. The sequences upstream of the junction could form part of a promoter required for the initiation of subgenomic RNA synthesis. This hypothesis was supported by a study on RHDV which demonstrated a requirement for 60 nts upstream of the start of the subgenomic RNA for the *in vitro* synthesis of a subgenomic RNA from a negative sense genomic RNA template by the viral RdRp (Morales et al., 2004). As the sequence downstream of MNV ORF1-ORF2 junction has been predicted to accommodate an alternative ORF (ORF4), alterations in RNA structures of this region are rather limited by the requirement to maintain two overlapping protein sequences. So, the computational predictions focused on the sequence upstream of the sgRNA initiation site. A stem loop structure was predicted in this region, however, based on the mean free energy difference, it was predicted to form with a slightly higher probability in the negative sense RNA than the positive sense. This fact led us to draw the structure in its negative sense form (SLa5045, **Fig. 4.1a**). Such a stem loop could be predicted for all caliciviruses and was invariably situated 6 nucleotides upstream of the start of the sgRNA (**Fig. 4.2**). Three nucleotide changes that were permitted by the conservation

of amino acid sequence were introduced in the lower 7-nucleotide stem in order to destabilise the structure (m53, **Fig. 4.1a**). Unfortunately, due to the limited choices of alternative synonymous nucleotides, rather than complete disruption of base pairing, the introduced mutations led to the formation of three wobble G•U base pairs. In each case however, these mutations were predicted to lower the likelihood of structure, as the G•U pairs are thermodynamically less stable than A-U or G-C pairs which they replaced. As in the case of m51, the introduced mutations were designed in such a way that compensatory mutations could restore the stem without affecting the amino-acid sequence.

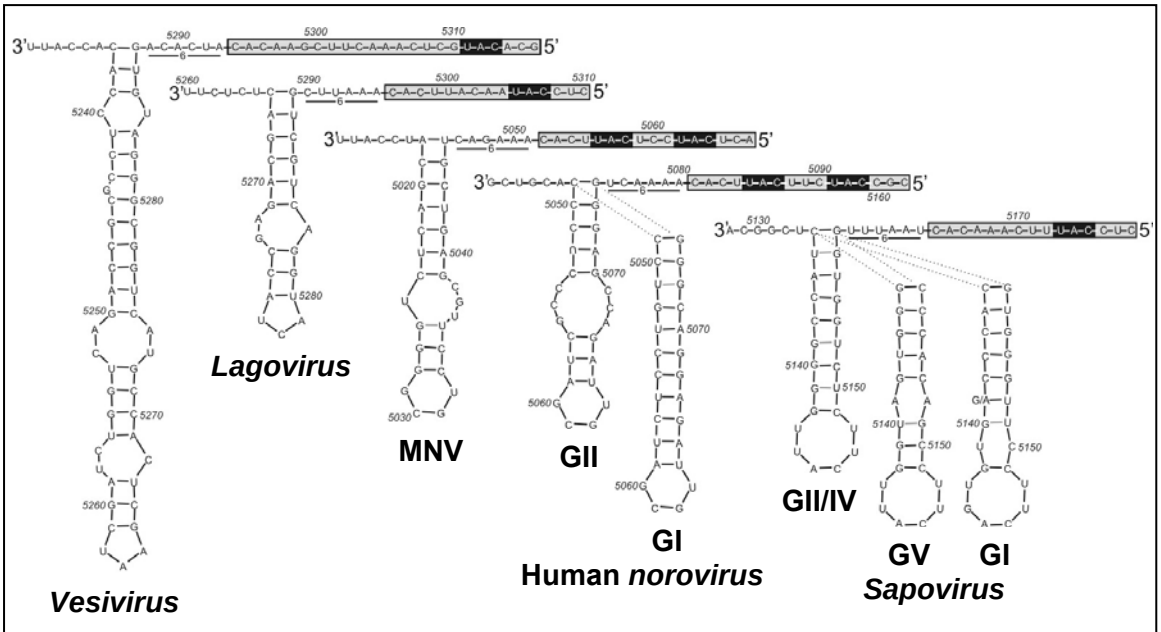


Figure 4.2. A stem loop structure upstream of the subgenomic RNA start is predicted for a variety of representative caliciviruses. The structure of the stem loop structure is drawn in the negative sense orientation. The framed nucleotides represent the template of the subgenomic RNA, while the C at the beginning is the template for the first nucleotide of the subgenomic RNA. The 6 nucleotides between the start of the subgenomic RNA template and the predicted stem-loop are highlighted. (GI and GII are to genogroups of human noroviruses; GI, GII, GIV and GV are genogroups of sapoviruses. The initiation codons (AUG) are highlighted in black

The last region to show a potential to form higher order RNA secondary structures was the 3' UTR. A stable stem loop structure was predicted at the 3' end of MNV 3'UTR (SL7330, **Fig. 4.1a**). As shown in **Figure 4.3** the sequence in the region that corresponded to the two stems was conserved among MNV strains, while the region that corresponded to the loop was highly variable. This fact increased the "predictability" of the stem loop structure, especially in alignment based RNA structure prediction algorithms such as p-fold. In order to assess the requirement of this 3' end stem loop 6 mutations were introduced in the top stem (m54, **Fig. 4.1a**). The fact that in the 3' UTR, the sequence of the RNA was not limited by a requirement to conserve the amino-acid sequence, meant that there was greater flexibility in the changes which could be introduced, compared to m50, m51 and m53 which are all coding.

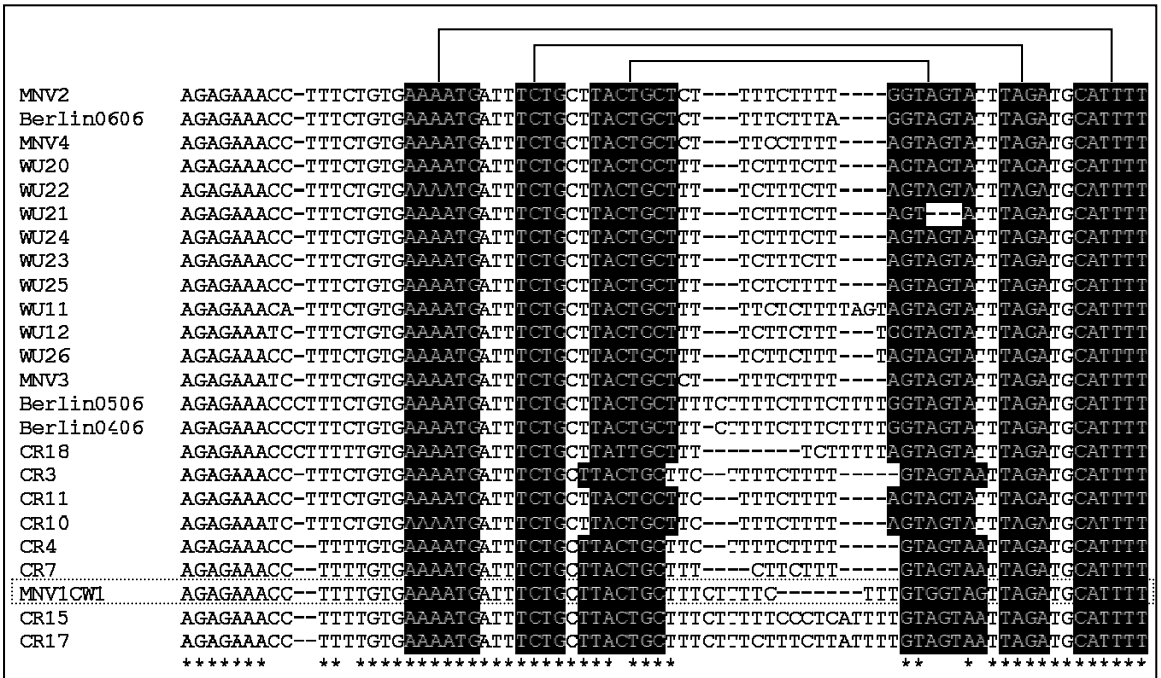


Figure 4.3. Alignment of the 3' end stem loop of MNV RNA. ClustalW alignment of all the MNV strains available in GenBank (NCBI) for the last 70 nts of the MNV1 genome. Highlighted in black are the nucleotides that form the three stems of the 3' end stem loop. The innermost bracket encompasses the highly variable polypyrimidine hairpin loop. The sequence of the MNV1 infectious cDNA clone used in all the experiments is highlighted in the dotted box.

4.3. Specific RNA structures are required for the MNV replication

The mutations in the RNA structures mentioned above were cloned into the full length MNV-1 infectious clone (pT7MNV:3'RZ). The mutated clones were tested for their ability to produce virus after transfection in BSRT7 cells infected with a fowl pox virus expressing T7 RNA polymerase (FPVT7) (Chaudhry et al., 2007). The viruses produced after 24 h in this reverse genetics system represent a single replication cycle as although MNV can replicate in BSRT7 cells, it cannot infect them (Chaudhry et al., 2007). The SL8 disrupting mutations in m50 resulted in a significantly reduced viral titre (approximately 20 times lower than the wild type virus) while the recovered virus also produced a small plaque phenotype (**Fig. 4.4**). The recovery of the viral clone which contained mutations in SL29 (m51) yielded about 16 times less virus than the wild type, while no alteration to the plaque phenotype was observed (**Fig. 4.4**). Considering the conservation of the region where both m50 and m51 mutations are situated it was rather surprising to see such a small effect on virus replication. In the m50 mutant the virus showed limited but not absolute dependence on the stability of the first 5' end stem loop, SL8. The mutations in the second 5' end stem loop (SL29 as disrupted in m51), demonstrated either that there is a limited requirement of this region for the efficient recovery of virus, or that the introduced mutations were not able to efficiently disrupt the stem loop *in vivo*.

A more profound effect was observed for the m53 mutant that disrupted the stem loop upstream of ORF1-ORF2 junction (SLa5045). The introduced mutations resulted in a lethal phenotype signifying that the mutated RNA structure is important for viral replication (**Fig. 4.4)**. A lethal phenotype was also produced by the mutations

in the 3' UTR stem loop (SL7330), again demonstrating a dependence of this region for virus replication (**Fig. 4.4)**. An important observation was that one of MNV strain isolated from *Rag1*$^{-/-}$ IFN-γR$^{-/-}$ laboratory mice lacked two of the nucleotides mutated in m54 (nts 7366 and 7367) (**Fig. 4.3**) (Thackray et al., 2007). Therefore it is possible that the observed lethal phenotype was caused by one or more of the other introduced mutations or that at least some of the base pairing is required for the formation of a functional structure.

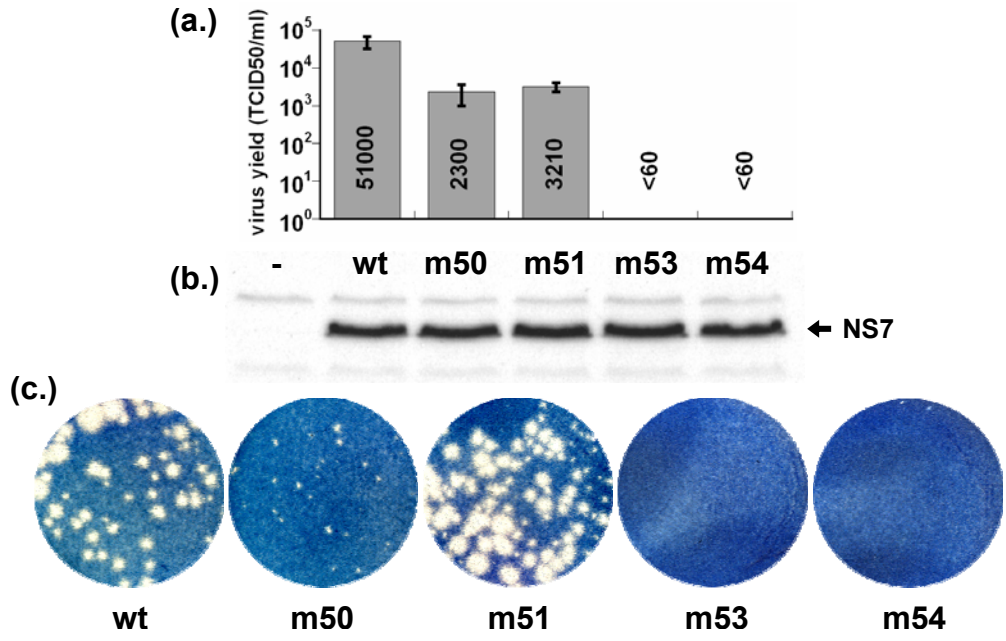


Figure 4.4. Phenotypes of the mutated viruses recovered by reverse genetics. (**a.**) The titres of the viruses produced during the recovery procedure after transfection of the mutated viral cDNA clones into BSRT7 cells infected with FPVT7 virus. (b.) Western blot for the NS7 protein for all different mutant cDNA clones that shows the ability of all the cDNA clones to produce and process the viral polyprotein. (c.) Plaques formed by the recovered mutant viruses on a monolayer of RAW 264.7 cells. Recovery and plaque phenotype are evaluated by comparison to the wild-type (wt) virus recovery. Error bars represent the standard deviation determined by 5 experiments and the limit of detection was 60 TCID50/ml.

In order to exclude the possibility that additional spurious mutations arose, outside of the manipulated region which was subsequently fully sequenced, every mutated MNV genome was represented by at least two independent clones. Furthermore, lysates of the cells infected with FPVT7 and transfected with the virus mutant MNV clones were probed for the NS7 protein (**Fig. 4.4**). The NS7 Western blot demonstrated that the mutant clones produced NS7 levels similar to wild-type clone during the recovery and served as a good indication that every clone had the same potential for the production of virus.

4.4. Deletion of the MNV 3' UTR polypyrimidine hairpin loop does not affect viral replication in tissue culture.

During the preliminary computational analysis of the predicted RNA structures in the 3' UTR of the MNV genome, a region which corresponded to the loop region of SL7330 was observed to be highly variable between different MNV strains (**Fig. 4.3**). The conservation of a poly(U/C) context appeared to be the only restriction in the changes observed. Furthermore, a specific motif, similar to the PTB consensus binding sequence of UCUU, was present in a variable number of repeats. The conservation of such a motif signified a potential involvement of the loop in the regulation of some aspect of the virus life cycle. To assess this hypothesis the polypyrimidine tract was substituted by a GNRA tetraloop which is well known to stabilise stem-loop structures (Correll & Swinger, 2003). This motif was introduced in order to minimise any disruption of the secondary structure which may have been caused by a full deletion of the poly(U/C) loop (**Fig. 4.5**). The mutated region was subsequently cloned into the MNV-1 full length clone to generate the mutant m52.

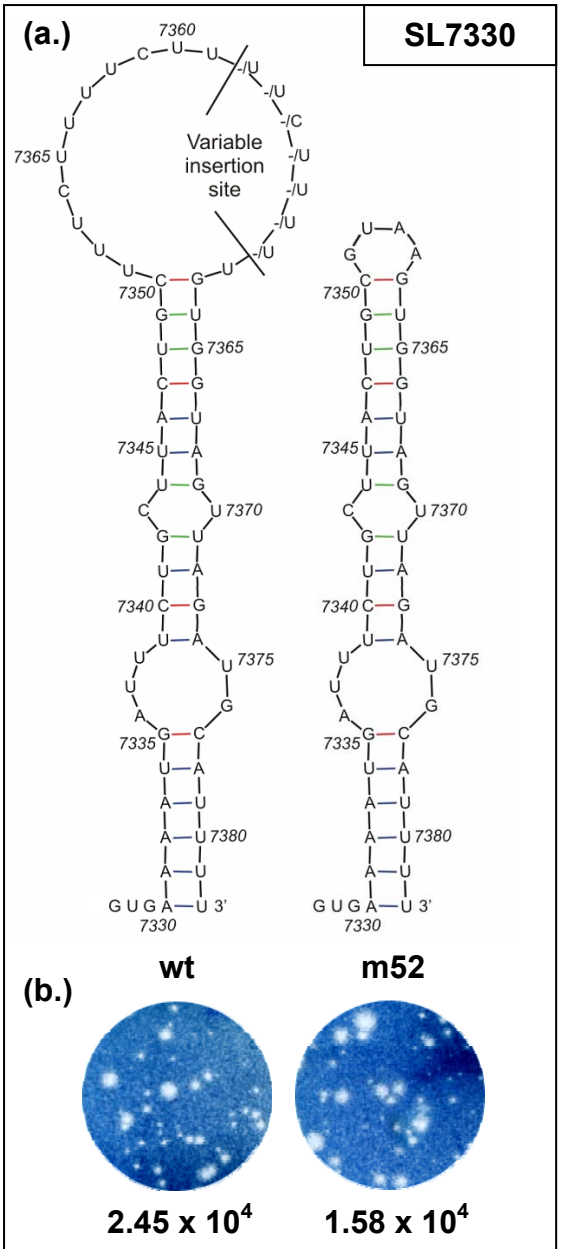


Figure 4.5. Phenotype of the 3' polypyrimidine loop-deletion virus after reverse genetics recovery. (**a.**) The predicted structure of the wild-type (wt) SL7330 stem-loop structure and the structure of the same stem loop after substitution of the loop by a GNRA motif (m52). (**b.**) Plaques formed by the recovered m52 virus on a monolayer of RAW 264.7 cells. Recovery and plaque phenotype are evaluated by comparison to the wt virus recovery.

The m52 mutated virus recovered at similar to wild-type titres while the plaque phenotype was also indistinguishable to wild-type. The kinetics of m52 replication was tested in high (4) and low (0.01) multiplicity of infection in comparison to the wild-type virus (**Fig. 4.6a,b**). While the titre of the virus yield was approximately the same for every time point of the growth curves, western blot analysis reproducibly demonstrated significantly higher levels of NS7 and VP1 proteins were produced in the m52 infected cells (**Fig. 4.6c,d**). The fact that the effect was not amplified when the virus was allowed to go through multiple replication cycles signified that the observed increase in protein levels did not affect the replication efficiency or the production of infectious virus. The increased protein levels of the m52 virus may indicate that either the poly(U/C)

tract of 3' UTR acts as a repressor of translation or that the inserted GNRA motif further stabilises SL7330, which is crucial for viral growth (as shown by the mutational analysis of this region).

As has been stated previously in **Chapter 3**, the stability of RNA structures is greatly altered by variations in the temperature at which they fold. For this reason the growth of the m52 mutant virus was examined across a temperature gradient (**Fig. 4.6e**). At high temperatures (39 ^{o}C) the mutant virus produced more NS7 protein than the wild-type, while the same was observed at the normal culture temperature of 37 ^{o}C. However, at low temperatures (32 ^{o}C) the positive effect of the mutation disappeared and the two viruses produced similar levels of NS7 protein. A possible explanation could be that the stabilisation of the stem loop by the GNRA tetraloop was more obvious at high temperatures as the destabilising effect of a large hairpin loop may be much greater than at lower temperatures, where RNA structures are stabilised. In other words, at lower temperatures the stabilisation of the RNA structure might be efficient enough that the additional thermodynamic stability conferred by the GNRA is less apparent.

Further study of the SL7330 stem-loop in **Chapter 5** demonstrated that RNA-binding proteins such as PTB and PCBP2 interact with the polypyrimidine loop of this RNA structure. The interaction was severely reduced when the loop was substituted by the GNRA motif used for the construction of the m52 mutant.

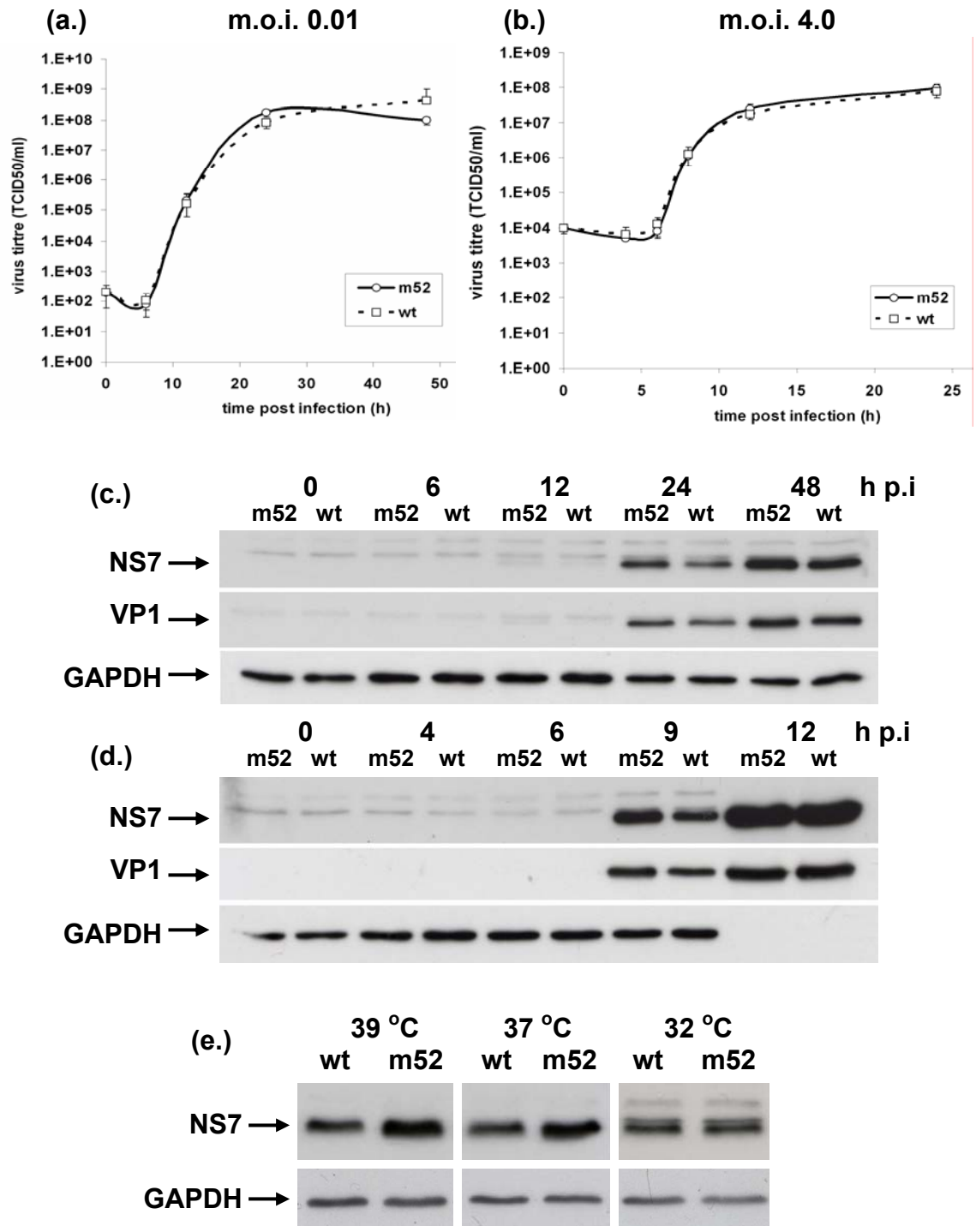


Figure 4.6. Growth kinetics and temperature sensitivity analysis of the 3' end polypyrimidine loop deletion virus (m52). (**a.**) Virus yield (in TCID50/ml) during the infection of RAW 264.7 cells with a low m.o.i. (0.01) of m52 and wt virus. (**b.**) Virus yield (in TCID50/ml) during the infection of RAW 264.7 cells with a high m.o.i. (4.0) of m52 and wt virus. (**c.** and **d.**) Probing for NS7 (polymerase), VP1 (major capsid protein) and GAPDH (control) of infected lysates at different time points of the viral growth at a low (c.) and high (d.) m.o.i. (**e.**) Western blot for NS7 (polymerase) and GAPDH (control) showing the NS7 levels produced during the replication of the m52 virus compared to wild-type virus (wt) in RAW 264.7 cells across a temperature gradient

4.5. Characterisation of naturally revertant viruses

Reverse genetics systems which are based on T7 RNA polymerase activity show an increased probability of introducing mutations into newly transcribed RNA as T7 polymerase is a highly error prone polymerase (Huang et al., 2000, Nesser et al., 2006). Indeed, in one of the attempts to recover the m53 mutant virus, a viable strain was produced. Sequencing of the full genome of the virus revealed that the initially introduced mutations in SLa5045 were still present, even after a third passage of the virus in cell culture (**Fig. 4.7a**). However, an additional mutation had been introduced which changed nucleotide 4922 from C to U (**Fig. 4.7a**). This position was 97 nucleotides upstream of the initial mutations in SLa5045 and lay within the NS7 coding region, however the alteration has no effect on the sequence of NS7 (**Fig. 4.7a**). To verify that this was the only mutation required for the suppression of the lethal phenotype, the corresponding region was cloned into the m53 full length cDNA clone. The recovery of the virus from this new clone (m53RevA) produced approximately 50 times less virus than the wild type clone (**Fig. 4.8a**). In addition, plaque assay performed using the recovered m53RevA virus demonstrated a small plaque phenotype (**Fig. 4.8a**), while the virus growth during a multistep growth curve was significantly reduced (**Fig. 4.8b**). The mutation which resulted in the suppressor phenotype (T4922C) is predicted not to participate in any of the predicted (optimal and suboptimal) RNA structures and the mechanism of the reversion remains to be revealed. Considering that the suppression nucleotide change was so far upstream the initial mutations, it seems likely that the predicted stem loop is part of a larger secondary (or maybe tertiary) structure that altogether forms a functional RNA domain, probably involved in the initiation of sgRNA synthesis.

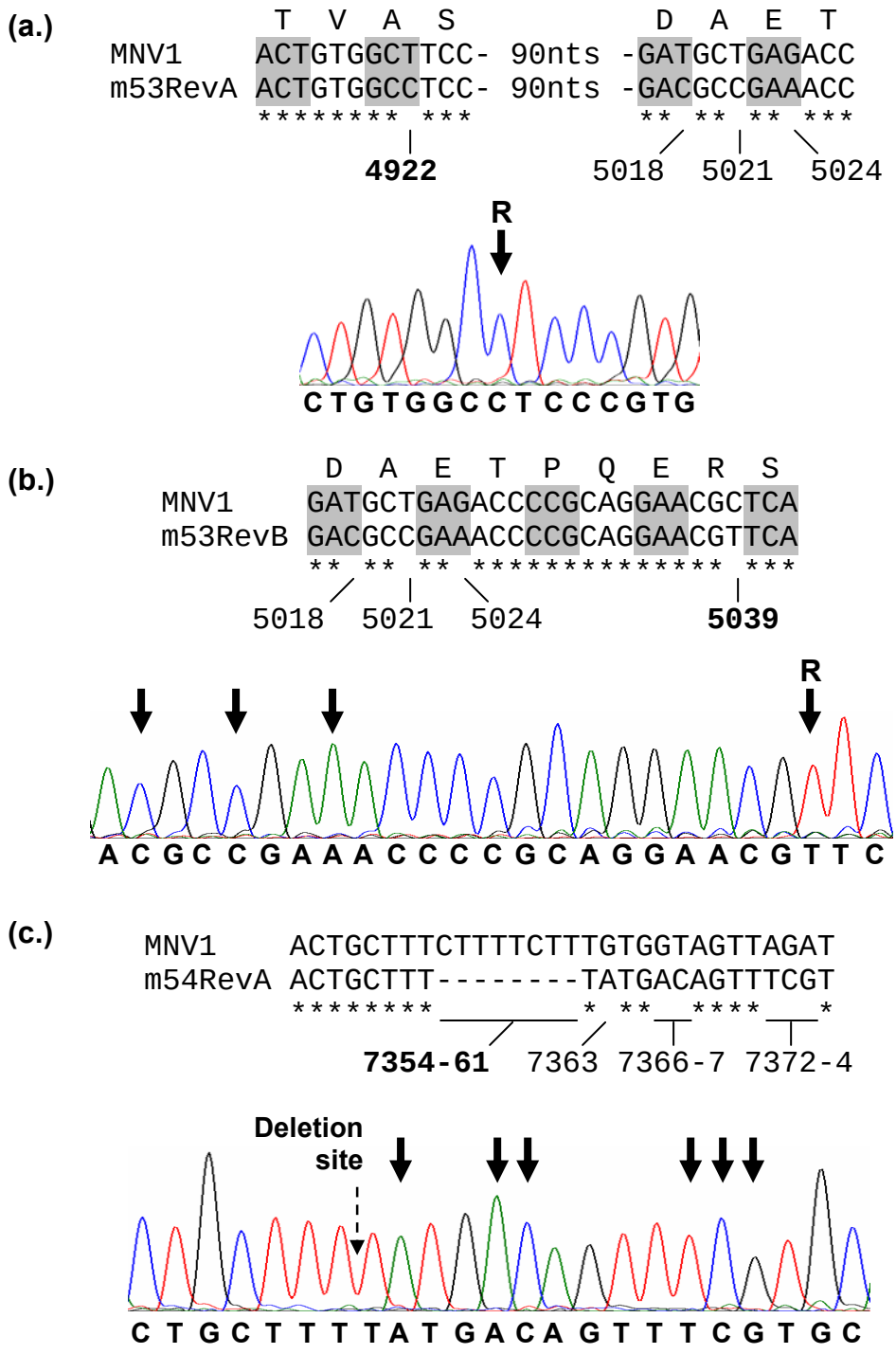


Figure 4.7. Reversion determinants of naturally revertant viruses. Sequencing of the viruses that showed reversion of the lethal phenotype caused by mutations m53 and m54 (**a., b., c.**) Alignments of the m53RevA (a) m53RevB (b) and m54RevA (c) virus sequence compared to wild-type MNV1. The nucleotide position numbers in **bold** highlight the mutations that were found in the revertant viruses, while the remaining are the mutations originally introduced. Over the alignments the respective amino-acid sequences (when applicable) are presented. Each alignment is followed by a chromatogram of the respective sequencing reaction shows the absence of major quasispecies in the initial (↓) and supression (**R**↓) mutations. The dashed arrow points at the site where the deletion of the polypyrimidine stretch occurred in m54RevA.

A second reversion of the m53 lethal phenotype was identified from an independent set of virus recoveries. In this instance, blind passage was required to obtain full cytopathic effect. Five clonal isolates from the revertant virus stock (m53RevB) were isolated by limiting dilution and partially sequenced. In addition to the originally introduced mutations in m53, all five isolates had a common nucleotide change, compared to the wild-type, (**Fig. 4.7b**). The observed C to U substitution in position 5039 was a synonymous nucleotide change that resulted in a partial reformation of the disrupted stem loop (**Fig. 4.1**). The G5024A or C5024U mutations in positive (+) or negative (-) strand RNA respectively in the m53 mutant led to the disruption of the wild-type G_{5024}-C_{5039} (+) or C_{5024}-G_{5039} (-) base pair. The C5039U alteration, generated by natural selection, reformed the base paring between the two nucleotide positions: A_{5024}-U_{5039} (+) or U_{5024}-A_{5039} (-). This reversion verified the dependence of viral replication on the formation of SLa5045 upstream of the subgenomic RNA start.

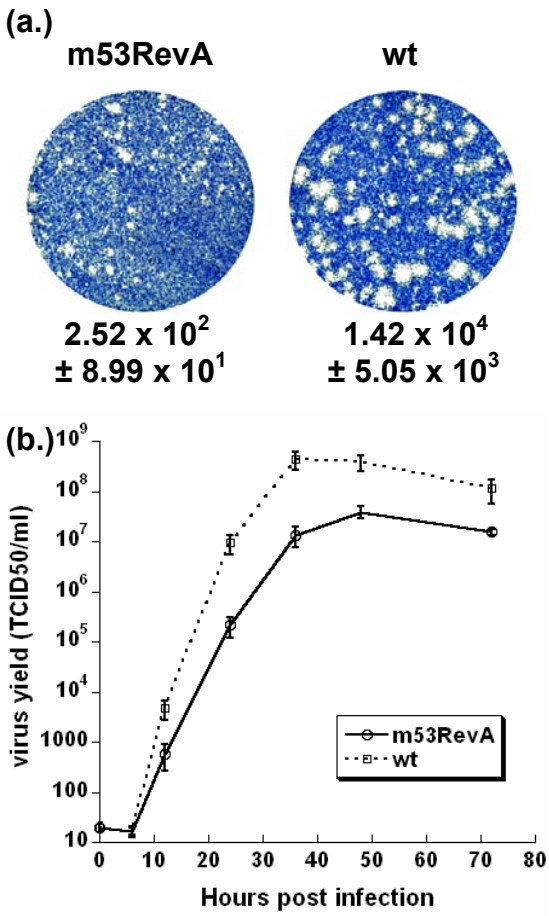


Figure 4.8. Phenotype of the m53RevA revertant of the m53 lethal phenotype. (**a.**) Titre of the m53RevA virus produced after transfection of the mutated viral cDNA clone into BSRT7 cells infected with FPVT7 and plaques formed by the recovered m53RevA virus on a monolayer of RAW 264.7 cells. Recovery and plaque phenotype are evaluated by comparison to the wild-type (wt) virus recovery. (b.) Kinetics of the m53RevA growth at an m.o.i. of 0.01 in RAW 264.7 cells.

Another intriguing suppression mutation was observed during the recovery attempts of the m54 mutant. A phenotypically reverted virus (m54RevA) was isolated by limiting dilutions of the population after blind passage and was partially sequenced in the 3' UTR region. Much to our surprise we found that the originally introduced m54 mutations were conserved in the m54RevA virus, while a large region of the polypyrimidine hairpin loop had also been deleted (7354-7361 nts, **Fig. 4.7b**). A possible explanation of the effect of such a deletion could be that by deleting the polypyrimidine tract the lower stem can reform (**Fig. 4.9b**). An indication that replication might be dependent on the lower stem is supported by the observation that the interruption of the bottommost base pair by a U to C mutation is lethal (Chaudhry et al., 2007). By re-evaluating the 3'UTR structure using the Kinefold algorithm which can predict the formation of pseudoknots (Xayaphoummine et al., 2005), a thermodynamically stable pseudoknot was predicted to form between the polypyrimidine tract nucleotides and a G/A rich tract just upstream of SL7330 (**Fig. 4.9a**). The question that arose after the identification of this new element was its involvement in a possible explanation of the observed reverted phenotype in m54RevA. Upon disruption of the upper stem of SL7330, the pseudoknot which conferred a $\delta G = -12.5$ kcal/mol in the free energy of the molecule, competed with the lower stem of SL7330 that conferred only a $\delta G = -5.9$ kcal/mol. The significantly lower free energy of the pseudoknot base stacking favoured an alternative structure presented in **Figure 4.9b**. When a structure is changed so dramatically, it is likely that there will be a dramatic effect on the functionality of the respective RNA domain. It is now intelligible why the disruption of such a dominating misfold by the deletion of the polypyrimidine tract in m54RevA was able to reverse the lethal phenotype of the original m54 mutant, as this deletion possibly favoured the formation of the lower

stem of the wild-type SL7330 (**Fig. 4.9c**) or reversed a possible negative effect of the stem formed between the poly(U/C) and the GA rich tracts (**Fig. 4.9b**). Due to the lack of time I was unable to confirm that the mutations in 53RevB and 54RevA were responsible for the revertant phenotype by the procedure followed for 53RevA, which would involve full genome sequencing and cloning of the mutated region back into the original m53 and m54 mutants.

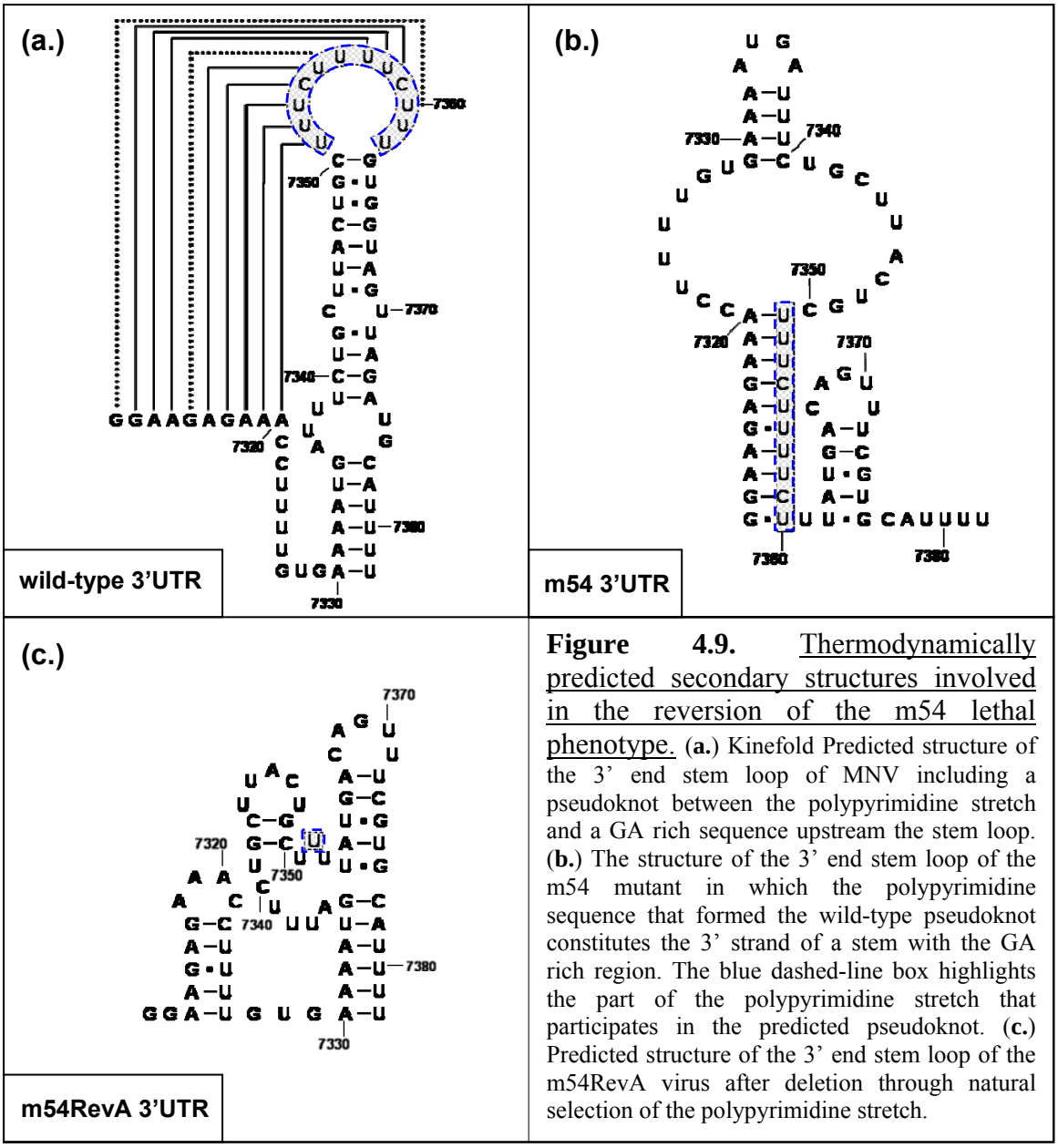


Figure 4.9. Thermodynamically predicted secondary structures involved in the reversion of the m54 lethal phenotype. (**a.**) Kinefold Predicted structure of the 3' end stem loop of MNV including a pseudoknot between the polypyrimidine stretch and a GA rich sequence upstream the stem loop. (**b.**) The structure of the 3' end stem loop of the m54 mutant in which the polypyrimidine sequence that formed the wild-type pseudoknot constitutes the 3' strand of a stem with the GA rich region. The blue dashed-line box highlights the part of the polypyrimidine stretch that participates in the predicted pseudoknot. (**c.**) Predicted structure of the 3' end stem loop of the m54RevA virus after deletion through natural selection of the polypyrimidine stretch.

4.6. Compensation of the disrupting mutations

Often to verify the need of an RNA secondary structure rather than primary sequence, mutations which disrupt its formation can be compensated by additional mutations that restore the base pairing in a stem. A drawback of such an approach is that sometimes it is not only a particular structure which is required for function but also the specific primary sequence within the secondary structure. Another problem is that in some structures which are located in coding regions, the introduction of compensatory mutations is prohibited if the mutations are not in the same reading frame. In simple terms, this means that if both the disruptive and compensatory mutation are not at third nucleotide positions of a codon, in the vast majority of cases the compensation is forbidden by the conservation of amino-acid sequence.

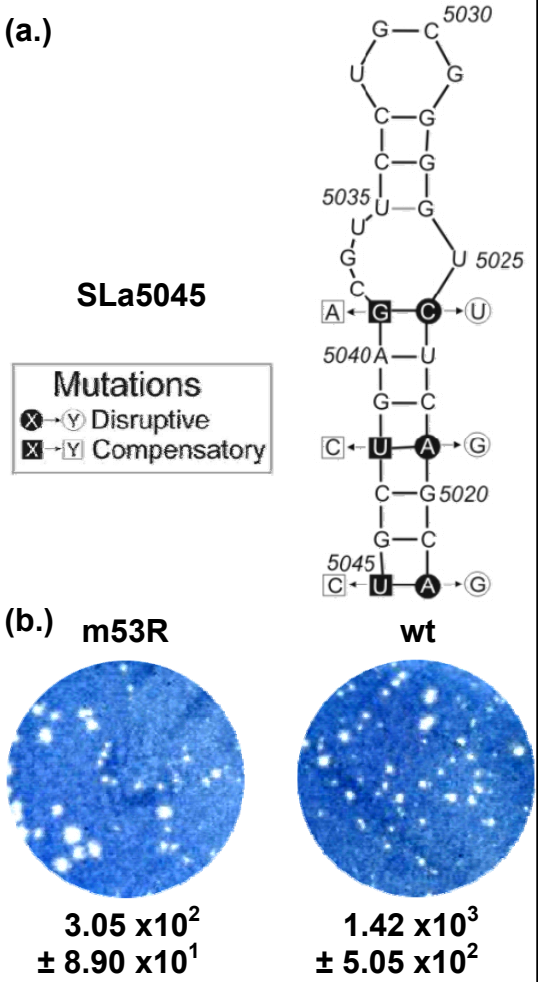


Figure 4.10. Compensation of the stem loop upstream of the subgenomic RNA start. (**a.**) Original m53 (circles) and the compensatory (boxes) mutations in m53R as depicted on the wild-type structure of SLa5045. (**b.**) Plaque phenotype of m53R on a monolayer of RAW 264.5 cells compared to the wild-type virus (wt). Underneath the plaque assay the titres of each virus during the recovery are presented.

For mutant m53 compensatory mutations could be introduced in order to reform the disrupted stem. The wild-type G_{5039}-C_{5024} pair was substituted in the m53R

MNV clone by an A-U pair, while the U_{5042}-A_{5021} and U_{5045}-A_{5018} base pairs were substituted by a C-G pair (**Fig. 4.10a**). The compensatory mutations were introduced into the m53 clone and the ability of the new clone, referred to as m53R, to produce virus was assessed. The restoring mutations in SLa5045 partially compensated the lethal phenotype of m53 (**Fig. 4.10b**). The yield of the recovered virus was lower than the wild-type, while its plaque phenotype had no obvious differences from the wild-type virus. The nearly total reversion of the viral phenotype upon restoration of the stem further verified the notion that the formation of SLa5045 is mandatory for the replication of MNV. The fact that the compensatory mutations were able to reform the stem loop in both positive and negative sense RNAs, prevents however a conclusion being drawn concerning the polarity of the functional structure.

4.7. Discussion

Nowadays it is common knowledge that all positive strand RNA viruses use a plethora of RNA structures to promote and regulate different aspects of their replication. Picornaviruses and flaviviruses, which are among the best studied mammalian positive strand RNA viruses, provide a good example of the dependence of virus replication on such *cis*-acting RNA elements (*cre*) (Witwer et al., 2001, Goodfellow et al., 2003b, Luo et al., 2003). Picornaviruses and flaviviruses accommodate in their extensive 5'UTRs the IRES element required for the viral translation (Belsham & Sonenberg, 1996, Kikuchi et al., 2005) and a 5' proximal RNA element that is required for the replication of the virus (Barton et al., 2001, Luo et al., 2003). Functional RNA elements are also situated in the 3'UTRs of these viruses that are important for the replication (Rohll et al., 1995, Yanagi et al., 1999)

and translation (Bradrick et al., 2006) of the viral RNA. Functional RNA elements have been also identified in the coding sequence of positive strand RNA viruses such as the 2C-*cre* element of picornaviruses that is required for VPg uridylation (Goodfellow et al., 2003b) and a structure in the NS5B region of HCV that is required for the replication of the virus (You et al., 2004).

To date our understanding of the RNA structures or sequences required for calicivirus translation and replication has been very limited due to the problems in cultivating human caliciviruses. The identification and propagation in tissue culture of the murine norovirus created the best model for the replication of human noroviruses (Wobus et al., 2004, Wobus et al., 2006). The development of a reverse genetics system for MNV provided a powerful tool which for the first time allowed the introduction of mutations in the norovirus genome (Chaudhry et al., 2007). In the present study, norovirus mutants were created taking advantage of this reverse genetics system. The mutations aimed at the disruption of certain RNA elements that were predicted by bioinformatics analysis. This analysis included the identification of regions in the viral RNA that presented a low free energy (thermodynamics RNA structure prediction algorithms) and a low variation in codon usage (suppression of synonymous site variation analysis) both of which are characteristics of conserved RNA elements.

Calicivirus genomes in contrast to other related viruses such as picornaviruses have short 5' UTRs (5 and 4 nucleotides in the case of the MNV genomic and sgRNAs respectively) and so any functional RNA elements are likely to be situated in the coding region. Also, it is known that calicivirus translation is not driven by an

IRES structure but rather by the VPg protein that is linked to the 5'end of the viral genomic and subgenomic RNA (Goodfellow et al., 2005). However, due to the unique nature of this translation mechanism, interestingly shared only between caliciviruses and a family of plant viruses, potyviruses (Leonard et al., 2000) it is not known whether any RNA elements at the 5'end of the viral genome are required for the translation initiation or its regulation. Mutagenesis of two conserved RNA elements at the 5' extremity of the viral genome (SL8, m50 and SL29, m51) showed a rather small contribution of these structures to viral replication in tissue culture. It is possible that the stem-loop sequences within the 5' end of the coding region contribute to viral translation through interactions with either canonical or non-canonical translation initiation factors (as discussed in **Chapter 3**) to direct ribosome assembly and translation initiation. It is also possible that the VPg protein is mainly responsible for the translation initiation and that the downstream RNA sequences have only regulatory role and so their importance in viral translation is either limited or cell type specific. The small plaque phenotype that was observed for the virus with a disrupted SL8 (m50) and the fact the initiation codon of ORF1 is situated within the 5' proximal stem loop of MNV (**Fig. 4.1a**) indicated a possible involvement of this structure in the regulation of MNV translation. Further studies would be required to examine this hypothesis

Many eukaryotic positive-strand RNA viruses regulate their gene expression by the synthesis of smaller subgenomic RNAs (sgRNAs) which can be translated and often replicated by the viral RdRp (van der Most et al., 1994, Morales et al., 2004, van den Born et al., 2005). Caliciviruses are among the viruses which produce a single subgenomic RNA that codes for the major and minor capsid proteins. It is believed

that the calicivirus subgenomic RNA is produced by internal initiation by the RdRp on the negative-strand genomic RNA. The process is thought to involve a promoter that by *in vitro* polymerase assays was identified to be located upstream of the subgenomic RNA region (Morales et al., 2004). In the search of such a subgenomic RNA synthesis promoter in the MNV genome, a conserved RNA structure upstream of the subgenomic RNA start (SLa5045) was disrupted. The lethal phenotype of the mutant virus confirmed the dependence of virus replication on this region. A lethal phenotype fitted with the hypothesis that this region formed part of a subgenomic RNA promoter as the loss of such an element would lead to the loss of capsid protein production. The occurrence of a suppression mutation within the SLa5045 (m53RevB) and the compensation of the m53 by the stem restoring mutations in m53R confirmed the requirement of the SLa5045 structure for virus replication.

Such RNA elements have been characterised in other positive strand RNA-viruses. In arteriviruses a similar stem-loop structure has been identified upstream of the sgRNA and serves as a promoter for the initiation of the sgRNA synthesis (van den Born et al., 2005). Also, in cucumber mosaic virus (CMV) a hairpin 5 nucleotides upstream of the sgRNA is required for the in-vitro synthesis of the sgRNA by the viral RdRp (Chen et al., 2000). A hairpin structure at the same region as SLa5045 was predicted for all caliciviruses. Interestingly in all cases the hairpin was 6 nucleotides upstream of the subgenomic RNA start site which may indicate a conserved mechanism among caliciviruses and a possible similarity with the mechanism described for sgRNA synthesis of CMV. The requirement of a region upstream of SLa5045 was also apparent as a suppressor mutation was identified ~100 nucleotides upstream of the stem-loop in the phenotypically revertant m53RevA. It is known that

in other positive strand RNA viruses sequences even 1000 bases upstream of the sgRNA start site are required for function of the sgRNA promoter through long-range RNA-RNA interactions (Zhang et al., 1999). Further studies are required to identify the role of the region in which m53RevA suppressor mutation is located.

The 3'extremity of the positive strand RNA viruses usually accommodate RNA elements that are required for the initiation of negative strand RNA synthesis or RNA elements that regulate the viral translation. However, in contrast to the rest of functional RNA structures, the role of 3' end structures is often controversial. For example the role of the 3'UTR of HCV in IRES function is still debated as HCV 3'UTR functions in a cell-type specific manner (Song et al., 2006). Similarly, a cell specific phenotype was observed with a poliovirus that lacked the 3'UTR as its requirement was obvious only in a neuroblastoma cell line (Brown et al., 2004). Thus, it is not surprising that the m52 MNV mutant that lacked the SL7330 polypyrimidine loop showed no defect in BSRT7 (baby-hamster kidney cells, modified BHK-21 cells) and RAW 264.7 cells (mouse leukemic macrophage cell line). It is possible that this region regulates an aspect of the virus life cycle upon interaction with a cell-type specific RNA binding protein (discussed in more details in **Chapter 5**). In contrast to the loop of SL7330, the importance of the stem was more apparent as the SL7330 disruption mutant (m54) showed a lethal phenotype. The fact that the lethal phenotype was reverted by the deletion of the polypyrimidine tract raised the question of the involvement of an extended pseudoknot, formed between the SL7330 loop and a GA-rich sequence upstream of the stem-loop. A strikingly similar pseudoknot structure has been characterised in the arterivirus 3' UTR, in which the 3'end-most hairpin loop

interacts with a sequence just upstream of the hairpin possibly regulating the negative strand RNA-synthesis (Beerens & Snijder, 2007).

The identification of functional RNA structures in a positive-strand RNA genome is the first step in understanding the mechanism by which an RNA self-regulates its replication through interaction with viral and cellular factors. In this study at least three important RNA elements were identified, however, their specific role remains to be elucidated in the future.

Chapter 5.

Characterisation of the Interaction of PCBPs and La with calicivirus RNA

5.1. Introduction

The majority of the ribonucleoprotein (RNP) complexes formed on an mRNA involve a large number of proteins. These proteins may function synergistically to perform a specific function on the particular RNA domain. For example, PCBP2 and PTB proteins cooperate for the formation of a functional IRES by binding to the 5' UTR of the *Bag-1* mRNA (Pickering et al., 2004). In other cases, proteins recruited on an mRNA have antagonistic functions, for example the recruitment of the TIA-1 protein on Fas mRNA promotes exon exclusion, while binding of PTB acts antagonistically by hindering the formation of the spliceosome and thereby promoting exon skipping (Izquierdo et al., 2005). Furthermore, alteration of the expression levels or localisation of RNA-binding proteins is often part of the regulatory network controlling the function of such RNPs. A similar network of RNA binding proteins seems to apply to the regulation of positive strand RNA virus replication. A variety of proteins have been shown to form large RNP complexes on the 5' and 3' extremities of many positive sense RNA viruses. The RNP complex formed on the 5' UTR of picornavirus genome has been demonstrated to accommodate the translation initiation factors eIF4G, eIF4A and eIF4B while the ITAFs: PTB, PCBP2, La and unr proteins have also been extensively studied for their roles in this RNP. Proteomics analysis of the RNP complex formed on the HCV IRES identified more than 30 proteins that interact with the IRES (Lu et al., 2004). Among them there were proteins such as PTB, La, PCBP2, hnRNP U, nucleolin and eIF3, the only translation initiation factor which interacts with the HCV IRES. Whether or not all the identified proteins are part of the functional RNP complex *in vivo* is not known.

The aim of this part of the study was to identify additional proteins that interact with the calicivirus RNA and characterise the properties of their binding. The identification of additional protein components of the RNPs formed on the viral RNA can shed more light in the regulatory network of calicivirus replication.

5.2. The MNV 5' genomic and 5' subgenomic RNA extremities interact with poly(C)-binding proteins

Bioinformatics analysis of the MNV 5' genomic RNA extremity identified at least four polypyrimidine tracts, most of which were predicted to be single stranded (**Fig. 5.1**). In contrast to the respective region in FCV, these polypyrimidine tracts (BS2-5) also had a substantially higher amount of cytosines (**Fig. 5.1**) that indicated a potential interaction with another important group of RNA-binding proteins, the poly(C)-binding proteins (PCBPs). PCBP1 and PCBP2 are arguably the most important representatives of this group and have been demonstrated to play a vital role in picornavirus translation and replication (Discussed in **Chapter 1**).

Recombinant PCBP1 and PCBP2[8] were expressed and purified then their ability to interact with the MNV 5'$G_{1\text{-}250}$ RNA examined using EMSA (**Fig. 5.2**). Both proteins showed a high affinity for the 5'$G_{1\text{-}250}$ RNA (**Fig. 5.2a**). The ability of PCBPs to bind to the 5' extremity of the subgenomic RNA (nts 1-200) was also assessed by titration of both PCBP1 and PCBP2 on the 5'$SG_{1\text{-}200}$ RNA probe. Both proteins were also able to bind the 5'$SG_{1\text{-}200}$ RNA probe, but with a lower affinity than the 5' genomic extremity (**Fig. 5.3**).

[8] The PCBP data was generated in collaboration with Lillian Chung as part of her master's project.

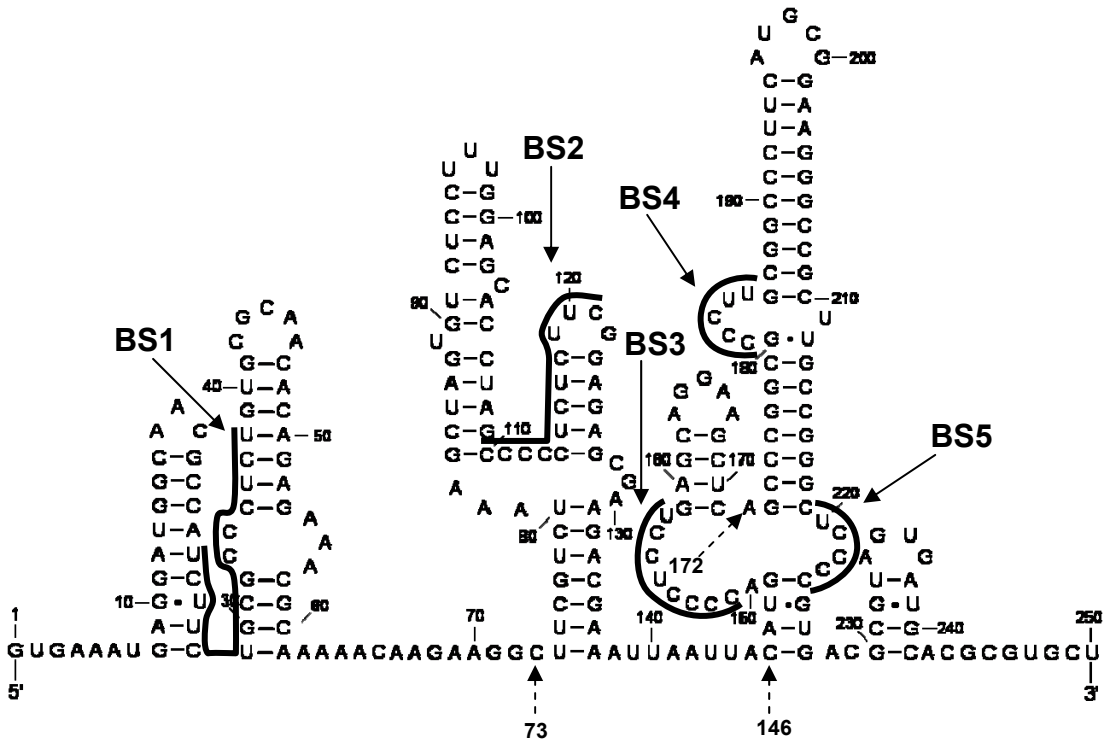


Figure 5.1. Bioinfomatically predicted secondary structure of the MNV 5'G$_{1\text{-}250}$. The potential binding sites (BS1-5) of PTB and PCBPs are highlighted. Dashed arrows indicate the nucleotide positions that constituted the terminal nucleotides of the 3' end truncations of the MNV 5'G$_{1\text{-}250}$ RNA or the first nucleotide of the 5' end truncations of the MNV 5'G$_{1\text{-}250}$ RNA

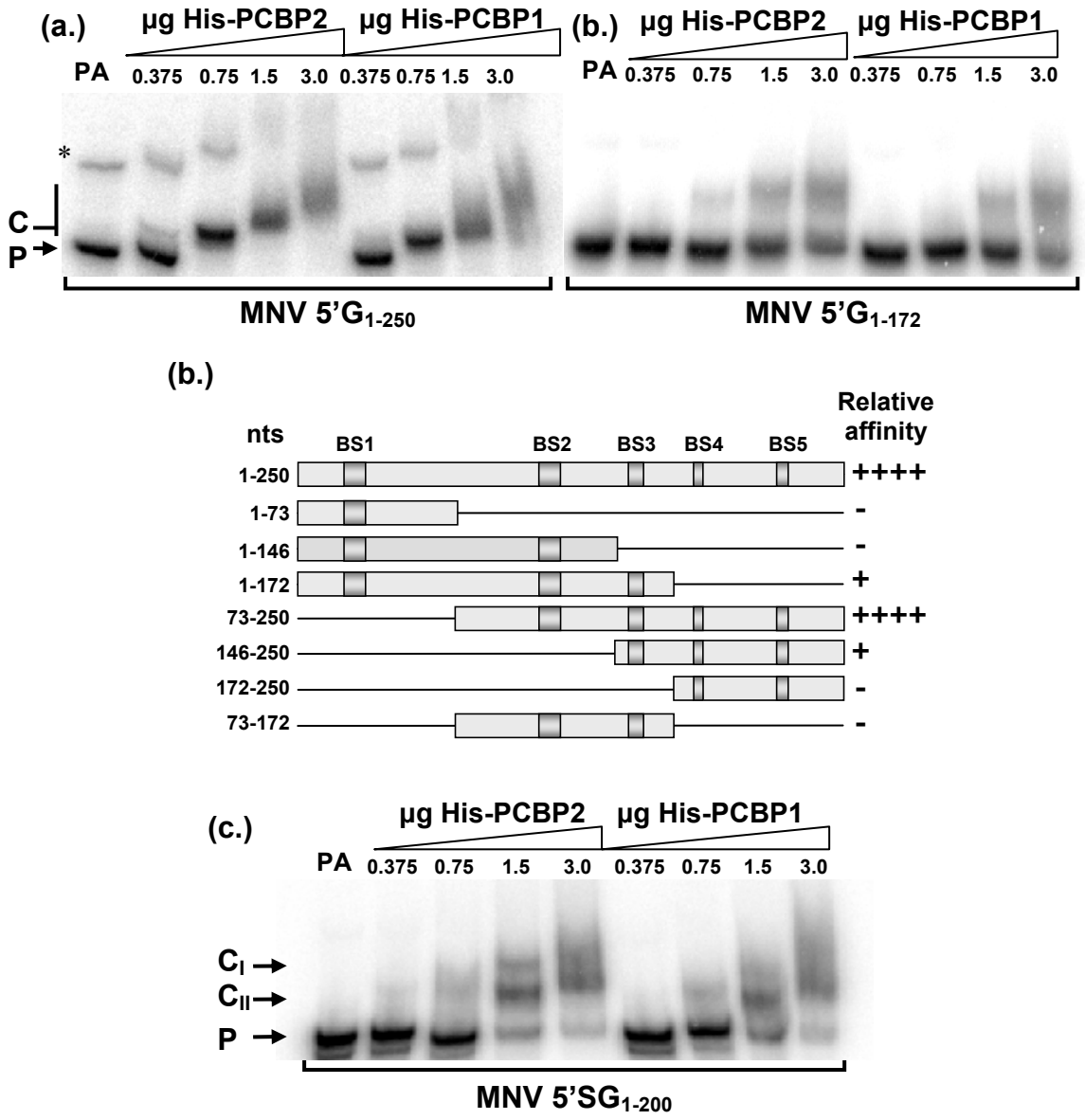


Figure 5.2. Interaction of PCBP1 and PCBP2 with the MNV 5'G$_{1-250}$ and 5'SG$_{1-200}$ RNAs. (**a.**) EMSA analysis examining the ability of PCBP1 and PCBP2 to interact with the 5' extremity of the MNV genome. RNA probes representing nts 1-250 and 1-172 of the genomic RNA were incubated with increasing concentrations of protein and the reactions separated on an 4 % native acrylamide gel. (**b.**) Chart that shows the affinity of the truncations tested for the binding of PCBP1 and PCBP2 relative to 5'G$_{1-250}$. PCBP1 and PCBP2 demonstrated similar binding characteristics (**c.**) EMSA analysis examining the ability of PCBP1 and PCBP2 to interact with the 5' extremity of the MNV subgenomic RNA. RNA probes representing nts 1-200 of the of MNV subgenomic RNA were incubated with increasing concentrations of protein and the reactions separated on an 4 % native acrylamide gel., C_I and C_{II} = complex I and II of PCBP1 or PCBP2 with the MNV 5'SG$_{1-200}$, P=free probe, PA=probe alone, *= alternative conformation of the probe or probe dimer)

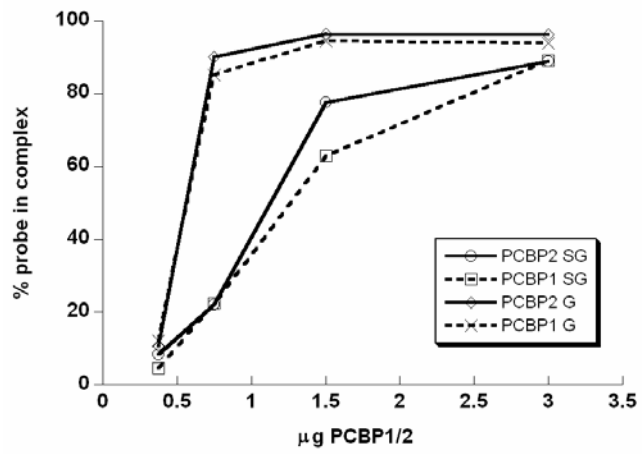


Figure 5.3. Comparison of the interaction of PCBP1 and PCBP2 with the MNV 5'G_{1-250} and 5'SG_{1-200} RNAs. Plot of the fraction (%) of the probe in complex with PCBP1 or PCBP2 with the MNV 5'G_{1-250} and 5'SG_{1-200} RNA probes from the respective EMSAs of Fig. 5.2

In order to identify the binding site(s) of PCBPs on the 5' end of the MNV genomic RNA, truncations of the original 5'G_{1-250} RNA were produced by T7 promoter driven *in vitro* transcription of different size PCR fragments representing various regions of the 5'G_{1-250} RNA. The distribution of the potential binding sites and the thermodynamically predicted RNA structure were taken into account during the design of the truncated transcripts as explained more extensively in **Chapter 3**. PCBP1 and PCBP2 demonstrated similar binding patterns and seemed to bind equally well to all the examined RNAs. Truncations from the 3' end of the 5'G_{1-250} RNA demonstrated that potential binding sites BS1 and BS2 did not contribute to PCBP binding as the transcripts that contained only BS1 (5'G_{1-73}) or BS1 and BS2 together (5'G_{1-146}) did not demonstrate any PCBP binding affinity (**Fig. 5.2a**). Addition of the sequence containing the potential binding site BS3 (5'G_{1-172}) demonstrated limited affinity to PCBP, signifying a small contribution of this region to PCBP binding (**Fig.**

5.2b). Truncations from the 5' end of the 5'G_{1-250} RNA demonstrated that deletion of the region which included BS1 (5'G_{73-250}) did not lead to any reduction in the affinity of the RNA for PCBP. Deletion of the region which contained BS2 (5'$G_{146-250}$), however, had a profound effect on PCBP binding, signifying a role for this region in the interaction. Further deletion of the BS3 region (5'$G_{172-250}$) resulted in the abolishment of PCBP binding, highlighting again the importance of the sequence that contained BS3. As the deletion analysis demonstrated that BS2 and BS3 were important for the interaction between 5'G_{1-250} and the PCBPs, an RNA transcript which contained only the regions containing BS2 and BS3 was examined for its ability to bind the PCBPs. This 5'G_{73-172} RNA demonstrated no affinity for PCBPs (**Fig. 5.2b**). From the above deletion analysis it was obvious that more than one binding sites on the MNV 5'extremity were required for the efficient interaction with the PCBPs.

5.3. The MNV 3' UTR interacts with PTB and PCBP2

Sequence analysis identified a pyrimidine rich region in the 3' UTR of MNV which localised to the loop region of the 3' stem-loop. Further analysis indicated that it had the potential to form a pseudoknot with upstream sequences (**Chapter 4, Fig. 4.9a**). Such a pyrimidine rich context was an obvious potential binding site for PTB and PCBP, hence this was characterised further. Such stretches of variable length have been identified in the 3'UTR of other viruses such as HCV and are well known to interact with PTB and PCBPs. EMSAs using an RNA probe representing the 3' extremity of MNV genome (nts 7133-7382) demonstrated that the region had a high

affinity for PTB and PCBP2 protein (**Fig. 5.4a,b**). The specificity of the interaction between PTB and the 3'extremity was assessed using a competition EMSA. Non-radiolabeled homologous transcripts representing the 3'extremity of the MNV genomic RNA and MNV 5'G_{1-250} were able to inhibit complex formation. FCV 3' extremity had some effect on the complex formation. However, this was insignificant as even 5'MNV that demonstrated residual binding for PTB inhibited better even at 10 times smaller concentration. This competition analysis confirmed that the interaction between PTB and the MNV 3' extremity was specific (**Fig. 5.5**).

In order to confirm that the region responsible for the binding was the pyrimidine rich loop of the 3' extremity of the MNV genome, the polypyrimidine tract was substituted by a GNRA tetranucleotide to generate the MNV mutant m52. The replication characteristics of this virus were identical to WT MNV and have already been described in **Chapter 4**. The mutated 3' extremity was used as an RNA probe in EMSA reactions, where it demonstrated that the removal of the polypyrimidine tract had a dramatic effect on PCBP2 and PTB binding (**Fig. 5.4c,d**).

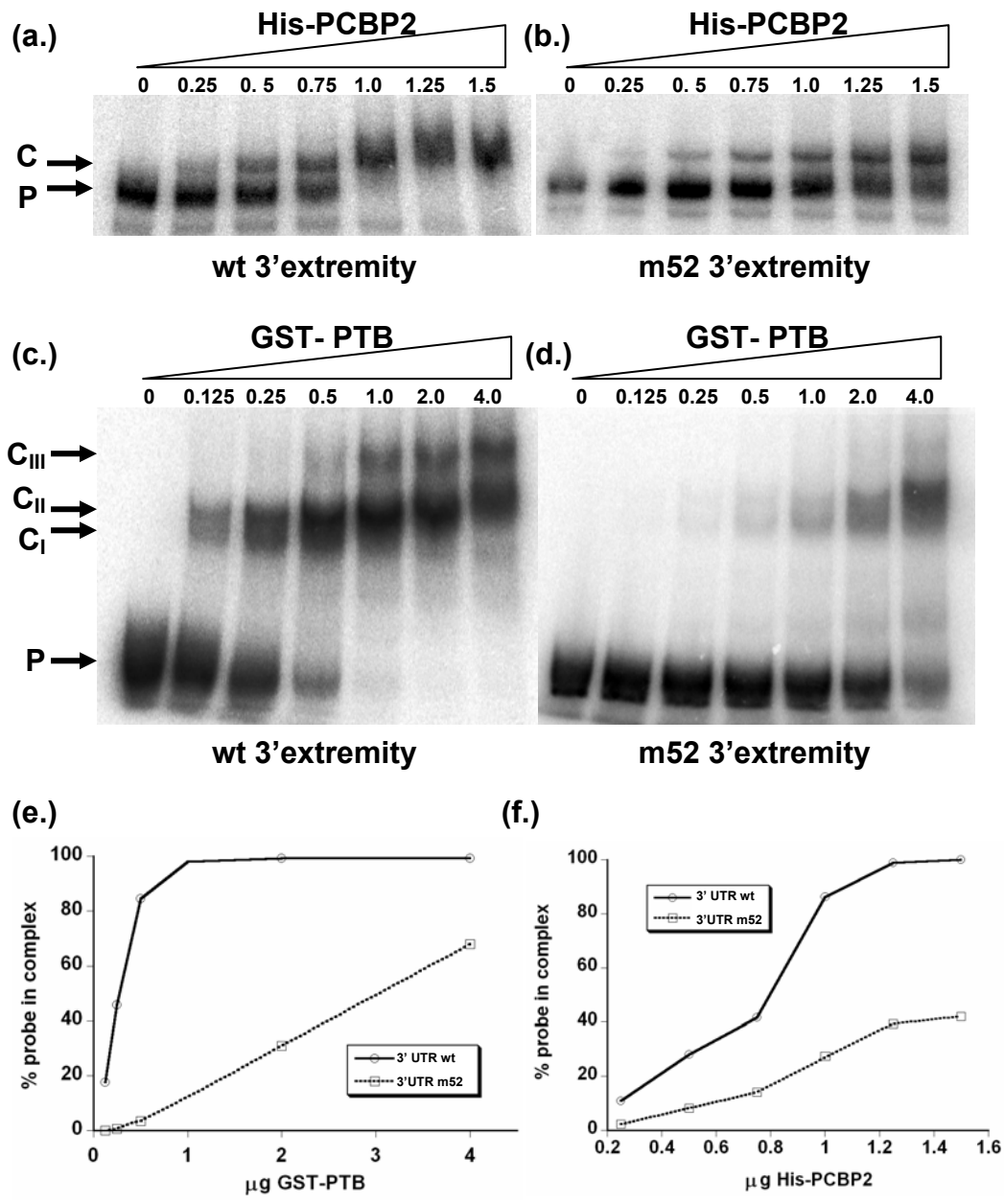


Figure 5.4. PCBP2 and PTB interact with the 3' extremity of the MNV genome. (**a.**, **b.**, **c.**, **d.**,) EMSA analysis examining the ability of PCBP2 and PTB to interact with the 3' extremity of the MNV genome. RNA probes encompassing nts 7133-7382 from either the wild-type virus or the m52 mutant lacking the polypyrimidine tract, were incubated with increasing concentrations of protein and the reactions separated on an 4 % native acrylamide gel. (**e.**, **f.**) Plot of the fraction of wt and mutated (m52) 3' extremity probe in complex with the PTB or PCBP2 under increasing amounts of protein. (C = complex of PCBP and the MNV 3'extremity, C_I, C_{II} and C_{III} = complex I, II, III of PTB and the MNV 3' extremity, P=free probe, PA=probe alone)

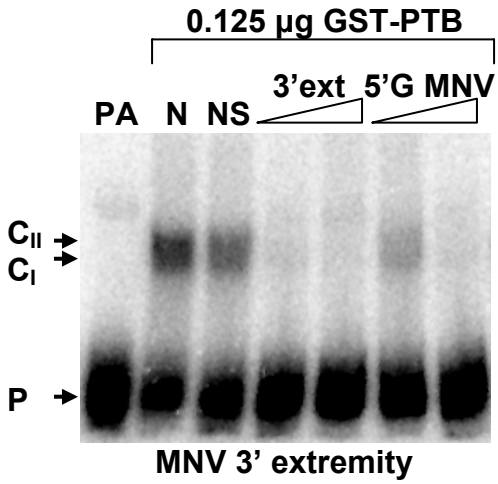


Figure 5.5. PTB interacts specifically with the 3' extremity of the MNV genome. The formation of a complex between an RNA probe encompassing nts 7133-7382 of the MNV 3' extremity and PTB is challenged by the addition of non-labelled 3'extremity homologous RNA (3'ext), 5'G_{1-250} RNA (5'GMNV) and the 3' extremity of FCV (nts 7493-7683, NS). (PA = probe alone, N = no competitor, NS = non-specific competitor, C_I and C_{II} the two complexes between PTB and the MNV 3' extremity.)

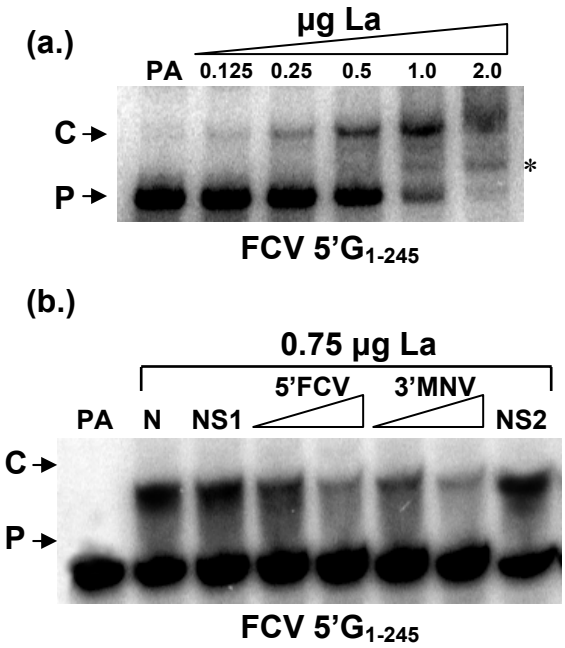


Figure 5.6. La protein interacts specifically with the 5' end of the FCV genomic RNA. (**a.**) EMSA analysis examining the ability of La to interact with the 5' extremity (5'G_{1-245}) of FCV genome. RNA probes encompassing nts 1-245 of FCV genomic RNA were incubated with increasing amounts of protein and the reactions separated on a 4 % native acrylamide gel. (**b.**) Competition EMSA in which the formation of complex between FCV 5'G_{1-245} and La protein is challenged with homologous FCV 5'G_{1-245} (5'FCV) MNV 3' extremity (nts 7133-7382, 3'MNV), poliovirus 2C-*Cre* (NS1) and FCV 3' extremity (nts 7493-7683, NS2). (C=complex, P= free probe, PA=probe alone, N=no competitor, *=complex of La with a smaller RNA fragment.)

5.4. The La protein interacts with the 5' extremity of FCV genomic RNA

A protein that has been demonstrated to participate in RNP complexes which also contain PTB is La autoantigen. The poliovirus 5' IRES RNA structure is one site of such an RNP complex (Svitkin et al., 1994), while the two proteins have also been identified to form a complex on the 3' UTR of Dengue 4 virus RNA (De Nova-

Ocampo et al., 2002). Similarly, PTB and La are part of the RNP complexes formed at the 5' and 3' extremities of Norwalk virus RNA (Gutierrez-Escolano et al., 2000, Gutierrez-Escolano et al., 2003). To address if similar PTB and La containing complexes can form on the genomes of other caliciviruses, purified recombinant La protein was first examined for its ability to bind on the 5' extremity of FCV. In EMSA reactions that contained the FCV 5'G_{1-245} RNA probe, La protein was found to form a stable complex with the FCV 5'G extremity (**Fig. 5.6a**). Titration of unlabelled RNA transcripts encompassing nts 1-245 of the FCV genomic RNA, homologous to the probe, into EMSA reactions inhibited complex formation (**Fig. 5.6b**). The same effect was also observed with RNA transcripts that represented the MNV 3'UTR, while the poliovirus 2C-cre (NS1) and the FCV 3' extremity (NS2) did not inhibit complex formation (**Fig. 5.6b**). This competition assay verified the specificity of the interaction between La and the FCV 5'G_{1-245} RNA probe. Furthermore, the specific inhibition of the complex by the MNV 3'UTR revealed another potential binding site of this host-cell factor.

5.5 La protein assists PTB binding to the 5' extremity of the FCV genomic RNA

Often proteins that form one component of a RNP complex may facilitate the binding of other components of the complex to the RNA, usually by helping the RNA adopt a more favourable conformation for binding. An example of such activity is the induction of PCBP2 binding on the 5' cloverleaf structure of the poliovirus genome, which occurs as a consequence of 3CD binding on the same structure (Parsley et al., 1997). A combined La and PTB EMSA analysis was performed in order to reveal any

potential cooperativity in binding between the two proteins. Recombinant La protein was titrated into reactions containing a standard amount of PTB in a series of EMSA reactions using the FCV 5'G_{1-245} RNA probe. Increasing amounts of La resulted in an increased intensity of the band corresponding to the complex formed by PTB and 5'G_{1-245} RNA in the absence of La (PTB C_I, **Fig. 5.7a**). A low amount of PTB (0.25 μg) was used in the binding assays to allow any increase in complex formation, which might occur as a result of La binding, to be observed. When PTB was titrated on top of a standard amount of La protein, increasing amounts of PTB resulted in the reduction of the intensity of the band that corresponded to the complex between La and the 5'G_{1-245} RNA in the absence of PTB (La C, **Fig. 5.7b**). This observation demonstrated that PTB either displaced La from its binding site on the 5'G_{1-245} or that both proteins formed a complex that had a mobility very similar to the mobility of the PTB-5'G_{1-245} complex. One fact that was clear from these EMSA reactions was that upon addition of La protein, the binding of PTB to the 5'G_{1-245} RNA was more favoured.

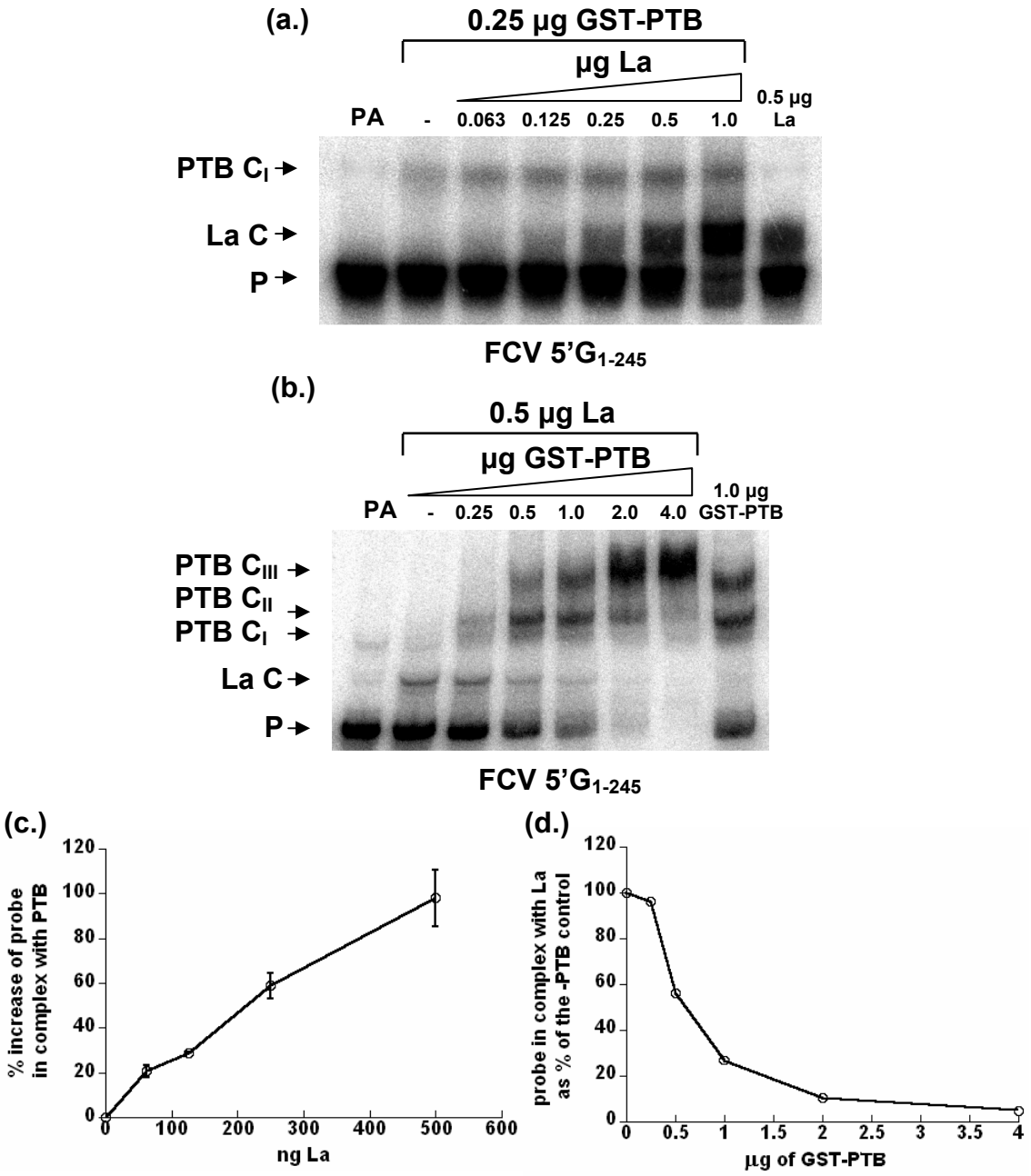


Figure 5.7. La assists PTB binding on the 5' end of the FCV genomic RNA. EMSA analysis of combined interaction of La and PTB with the 5' extremity (5'G_{1-245}) of FCV genome. (**a.**) RNA probes encompassing nts 1-245 of FCV genomic RNA with a constant amount of PTB were incubated with increasing amounts of La and the reactions separated on an 4 % native acrylamide gel. (**b.**) RNA probes encompassing nts 1-245 of FCV genomic RNA with a constant amount of La were incubated with increasing amounts of PTB and the reactions separated on an 4 % native acrylamide gel. (**c.**) Plot of the % increase in the complex between PTB and the 5'G_{1-245} probe upon addition of increasing amounts of La. (**d.**) Plot of the fraction (%) of 5'G_{1-245}probe in complex with La upon addition of increasing amounts of PTB. (PTB C_I C_{II} C_{III} = complex I II and III of PTB with the 5'G_{1-245}, La C = complex of La with the 5'G_{1-245}, P=free probe, PA=probe alone)

5.6 Discussion

Cooperative assembly of RNP complexes is a conserved mechanism for the regulation of many cellular processes. RNA viruses and especially positive strand RNA viruses take advantage of the abundance of host RNA-binding proteins for the regulation of their own translation and replication processes. During this part of the study the interaction of a number of host RNA-binding proteins with the calicivirus RNA was examined in order to identify additional components of the viral RNPs.

Poly(C)-binding proteins (PCBPs) are a large group of RNA-binding proteins that are involved in the regulation of translation and replication of a number of positive strand RNA viruses. In poliovirus, PCBPs play a dual role as they are required for the efficient IRES-mediated translation, while through interaction with a 5' extremity *cis*-replication element (cloverleaf) they also regulate poliovirus replication (Gamarnik & Andino, 1998). PCBP1 and PCBP2 were demonstrated to interact with the 5' extremity of the MNV genomic RNA and an attempt to roughly map their binding site(s) on the RNA was made. According to the deletion analysis, potential binding sites BS2 and BS3 on the MNV 5' extremity contributed greatly to the binding of the PCBPs. However, BS2 and BS3 were not sufficient for PCBP binding. It is highly possible structural rearrangements in the truncated RNA masked or altered the tertiary positions of the pyrimidine tracts inhibiting PCBP binding. For example, it is known that the alteration of the secondary structure of the poliovirus type 3 IRES and not the actual alteration of its binding site due to a mutation present in Sabin type 3 vaccine strain is probably responsible for the inefficient binding of PTB (Guest et al., 2004). Mutational analysis of BS2 and BS3 binding sites would

elucidate their involvement in the interaction between MNV 5'G_{1-250} and the PCBPs, but time constrains did not allow further study of PCBP binding to the MNV 5' genomic extremity. Nevertheless, it was clear that PCBP binding involved more than one region of the RNA.

The interaction of PCBPs with additional regions of the MNV genomic RNA was assessed by EMSAs that contained the 5' extremity of the subgenomic RNA and the 3' extremity of the MNV genome. Both regions demonstrated some affinity for the PCBPs, while the pyrimidine rich loop of the 3'end stem-loop was the major binding determinant of the 3' extremity for both PCBP2 and PTB. The simultaneous high affinity interaction of PCBP2 with both the MNV 5' and 3' extremities also suggested a possible role of PCBP2 in the formation of a protein bridge between the two ends of the viral RNA. Such an interaction has been demonstrated to be important for the efficient translation and/or replication of all the extensively studied mammalian positive strand RNA viruses. An interaction between PABP, that binds the 3' end poly(A) tail and PCBP, which binds the poliovirus IRES, is a well studied example of viral RNA circularisation that has been demonstrated to enhance the viral translation (Herold & Andino, 2001). In rotaviruses the 3' end partner, PABP, has been substituted by the virally encoded protein NSP3, which binds to a conserved sequence at the 3′ end (UGUGACC-3'OH) of all six segments of the rotavirus RNA genome (Vende et al., 2000). The fact that PCBP2 was recently demonstrated by X-ray crystallography and NMR to form a dimer through interaction between two KH1 domains or a KH1 and a KH2 domain (Du et al., 2007) indicated a PCBP2-PCBP2 interaction might be a potential bridge between the two extremities of the MNV viral RNA. Further studies are required to support this hypothesis.

Amongst the proteins that were identified to be part of the Norwalk virus 5'end RNP was the La autoantigen (Gutierrez-Escolano et al., 2000). However, after the initial finding, the interactions were not characterised either biochemically or functionally. During this study, La protein was demonstrated to interact specifically with the 5' extremity of the FCV genomic RNA, while in combination with PTB, the La protein demonstrated an assisting role in PTB binding. In the presence of the La protein, the viral RNA demonstrated an increased affinity for PTB. Enhancement of such an interaction could either signify that a direct interaction between La and PTB assisted the formation of a tripartite complex with the RNA or that La acted as an RNA chaperone, allosterically altering the conformation of the RNA which facilitated the binding of PTB. A direct interaction between La and PTB has never been reported, despite the fact that these proteins have been found together in several RNPs. On the other hand, La protein is well known for its RNA chaperone activity by inducing conformational changes of the RNA during mRNA *cis*-splicing (Belisova et al., 2005), while it has also been found to promote the correct folding of several pre-tRNAs (Wolin & Wurtmann, 2006). An allosterically assisted binding of a protein to RNA has been previously described during the study of RNP complex assembly on the 16S ribosomal RNA (Recht & Williamson, 2004). In the presence of the ribosomal protein S15, the affinity of the 16S RNA for the S6/S18 heterodimer was significantly enhanced, while it is believed that the conformational change induced by the S15 is the cause of this shift in the affinity (Recht & Williamson, 2004).

Identification of the components of the viral RNPs is the first step in the elucidation of the regulatory network that controls calicivirus translation and

replication. Future demonstration of the functional role of these interactions will reveal the mechanism by which the above regulation takes place.

Chapter 6.

Conclusion and future work

RNA performs essential functions within the cell, regulating a wide range of processes though interaction with RNA-binding proteins (Ciesla, 2006, Rodriguez-Trelles et al., 2006). Viruses taking advantage of this regulatory network use cellular RNA-binding proteins for their own translation and replication (Belsham & Sonenberg, 2000). The study of these interactions can offer insights in the mechanisms that regulate the virus life cycle.

The study of RNA-protein interactions and RNA structures in caliciviruses and most importantly in human caliciviruses was particularly difficult due to the lack of a tissue culture system to support human norovirus infection. Recently, a research group managed to apply a 3D-culture system in which cells could differentiate mimicking the small intestinal epithelium that could support the growth of human noroviruses (Straub et al., 2007). However, this system is difficult to establish as the cells need at least a month of preparation for every infectivity assay and although this finding was a breakthrough in the study of human noroviruses, in practice the FCV and MNV model systems remain the best for the study of calicivirus replication.

Throughout this project a number of RNP complexes formed on the calicivirus RNA were dissected to allow the identification of the RNA-binding proteins that constitute the viral RNP complexes. Host-cell RNA binding proteins such as PTB, the PCBPs and La were demonstrated to interact with the extremities of the FCV and MNV genomic and subgenomic RNAs (**Table 6.1**). PTB protein had an intriguingly diverse affinity for the extremities of the FCV and MNV genomic RNA. The 5' extremity of the FCV genome could interact with PTB while its 3' extremity did not demonstrate any affinity. The opposite was observed for the MNV genomic RNA,

which had residual binding affinity for PTB at the 5' extremity, while the 3' extremity demonstrated a good binding affinity for PTB. The opposite polarity of PTB binding on the FCV and MNV genomic RNA could indicate a possible alternative regulation of FCV and MNV replication by PTB. It is has been already demonstrated that FCV and MNV may have different mechanisms for the regulation of their gene expression as they differ in their requirements for canonical translation initiation factors (Chaudhry et al., 2006). In contrast to PTB, PCBPs could interact with both extremities of the MNV genome indicating a possible role in the circularisation of the viral RNA that has been shown to be important for other positive strand RNA viruses (Edgil & Harris, 2006). The attribution of such a role to PCBPs, however, requires additional study that will demonstrate the formation of such a protein bridge between the two ends of the viral RNA *in vitro* and also the requirement of such an interaction in viral replication.

Table 6.1. RNA-protein interactions in FCV and MNV

Protein / Viral RNA	PTB †	PCBPs ‡	La ¶
FCV 5'G extremity	++++	?	Yes
FCV 5'SG extremity	++++	?	?
FCV 3'extremity	-	?	No
MNV 5'G extremity	+	++++	Yes
MNV 5'SG extremity	++++	+++	?
MNV 3'extremity	+++++	+++++	Yes

† ++++ = relative affinity of PTB for FCV 5'G_{1-245}
‡ ++++ = relative affinity of PCBPs for MNV 5'G_{1-250}
¶ the lack of comparative study for La binding limited the designation to Yes for some affinity and No for no affinity
? = not assayed, - = no affinity

The interaction of PTB with the FCV RNA was thoroughly studied during this project and PTB demonstrated a potential RNA chaperone activity in the regulation of FCV translation. The negative regulation of FCV translation by PTB was the first

functional analysis for an RNA-binding protein in the life cycle of any calicivirus. It is hypothesised that translation of viral proteins causes PTB to move out of the nucleus late in the infection to down-regulate translation in order to facilitate the assembly of the replication machinery (**Fig. 6.1**). The hypothesis that PTB may be part of the switch between translation and replication requires additional study in isolated active replication complexes (Green et al., 2002) and in cell culture. The assistance of PTB recruitment on the 5' extremity by La protein added another component in the RNP complex that possibly regulates the translation of FCV RNA (**Fig. 6.2**).

The identification of functional RNA structures in the viral genomes has been a well known alternative path for the elucidation of the role of viral RNP complexes. The poliovirus 2C-*Cre* structure is an example of an RNA element that was identified by computational analysis of the poliovirus genome (Goodfellow et al., 2000) and was subsequently demonstrated to be crucial for poliovirus replication (Goodfellow et al., 2003a). Functional RNA structures were identified in the MNV genome by computational and mutational analysis using the recently described MNV reverse genetics system (Chaudhry et al., 2007). This study revealed a potential subgenomic RNA synthesis promoter upstream of the subgenomic RNA start site. *In vitro* studies of subgenomic RNA synthesis initiation by the viral RdRp (Morales et al., 2004) on wild-type and mutated (m53, **Chapter 4**) negative strand RNA templates would elucidate the role of this important MNV RNA element. Moreover, further study of the phenotypically reventant viruses (m53RevA and m53RevB, **Chapter 4**) could aid the dissection of the mechanism that lies behind the subgenomic RNA synthesis in MNV.

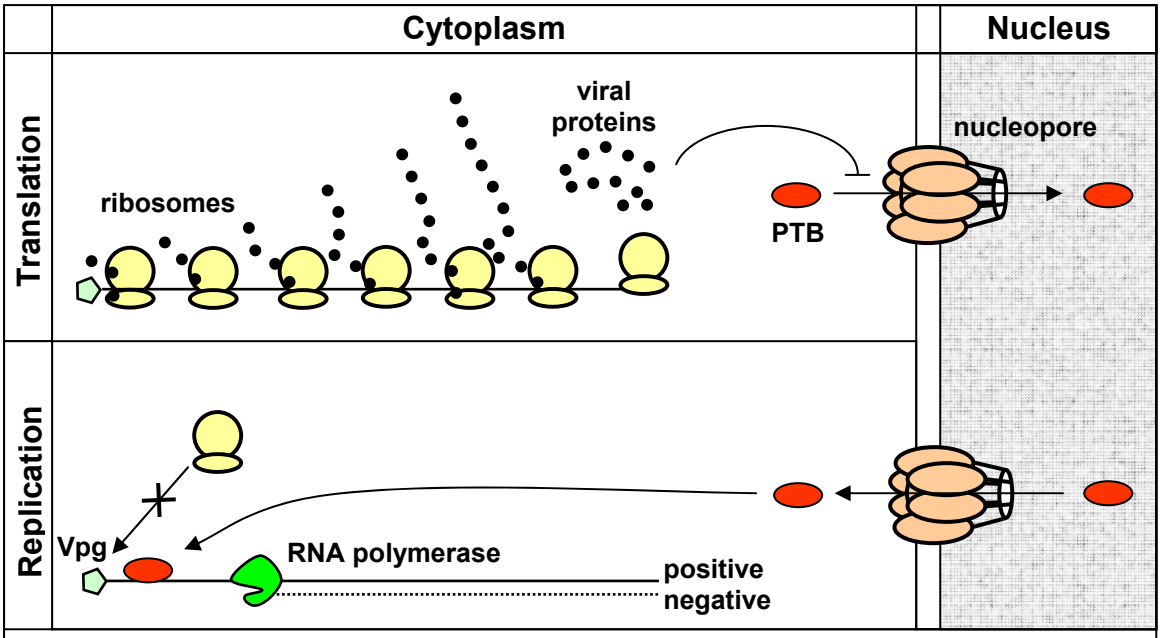


Figure 6.1. The hypothesis for the regulation of FCV replication by PTB. The viral RNA is translated producing the viral proteins. The viral proteins later during the infection inhibit the shuttling of PTB to the nucleus either directly or indirectly and promote the translocation of PTB to the cytoplasm. PTB inhibits the recruitment of the ribosomes at the 5' end of the positive strand viral RNA and the RNA-dependent RNA polymerase can produce the negative strand RNA.

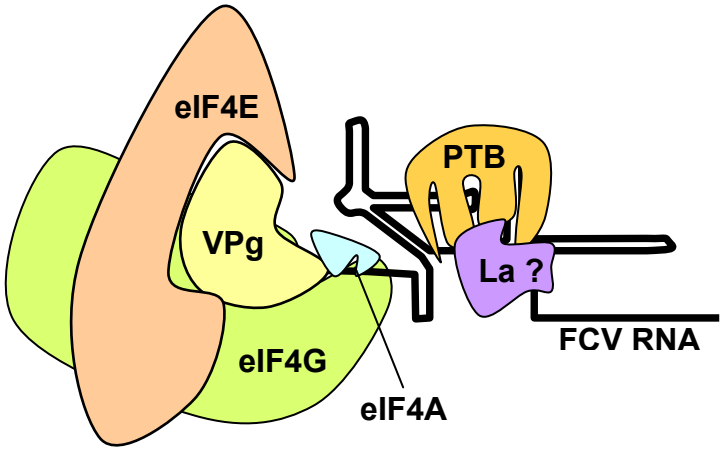


Figure 6.2. The RNP complex that regulates FCV translation. The canonical translation initiation factors eIF4E, eIF4G and eIF4A that are recruited on the 5' end of the FCV RNA through interaction with VPg and possibly with the viral RNA (Chaudhry et al., 2006). PTB and possibly La protein interact with the viral RNA for the regulation of the translation.

MNV replication demonstrated a dependence on RNA elements situated in the 5' and 3' extremities of the MNV genome. The dependence of MNV replication on 5' end RNA structures was less apparent than the requirement of RNA elements in the 3'extremity. The unique translation initiation mechanism of caliciviruses has potentially resulted in the reduction of the regulatory role of the 5' extremity structures during the evolution, as the extremely short 5' UTR would indicate. In contrast the 3' extremity stem-loop (SL7330, **Chapter 4**) is required for the production of viable viruses. If the conserved motifs that form the polypyrimidine loop of this structure are required for the replication of the virus in the *in vivo* mouse model, then strains such as m54RevA could serve as candidates for live-attenuated vaccine.

The identification of RNA-binding proteins that regulate calicivirus translation and replication may reveal new targets for the production of drugs against human caliciviruses. Finally, the construction of attenuated mutant viruses, which are defective in the interaction of their RNA with a cellular protein, could lead to the production of a vaccine strain for a disease that affects millions of people worldwide.

References

Adler, JL. & Zickl R. (1969). Winter vomiting disease. *J Infect Dis* **119**, 668-73

Agirre, A., Barco, A., Carrasco, L. & Nieva, J. L. (2002). Viroporin-mediated membrane permeabilization. Pore formation by nonstructural poliovirus 2B protein. *J Biol Chem* **277**, 40434-41.

Al-Molawi, N., Beardmore, V. A., Carter, M. J., Kass, G. E. & Roberts, L. O. (2003). Caspase-mediated cleavage of the feline calicivirus capsid protein. *J Gen Virol* **84**, 1237-44.

Ali, N. & Siddiqui, A. (1995). Interaction of polypyrimidine tract-binding protein with the 5' noncoding region of the hepatitis C virus RNA genome and its functional requirement in internal initiation of translation. *J Virol* **69**, 6367-75.

Ali, N. & Siddiqui, A. (1997). The La antigen binds 5' noncoding region of the hepatitis C virus RNA in the context of the initiator AUG codon and stimulates internal ribosome entry site-mediated translation. *Proc Natl Acad Sci U S A* **94**, 2249-54.

Andino, R., Rieckhof, G. E., Achacoso, P. L. & Baltimore, D. (1993). Poliovirus RNA Synthesis Utilizes an RNP Complex Formed Around the 5'-End of Viral RNA. *EMBO J* **12**, 3587-3598.

Anwar, A., Ali, N., Tanveer, R. & Siddiqui, A. (2000). Demonstration of Functional Requirement of Polypyrimidine Tract-binding Protein by SELEX RNA during Hepatitis C Virus Internal Ribosome Entry Site-mediated Translation Initiation. *J Biol Chem* **275**, 34231-34235.

Asanaka, M., Atmar, R. L., Ruvolo, V., Crawford, S. E., Neill, F. H. & Estes, M. K. (2005). Replication and packaging of Norwalk virus RNA in cultured mammalian cells. *Proc Natl Acad Sci U S A* **102**, 10327-10332.

Ashiya, M. & Grabowski, P. J. (1997). A neuron-specific splicing switch mediated by an array of pre-mRNA repressor sites: evidence of a regulatory role for the polypyrimidine tract binding protein and a brain-specific PTB counterpart. *RNA* **3**, 996-1015.

Atmar, R. L. & Estes, M. K. (2001). Diagnosis of noncultivatable gastroenteritis viruses, the human caliciviruses. *Clin Microbiol Rev* **14**, 15-37.

Ayukawa, K., Taniguchi, S., Masumoto, J., Hashimoto, S., Sarvotham, H., Hara, A., Aoyama, T. & Sagara, J. (2000). La autoantigen is cleaved in the COOH terminus and loses the nuclear localization signal during apoptosis. *J Biol Chem* **275**, 34465-70.

Bachmann, M., Pfeifer, K., Schroder, H. C. & Muller, W. E. (1989). The La antigen shuttles between the nucleus and the cytoplasm in CV-1 cells. *Mol Cell Biochem* **85**, 103-14.

Back, S. H., Kim, Y. K., Kim, W. J., Cho, S., Oh, H. R., Kim, J. E. & Jang, S. K. (2002a). Translation of polioviral mRNA is inhibited by cleavage of polypyrimidine tract-binding proteins executed by polioviral 3C(pro). *J Virol* **76**, 2529-42.

Back, S. H., Shin, S. & Jang, S. K. (2002b). Polypyrimidine tract-binding proteins are cleaved by caspase-3 during apoptosis. *J Biol Chem* **277**, 27200-9.

Baird, S. D., Turcotte, M., Korneluk, R. G. & Holcik, M. (2006). Searching for IRES. *RNA* **12**, 1755-85.

Bakheet, T., Frevel, M., Williams, B. R., Greer, W. & Khabar, K. S. (2001). ARED: human AU-rich element-containing mRNA database reveals an unexpectedly diverse functional repertoire of encoded proteins. *Nucleic Acids Res* **29**, 246-54.

Barreau, C., Paillard, L. & Osborne, H. B. (2005). AU-rich elements and associated factors: are there unifying principles? *Nucleic Acids Res* **33**, 7138-50.

Barton, D. J., Morasco, B. J. & Flanegan, J. B. (1999). Translating ribosomes inhibit poliovirus negative-strand RNA synthesis. *J Virol* **73**, 10104-12.

Barton, D. J., O'Donnell, B. J. & Flanegan, J. B. (2001). 5' cloverleaf in poliovirus RNA is a *cis*-acting replication element required for negative-strand synthesis. *EMBO J* **20**, 1439-48.

Beerens, N. & Snijder, E. J. (2007). An RNA pseudoknot in the 3' end of the arterivirus genome has a critical role in regulating viral RNA synthesis. *J Virol* **81**, 9426-36.

Belisova, A., Semrad, K., Mayer, O., Kocian, G., Waigmann, E., Schroeder, R. & Steiner, G. (2005). RNA chaperone activity of protein components of human Ro RNPs. *RNA* **11**, 1084-94.

Belliot, G., Sosnovtsev, S. V., Chang, K. O., Babu, V., Uche, U., Arnold, J. J., Cameron, C. E. & Green, K. Y. (2005). Norovirus proteinase-polymerase and polymerase are both active forms of RNA-dependent RNA polymerase. *J Virol* **79**, 2393-403.

Belsham, G. J. & Sonenberg, N. (1996). RNA-Protein Interactions in Regulation of Picornavirus RNA Translation. *Microbiological Reviews* **60**, 499.

Belsham, G. J. & Sonenberg, N. (2000). Picornavirus RNA translation: roles for cellular proteins. *Trends Microbiol* **8**, 330-5.

Bertolotti-Ciarlet, A., Crawford, S. E., Hutson, A. M. & Estes, M. K. (2003). The 3' end of Norwalk virus mRNA contains determinants that regulate the expression and stability of the viral capsid protein VP1: a novel function for the VP2 protein. *J Virol* **77**, 11603-15.

Bertolotti-Ciarlet, A., White, L. J., Chen, R., Prasad, B. V. & Estes, M. K. (2002). Structural requirements for the assembly of Norwalk virus-like particles. *J Virol* **76**, 4044-55.

Birney, E., Kumar, S. & Krainer, A. R. (1993). Analysis of the RNA-recognition motif and RS and RGG domains: conservation in metazoan pre-mRNA splicing factors. *Nucleic Acids Res* **21**, 5803-16.

Blakeney, S. J., Cahill, A. & Reilly, P. A. (2003). Processing of Norwalk virus nonstructural proteins by a 3C-like cysteine proteinase. *Virology* **308**, 216-24.

Blyn, L. B., Swiderek, K. M., Richards, O., Stahl, D. C., Semler, B. L. & Ehrenfeld, E. (1996). Poly(rC) binding protein 2 binds to stem-loop IV of the poliovirus RNA 5' noncoding region: identification by automated liquid chromatography-tandem mass spectrometry. *Proc Natl Acad Sci U S A* **93**, 11115-20.

Borman, A., Howell, M. T., Patton, J. G. & Jackson, R. J. (1993). The involvement of a spliceosome component in internal initiation of human rhinovirus RNA translation. *J Gen Virol* **74**, 1775-1788.

Boussadia, O., Niepmann, M., Creancier, L., Prats, A.-C., Dautry, F. & Jacquemin-Sablon, H. (2003). Unr Is Required In Vivo for Efficient Initiation of Translation from the Internal Ribosome Entry Sites of both Rhinovirus and Poliovirus. *J. Virol.* **77**, 3353-3359.

Bradrick, S. S., Walters, R. W. & Gromeier, M. (2006). The hepatitis C virus 3'-untranslated region or a poly(A) tract promote efficient translation subsequent to the initiation phase. *Nucleic Acids Res* **34**, 1293-303.

Brenet, F., Dussault, N., Borch, J., Ferracci, G., Delfino, C., Roepstorff, P., Miquelis, R. & Ouafik, L. (2005). Mammalian peptidylglycine alpha-amidating monooxygenase mRNA expression can be modulated by the La autoantigen. *Mol Cell Biol* **25**, 7505-21.

Brown, D. M., Kauder, S. E., Cornell, C. T., Jang, G. M., Racaniello, V. R. & Semler, B. L. (2004). Cell-dependent role for the poliovirus 3' noncoding region in positive-strand RNA synthesis. *J Virol* **78**, 1344-51.

Büchen-Osmond, C. E. (2003). 00.012. Caliciviridae. In: *ICTVdB - The Universal Virus Database*, version 3. *ICTVdB*.

Burroughs, J. N. & Brown, F. (1978). Presence of a covalently linked protein on calicivirus RNA. *J Gen Virol* **41**, 443-6.

Buyon, J. P. (1989). Neonatal lupus and congenital complete heart block: manifestations of passively acquired autoimmunity. *Clin Exp Rheumatol* **7 Suppl 3**, S199-203.

Caput, D., Beutler, B., Hartog, K., Thayer, R., Brown-Shimer, S. & Cerami, A. (1986). Identification of a common nucleotide sequence in the 3'-untranslated region of mRNA molecules specifying inflammatory mediators. *Proc Natl Acad Sci U S A* **83**, 1670-4.

Chanfreau, G., Elela, S. A., Ares, M., Jr. & Guthrie, C. (1997). Alternative 3'-end processing of U5 snRNA by RNase III. *Genes Dev* **11**, 2741-51.

Chang, K. H., Brown, E. A. & Lemon, S. M. (1993). Cell-type-specific proteins which interact with the 5' nontranslated region of hepatitis-A virus-RNA. *J Virol* **67**, 6716-6725.

Chang, K. O., Sosnovtsev, S. V., Belliot, G., King, A. D. & Green, K. Y. (2006). Stable expression of a Norwalk virus RNA replicon in a human hepatoma cell line. *Virology* **353**, 463-73.

Chang, K. S. & Luo, G. (2006). The polypyrimidine tract-binding protein (PTB) is required for efficient replication of hepatitis C virus (HCV) RNA. *Virus Res* **115**, 1-8.

Chaudhry, Y., Nayak, A., Bordeleau, M. E., Tanaka, J., Pelletier, J., Belsham, G. J., Roberts, L. O. & Goodfellow, I. G. (2006). Caliciviruses differ in their functional requirements for eIF4F components. *J Biol Chem* **281**, 25315-25.

Chaudhry, Y., Skinner, M. A. & Goodfellow, I. G. (2007). Recovery of genetically defined murine norovirus in tissue culture by using a fowlpox virus expressing T7 RNA polymerase. *J Gen Virol* **88**, 2091-100.

Cheetham, S., Souza, M., Meulia, T., Grimes, S., Han, M. G. & Saif, L. J. (2006). Pathogenesis of a genogroup II human norovirus in gnotobiotic pigs. *J Virol* **80**, 10372-81.

Chen, C. Y. & Shyu, A. B. (1994). Selective degradation of early-response-gene mRNAs: functional analyses of sequence features of the AU-rich elements. *Mol Cell Biol* **14**, 8471-82.

Chen, M. H., Roossinck, M. J. & Kao, C. C. (2000). Efficient and specific initiation of subgenomic RNA synthesis by cucumber mosaic virus replicase in vitro requires an upstream RNA stem-loop. *J Virol* **74**, 11201-9.

Chkheidze, A. N., Lyakhov, D. L., Makeyev, A. V., Morales, J., Kong, J. & Liebhaber, S. A. (1999). Assembly of the alpha-globin mRNA stability complex reflects binary interaction between the pyrimidine-rich 3' untranslated region determinant and poly(C) binding protein alphaCP. *Mol Cell Biol* **19**, 4572-81.

Ciesla, J. (2006). Metabolic enzymes that bind RNA: yet another level of cellular regulatory network? *Acta Biochim Pol* **53**, 11-32.

Clarke, I. N. & Lambden, P. R. (1997). The molecular biology of caliciviruses. *J Gen Virol* **78**, 291-301.

Correll, C. C. & Swinger, K. (2003). Common and distinctive features of GNRA tetraloops based on a GUAA tetraloop structure at 1.4 A resolution. *RNA* **9**, 355-63.

Costa-Mattioli, M., Svitkin, Y. & Sonenberg, N. (2004). La autoantigen is necessary for optimal function of the poliovirus and hepatitis C virus internal ribosome entry site in vivo and in vitro. *Mol Cell Biol* **24**, 6861-70.

Cote, C. A., Gautreau, D., Denegre, J. M., Kress, T. L., Terry, N. A. & Mowry, K. L. (1999). A Xenopus protein related to hnRNP I has a role in cytoplasmic RNA localization. *Mol Cell* **4**, 431-7.

Coyne, K. P., Jones, B. R., Kipar, A., Chantrey, J., Porter, C. J., Barber, P. J., Dawson, S., Gaskell, R. M. & Radford, A. D. (2006). Lethal outbreak of disease associated with feline calicivirus infection in cats. *Vet Rec* **158**, 544-50.

Daughenbaugh, K. F., Fraser, C. S., Hershey, J. W. & Hardy, M. E. (2003). The genome-linked protein VPg of the Norwalk virus binds eIF3, suggesting its role in translation initiation complex recruitment. *EMBO J* **22**, 2852-9.

De Nova-Ocampo, M., Villegas-Sepulveda, N. & del Angel, R. M. (2002). Translation elongation factor-1alpha, La, and PTB interact with the 3' untranslated region of dengue 4 virus RNA. *Virology* **295**, 337-47.

Dejgaard, K. & Leffers, H. (1996). Characterisation of the nucleic-acid-binding activity of KH domains. Different properties of different domains. *Eur J Biochem* **241**, 425-31.

DeMaria, C. T. & Brewer, G. (1996). AUF1 binding affinity to A+U-rich elements correlates with rapid mRNA degradation. *J Biol Chem* **271**, 12179-84.

Domitrovich, A. M., Diebel, K. W., Ali, N., Sarker, S. & Siddiqui, A. (2005). Role of La autoantigen and polypyrimidine tract-binding protein in HCV replication. *Virology* **335**, 72-86.

Dorner, A. J., Semler, B. L., Jackson, R. J., Hanecak, R., Duprey, E. & Wimmer, E. (1984). In Vitro translation of poliovirus RNA: Utilisation of internal initiation sites in reticulocyte lysates. *J Virol* **50 (2)**, 507-514.

Du, Q., Melnikova, I. N. & Gardner, P. D. (1998). Differential effects of heterogeneous nuclear ribonucleoprotein K on Sp1- and Sp3-mediated transcriptional activation of a neuronal nicotinic acetylcholine receptor promoter. *J Biol Chem* **273**, 19877-83.

Du, Z., Lee, J. K., Fenn, S., Tjhen, R., Stroud, R. M. & James, T. L. (2007). X-ray crystallographic and NMR studies of protein-protein and protein-nucleic acid interactions involving the KH domains from human poly(C)-binding protein-2. *RNA* **13**, 1043-51.

Edgil, D. & Harris, E. (2006). End-to-end communication in the modulation of translation by mammalian RNA viruses. *Virus Res* **119**, 43-51.

Elbashir, S. M., Harborth, J., Lendeckel, W., Yalcin, A., Weber, K. & Tuschl, T. (2001). Duplexes of 21-nucleotide RNAs mediate RNA interference in cultured mammalian cells. *Nature* **411**, 494-8.

Erlitzki, R., Long, J. C. & Theil, E. C. (2002). Multiple, conserved iron-responsive elements in the 3'-untranslated region of transferrin receptor mRNA enhance binding of iron regulatory protein 2. *J Biol Chem* **277**, 42579-87.

Ettayebi, K. & Hardy, M. E. (2003). Norwalk virus nonstructural protein p48 forms a complex with the SNARE regulator VAP-A and prevents cell surface expression of vesicular stomatitis virus G protein. *J Virol* **77**, 11790-7.

Fang, J. W. & Moyer, R. W. (2000). The effects of the conserved extreme 3' end sequence of hepatitis C virus (HCV) RNA on the in vitro stabilization and translation of the HCV RNA genome. *J Hepatol* **33**, 632-9.

FeRNAndez-Vega, V., Sosnovtsev, S. V., Belliot, G., King, A. D., Mitra, T., Gorbalenya, A. & Green, K. Y. (2004). Norwalk virus N-terminal nonstructural protein is associated with disassembly of the Golgi complex in transfected cells. *J Virol* **78**, 4827-37.

Fire, A., Xu, S., Montgomery, M. K., Kostas, S. A., Driver, S. E. & Mello, C. C. (1998). Potent and specific genetic interference by double-stranded RNA in Caenorhabditis elegans. *Nature* **391**, 806-11.

Fletcher, S. P. & Jackson, R. J. (2002). Pestivirus internal ribosome entry site (IRES) structure and function: elements in the 5' untranslated region important for IRES function. *J Virol* **76**, 5024-33.

Florez, P. M., Sessions, O. M., Wagner, E. J., Gromeier, M. & Garcia-Blanco, M. A. (2005). The polypyrimidine tract binding protein is required for efficient picornavirus gene expression and propagation. *J Virol* **79**, 6172-9.

Friebe, P. & Bartenschlager, R. (2002). Genetic analysis of sequences in the 3' nontranslated region of hepatitis C virus that are important for RNA replication. *J Virol* **76**, 5326-38.

Fukushi, S., Kojima, S., Takai, R., Hoshino, F. B., Oka, T., Takeda, N., Katayama, K. & Kageyama, T. (2004). Poly(A)- and primer-independent RNA polymerase of Norovirus. *J Virol* **78**, 3889-96.

Fullerton, S. W., Blaschke, M., Coutard, B., Gebhardt, J., Gorbalenya, A., Canard, B., Tucker, P. A. & Rohayem, J. (2007). Structural and Functional Characterization of Sapovirus RNA-Dependent RNA Polymerase. *J Virol* **81**, 1858-71.

Gamarnik, A. V. & Andino, R. (1998). Switch from translation to RNA replication in a positive-stranded RNA virus. *Genes Dev* **12**, 2293-304.

Gamarnik, A. V. & Andino, R. (2000). Interactions of viral protein 3CD and poly(rC) binding protein with the 5' untranslated region of the poliovirus genome. *J Virol* **74**, 2219-26.

Geissler, K., Parrish, C. R., Schneider, K. & Truyen, U. (1999). Feline calicivirus capsid protein expression and self-assembly in cultured feline cells. *Vet Microbiol* **69**, 63-6.

Glass, P. J., White, L. J., Ball, J. M., Leparc-Goffart, I., Hardy, M. E. & Estes, M. K. (2000). Norwalk virus open reading frame 3 encodes a minor structural protein. *J Virol* **74**, 6581-91.

Glass, P. J., Zeng, C. Q. & Estes, M. K. (2003). Two nonoverlapping domains on the Norwalk virus open reading frame 3 (ORF3) protein are involved in the formation of the phosphorylated 35K protein and in ORF3-capsid protein interactions. *J Virol* **77**, 3569-77.

Goessling, L. S., Mascotti, D. P. & Thach, R. E. (1998). Involvement of heme in the degradation of iron-regulatory protein 2. *J Biol Chem* **273**, 12555-7.

Gohara, D. W., Crotty, S., Arnold, J. J., Yoder, J. D., Andino, R. & Cameron, C. E. (2000). Poliovirus RNA-dependent RNA polymerase (3Dpol): structural, biochemical, and biological analysis of conserved structural motifs A and B. *J Biol Chem* **275**, 25523-32.

Goodfellow, I., Chaudhry, Y., Gioldasi, I., Gerondopoulos, A., Natoni, A., Labrie, L., Laliberte, J. & Roberts, L. (2005). Calicivirus translation initiation requires an interaction between VPg and eIF4E. *EMBO Reports* **6**, 968–972.

Goodfellow, I. G., Chaudhry, Y., Richardson, A., Meredith, J. M., Almond, J. W., Barclay, W. S. & Evans, D. J. (2000). Identification of a *cis*-acting replication element (CRE) within the poliovirus coding region. *J Virol* **74**, 4590-4600.

Goodfellow, I. G., Kerrigan, D. & Evans, D. J. (2003a). Structure and function analysis of the poliovirus cis-acting replication element (CRE). *RNA* **9**, 124-37.

Goodfellow, I. G., Polacek, C., Andino, R. & Evans, D. J. (2003b). The poliovirus 2C cis-acting replication element-mediated uridylylation of VPg is not required for synthesis of negative-sense genomes. *J Gen Virol* **84**, 2359-63.

Gosert, R., Chang, K. H., Rijnbrand, R., Yi, M., Sangar, D. V. & Lemon, S. M. (2000). Transient expression of cellular polypyrimidine-tract binding protein stimulates cap-independent translation directed by both picornaviral and flaviviral internal ribosome entry sites In vivo. *Mol Cell Biol* **20**, 1583-95.

Graham, D. Y., Jiang, X., Tanaka, T., Opekun, A. R., Madore, H. P. & Estes, M. K. (1994). Norwalk virus infection of volunteers: new insights based on improved assays. *J Infect Dis* **170**, 34-43.

Graus, F., Cordon-Cardo, C., Bonfa, E. & Elkon, K. B. (1985). Immunohistochemical localization of La nuclear antigen in brain. Selective concentration of the La protein in neuronal nucleoli. *J Neuroimmunol* **9**, 307-19.

Green, K. Y., Mory, A., Fogg, M. H., Weisberg, A., Belliot, G., Wagner, M., Mitra, T., Ehrenfeld, E., Cameron, C. E. & Sosnovtsev, S. V. (2002). Isolation of

enzymatically active replication complexes from feline calicivirus-infected cells. *J Virol* **76**, 8582-95.

Guerrier-Takada, C., Gardiner, K., Marsh, T., Pace, N. & Altman, S. (1983). The RNA moiety of ribonuclease P is the catalytic subunit of the enzyme. *Cell* **35**, 849-57.

Guest, S., Pilipenko, E., Sharma, K., Chumakov, K. & Roos, R. P. (2004). Molecular mechanisms of attenuation of the Sabin strain of poliovirus type 3. *J Virol* **78**, 11097-107.

Gustin, K. E. & Sarnow, P. (2001). Effects of poliovirus infection on nucleo-cytoplasmic trafficking and nuclear pore complex composition. *EMBO J* **20**, 240-9.

Gustin, K. E. & Sarnow, P. (2002). Inhibition of nuclear import and alteration of nuclear pore complex composition by rhinovirus. *J Virol* **76**, 8787-96.

Gutierrez-Escolano, A. L., Brito, Z. U., del Angel, R. M. & Jiang, X. (2000). Interaction of cellular proteins with the 5' end of Norwalk virus genomic RNA. *J Virol* **74**, 8558-62.

Gutierrez-Escolano, A. L., Vazquez-Ochoa, M., Escobar-Herrera, J. & Hernandez-Acosta, J. (2003). La, PTB, and PAB proteins bind to the 3(') untranslated region of Norwalk virus genomic RNA. *Biochem Biophys Res Commun* **311**, 759-66.

Hamilton, B. J., Nagy, E., Malter, J. S., Arrick, B. A. & Rigby, W. F. (1993). Association of heterogeneous nuclear ribonucleoprotein A1 and C proteins with reiterated AUUUA sequences. *J Biol Chem* **268**, 8881-7.

Hellen, C. U., Witherell, G. W., Schmid, M., Shin, S. H., Pestova, T. V., Gil, A. & Wimmer, E. (1993a). A cytoplasmic 57-kDa protein that is required for translation of picornavirus RNA by internal ribosomal entry is identical to the nuclear pyrimidine tract-binding protein. *Proc Natl Acad Sci U S A* **90**, 7642-6.

Hellen, C. U. T., Witherell, G. W., Schmid, M., Shin, S. H., Pestova, T. V., Gil, A. & Wimmer, E. (1993b). A cytoplasmic 57-kda protein that is required for translation of picornavirus RNA by internal ribosomal entry is identical to the nuclear pyrimidine tract-binding protein. *Proc Natl Acad Sci U S A* **90**, 7642-7646.

Henics, T. & Zimmer, C. (2006). RNA delivery by heat shock protein-70 into mammalian cells: a preliminary study. *Cell Biol Int* **30**, 480-4.

Hennessy, E. P., Green, A. D., Connor, M. P., Darby, R. & MacDonald, P. (2003). Norwalk virus infection and disease is associated with ABO histo-blood group type. *J Infect Dis* **188**, 176-7.

Herbert, T. P., Brierley, I. & Brown, T. D. (1997). Identification of a protein linked to the genomic and subgenomic mRNAs of feline calicivirus and its role in translation. *J Gen Virol* **78**, 1033-40.

Herold, J. & Andino, R. (2001). Poliovirus RNA replication requires genome circularization through a protein-protein bridge. *Mol Cell* **7**, 581-91.

Herschlag, D. (1995). RNA chaperones and the RNA folding problem. *J Biol Chem* **270**, 20871-4.

Holcik, M. & Korneluk, R. G. (2000). Functional characterization of the X-linked inhibitor of apoptosis (XIAP) internal ribosome entry site element: role of La autoantigen in XIAP translation. *Mol Cell Biol* **20**, 4648-57.

Hollams, E. M., Giles, K. M., Thomson, A. M. & Leedman, P. J. (2002). mRNA stability and the control of gene expression: implications for human disease. *Neurochem Res* **27**, 957-80.

Hsu, C. C., Riley, L. K., Wills, H. M. & Livingston, R. S. (2006). Persistent infection with and serologic cross-reactivity of three novel murine noroviruses. *Comp Med* **56**, 247-51.

Huang, J., Brieba, L. G. & Sousa, R. (2000). Misincorporation by wild-type and mutant T7 RNA polymerases: identification of interactions that reduce misincorporation rates by stabilizing the catalytically incompetent open conformation. *Biochemistry* **39**, 11571-80.

Huang, P., Farkas, T., Marionneau, S., Zhong, W., Ruvoen-Clouet, N., Morrow, A. L., Altaye, M., Pickering, L. K., Newburg, D. S., LePendu, J. & Jiang, X. (2003). Noroviruses bind to human ABO, Lewis, and secretor histo-blood group antigens: identification of 4 distinct strain-specific patterns. *J Infect Dis* **188**, 19-31.

Huang, P. & Lai, M. M. (1999). Polypyrimidine tract-binding protein binds to the complementary strand of the mouse hepatitis virus 3' untranslated region, thereby altering RNA conformation. *J Virol* **73**, 9110-6.

Hunt, S. L., Hsuan, J. J., Totty, N. & Jackson, R. J. (1999). unr, a cellular cytoplasmic RNA-binding protein with five cold-shock domains, is required for internal initiation of translation of human rhinovirus RNA. *Genes Dev* **13**, 437-448.

Hunt, S. L. & Jackson, R. J. (1999). Polypyrimidine-tract binding protein (PTB) is necessary, but not sufficient, for efficient internal initiation of translation of human rhinovirus-2 RNA. *RNA* **5**, 344-359.

Ito, T. & Lai, M. M. (1999). An internal polypyrimidine-tract-binding protein-binding site in the hepatitis C virus RNA attenuates translation, which is relieved by the 3'-untranslated sequence. *Virology* **254**, 288-96.

Ito, T., Tahara, S. M. & Lai, M. M. (1998). The 3'-untranslated region of hepatitis C virus RNA enhances translation from an internal ribosomal entry site. *J Virol* **72**, 8789-96.

Iwaoka, S., Nakamura, T., Takano, S., Tsuchiya, S. & Aramaki, Y. (2006). Cationic liposomes induce apoptosis through p38 MAP kinase-caspase-8-Bid pathway in macrophage-like RAW264.7 cells. *J Leukoc Biol* **79**, 184-91.

Izquierdo, J. M., Majos, N., Bonnal, S., Martinez, C., Castelo, R., Guigo, R., Bilbao, D. & Valcarcel, J. (2005). Regulation of Fas alternative splicing by antagonistic effects of TIA-1 and PTB on exon definition. *Mol Cell* **19**, 475-84.

Jackson, R. J. (2005). Alternative mechanisms of initiating translation of mammalian mRNAs. *Biochem Soc Trans* **33**, 1231-41.

Jan, E. & Sarnow, P. (2002). Factorless ribosome assembly on the internal ribosome entry site of cricket paralysis virus. *J Mol Biol* **324**, 889-902.

Jang, S. K. (2006). Internal initiation: IRES elements of picornaviruses and hepatitis c virus. *Virus Res* **119**, 2-15.

Jang, S. K. & Wimmer, E. (1990). Cap-independent translation of encephalomyocarditis virus RNA: structural elements of the internal ribosomal entry site and involvement of a cellular 57-kD RNA-binding protein. *Genes Dev* **4**, 1560-1572.

Jansen, R. P. (2001). mRNA localization: message on the move. *Nat Rev Mol Cell Biol* **2**, 247-56.

Jiang, X., Wang, M., Wang, K. & Estes, M. K. (1993). Sequence and genomic organization of Norwalk virus. *Virology* **195**, 51-61.

Kaiser, W. J., Chaudhry, Y., Sosnovtsev, S. V. & Goodfellow, I. G. (2006). Analysis of protein-protein interactions in the feline calicivirus replication complex. *J Gen Virol* **87**, 363-8.

Kalliampakou, K. I., Kalamvoki, M. & Mavromara, P. (2005). Hepatitis C virus (HCV) NS5A protein downregulates HCV IRES-dependent translation. *J Gen Virol* **86**, 1015-25.

Kamath, R. V., Leary, D. J. & Huang, S. (2001). Nucleocytoplasmic shuttling of polypyrimidine tract-binding protein is uncoupled from RNA export. *Mol Biol Cell* **12**, 3808-20.

Kaminski, A., Hunt, S. L., Patton, J. G. & Jackson, R. J. (1995). Direct evidence that polypyrimidine tract binding-protein (PTB) is essential for internal initiation of translation of encephalomyocarditis virus-RNA. *RNA* **1**, 924-938.

Kaminski, A. & Jackson, R. J. (1998). The polypyrimidine tract binding protein (PTB) requirement for internal initiation of translation of cardiovirus RNAs is conditional rather than absolute. *RNA* **4**, 626-38.

Karst, S. M., Wobus, C. E., Lay, M., Davidson, J. & Virgin, H. W. t. (2003). STAT1-dependent innate immunity to a Norwalk-like virus. *Science* **299**, 1575-8.

Kikovska, E., Svard, S. G. & Kirsebom, L. A. (2007). Eukaryotic RNase P RNA mediates cleavage in the absence of protein. *Proc Natl Acad Sci U S A* **104**, 2062-7.

Kikuchi, K., Umehara, T., Fukuda, K., Kuno, A., Hasegawa, T. & Nishikawa, S. (2005). A hepatitis C virus (HCV) internal ribosome entry site (IRES) domain III-IV-targeted aptamer inhibits translation by binding to an apical loop of domain IIId. *Nucleic Acids Res* **33**, 683-92.

Kim, S. S., Pandey, K. K., Choi, H. S., Kim, S. Y., Law, P. Y., Wei, L. N. & Loh, H. H. (2005). Poly(C) binding protein family is a transcription factor in mu-opioid receptor gene expression. *Mol Pharmacol* **68**, 729-36.

Kim, Y. K., Back, S. H., Rho, J., Lee, S. H. & Jang, S. K. (2001). La autoantigen enhances translation of BiP mRNA. *Nucleic Acids Res* **29**, 5009-16.

Knudsen, B. & Hein, J. (2003). Pfold: RNA secondary structure prediction using stochastic context-free grammars. *Nucleic Acids Res* **31**, 3423-8.

Kolupaeva, V. G., Hellen, C. U. T. & Shatsky, I. N. (1996). Structural-analysis of the interaction of the pyrimidine tract- binding protein with the internal ribosomal

entry site of encephalomyocarditis virus and foot-and-mouth-disease virus RNAs. *RNA* **2**, 1199-1212.

Kolupaeva, V. G., Lomakin, I. B., Pestova, T. V. & Hellen, C. U. (2003). Eukaryotic initiation factors 4G and 4A mediate conformational changes downstream of the initiation codon of the encephalomyocarditis virus internal ribosomal entry site. *Mol Cell Biol* **23**, 687-98.

Kolupaeva, V. G., Pestova, T. V., Hellen, C. U. & Shatsky, I. N. (1998). Translation eukaryotic initiation factor 4G recognizes a specific structural element within the internal ribosome entry site of encephalomyocarditis virus RNA. *J Biol Chem* **273**, 18599-604.

Kong, J., Ji, X. & Liebhaber, S. A. (2003). The KH-domain protein alpha CP has a direct role in mRNA stabilization independent of its cognate binding site. *Mol Cell Biol* **23**, 1125-34.

Konig, M., Thiel, H. J. & Meyers, G. (1998). Detection of viral proteins after infection of cultured hepatocytes with rabbit hemorrhagic disease virus. *J Virol* **72**, 4492-7.

Kozak, M. (2005). Regulation of translation via mRNA structure in prokaryotes and eukaryotes. *Gene* **361**, 13-37.

Kruger, K., Grabowski, P. J., Zaug, A. J., Sands, J., Gottschling, D. E. & Cech, T. R. (1982). Self-splicing RNA: autoexcision and autocyclization of the ribosomal RNA intervening sequence of Tetrahymena. *Cell* **31**, 147-57.

Kuyumcu-Martinez, M., Belliot, G., Sosnovtsev, S. V., Chang, K. O., Green, K. Y. & Lloyd, R. E. (2004). Calicivirus 3C-like proteinase inhibits cellular translation by cleavage of poly(A)-binding protein. *J Virol* **78**, 8172-82.

Lai, E. C. (2002). Micro RNAs are complementary to 3' UTR sequence motifs that mediate negative post-transcriptional regulation. *Nat Genet* **30**, 363-4.

Lai, M. M. (1998). Cellular factors in the transcription and replication of viral RNA genomes: a parallel to DNA-dependent RNA transcription. *Virology* **244**, 1-12.

Le, S., Sternglanz, R. & Greider, C. W. (2000). Identification of two RNA-binding proteins associated with human telomerase RNA. *Mol Biol Cell* **11**, 999-1010.

Leonard, S., Plante, D., Wittmann, S., Daigneault, N., Fortin, M. G. & Laliberte, J. F. (2000). Complex formation between potyvirus VPg and translation eukaryotic initiation factor 4E correlates with virus infectivity. *J Virol* **74**, 7730-7.

Li, H. P., Huang, P., Park, S. & Lai, M. M. (1999). Polypyrimidine tract-binding protein binds to the leader RNA of mouse hepatitis virus and serves as a regulator of viral transcription. *J Virol* **73**, 772-7.

Lindesmith, L., Moe, C., Marionneau, S., Ruvoen, N., Jiang, X., Lindblad, L., Stewart, P., LePendu, J. & Baric, R. (2003). Human susceptibility and resistance to Norwalk virus infection. *Nat Med* **9**, 548-53.

Lomakin, I. B., Hellen, C. U. & Pestova, T. V. (2000). Physical association of eukaryotic initiation factor 4G (eIF4G) with eIF4A strongly enhances binding of eIF4G to the internal ribosomal entry site of encephalomyocarditis virus and is required for internal initiation of translation. *Mol Cell Biol* **20**, 6019-29.

Lopman, B. A., Brown, D. W. & Koopmans, M. (2002). Human caliciviruses in Europe. *J Clin Virol* **24**, 137-60.

Lopman, B. A., Reacher, M. H., Vipond, I. B., Hill, D., Perry, C., Halladay, T., Brown, D. W., Edmunds, W. J. & Sarangi, J. (2004). Epidemiology and cost of nosocomial gastroenteritis, Avon, England, 2002-2003. *Emerg Infect Dis* **10**, 1827-34.

Lou, H., Helfman, D. M., Gagel, R. F. & Berget, S. M. (1999). Polypyrimidine tract-binding protein positively regulates inclusion of an alternative 3'-terminal exon. *Mol Cell Biol* **19**, 78-85.

Lu, H., Li, W., Noble, W. S., Payan, D. & Anderson, D. C. (2004). Riboproteomics of the hepatitis C virus internal ribosomal entry site. *J Proteome Res* **3**, 949-57.

Luo, G., Xin, S. & Cai, Z. (2003). Role of the 5'-proximal stem-loop structure of the 5' untranslated region in replication and translation of hepatitis C virus RNA. *J Virol* **77**, 3312-8.

Luttermann, C. & Meyers, G. (2007). A bipartite sequence motif induces translation reinitiation in feline calicivirus RNA. *J Biol Chem*.

Luz, N. & Beck, E. (1991). Interaction of a Cellular 57-Kilodalton Protein with the Internal Translation Initiation Site of Foot-and-Mouth Disease Virus. *J Virol* **65**, 6486-6494.

Lyons, T., Murray, K. E., Roberts, A. W. & Barton, D. J. (2001). Poliovirus 5'-terminal cloverleaf RNA is required in cis for VPg uridylylation and the initiation of negative-strand RNA synthesis. *J Virol* **75**, 10696-708.

Makeyev, A. V. & Liebhaber, S. A. (2002). The poly(C)-binding proteins: a multiplicity of functions and a search for mechanisms. *RNA* **8**, 265-78.

Makino, A., Shimojima, M., Miyazawa, T., Kato, K., Tohya, Y. & Akashi, H. (2006). Junctional adhesion molecule 1 is a functional receptor for feline calicivirus. *J Virol* **80**, 4482-90.

Marin, M. S., Casais, R., Alonso, J. M. & Parra, F. (2000). ATP binding and ATPase activities associated with recombinant rabbit hemorrhagic disease virus 2C-like polypeptide. *J Virol* **74**, 10846-51.

Marinescu, V., Loomis, P. A., Ehmann, S., Beales, M. & Potashkin, J. A. (2007). Regulation of retention of FosB intron 4 by PTB. *PLoS ONE* **2**, e828.

Martin Alonso, J. M., Casais, R., Boga, J. A. & Parra, F. (1996). Processing of rabbit hemorrhagic disease virus polyprotein. *J Virol* **70**, 1261-5.

Martinez-Salas, E., Ramos, R., Lafuente, E. & Lopez de Quinto, S. (2001). Functional interactions in internal translation initiation directed by viral and cellular IRES elements. *J Gen Virol* **82**, 973-84.

Mattick, J. S. (2001). Non-coding RNAs: the architects of eukaryotic complexity. *EMBO Rep* **2**, 986-91.

Mattick, J. S. (2004). RNA regulation: a new genetics? *Nat Rev Genet* **5**, 316-23.

McCaffrey, A. P., Ohashi, K., Meuse, L., Shen, S., Lancaster, A. M., Lukavsky, P. J., Sarnow, P. & Kay, M. A. (2002). Determinants of hepatitis C translational initiation in vitro, in cultured cells and mice. *Mol Ther* **5**, 676-84.

Mead, P. S., Slutsker, L., Dietz, V., McCaig, L. F., Bresee, J. S., Shapiro, C., Griffin, P. M. & Tauxe, R. V. (1999). Food-related illness and death in the United States. *Emerg Infect Dis* **5**, 607-25.

Meerovitch, K., Svitkin, Y. V., Lee, H. S., Lejbkowicz, F., Kenan, D. J., Chan, E. K. L., Agol, V. I., Keene, J. D. & Sonenberg, N. (1993). La Autoantigen Enhances and Corrects Aberrant Translation of Poliovirus RNA in Reticulocyte Lysate. *J Virol* **67**, 3798-3807.

Merrill, M. K., Dobrikova, E. Y. & Gromeier, M. (2006). Cell-type-specific repression of internal ribosome entry site activity by double-stranded RNA-binding protein 76. *J Virol* **80**, 3147-56.

Meyers, G. (2003). Translation of the minor capsid protein of a calicivirus is initiated by a novel termination-dependent reinitiation mechanism. *J Biol Chem* **278**, 34051-60.

Meyers, G., Wirblich, C. & Thiel, H. J. (1991). Genomic and subgenomic RNAs of rabbit hemorrhagic disease virus are both protein-linked and packaged into particles. *Virology* **184**, 677-86.

Michel, Y. M., Borman, A. M., Paulous, S. & Kean, K. M. (2001). Eukaryotic initiation factor 4G-poly(A) binding protein interaction is required for poly(A) tail-mediated stimulation of picornavirus internal ribosome entry segment-driven translation but not for X-mediated stimulation of hepatitis C virus translation. *Mol Cell Biol* **21**, 4097-109.

Mitra, T., Sosnovtsev, S. V. & Green, K. Y. (2004). Mutagenesis of tyrosine 24 in the VPg protein is lethal for feline calicivirus. *J Virol* **78**, 4931-5.

Monie, T. P., Perrin, A. J., Birtley, J. R., Sweeney, T. R., Karakasiliotis, I., Chaudhry, Y., Roberts, L. O., Matthews, S., Goodfellow, I. G. & Curry, S. (2007). Structural insights into the transcriptional and translational roles of Ebp1. *EMBO J* **26**, 3936-44.

Morales, M., Barcena, J., Ramirez, M. A., Boga, J. A., Parra, F. & Torres, J. M. (2004). Synthesis in vitro of rabbit hemorrhagic disease virus subgenomic RNA by internal initiation on (-)sense genomic RNA: mapping of a subgenomic promoter. *J Biol Chem* **279**, 17013-8.

Moulton, V., Gardner, P. P., Pointon, R. F., Creamer, L. K., Jameson, G. B. & Penny, D. (2000). RNA folding argues against a hot-start origin of life. *J Mol Evol* **51**, 416-21.

Muckenthaler, M., Gray, N. K. & Hentze, M. W. (1998). IRP-1 binding to ferritin mRNA prevents the recruitment of the small ribosomal subunit by the cap-binding complex eIF4F. *Mol Cell* **2**, 383-8.

Muller, B., Klemm, U., Mas Marques, A. & Schreier, E. (2007). Genetic diversity and recombination of murine noroviruses in immunocompromised mice. *Arch Virol* **152**, 1709-19.

Murakami, K., Abe, M., Kageyama, T., Kamoshita, N. & Nomoto, A. (2001). Down-regulation of translation driven by hepatitis C virus internal ribosomal entry site by the 3' untranslated region of RNA. *Arch Virol* **146**, 729-41.

Neill, J. D. (2002). The subgenomic RNA of feline calicivirus is packaged into viral particles during infection. *Virus Res* **87**, 89-93.

Nesser, N. K., Peterson, D. O. & Hawley, D. K. (2006). RNA polymerase II subunit Rpb9 is important for transcriptional fidelity in vivo. *Proc Natl Acad Sci U S A* **103**, 3268-73.

Ng, K. K., Cherney, M. M., Vazquez, A. L., Machin, A., Alonso, J. M., Parra, F. & James, M. N. (2002). Crystal structures of active and inactive conformations of a caliciviral RNA-dependent RNA polymerase. *J Biol Chem* **277**, 1381-7.

Niepmann, M., Petersen, A., Meyer, K. & Beck, E. (1997). Functional involvement of polypyrimidine tract-binding protein in translation initiation complexes with the internal ribosome entry site of foot-and-mouth disease virus. *J Virol* **71**, 8330-9.

Nissen, P., Hansen, J., Ban, N., Moore, P. B. & Steitz, T. A. (2000). The structural basis of ribosome activity in peptide bond synthesis. *Science* **289**, 920-30.

Ochs, K., Saleh, L., Bassili, G., Sonntag, V. H., Zeller, A. & Niepmann, M. (2002). Interaction of translation initiation factor eIF4B with the poliovirus internal ribosome entry site. *J Virol* **76**, 2113-22.

Ochs, K., Zeller, A., Saleh, L., Bassili, G., Song, Y., Sonntag, A. & Niepmann, M. (2003). Impaired binding of standard initiation factors mediates poliovirus translation attenuation. *J Virol* **77**, 115-22.

Ostareck, D. H., Ostareck-Lederer, A., Shatsky, I. N. & Hentze, M. W. (2001). Lipoxygenase mRNA silencing in erythroid differentiation: The 3'UTR regulatory complex controls 60S ribosomal subunit joining. *Cell* **104**, 281-90.

Ostareck, D. H., Ostareck-Lederer, A., Wilm, M., Thiele, B. J., Mann, M. & Hentze, M. W. (1997). mRNA silencing in erythroid differentiation: hnRNP K and hnRNP E1 regulate 15-lipoxygenase translation from the 3' end. *Cell* **89**, 597-606.

Parsley, T. B., Towner, J. S., Blyn, L. B., Ehrenfeld, E. & Semler, B. L. (1997). Poly (rC) binding protein 2 forms a teRNAry complex with the 5'- terminal sequences of poliovirus RNA and the viral 3CD proteinase. *RNA* **3**, 1124-34.

Pautz, A., Linker, K., Hubrich, T., Korhonen, R., Altenhofer, S. & Kleinert, H. (2006). The polypyrimidine tract-binding protein (PTB) is involved in the post-transcriptional regulation of human inducible nitric oxide synthase expression. *J Biol Chem* **281**, 32294-302.

Pedersen, N. C., Elliott, J. B., Glasgow, A., Poland, A. & Keel, K. (2000). An isolated epizootic of hemorrhagic-like fever in cats caused by a novel and highly virulent strain of feline calicivirus. *Vet Microbiol* **73**, 281-300.

Pelletier, J. & Sonenberg, N. (1988). Internal initiation of translation of eukaryotic mRNA directed by a sequence derived from poliovirus RNA. *Nature* **334**, 320-325.

Perera, R., Daijogo, S., Walter, B. L., Nguyen, J. H. & Semler, B. L. (2007). Cellular protein modification by poliovirus: the two faces of poly(rC)-binding protein. *J Virol*.

Pestova, T. V., Shatsky, I. N., Fletcher, S. P., Jackson, R. J. & Hellen, C. U. (1998). A prokaryotic-like mode of cytoplasmic eukaryotic ribosome binding to the initiation codon during internal translation initiation of hepatitis C and classical swine fever virus RNAs. *Genes Dev* **12**, 67-83.

Pfister, T. & Wimmer, E. (2001). Polypeptide p41 of a Norwalk-like virus is a nucleic acid-independent nucleoside triphosphatase. *J Virol* **75**, 1611-9.

Pickering, B. M., Mitchell, S. A., Spriggs, K. A., Stoneley, M. & Willis, A. E. (2004). Bag-1 internal ribosome entry segment activity is promoted by structural changes mediated by poly(rC) binding protein 1 and recruitment of polypyrimidine tract binding protein 1. *Mol Cell Biol* **24**, 5595-605.

Piecyk, M., Wax, S., Beck, A. R., Kedersha, N., Gupta, M., Maritim, B., Chen, S., Gueydan, C., Kruys, V., Streuli, M. & Anderson, P. (2000). TIA-1 is a translational silencer that selectively regulates the expression of TNF-alpha. *EMBO J* **19**, 4154-63.

Pilipenko, E. V., Gmyl, A. P., Maslova, S. V., Svitkin, Y. V., Sinyakov, A. N. & Agol, V. I. (1992). Prokaryotic-Like Cis Elements in the Cap-Independent Internal Initiation of Translation on Picornavirus RNA. *Cell* **68**, 119-131.

Pilipenko, E. V., Pestova, T. V., Kolupaeva, V. G., Khitrina, E. V., Poperechnaya, A. N., Agol, V. I. & Hellen, C. U. (2000). A cell cycle-dependent protein serves as a template-specific translation initiation factor. *Genes Dev* **14**, 2028-45.

Pilipenko, E. V., Viktorova, E. G., Guest, S. T., Agol, V. I. & Roos, R. P. (2001). Cell-specific proteins regulate viral RNA translation and virus-induced disease. *EMBO J* **20**, 6899-908.

Pisarev, A. V., Chard, L. S., Kaku, Y., Johns, H. L., Shatsky, I. N. & Belsham, G. J. (2004). Functional and structural similarities between the internal ribosome

entry sites of hepatitis C virus and porcine teschovirus, a picornavirus. *J Virol* **78**, 4487-97.

Popovic, Z. & Templeton, D. M. (2005). A Northwestern blotting approach for studying iron regulatory element-binding proteins. *Mol Cell Biochem* **268**, 67-74.

Poulet, H., Brunet, S., Leroy, V. & Chappuis, G. (2005). Immunisation with a combination of two complementary feline calicivirus strains induces a broad cross-protection against heterologous challenges. *Vet Microbiol* **106**, 17-31.

Prasad, B. V., Hardy, M. E., Dokland, T., Bella, J., Rossmann, M. G. & Estes, M. K. (1999). X-ray crystallographic structure of the Norwalk virus capsid. *Science* **286**, 287-90.

Radford, A. D., Coyne, K. P., Dawson, S., Porter, C. J. & Gaskell, R. M. (2007). Feline calicivirus. *Vet Res* **38**, 319-35.

Ray, D., Shah, A., Tilgner, M., Guo, Y., Zhao, Y., Dong, H., Deas, T. S., Zhou, Y., Li, H. & Shi, P. Y. (2006). West Nile virus 5'-cap structure is formed by sequential guanine N-7 and ribose 2'-O methylations by nonstructural protein 5. *J Virol* **80**, 8362-70.

Recht, M. I. & Williamson, J. R. (2004). RNA tertiary structure and cooperative assembly of a large ribonucleoprotein complex. *J Mol Biol* **344**, 395-407.

Rodriguez-Trelles, F., Tarrio, R. & Ayala, F. J. (2006). Origins and evolution of spliceosomal introns. *Annu Rev Genet* **40**, 47-76.

Rohll, J. B., Moon, D. H., Evans, D. J. & Almond, J. W. (1995). The 3'-untranslated region of picornavirus RNA - features required for efficient genome replication. *J Virol* **69**, 7835-7844.

Rouault, T. A. (2006). The role of iron regulatory proteins in mammalian iron homeostasis and disease. *Nat Chem Biol* **2**, 406-14.

Sambrook, J. R., D. W. (2001). Molecular cloning: a laboratory manual 3rd ed.

Schwartz, M., Chen, J., Lee, W. M., Janda, M. & Ahlquist, P. (2004). Alternate, virus-induced membrane rearrangements support positive-strand RNA virus genome replication. *Proc Natl Acad Sci U S A* **101**, 11263-8.

Shaw, G. & Kamen, R. (1986). A conserved AU sequence from the 3' untranslated region of GM-CSF mRNA mediates selective mRNA degradation. *Cell* **46**, 659-67.

Singh, R. (2002). RNA–Protein Interactions That Regulate Pre-mRNA Splicing. *Gene Expression* **10**, 79-92.

Siomi, H., Choi, M., Siomi, M. C., Nussbaum, R. L. & Dreyfuss, G. (1994). Essential role for KH domains in RNA binding: impaired RNA binding by a mutation in the KH domain of FMR1 that causes fragile X syndrome. *Cell* **77**, 33-9.

Smith, A. W., Iversen, P. L., Skilling, D. E., Stein, D. A., Bok, K. & Matson, D. O. (2006). Vesivirus viremia and seroprevalence in humans. *J Med Virol* **78**, 693-701.

Someya, Y., Takeda, N. & Miyamura, T. (2000). Complete nucleotide sequence of the chiba virus genome and functional expression of the 3C-like protease in Escherichia coli. *Virology* **278**, 490-500.

Song, Y., Friebe, P., Tzima, E., Junemann, C., Bartenschlager, R. & Niepmann, M. (2006). The hepatitis C virus RNA 3'-untranslated region strongly enhances translation directed by the internal ribosome entry site. *J Virol* **80**, 11579-88.

Song, Y., Tzima, E., Ochs, K., Bassili, G., Trusheim, H., Linder, M., Preissner, K. T. & Niepmann, M. (2005). Evidence for an RNA chaperone function of polypyrimidine tract-binding protein in picornavirus translation. *RNA* **11**, 1809-24.

Sosnovtsev, S. & Green, K. Y. (1995). RNA transcripts derived from a cloned full-length copy of the feline calicivirus genome do not require VPg for infectivity. *Virology* **210**, 383-90.

Sosnovtsev, S. V., Belliot, G., Chang, K.-O., Onwudiwe, O. & Green, K. Y. (2005). Feline Calicivirus VP2 Is Essential for the Production of Infectious Virions. *J. Virol.* **79**, 4012-4024.

Sosnovtsev, S. V., Belliot, G., Chang, K. O., Prikhodko, V. G., Thackray, L. B., Wobus, C. E., Karst, S. M., Virgin, H. W. & Green, K. Y. (2006). Cleavage map and proteolytic processing of the murine norovirus nonstructural polyprotein in infected cells. *J Virol* **80**, 7816-31.

Sosnovtsev, S. V., Garfield, M. & Green, K. Y. (2002). Processing map and essential cleavage sites of the nonstructural polyprotein encoded by ORF1 of the feline calicivirus genome. *J Virol* **76**, 7060-72.

Sosnovtsev, S. V. & Green, K. Y. (2000). Identification and genomic mapping of the ORF3 and VPg proteins in feline calicivirus virions. *Virology* **277**, 193-203.

Sosnovtsev, S. V., Prikhod'ko, E. A., Belliot, G., Cohen, J. I. & Green, K. Y. (2003). Feline calicivirus replication induces apoptosis in cultured cells. *Virus Res* **94**, 1-10.

Southby, J., Gooding, C. & Smith, C. W. (1999). Polypyrimidine tract binding protein functions as a repressor to regulate alternative splicing of alpha-actinin mutally exclusive exons. *Mol Cell Biol* **19**, 2699-711.

Spahn, C. M., Jan, E., Mulder, A., Grassucci, R. A., Sarnow, P. & Frank, J. (2004). Cryo-EM visualization of a viral internal ribosome entry site bound to human ribosomes: the IRES functions as an RNA-based translation factor. *Cell* **118**, 465-75.

Spahn, C. M., Kieft, J. S., Grassucci, R. A., Penczek, P. A., Zhou, K., Doudna, J. A. & Frank, J. (2001). Hepatitis C virus IRES RNA-induced changes in the conformation of the 40s ribosomal subunit. *Science* **291**, 1959-62.

Staton, J. M., Thomson, A. M. & Leedman, P. J. (2000). Hormonal regulation of mRNA stability and RNA-protein interactions in the pituitary. *J Mol Endocrinol* **25**, 17-34.

Stefanovic, B., Hellerbrand, C., Holcik, M., Briendl, M., Aliebhaber, S. & Brenner, D. A. (1997). Posttranscriptional regulation of collagen alpha1(I) mRNA in hepatic stellate cells. *Mol Cell Biol* **17**, 5201-9.

Stoneley, M. & Willis, A. E. (2004). Cellular internal ribosome entry segments: structures, trans-acting factors and regulation of gene expression. *Oncogene* **23**, 3200-7.

Storz, G., Altuvia, S. & Wassarman, K. M. (2005). An abundance of RNA regulators. *Annu Rev Biochem* **74**, 199-217.

Straub, T. M., Honer zu Bentrup, K., Orosz-Coghlan, P., Dohnalkova, A., Mayer, B. K., Bartholomew, R. A., Valdez, C. O., Bruckner-Lea, C. J., Gerba, C. P., Abbaszadegan, M. & Nickerson, C. A. (2007). In vitro cell culture infectivity assay for human noroviruses. *Emerg Infect Dis* **13**, 396-403.

Stuart, A. D. & Brown, T. D. (2007). Alpha2,6-linked sialic acid acts as a receptor for Feline calicivirus. *J Gen Virol* **88**, 177-86.

Svitkin, Y. V., Meerovitch, K., Lee, H. S., Dholakia, J. N., Kenan, D. J., Agol, V. I. & Sonenberg, N. (1994). Internal translation initiation on poliovirus RNA - further characterization of la function in poliovirus translation in-vitro. *J Virol* **68**, 1544-1550.

Tan, M., Hegde, R. S. & Jiang, X. (2004). The P domain of norovirus capsid protein forms dimer and binds to histo-blood group antigen receptors. *J Virol* **78**, 6233-42.

TerWee, J., Lauritzen, A. Y., Sabara, M., Dreier, K. J. & Kokjohn, K. (1997). Comparison of the primary signs induced by experimental exposure to either a pneumotrophic or a 'limping' strain of feline calicivirus. *Vet Microbiol* **56**, 33-45.

Thackray, L. B., Wobus, C. E., Chachu, K. A., Liu, B., Alegre, E. R., Henderson, K. S., Kelley, S. T. & Virgin, H. W. t. (2007). Murine noroviruses comprising a single genogroup exhibit biological diversity despite limited sequence divergence. *J Virol*. **81**, 10460-73

Thomson, A. M., Cahill, C. M., Cho, H. H., Kassachau, K. D., Epis, M. R., Bridges, K. R., Leedman, P. J. & Rogers, J. T. (2005). The acute box cis-element in human heavy ferritin mRNA 5'-untranslated region is a unique translation enhancer that binds poly(C)-binding proteins. *J Biol Chem* **280**, 30032-45.

Thomson, A. M., Rogers, J. T. & Leedman, P. J. (1999). Iron-regulatory proteins, iron-responsive elements and ferritin mRNA translation. *Int J Biochem Cell Biol* **31**, 1139-52.

Thorven, M., Grahn, A., Hedlund, K. O., Johansson, H., Wahlfrid, C., Larson, G. & Svensson, L. (2005). A homozygous nonsense mutation (428G-->A) in the human secretor (FUT2) gene provides resistance to symptomatic norovirus (GGII) infections. *J Virol* **79**, 15351-5.

Tischendorf, J. J., Beger, C., Korf, M., Manns, M. P. & Kruger, M. (2004). Polypyrimidine tract-binding protein (PTB) inhibits Hepatitis C virus internal ribosome entry site (HCV IRES)-mediated translation, but does not affect HCV replication. *Arch Virol* **149**, 1955-70.

Tomonaga, T. & Levens, D. (1996). Activating transcription from single stranded DNA. *Proc Natl Acad Sci U S A* **93**, 5830-5.

Toyoda, H., Koide, N., Kamiyama, M., Tobita, K., Mizumoto, K. & Imura, N. (1994). Host factors required for internal initiation of translation on poliovirus RNA. *Arch Virol* **138**, 1-15.

Treiber, D. K. & Williamson, J. R. (2001). Concerted kinetic folding of a multidomain ribozyme with a disrupted loop-receptor interaction. *J Mol Biol* **305**, 11-21.

Tsuchihara, K., Tanaka, T., Hijikata, M., Kuge, S., Toyoda, H., Nomoto, A., Yamamoto, N. & Shimotohno, K. (1997). Specific interaction of polypyrimidine tract-binding protein with the extreme 3'-terminal structure of the hepatitis C virus genome, the 3'X. *J Virol* **71**, 6720-6.

Valcarcel, J. & Gebauer, F. (1997). Post-transcriptional regulation: the dawn of PTB. *Curr Biol* **7**, R705-8.

van den Born, E., Posthuma, C. C., Gultyaev, A. P. & Snijder, E. J. (2005). Discontinuous subgenomic RNA synthesis in arteriviruses is guided by an RNA hairpin structure located in the genomic leader region. *J Virol* **79**, 6312-24.

van der Most, R. G., de Groot, R. J. & Spaan, W. J. (1994). Subgenomic RNA synthesis directed by a synthetic defective interfering RNA of mouse hepatitis virus: a study of coronavirus transcription initiation. *J Virol* **68**, 3656-66.

van Kuppeveld, F. J., Hoenderop, J. G., Smeets, R. L., Willems, P. H., Dijkman, H. B., Galama, J. M. & Melchers, W. J. (1997). Coxsackievirus protein 2B modifies endoplasmic reticulum membrane and plasma membrane permeability and facilitates virus release. *EMBO J* **16**, 3519-32.

Vende, P., Piron, M., Castagne, N. & Poncet, D. (2000). Efficient translation of rotavirus mRNA requires simultaneous interaction of NSP3 with the eukaryotic translation initiation factor eIF4G and the mRNA 3' end. *J Virol* **74**, 7064-71.

Wagner, E. J. & Garcia-Blanco, M. A. (2001). Polypyrimidine tract binding protein antagonizes exon definition. *Mol Cell Biol* **21**, 3281-8.

Walter, B. L., Parsley, T. B., Ehrenfeld, E. & Semler, B. L. (2002). Distinct Poly(rC) Binding Protein KH Domain Determinants for Poliovirus Translation Initiation and Viral RNA Replication. *J. Virol.* **76**, 12008-12022.

Wang, W., Furneaux, H., Cheng, H., Caldwell, M. C., Hutter, D., Liu, Y., Holbrook, N. & Gorospe, M. (2000). HuR regulates p21 mRNA stabilization by UV light. *Mol Cell Biol* **20**, 760-9.

Ward, V. K., McCormick, C. J., Clarke, I. N., Salim, O., Wobus, C. E., Thackray, L. B., Virgin, H. W. t. & Lambden, P. R. (2007). Recovery of infectious murine norovirus using pol II-driven expression of full-length cDNA. *Proc Natl Acad Sci U S A* **104**, 11050-5.

Wei, L., Huhn, J. S., Mory, A., Pathak, H. B., Sosnovtsev, S. V., Green, K. Y. & Cameron, C. E. (2001). Proteinase-polymerase precursor as the active form of feline calicivirus RNA-dependent RNA polymerase. *J Virol* **75**, 1211-9.

Weiss, I. M. & Liebhaber, S. A. (1995). Erythroid cell-specific mRNA stability elements in the alpha 2-globin 3' nontranslated region. *Mol Cell Biol* **15**, 2457-65.

Willcocks, M. M., Carter, M. J. & Roberts, L. O. (2004). Cleavage of eukaryotic initiation factor eIF4G and inhibition of host-cell protein synthesis during feline calicivirus infection. *J Gen Virol* **85**, 1125-30.

Witwer, C., Rauscher, S., Hofacker, I. L. & Stadler, P. F. (2001). Conserved RNA secondary structures in Picornaviridae genomes. *Nucleic Acids Res* **29**, 5079-89.

Wobus, C. E., Karst, S. M., Thackray, L. B., Chang, K. O., Sosnovtsev, S. V., Belliot, G., Krug, A., Mackenzie, J. M., Green, K. Y. & Virgin, H. W. (2004). Replication of Norovirus in cell culture reveals a tropism for dendritic cells and macrophages. *PLoS Biol* **2**, e432.

Wobus, C. E., Thackray, L. B. & Virgin, H. W. 4th. (2006). Murine norovirus: a model system to study norovirus biology and pathogenesis. *J Virol* **80**, 5104-12.

Wolin, S. L. & Cedervall, T. (2002). The La protein. *Annu Rev Biochem* **71**, 375-403.

Wolin, S. L. & Wurtmann, E. J. (2006). Molecular chaperones and quality control in noncoding RNA biogenesis. *Cold Spring Harb Symp Quant Biol* **71**, 505-11.

Xayaphoummine, A., Bucher, T. & Isambert, H. (2005). Kinefold web server for RNA/DNA folding path and structure prediction including pseudoknots and knots. *Nucleic Acids Res* **33**, W605-10.

Xie, J., Lee, J. A., Kress, T. L., Mowry, K. L. & Black, D. L. (2003). Protein kinase A phosphorylation modulates transport of the polypyrimidine tract-binding protein. *Proc Natl Acad Sci U S A* **100**, 8776-81.

Xue, D., Rubinson, D. A., Pannone, B. K., Yoo, C. J. & Wolin, S. L. (2000). U snRNP assembly in yeast involves the La protein. *EMBO J* **19**, 1650-60.

Yanagi, M., St Claire, M., Emerson, S. U., Purcell, R. H. & Bukh, J. (1999). In vivo analysis of the 3' untranslated region of the hepatitis C virus after in vitro mutagenesis of an infectious cDNA clone. *Proc Natl Acad Sci U S A* **96**, 2291-5.

Yocupicio-Monroy, M., Padmanabhan, R., Medina, F. & del Angel, R. M. (2007). Mosquito La protein binds to the 3' untranslated region of the positive and negative polarity dengue virus RNAs and relocates to the cytoplasm of infected cells. *Virology* **357**, 29-40.

Yoo, C. J. & Wolin, S. L. (1997). The yeast La protein is required for the 3' endonucleolytic cleavage that matures tRNA precursors. *Cell* **89**, 393-402.

You, S., Stump, D. D., Branch, A. D. & Rice, C. M. (2004). A cis-acting replication element in the sequence encoding the NS5B RNA-dependent RNA polymerase is required for hepatitis C virus RNA replication. *J Virol* **78**, 1352-66.

Yu, J. & Russell, J. E. (2001). Structural and functional analysis of an mRNP complex that mediates the high stability of human beta-globin mRNA. *Mol Cell Biol* **21**, 5879-88.

Zhang, G., Slowinski, V. & White, K. A. (1999). Subgenomic mRNA regulation by a distal RNA element in a (+)-strand RNA virus. *RNA* **5**, 550-61.

Zhang, J., Yamada, O., Yoshida, H., Iwai, T. & Araki, H. (2002). Autogenous translational inhibition of core protein: implication for switch from translation to RNA replication in hepatitis C virus. *Virology* **293**, 141-50.

Zuker, M. (2003). Mfold web server for nucleic acid folding and hybridization prediction. *Nucleic Acids Res* **31**, 3406-15.